



Multifactorial analysis of mesenchymal stem cell properties for storage and transportation

A thesis submitted by

Fabio Salvatore D'Agostino

For the award of Engineering Doctorate
in Biopharmaceutical Process Development

Biopharmaceutical and Bioprocessing Technology Centre
School of Chemical Engineering and Advanced Materials

Newcastle University

March 2017

Abstract

Using living cells to treat disease is known as cell therapy and holds the potential to revolutionize healthcare. An increasing number of cell-based products are approaching the late clinical development phase, with human mesenchymal stem cells, which have chondrogenic, osteogenic and adipogenic differentiation capacity, being one of the most widely studied. For these new medicinal products, preserving their therapeutic potential throughout the supply chain is challenging. Current approaches are based on cryopreservation, where cells are cooled to $-80\text{ }^{\circ}\text{C}$ or lower, on hypothermic preservation, where cells are cooled to $2\text{-}8\text{ }^{\circ}\text{C}$, and on controlled room temperatures, with cells at $15\text{-}25\text{ }^{\circ}\text{C}$. However, these methods suffer from limitations and alternative approaches are required.

The aim of this thesis was to investigate a novel temperature range ($26\text{-}37\text{ }^{\circ}\text{C}$) for storage and transportation and, for the first time, to combine temperature with a variable oxygen tension ($3\text{-}20\%$) over a simulated shelf life of 5 or 7 days. Two models were investigated: undifferentiated human bone marrow derived mesenchymal stem cells and cartilage discs derived from these cells. The investigation was based on the use of a statistical design of experiment where temperature, oxygen and storage duration are the input factors while viability, metabolite concentrations and gene expression are the output factors.

The results showed that temperature and oxygen modulate metabolic activity and subsequent differentiation potential, with interaction effects between temperature and oxygen being readily identifiable. Predictive models were subsequently developed, with case studies demonstrating how such models can be used as a decision support tool for the design of a transportation device for mesenchymal stem cells and their differentiated products.

Overall, this thesis demonstrates the need for a multifactorial approach for the development of a storage and transportation solution of cell-based medicinal products and offers guidance as to how this may be possible.

Acknowledgements

I would like to thank all my colleagues at the Musculoskeletal Research Group for their help during my EngD.

I would like to thank my supervisor Prof John Loughlin for his help, support and for making this research project possible within his lab.

I would like to thank Prof Elaine Martin for her help and motivation during the challenging times of the project.

I would like to thank Dr Ivan Wall and Dr Carlotta Peticone at UCL for allowing me to use their equipment.

I would like to thank Dr Dennis Lendrem for his help with the implementation of the statistical design of experiment.

I would like to thank the Engineering and Physical Sciences Research Council (EPSRC) and Tower Cold Chain for funding.

I would also like to thank all the friends I have made during my EngD here in Newcastle.

A special thank you goes to my girlfriend Eleni for her support, motivation and for always being there for me.

Dedication

To my uncle Alfredo and my grandparents.

List of publications

D'Agostino F., Martin E., Loughlin J. (2015) Development of successful bio-preservation strategies for cell therapy medicinal products *Cytotherapy*, Vol. 17, Issue 6, S32 Published in issue: June, 2015

D'Agostino F., ISCT 2015 Annual Meeting Conference Report
Cell Gene Therapy Insights 2015; 1(1), 49-63.

Lendrem DW., Lendrem BC., Rowland-Jones R., **D'Agostino F.**, Linsley M., Owen MR., Isaacs JD. Teaching Examples for the Design of Experiments: Geographical Sensitivity and the Self-Fulfilling Prophecy. *Pharmaceutical Statistics*. 2016 Jan-Feb;15(1):90-2.

Table of contents

List of Figures	p.10
List of Tables	p.21
List of Abbreviations	p.23

Chapter 1: Introduction

1.1 Cell therapy industry overview.....	p.25
1.2 Human cells as active pharmaceutical ingredients.....	p.27
1.3 Human mesenchymal/stromal stem cells.....	p.28
1.4 Manufacturing and delivery of cell based medicinal products.....	p.32
1.5 Preservation methods for cell based medicinal products.....	p.35
1.6 Statistical Design of Experiment (DoE) for cell therapy development.....	p.41
1.7 Scope and aim of research.....	p.43
1.8 Thesis overview.....	p.45

Chapter 2: Investigating storage properties of scaffold free bone marrow derived cartilage discs

Introduction.....	p.47
2.1 Materials and methods.....	p.51
2.1.1 Human Bone Marrow derived MSCs culture.....	p.51
2.1.2 Chondrogenic differentiation of hMSCs using the tranwell method.....	p.52
2.1.3 Alamar blue assay for scaffold-free bone marrow derived cartilage disc.....	p.53
2.1.4 Quantitative viability indicator.....	p.55
2.1.5 Storage of cartilage discs.....	p.58
2.1.6 Spent medium analysis.....	p.59
2.1.7 Extraction of total RNA.....	p.60
2.1.8 Gene Expression analysis.....	p.61
2.1.8.1 cDNA synthesis.....	p.61
2.1.8.2 Quantitative real-time PCR.....	p.61
2.1.9 Statistical analysis.....	p.63
2.2 Results.....	p.64
2.2.1 Alamar blue assay for cartilage discs.....	p.64
2.2.2 Post storage viability of scaffold-free bone marrow derived cartilage discs...	p.66

2.2.2 Post storage metabolites concentration.....	p.72
2.2.2.1 Glucose and lactate.....	p.72
2.2.2.2 Glutamine and ammonia.....	p.78
2.2.3 Post storage gene expression analysis.....	p.84
2.3 Brief summary of data described.....	p.93
2.4 Discussion.....	p.94

Chapter 3: Factorial experimental design as an investigational and decision support tool for cell therapy product development

Introduction.....	p.98
3.1 Material and methods.....	p.101
3.1.1 Factorial Design of Experiment.....	p.101
3.1.2 Model adequacy checking.....	p.102
3.1.3 Centre points and linearity assumption.....	p.103
3.1.4 Case study 1.....	p.104
3.1.5 Case study 2.....	p.104
3.2 Results.....	p.106
3.2.1 Analysis of post-storage viability response model.....	p.106
3.2.2 Analysis of post-storage glucose and lactate response models.....	p.109
3.2.3 Analysis of post-storage glutamine and ammonia response models.....	p.116
3.2.4 Analysis of post-storage gene expressions response models.....	p.122
3.4 Linearity testing and centre points.....	p.129
3.5 Case study 1.....	p.132
3.6 Case study 2.....	p.135
3.7 Discussion.....	p.138

Chapter 4: Investigating storage properties of hMSCs prior to their differentiation

Introduction.....	p.141
4.1 Materials and methods.....	p.143
4.1.1 Storage of hMSCs in tissue culture flasks and plates.....	p.143
4.1.2 Spent medium analysis.....	p.146

4.1.3 Post-storage chondrogenic differentiation in micropellets.....	p.146
4.1.4 Post-Storage osteogenic differentiation.....	p.147
4.1.5 Post storage adipogenic differentiation.....	p.147
4.1.6 Post storage GAGs assay.....	p.149
4.1.7 Post-storage alkaline phosphatase assay and osteogenic staining.....	p.151
4.1.8 Post storage adipogenic staining of hMSCs.....	p.152
4.1.9 Gene expression analysis from micropellets and hMSCs.....	p.153
4.1.10 Factorial design of experiment for hMSCs storage.....	p.154
4.2 Results.....	p.155
4.2.1 Post storage metabolites concentration for undifferentiated hMSCs.....	p.155
4.2.2 Post storage chondrogenic differentiation of hMSC in micropellets.....	p.162
4.2.3 Post storage osteogenic differentiation of hMSC.....	p.167
4.2.4 Post storage adipogenic differentiation of hMSC.....	p.172
4.3 Brief summary of data described.....	p.177
4.4 Discussion.....	p.178

Chapter 5 General discussion

5.1 Key findings.....	p.182
5.1.2 Metabolites.....	p.184
5.1.3 Chondrogenic potential.....	p.186
5.1.4 Osteogenic potential.....	p.188
5.1.5 Adipogenic potential.....	p.189
5.1.6 DoE as an investigational and decision support tool.....	p.190
5.2 Challenges and limitations.....	p.192
5.3 Future work.....	p.194
5.4 Conclusion.....	p.198

References.....	p.200
------------------------	--------------

Appendix I.....	p.215
------------------------	--------------

List of Figures

Fig.1.1 Schematic summarizing the main sources and properties of mesenchymal stem cells (modified from (Eberli et al., 2014))......p.30

Fig. 1.2 Allogeneic versus autologous manufacturing models. Autologous products are patient specific; one batch will correspond to one patient. Starting from a biopsy isolated from the patients, cells will need to be processed to generate the number of doses required for that treatment and to allow quality testing. For allogeneic products, cells from one universal donor are isolated, validated and generate a master cell bank. This is further expanded into a working cell bank. When a production lot is required, patient doses will be generated from the working cell bank and will be used to treat multiple patients (modified from (Brandenberger et al., 2011))......p.34

Figure 2.1 Multifactorial space under investigation. Eight storage conditions were defined by combining two levels (high and low) for the three factors: temperature, oxygen and storage duration......p.50

Figure 2.2 Schematic view of the Alamar blue assay cartilage disc. Three technical replicates are sampled by cutting the discs into four quarters with a scapel blade. Three of the quarters are used for the Alamar blue assay. Each quarter was added to 100 μ l chondrogenic medium and 10 μ l Alamar blue reagent in a 96 well plate. Negative controls containing no cells were included. A mix of chondrogenic medium + 10% Alamar blue reagent was autoclaved and used as positive control as resazurin contained in the Alamar blue is completely reduced to resorufin. The plate was incubated at 37 °C and Alamar blue fluorescence values were measured every hour for eight hours. (Ex λ = excitation wavelength; Em λ = emission wavelength)......p.52

Figure 2.3. Schematic view of the quantitative viability indicator assay for scaffold-free bone marrow derived cartilage discs. The assay is based on Alamar blue and Picogreen assays performed on the same sample. Each disc was cut into four quarters; three were used for Alamar blue and Picogreen assays and one was used for gene expression analysis. For each disc, three technical replicates were available (samples A, B, and C). Alamar blue fluorescence values were measured for each sample (Ex λ =560 nm, Em λ = 590 nm). For each sample, the amount of DNA was then quantified by Picogreen assay. Alamar blue fluorescence values were normalized by the amount of DNA per each sample. The resulting values were defined as viability indicator. (Ex λ = excitation wavelength; Em λ = emission wavelength)......p.57

Figure 2.4 Schematic view of the storage experiment of scaffold-free bone marrow derived cartilage discs......p.59

Figure 2.5 Chondrogenic differentiation of hMSCs into cartilage discs. Cells were cultured for 14 days in a transwell with chondrogenic medium (Table 1) forming a 7 mm diameter disc which has been used as cell therapy product model for subsequent experiments. Scale bar= 500 μ m)......p.66

Fig 2.6 Alamar blue fluorescence (Relative fluorescence units, RFU) of four cartilage discs during 8 h incubation at 37 °C. Each disc was prepared as described in 3.1.2 using hMSCs isolated from 1 healthy donor. For each time point, results are represented as mean \pm standard deviation for three technical replicates. These were sampled by cutting each disc into four quarters and using three for the Alamar blue assay. Negative control samples were included (chondrogenic medium plus Alamar blue reagent only). Positive control was created by

preliminary autoclaving chondrogenic medium and Alamar blue reagent. Resazurin contained in the Alamar blue reagent is reduced and changes color from blue to pink.....p.68

Figure 2.7 Post-storage viability indicator of cartilage discs measured via Alamar blue and Picogreen assays. Discs were prepared using bone marrow derived hMSCs isolated from three healthy donors. Discs were exposed to storage conditions listed in Table 2. For each disc, Alamar blue fluorescence was measured by cutting the disc into four quarters (three quarters were used for Alamar Blue and Picogreen Assay). For each quarter, Alamar blue fluorescence was normalized by the amount of DNA measured via Picogreen assay. This was defined as the viability indicator. Viability indicator values for all storage conditions and all three donors are plotted relative to a disc not exposed to storage conditions (storage start, day 0). Values are plotted as mean and standard error of the mean (n=3). (37 C=37 °C, O₂=pO₂ oxygen tension, D5= day 5, D7= day 7).....p.70

Figure 2.8 Least square means for viability indicator for cartilage discs following storage conditions listed in table 2 for donor 1 (A), 2 (B) and 3(C) respectively. Least square means (LS-means) were estimated using JMP SAS software. Viability indicator raw data used to estimate the LS-means were expressed as % relative to untreated samples which were not exposed to any storage condition. Storage conditions were defined by combining high (+) and low(-) levels of the three parameters under investigation: temperature (37 -26 °C), oxygen (3-20 % O₂) and storage duration (5-7 days). This method allows to compare by compensating for donor to donor variability. Left (A,B,C), least square means for viability indicator (%) for each storage condition. Right (A,B,C), least square means for each donor calculated across all storage conditions. Error bars represent 95% CI. Confidence intervals that do not overlap represent storage conditions which were consistently different across the three donors. Statistically different storage conditions or donors can be identified by non-overlapping CIs.....p.71

Figure 2.9 Control charts for total DNA (ng) contained in three quarters of scaffold-free bone marrow derived cartilage disc measured via Picogreen assay. Each control chart (A, B and C) shows the average amount of DNA (Avg) for the three quarters for all discs used in the storage experiment for donor 1, 2 and 3 respectively. For each donor, day 0 corresponds to the disc used as control (storage start). Avg (green line) is the center line. Upper control limit (UCL) and lower control limit (LCL) represent +3 SD and - 3 SD respectively. All points are between the control limits.....p.73

Figure 2.10 Post-storage glucose concentrations (g/l) in spent medium. Scaffold-free bone marrow derived cartilage discs were prepared using bone marrow hMSCs isolated from three healthy donors. Discs were exposed to storage conditions listed in Table 2. Dotted line represents initial glucose concentration in fresh medium (i.e.) (4.5 g/l). Each measurement requires 1 ml of spent medium. As only 2 ml of spent medium were available for each storage condition, two technical replicates only were possible. Values are plotted as mean and standard error of the mean (n=2). (37 C=37 °C, O₂=pO₂ oxygen tension, D5= day 5, D7= day 7).....p.74

Figure 2.11 Least square means for glucose for scaffold-free bone marrow derived cartilage discs following storage conditions listed in table 2 for donor 1 (A), 2 (B) and 3(C) respectively. Least square means (LS-means) were estimated using JMP SAS software. Storage conditions were defined by combining high (+) and low(-) levels of the three parameters under investigation: temperature (37 -26 °C), oxygen (3-20 % O₂) and storage duration (5-7 days). This method allows to compare by compensating for donor to donor variability. Left (A,B,C), least square means for glucose for each storage condition. Right (A,B,C), least square means for each donor calculated across all storage conditions. Error bars represent 95% CI. Confidence intervals that do not overlap represent storage conditions which were consistently different across the three donors. Statistically different storage conditions or donors can be identified by non-overlapping CIs.....p.75

Figure 2.12 Post-storage lactate concentrations (g/l) in spent medium. Initial concentration is 0 g/l. Scaffold-free bone marrow derived cartilage discs were prepared using bone marrow hMSCs isolated from three healthy donors. Discs were exposed to storage conditions listed in Table 2. Each measurement requires 1 ml of spent medium. As only 2 ml of spent medium were available for each storage condition, two technical replicates only were possible. Values are plotted as mean and standard error of the mean (n=2). (37 C=37 °C, O2=pO₂ oxygen tension, D5= day 5, D7= day 7).....p.77

Figure 2.13 Least square means for lactate for scaffold-free bone marrow derived cartilage discs following storage conditions listed in table 2 for donor 1 (A), 2 (B) and 3(C) respectively. Least square means (LS-means) were estimated using JMP SAS software. Storage conditions were defined by combining high (+) and low(-) levels of the three parameters under investigation: temperature (37 -26°C), oxygen (3-20 % O₂)and storage duration (5-7 days). This method allows to compare by compensating for donor to donor variability. Left (A,B,C), least square means for lactate (%) for each storage condition. Right (A,B,C), least square means for each donor calculated across all storage conditions. Error bars represent 95% CI. Confidence intervals that do not overlap represent storage conditions which were consistently different across the three donors. Statistically different storage conditions or donors can be identified by non-overlapping CIs.....p.78

Figure 2.14 Post-storage glutamine concentrations (mM) in spent medium. Scaffold-free bone marrow derived cartilage discs were prepared using bone marrow hMSCs isolated from three healthy donors. Discs were exposed to storage conditions listed in Table 2. Dotted line represents initial glutamine concentration in fresh medium (i.c.) (2 mM). Each measurement requires 1 ml of spent medium. As only 2 ml of spent medium were available for each storage condition, two technical replicates only were possible. Values are plotted as mean and standard error of the mean (n=2). (37 C=37 °C, O2=pO₂ oxygen tension, D5= day 5, D7= day 7).....p.79

Figure 2.15 Least square means for glutamine for scaffold-free bone marrow derived cartilage discs following storage conditions listed in table 2 for donor 1 (A), 2 (B) and 3(C) respectively. Least square means (LS-means) were estimated using JMP SAS software. Storage conditions were defined by combining high (+) and low(-) levels of the three parameters under investigation: temperature (37 -26°C), oxygen (3-20 % O₂)and storage duration (5-7 days). This method allows to compare by compensating for donor to donor variability. Left (A,B,C), least square means for glutamine for each storage condition. Right (A,B,C), least square means for each donor calculated across all storage conditions. Error bars represent 95% CI. Confidence intervals that do not overlap represent storage conditions which were consistently different across the three donors. Statistically different storage conditions or donors can be identified by non-overlapping CIs.....p.80

Figure 2.16 Post-storage NH₃ concentrations (mM) in spent medium. Scaffold-free bone marrow derived cartilage discs were prepared using bone marrow hMSCs isolated from three healthy donors. Discs were exposed to storage conditions listed in Table 2. Initial NH₃ concentration was 0 mM. Each measurement requires 1 ml of spent medium. As only 2 ml of spent medium were available for each storage condition, two technical replicates only were possible. Values are plotted as mean and standard error of the mean (n=2). (37 C=37 °C, O2=pO₂ oxygen tension, D5= day 5, D7= day 7).....p.81

Figure 2.17 Least square means for NH₃ for scaffold-free bone marrow derived cartilage discs following storage conditions listed in table 2 for donor 1 (A), 2 (B) and 3(C) respectively. Least square means (LS-means) were estimated using JMP SAS software. Storage conditions were defined by combining high (+) and low(-) levels of the three parameters under investigation: temperature (37 -26°C), oxygen (3-20 % O₂)and storage duration (5-7 days). This method allows to compare by compensating for donor to donor variability. Left (A,B,C), least square means

for viability indicator (%) for each storage condition. Right (A,B,C), least square means for each donor calculated across all storage conditions. Error bars represent 95% CI. Confidence intervals that do not overlap represent storage conditions which were consistently different across the three donors. Statistically different storage conditions or donors can be identified by non-overlapping CIs.....p.83

Figure 2.18 Fold change in *COL2A1* gene expression in response to storage. Scaffold-free bone marrow derived cartilage discs were prepared using bone marrow hMSCs isolated from three healthy donors. Discs were exposed to storage conditions listed in Table 2. Fold change values are relative to an unstored disc and plotted as mean and standard error of the mean for three technical replicates for each donor. (37 C=37 °C, O₂=pO₂ oxygen tension, D5= day 5, D7= day 7).....p.84

Figure 2.19 Least square means for *COL2A1* fold change for scaffold-free bone marrow derived cartilage discs following storage conditions listed in table 2 for donor 1 (A), 2 (B) and 3(C) respectively. Least square means (LS-means) were estimated using JMP SAS software. Fold changes are relative to untreated samples which were not exposed to any storage condition. Storage conditions were defined by combining high (+) and low(-) levels of the three parameters under investigation: temperature (37 -26 °C), oxygen (3-20 % O₂)and storage duration (5-7 days). This method allows to compare by compensating for donor to donor variability. Left (A,B,C), least square means for *COL2A1* fold change for each storage condition. Right (A,B,C), least square means for each donor calculated across all storage conditions. Error bars represent 95% CI. Confidence intervals that do not overlap represent storage conditions which were consistently different across the three donors. Statistically different storage conditions or donors can be identified by non-overlapping CIs.....p.86

Figure 2.20 Fold change in *ACAN* gene expression in response to storage. Scaffold-free bone marrow derived cartilage discs were prepared using bone marrow hMSCs isolated from three healthy donors. Discs were exposed to storage conditions listed in Table 2. Fold change values are relative to an unstored disc and plotted as mean and standard error of the mean for three technical replicates for each donor. (37 C=37 °C, O₂=pO₂ oxygen tension, D5= day 5, D7= day 7).....p.87

Figure 21 Least square means for *ACAN* fold change for scaffold-free bone marrow derived cartilage discs following storage conditions listed in table 2 for donor 1 (A), 2 (B) and 3(C) respectively. Least square means (LS-means) were estimated using JMP SAS software. Fold changes are relative to untreated samples which were not exposed to any storage condition. Storage conditions were defined by combining high (+) and low(-) levels of the three parameters under investigation: temperature (37 -26 °C), oxygen (3-20 % O₂)and storage duration (5-7 days). This method allows to compare by compensating for donor to donor variability. Left (A,B,C), least square means for *ACAN* fold change for each storage condition. Right (A,B,C), least square means for each donor calculated across all storage conditions. Error bars represent 95% CI. Confidence intervals that do not overlap represent storage conditions which were consistently different across the three donors. Statistically different storage conditions or donors can be identified by non-overlapping CIs.....p.89

Figure 2.22 Fold change in *COL1A1* gene expression in response to storage. Scaffold-free bone marrow derived cartilage discs were prepared using bone marrow hMSCs isolated from three healthy donors. Discs were exposed to storage conditions listed in Table 2. Fold change values are relative to an unstored disc and plotted as mean and standard error of the mean for three

technical replicates for each donor. (37 C=37 °C, O2=pO₂ oxygen tension, D5= day 5, D7= day 7).....p.90

Figure 2.23 Least square means for *COL1A1* fold changes for scaffold-free bone marrow derived cartilage discs following storage conditions listed in table 2 for donor 1 (A), 2 (B) and 3(C) respectively. Least square means (LS-means) were estimated using JMP SAS software. Fold changes are relative to untreated samples which were not exposed to any storage condition. Storage conditions were defined by combining high (+) and low(-) levels of the three parameters under investigation: temperature (37 -26 °C), oxygen (3-20 % O₂)and storage duration (5-7 days). This method allows to compare by compensating for donor to donor variability. Left (A,B,C), least square means for *COL1A1* fold changes for each storage condition. Right (A,B,C), least square means for each donor calculated across all storage conditions. Error bars represent 95% CI. Confidence intervals that do not overlap represent storage conditions which were consistently different across the three donors. Statistically different storage conditions or donors can be identified by non-overlapping CIs.....p.92

Fig. 3.1 Statistical design of experiment schematic showing input and output factors selected. This system represents the storage of a cartilage disc, used as cell therapy model. For each input factor, two levels (high and low) have been selected creating eight combinations. Output values were measured for each sample as described in chapter 3. The experiment was performed for three healthy donors. As output data showed inter donor variability, one additional nominal variable, donor, has been introduced in the design to account for known variability introduced by noise (donor number) on the output factors.....p.99

Fig. 3.2 Analysis of residuals for viability model. Residuals are plotted versus viability predicted values (A) and versus experimental run number (B) to confirm the hypothesis of constant variance. As no trend nor pattern is shown in (A) and (B) the model is valid. (C) shows goodness of fit by plotting viability actual values versus viability predicted values. RSq= r², RMSE=root mean square error.....p.107

Fig. 3.3 Post-storage viability models for the process space under investigation. Models' parameters estimation performed via least square estimation. Variability values are predicted for temperature range (26-37 °C), oxygen range (3-20%), storage duration 5-7 days and for donor 1 (A), 2 (B) and 3 (C) respectively. In red, viability predicted values for T= 31.5 °C, oxygen= 11.5 % and 6 day storage. Blue dashed lines and blue error bars represent 95 % confidence intervals. Temperature and storage duration have a statistical significant effect on viability, although the former is greater than the latter. Viability decreases as temperature and storage duration increase, while oxygen tension show no significant effect. Samples from the three donors studied showed consistent trends and inter-donor variability was not significant.....p.108

Fig.3.4 Analysis of residuals for glucose model. Residuals are plotted vs glucose predicted values (A) and versus experimental run number (B) to confirm the hypothesis of constant variance. As no trend nor pattern is shown in (A) and (B) the model is valid. (C) shows goodness of fit by plotting glucose actual values versus glucose predicted values. RSq= r², RMSE=root mean square error.....p.110

Fig. 3.5 Post-storage glucose concentration models for the process space under investigation. Models' parameters estimation performed via least square estimation. Glucose values are predicted for temperature range (26-37 °C), oxygen range (3-20%), storage duration 5-7 days and for donor 1 (A), 2 (B) and 3 (C) respectively. In red, glucose predicted values for T= 31.5 °C, oxygen= 11.5 % and 6 day storage. Blue dashed lines and blue error bars represent confidence intervals. Temperature and storage duration have a statistical significant effect on glucose consumption, although the former is greater than the latter. Final glucose concentration decreases as temperature and storage duration increase, while oxygen tension did not show significant effect. Samples from the three donors studied showed consistent trends but donor 2 was statistically different.....p.111

Fig.3.6 Analysis of residuals for lactate model. Residuals are plotted versus lactate predicted values (a) and versus experimental run number (b) to confirm the hypothesis of constant variance. As no trend nor pattern is shown in (a) and (b) the model is valid. (c) shows goodnees of fit by plotting lactate actual values versus lactate predicted values. RSq= r², RMSE=root mean square error.....p.113

Fig.3.7 Post-storage lactate concentration models for the process space under investigation. Models' parameters estimation performed via least square estimation. Lactate values are predicted for temperature range (26-37 °C), oxygen range (3-20%), storage duration 5-7 days and for donor 1 (A), 2 (B) and 3 (C) respectively. In red, lactate predicted values for T= 31.5 °C, oxygen= 3-20 % and 6 day storage. Blue dashed lines and blue error bars represent confidence intervals. Temperature and storage duration have a statistical significant effect on lactate release, although the former is greater than the latter. Post storage concentration increases as temperature and storage duration increase, while oxygen tension did not show significant effect. Samples from the three donors studied showed consistent trends but donor 2 was statistically different.....p.114

Fig. 3.8 Interaction plots for post storage lactate concentration model. All possible combinations of input variables (temperature, oxygen and storage duration) are shown. For each variable, red line represents low levels while blue line represents high levels. Statistically significant interactions towards post storage lactate concentration are represented by crossing lines. Oxygen and temperature interaction was statistically significant.....p.115

Fig 3.9 Analysis of residuals for glutamine model. Residuals are plotted vs glutamine predicted values (a) and versus experimental run number (b) to confirm the hypothesis of constant variance. As no trend nor pattern is shown in (a) and (b) the model is valid. (c) shows goodnees of fit by plotting glutamine actual values versus glutamine predicted values. RSq= r², RMSE=root mean square error.....p.116

Fig. 3.10 Post-storage glutamine concentration models for the process space under investigation. Models' parameters estimation performed via least square estimation. Glutamine values are predicted for temperature range (26-37 °C), oxygen range (3-20%), storage duration 5-7 days and for donor 1 (A), 2 (B) and 3 (C) respectively. In red, glutamine predicted values for T= 31.5 °C, oxygen= 3-20 % and 6 day storage. Blue dashed lines and blue error bars represent confidence intervals. Temperature, oxygen and storage duration have a statistical significant effect on glutamine consumption, although the former is much greater. Post storage glutamine

concentration decreases as temperature, oxygen and storage duration increase. Samples from the three donors studied showed consistent trends but donor 2 was statistically different...p.117

Fig. 3.11 Analysis of residuals for NH₃ model. Residuals are plotted vs ammonia predicted values (a) and versus experimental run number (b) to confirm the hypothesis of constant variance. As no trend nor pattern is shown in (a) and (b) the model is valid. (c) shows goodness of fit by plotting ammonia actual values versus ammonia predicted values. RSq= r², RMSE=root mean square error.....p.119

Fig.12 Post-storage NH₃ concentration models for the process space under investigation. Models' parameters estimation performed via least square estimation. NH₄⁺ values are predicted for temperature range (26-37 °C), oxygen range (3-20%), storage duration 5-7 days and for donor 1 (A), 2 (B) and 3 (C) respectively. In red, NH₄⁺ predicted values for T= 31.5 °C, oxygen= 3-20 % and 6 day storage. Blue dashed lines and blue error bars represent confidence intervals. Temperature, oxygen and storage duration have a statistical significant effect on ammonia release, although the former is greater. Post storage ammonia concentration increases as temperature, oxygen and storage duration increase, while oxygen tension did not show significant effect. Samples from the three donors studied showed consistent trends but donor 2 was statistically different.....p.120

Fig. 3.13 Interaction plots for post storage NH₃ concentration model. All possible combinations of input variables (temperature, oxygen and storage duration) are shown. For each variable, red line represents low levels while blue line represents high levels. Statistically significant interactions towards post storage lactate concentration are represented by crossing lines. Oxygen and temperature interaction was statistically significant.....p.121

Fig. 3.14 Analysis of residuals for COL2A1 model. Residuals are plotted vs COL2A1 predicted values (a). Residuals showed uneven spreading (fanning effect) which violates the assumption of constant variance. COL2A1 values were transformed by log₁₀. Residuals for the transformed COL2A1 values (LOG10COL2A1) are plotted versus predicted LOG10COL2A1 (b). No fanning is shown in (b) and the model can therefore be considered valid. (c) shows goodness of fit by plotting LOG10COL2A1 actual values versus predicted values. RSq= r², RMSE=root mean square error.....p.123

Fig. 3.15 Post storage COL2A1 expression fold change relative to non-stored samples models for the process space under investigation. Fold change values were transformed by log₁₀. Models' parameters estimation performed via least square estimation. Log₁₀ of COL2A1 fold change values are predicted for temperature range (26-37 °C), oxygen range (3-20%), storage duration 5-7 days and for donor 1 (A), 2 (B) and 3 (C) respectively. In red, log₁₀ fold changes COL2A1 predicted values for T= 31.5 °C, oxygen= 3-20 % and 6 day storage. Blue dashed lines and blue error bars represent confidence intervals. Temperature, oxygen tension and storage duration did not have a statistical significant effect on COL2A1 expression. Samples from the three donors.....p.124

Fig. 3.16 Analysis of residuals for ACAN model. Residuals are plotted vs ACAN predicted values (a). Residuals showed uneven spreading (fanning effect) which violates the assumption of constant variance. ACAN values were transformed by log₁₀. Residuals for the transformed ACAN values (LOG10ACAN) are plotted versus predicted LOG10ACAN (b). No fanning is shown in (b) and the model can therefore be considered valid. (c) shows goodness of fit by plotting LOG10ACAN actual values versus predicted values. RSq= r², RMSE=root mean square error.....p.125

Fig. 3.17 Post storage ACAN expression fold change relative to non-stored samples models for the process space under investigation. Fold change values were transformed by log₁₀. Models' parameters estimation performed via least square estimation. Log₁₀ of ACAN fold change values are predicted for temperature range (26-37 °C), oxygen range (3-20%), storage duration 5-7 days and for donor 1 (A), 2 (B) and 3 (C) respectively. In red, log₁₀ fold changes ACAN predicted values for T= 31.5 °C, oxygen= 3-20 % and 6 day storage. Blue dashed lines and blue error bars represent confidence intervals. Temperature, oxygen tension and storage duration did not have a statistical significant effect on ACAN expression. Samples from the three donors studied showed consistent trends but donor 1 was statistically different.....p.126

Fig. 3.18 Analysis of residuals for COL1A1 model. Residuals are plotted vs COL1A1 predicted values (a). Residuals showed uneven spreading (fanning effect) which violets the assumption of constant variance. COL1A1 values were transformed by log₁₀. Residuals for the transformed COL1A1 values (LOG10COL1A1) are plotted versus predicted LOG10COL1A1 (b). No fanning is shown in (b) and the model can therefore be considered valid. (c) shows goodness of fit by plotting LOG10COL1A1 actual values versus predicted values. RSq= r², RMSE=root mean square error.....p.127

Fig. 3.19 Post storage COL1A1 expression fold change relative to non-stored samples models for the process space under investigation. Fold change values were transformed by log₁₀. Models' parameters estimation performed via least square estimation. Log₁₀ of COL1A1 fold change values are predicted for temperature range (26-37 °C), oxygen range (3-20%), storage duration 5-7 days and for donor 1 (A), 2 (B) and 3 (C) respectively. In red, log₁₀ fold changes COL1A1 predicted values for T= 31.5 °C, oxygen= 3-20 % and 6 day storage. Blue dashed lines and blue error bars represent confidence intervals. Temperature, oxygen tension and storage duration did not have a statistical significant effect on COL2A1 expression. Samples from the three donors studied showed consistent trends but were statistically different.....p.128

Fig. 3.20 Center points analysis on viability model. (Top) Viability model with center points. Viability values measured plotted versus predicted values showing the presence of two outliers which correspond to center points (blue circle) (a) Lack of fit due to center points was observed. Residuals are plotted versus predicted values (b) and versus experimental run (c), confirming the presence of outliers (centre points). (Bottom) Viability model after center points removal (d). No lack of fit was observed. Residuals plotted versus predicted values (e) and experimental run (f) showed no correlations and no trends confirming the hypothesis of constant variance.....p.131

Fig. 3.21 Output values prediction for simulated storage condition A (T = 32 °C, oxygen = 20 %, storage duration= 6 days). Vertical red dashed lines indicate selected input values in the Profiler function in JMP SAS software. Horizontal red dashed lines represent output predicted values for each response variable. Predicted values are also indicated in red for each response variable.....p.133

Fig. 3.22 Output values prediction for simulated storage condition B (T=28 °C, oxygen = 5 %, storage duration= 7 days). Vertical red dashed lines indicate selected input values in the Profiler function in JMP SAS software. Horizontal red dashed lines represent output predicted values for each response variable. Predicted values are also indicated in red for each response variable with 95 % confidence intervals (CIs). Blue dashed lines represent 95 % CIs for the predicted values within the investigated range of input factors.....p.134

Fig.3.23 Contour plots 7 day storage of cartilage disc. The set specifications were (B) viability \geq 80 %, (C) lactate concentration in spent medium after storage 0-1.5 g/l, (D) NH_3 concentration 0-0.5 mM, (E) \log_{10} of COL2A1 fold change relative to non-stored discs 0.4-0.55, (F) \log_{10} of ACAN fold change relative to non-stored discs 0.40-0.6 (G) \log_{10} of COL1A1 fold change relative to non-stored discs -0.35 to -0.25 (H) Design space for the process space under investigation. White areas represent combinations of temperature and oxygen which would meet the set specifications (B-G). Design space shown in H is given by overlapping colored areas B-G. Each point within the white area in H will meet all specifications. A point can be selected within the design space to test the robustness of the system (I).....p.137

Fig. 4.1 Multifactorial space under investigation for hMSCs. Four storage conditions were defined by combining two levels (high and low) for the two factors: temperature and oxygen.....p.142

Fig. 4.2 Storage experiments schematic. hMSCs from three healthy donors were seeded in T25 flasks and exposed to different combinations of temperature and oxygen for 5 days (Table 4.1). Stored hMSCs were then differentiated towards chondrogenic (A), osteogenic (B) and adipogenic (C) lineages. Non stored hMSCs were also differentiated towards the three lineages on the day the storage period started (day 0) and used as control. Spent medium was also analysed for glucose, lactate, glutamine and NH_3 concentrations. For osteogenic (B) and adipogenic (C) lineages hMSCs were also seeded, stored and differentiated in 24 well plates.....p.145

Fig. 4.3 Post-storage glucose concentrations (g/l) in spent medium for hMSCs seeded and stored in T25 flasks. hMSCs were isolated from three healthy donors and exposed to storage conditions listed in Table 4.1. Dashed line represents initial glucose concentration (i.g.c.)(1 g/l). Each measurement requires 1 ml of spent medium. Values are plotted as mean and standard error of the mean (n=3) for three technical replicates. For each storage condition, donors average represents the mean value of glucose concentration post storage for the three donors. (37 C= 37°C, O2= pO₂, oxygen tension, D5= day 5).....p.157

Fig. 4.4 Post-storage lactate concentrations (g/l) in spent medium for hMSCs seeded and stored in T25 flasks. hMSCs were isolated from three healthy donors and exposed to storage conditions listed in Table 4.1. Each measurement requires 1 ml of spent medium. Values are plotted as mean and standard error of the mean (n=3) for three technical replicates. For each storage condition, donors average represents the mean value of lactate concentration post storage for the three donors. (37 C= 37°C, O2= pO₂, oxygen tension, D5= day 5).....p.158

Fig. 4.5 Post-storage glutamine concentrations (mM) in spent medium for hMSCs seeded and stored in T25 flasks. hMSCs were isolated from three healthy donors and exposed to storage conditions listed in Table 4.1. Dashed line represents initial glutamine concentration (i.g.c.) (3.1 mM). Each measurement requires 1 ml of spent medium. Values are plotted as mean and standard error of the mean (n=3) for three technical replicates. For each storage condition, donors average represents the mean value of glucose concentration post storage for the three donors. (37 C= 37°C, O2= pO₂, oxygen tension, D5= day 5).....p.159

Fig. 4.6 Post-storage NH_3 concentrations (mM) in spent medium for hMSCs seeded and stored in T25 flasks. hMSCs were isolated from three healthy donors and exposed to storage conditions listed in Table 4.1. Each measurement requires 1 ml of spent medium. Values are plotted as mean and standard error of the mean (n=3) for three technical replicates. For each storage condition, donors average represents the mean value of glucose concentration post storage for the three donors. (37 C= 37°C, O2= pO₂, oxygen tension, D5= day 5).....p.161

Fig. 4.7 Fold change in *COL2A1* gene expression in response to storage. hMSCs isolated from three healthy donors and exposed to storage conditions listed in Table 4.1. Fold changes values are relative to non-stored hMSCs (day 0) and are plotted as mean and standard error of the mean for three technical replicates for each donor. The average fold change values for the three healthy donors is also plotted for each storage condition. Data on y-axis are on logarithmic scale (log10). (37 C= 37°C, O2= pO₂, oxygen tension, D5= day 5).....p.163

Fig. 4.8 Fold change in *ACAN* gene expression in response to storage. hMSCs isolated from three healthy donors and exposed to storage conditions listed in Table 4.1. Fold changes values are relative to non-stored hMSCs (day 0) and are plotted as mean and standard error of the mean for three technical replicates for each donor. The average fold change values for the three healthy donors is also plotted for each storage condition. Data on y-axis are on logarithmic scale (log10). (37 C= 37°C, O2= pO₂, oxygen tension, D5= day 5).....p.164

Fig. 4.9 Fold change in *COL1A1* gene expression in response to storage. hMSCs isolated from three healthy donors and exposed to storage conditions listed in Table 4.1. Fold changes values are relative to non-stored hMSCs (day 0) and are plotted as mean and standard error of the mean for three technical replicates for each donor. The average fold change values for the three healthy donors is also plotted for each storage condition. Data on y-axis are on logarithmic scale (log10). (37 C= 37°C, O2= pO₂, oxygen tension, D5= day 5).....p.165

Fig. 4.10 Post storage GAGs accumulations in micropellets. hMSCs isolated from three healthy donors and exposed to storage conditions listed in Table 4.1. Fold changes values are relative to non-stored hMSCs (day 0) and are plotted as mean and standard error of the mean for three technical replicates for each donor. The average fold change values for the three healthy donors is also plotted for each storage condition. Data on y-axis are on logarithmic scale (log10). (37 C= 37°C, O2= pO₂, oxygen tension, D5= day 5).....p.166

Fig. 4.11 Fold change in *RUNX2* gene expression in response to storage. hMSCs isolated from three healthy donors and exposed to storage conditions listed in Table 4.1. Fold changes values are relative to non-stored hMSCs (day 0) and are plotted as mean and standard error of the mean for three technical replicates for each donor. The average fold change values for the three healthy donors is also plotted for each storage condition. Data on y-axis are on logarithmic scale (log10). (37 C= 37°C, O2= pO₂, oxygen tension, D5= day 5).....p.168

Fig. 4.12 Fold change in *ALPL* gene expression in response to storage. hMSCs isolated from three healthy donors and exposed to storage conditions listed in Table 4.1. Fold changes values are relative to non-stored hMSCs (day 0) and are plotted as mean and standard error of the mean for three technical replicates for each donor. The average fold change values for the three healthy donors are also plotted for each storage condition. Data on y-axis are on logarithmic scale (log10). (37 C= 37°C, O2= pO₂, oxygen tension, D5= day 5).....p.169

Fig. 4.13 Post storage ALP activity of hMSCs differentiated into osteogenic lineage. The ALP activity was measured with the pNPP assay and expressed relative to the ALP activity of differentiated non-stored hMSCs (day 0). hMSCs for one representative donor were used for

this experiments. Data are expressed as mean and standard error of the mean for three biological replicates. (37 C= 37°C, O2= pO₂, oxygen tension, D5= day 5).....p.170

Fig. 4.14 ALP staining of differentiated hMSCs following 5 day storage. hMSCs from the donor were differentiated towards osteogenic lineage for 14 days before performing the ALP assay and staining using a Fast blue salt. Representative field of views are shown for all four storage conditions (Table 4.1) in a matrix format (oxygen versus temperature). Representative field of view of differentiated non-stored hMSCs is also shown (top). ALP positively stained cells are shown in purple. (Scale bar = 100 µm).....p.171

Fig. 4.15 Fold change in *PPAR*γ gene expression in response to storage. hMSCs isolated from three healthy donors and exposed to storage conditions listed in Table 4.1. Fold changes values are relative to non-stored hMSCs (day 0) and are plotted as mean and standard error of the mean for three technical replicates for each donor. The average fold change values for the three healthy donors are also plotted for each storage condition. Data on y-axis are on logarithmic scale (log₁₀). (37 C= 37°C, O2= pO₂, oxygen tension, D5= day 5).....p.173

Fig. 4.16 Fold change in *FABP4* gene expression in response to storage. hMSCs isolated from three healthy donors and exposed to storage conditions listed in Table 4.1. Fold changes values are relative to non-stored hMSCs (day 0) and are plotted as mean and standard error of the mean for three technical replicates for each donor. The average fold change values for the three healthy donors are also plotted for each storage condition. Data on y-axis are on logarithmic scale (log₁₀). (37 C= 37°C, O2= pO₂, oxygen tension, D5= day 5).....p.174

Fig. 4.17 AdipoRed staining of adipocytes following 5 day storage. hMSCs from one healthy donor were differentiated towards adipogenic lineage for 14 days before being stained using AdipoRed staining (Lonza). AdipoRed positive cells represent adipocytes (in red) and were visualized by fluorescence microscopy (Zeiss Axio Imager II microscope) (excitation λ=485 nm; emission λ=535 nm). Representative fields of stained adipocytes are shown for all four storage conditions (Table 4.1) in a matrix format (oxygen versus temperature). Representative field of differentiated non-stored hMSCs is also shown (top). (Scale bar = 150 µm).....p.175

Fig. 4.18 Number of adipocytes for differentiated hMSCs following 5 day storage. Adipocytes were stained using the AdipoRed staining (Lonza), visualized by fluorescence microscopy (Zeiss Axio Imager II microscope) (excitation λ=485 nm; emission λ=535 nm) and counted by IMARIS software (BITPLANE, <http://www.bitplane.com/>). For each storage condition, three fields were taken for each of the three culture wells. The number of adipocytes has been calculated as the average of the three culture wells for each storage condition relative to differentiated hMSCs which were not exposed to any storage condition. (37 C= 37°C, O2= pO₂, oxygen tension, D5= day 5). Dashed line represents fold change equal to 1 (no change in number of adipocytes compared to not stored cells.).....p.176

Fig. 5.1 Schematic of an innovative primary container for the storage and transportation of cell and tissue products. The oxygen ‘enriched’ chamber would provide through the membrane the adequate oxygen supply for the effective preservation of viability and biological function of the product.....p.195

Fig. 5.2 Schematic illustration of the main temperature ranges that can be adopted for the transportation of pharmaceutical products.....p.197

List of Tables

Table 1.1 List of selected marketed cell-based medicinal products with their final formulation, shelf-life and storage conditions. PAP-GM-CSF= prostatic acid phosphatase-granulocyte-macrophage-colony-stimulating factor, DMEM=Dulbecco's modified eagles medium.....	p.36
Table 2.1 Chondrogenic medium composition.....	p.52
Table 2.2 Storage conditions. Two levels (low and high) were selected for each of the three parameters under investigation: Temperature, oxygen partial pressure (pO₂) and storage duration. Eight combinations were defined by combining low (-) and high (+) values for the three parameters.....	p.58
Table 2.3 Primers used for quantitative real time PCR.....	p.62
Table 2.4: Reaction mix for TaqMan assays. TFU: TaqMan Fast Universal PCR Master Mix (Applied Biosystems). Primer probe mix contains forward primer, reverse primer and probe.....	p.62
Table 2.5 Brief summary of key findings for the storage of cartilage discs in a controlled environment for 5 and 7 days.....	p.93
Table 3.2 Simulated storage conditions (A and B) for cartilage discs (Case study 1).....	p.104
Table 3.2: Hypothetical list of quality attributes and specifications which need to be satisfied by the cartilage disc following storage.....	p.105
Table 3.3 Centre points response values. CP1 (centre point 1), CP2 (centre point 2). Values are expressed as mean ±SEM for three technical replicates from one healthy donor.....	p.130
Table 4.1. Storage conditions for hMSCs seeded in T25 flasks and 24 well plates. Storage duration was 5 days.....	p.144
Table 4.2 Osteogenic medium.....	p.147
Table 4.3 Adipogenic induction medium.....	p.148
Table 4.4 Adipogenic maintenance medium.....	p.149
Table 4.5 Micropellet digestion solution.....	p.149

Table 4.6 Chondroitin sulphate calibration curve.....p.150

Table 4.7 Osteogenic staining solution.....p.152

Table 4.8 Primers used for quantitative real-time PCR.....p.153

Table 4.8 Input and output variables for the hMSCs storage system. Input and output variables of the full factorial design of experiments are presented.....p.155

Table 4.9 Brief summary of key findings for the storage of hMSCs in a controlled environment for 5 days.....p.177

List of Abbreviations

Adipose tissue (AT)

Bone marrow (BM)

Advanced Therapy Medicinal Products (ATMPs)

Affinity-enhanced T-cell receptor (TCR)

Alkaline phosphatase (ALP)

Chimeric antigen receptor (CAR)

Chinese Hamster Ovary (CHO)

Colony-Forming Unit-Fibroblasts (CFUFs)

Controlled room temperature (CRT)

Design of Experiment (DoE)

Dimethylmethylene blue (DMB)

Dimethyl-sulfoxide (DMSO)

Dulbecco's modified eagles medium (DMEM)

Embryonic stem cell (ESCs)

Ethylenediaminetetraacetic acid (EDTA)

Fetal Bovine Serum (FBS)

Glycosaminoglycan (GAG)

Graft-versus-host-disease (GvHD)

Heat shock proteins (HSP)

Human MSCs (hMSCs)

HypoThermosol (HTS)

Induced Pluripotent stem cells (iPSCs)

Insulin grow factor (IGF-1)

Isobutyl-1- methylxanthine (IBMX)

Least square means (LS-means)

Master cell bank (MCB)

Mesenchymal stromal/stem cells (MSCs)

Multipotent adult progenitor cells (MAPCs)

NN- Dimethylformaldehyde (DMF)

One Factor at a Time (OFAT)

Osteoarthritis (OA)

P-nitrophenol (pNPP)

Quality by Design (QbD)

Reverse transcriptase (RT)

Transforming Growth Factor (TGF)

Umbilical cord blood (UCB)

Chapter 1

Introduction

1.1 Cell therapy industry overview

Historically human cells have only been considered as the microscopic building blocks of the human body and it was not until the late 1950s that Dr. E. Donnall Thomas demonstrated that bone marrow can be used to cure patients dying from blood cancers (Appelbaum, 2007).

The administration of human cells to treat diseases is referred to as cell therapy (Mason, Brindley, Culme-Seymour, & Davie, 2011). Cell therapy has the great potential to target diseases that cannot be targeted with small molecules or biologics. However, their manufacturing is both more expensive and more complex (Salmikangas et al., 2015).

Compared to traditional biologics where cell lines, such as Chinese Hamster Ovary (CHO) and NS0, are used to produce the therapeutic protein that is normally secreted, for cell-based

medicinal products the actual living cell is the product. In Europe, cell-based products in which cells have been either substantially manipulated or are not intended to be used for the same essential function(s) in the recipient and the donor are regulated as medicinal products under the legal framework of Advanced Therapy Medicinal Products (ATMPs)

(http://www.ema.europa.eu/ema/index.jsp?curl=pages/regulation/general/general_content_000296.jsp) . In the US, cell-based products are regulated as biologics

(<http://www.fda.gov/BiologicsBloodVaccines/GuidanceComplianceRegulatoryInformation/Guidances/CellularandGeneTherapy/>). Many governments worldwide have been investing in

translating the last two decades of basic research into commercially viable cell therapy products. Examples are Japan, the US, Canada and, in Europe, the UK, Germany and Spain

(https://www.gov.uk/government/uploads/system/uploads/attachment_data/file/32459/11-1056-taking-stock-of-regenerative-medicine.pdf). Japan enacted a new Regenerative

Medicine Law regulating the development, approval and use of regenerative medicine products in November 2014. Conditional approvals can now be granted based on safety and

efficacy data from Phase II clinical trials, instead of full Phase III programs, and allow for commercial sales for up to seven years. This new approval process will encourage the

development of novel regenerative therapies and will also speed up product approvals

(Konomi, Tobita, Kimura, & Sato, 2015). Big Pharmaceutical companies are also

increasingly interested and investing in developing these new kinds of drugs with a market which is estimated to grow at a rate of roughly 40% from 2015 to 2020.

(<http://www.prnewswire.com/news-releases/stem-cell-therapy-market-growing-at-395-cagr-worldwide-to-2020-276525411.html>) .

1.2 Human cells as active pharmaceutical ingredients

A broad spectrum of cell types with different levels of *ex-vivo* manipulations are currently being evaluated in clinical trials (www.clinicaltrials.gov). These can be divided into two main categories: (1) stem cell-based and (2) non-stem cell-based therapies.

Stem cells pose the unique capacity to self-renew and to differentiate into cells of different lineages under specific stimuli (Ying et al., 2008). For these properties, they have generated great interest for drug screening, human tissue research and cell-based therapies (Ebert & Svendsen, 2010). Depending on their origin, they can be classified into two categories: adult and embryonic. Adult stem cells have limited proliferation and differentiation potential *in vitro* compared to embryonic stem cells (Ramalho-Santos et al., 2002). Embryonic stem cell (ESCs) are capable of differentiating into derivatives of all three germ layers, ectoderm, endoderm and mesoderm while maintaining high proliferation potential (Rippon & Bishop, 2004). This ability makes them an excellent candidate for use as a therapeutic agent as well as for toxicology testing and to investigate genetic disease (Deshmukh et al., 2012). As atherapeutic agent, ESC-based therapies are under development to treat diseases such as diabetes (D'Amour et al., 2006), macular degeneration (Schwartz et al., 2012) and Parkinson's disease (Brederlau et al., 2006). Ethical concerns associated with the use of ESCs along with the risk of teratoma formation *in vivo* and immunogenicity have limited their use for clinical application (M. J. Martin, Muotri, Gage, & Varki, 2005). In 2006, a new type of pluripotent stem cell was announced by Takahashi and Yamanaka (Takahashi & Yamanaka, 2006). Their study revealed the possibility for mouse fibroblast cells to be transfected with lentiviral vectors carrying Oct-4, Sox-2, Klf-4 and c-myc to become pluripotent. These cells are called "Induced Pluripotent stem cells" (iPSCs). This finding were later replicated in human cells (Pei, Xu, Zhuang, Tse, & Esteban, 2010). This new type of cell generated great

interest mainly for drug screening purposes. They have been tested on humans but the first clinical trial in Japan was suspended due to genomic issues

(<http://www.nature.com/news/next-generation-stem-cells-cleared-for-human-trial-1.15897>).

The most widely studied type of adult stem cells isolated from human tissue are referred to as mesenchymal stromal/stem cells (MSCs). On the other hand, the most investigated type of non-stem cell for clinical application are T-cells. T-cells can be engineered to overcome the natural protection mechanisms and target tumour cells either via a chimeric antigen receptor (CAR) or by affinity-enhanced T-cell receptor (TCR). The former has proven to be more effective for haematological malignancies as it can target antigen on the cell surface. The latter has the potential to target intracellular antigens and this makes it, potentially, a more suitable candidate for treating solid tumour (Fedorov, Sadelain, & Kloss, 2014).

1.3 Human mesenchymal/stromal stem cells

MSCs were isolated for the first time in the mid-1960s from rat bone marrow by Friedenstein and colleagues (Friedenstein et al. 1966). Since then, the presence of MSCs has been documented in many human specialized tissues and organs where they normally reside as rare and quiescent populations (Conget & Minguell, 1999).

Human MSCs (hMSCs) show many interesting properties that make them a good candidate for therapeutic applications, such as the ability to self-renew and to differentiate into mesodermal lineages (cartilage, bone, fat and muscle) (Nombela-Arrieta, Ritz, & Silberstein,

2011) (Fig.1.1). Their ability to trans-differentiate into cells of all three germ layers (mesodermal, endodermal and ectodermal) has also been demonstrated (Sasaki et al., 2008).

Bone marrow is one of the most common sources of hMSCs, where they are involved in tissue homeostasis and in the turnover of skeletal cell types (Bruder, Fink, & Caplan, 1994). The yield of hMSCs that can be isolated from bone marrow is, however, very low, ranging from 0.01 to 0.001 % of all cells (Panchalingam, Jung, Rosenberg, & Behie, 2015). Adipose tissue is, on the other hand, a more abundant source of hMSCs (Keung, Nelson, & Conrad, 2013).

Other sources include umbilical cord blood (H.-S. Wang et al., 2004), amniotic fluid (Sessarego et al., 2008), placenta (Makhoul, Chiu, & Cecere, 2013), synovium (Arufe, De la Fuente, Fuentes, de Toro, & Blanco, 2010) and peripheral blood (Kassis et al., 2006).

Compared to bone marrow, adipose tissue and umbilical cord blood can be isolated without a highly invasive procedure (Zhang et al., 2011).

However, hMSCs from different tissues show some differences in their differentiation potential and properties. Kern et al. compared hMSCs from umbilical cord blood (UCB), adipose tissue (AT) and bone marrow (BM) and found that UCB-MSCs show no adipogenic potential, unlike BM- and AT-MSCs (Kern, Eichler, Stoeve, Klüter, & Bieback, 2006). On the other hand, UCB-MSCs showed the highest proliferation capacity and therefore they are a source that facilitates high cell yields that might be necessary for therapeutic applications on a large scale (Simaria et al., 2014).

Currently, the methods used to characterize these cells are based on the International Society of Cellular Therapy guidelines (Dominici, 2006). According to these, the minimal criteria for hMSC characterization are the following: (a) MSCs must be plastic-adherent when

maintained in standard culture conditions and develop Colony-Forming Unit-Fibroblasts (CFUFs) (b) MSCs must express CD105, CD73 and CD90 and lack expression of CD45, CD34, CD14 or CD11b, CD79 α or CD19 and HLA-DR surface molecules and; (c) MSCs must also demonstrate tri-lineage differentiation into osteocytes, adipocytes and chondrocytes *in vitro* (Dominici et al., 2006).

However, there is considerable evidence showing that such marker-based classification is not sufficient to distinctively define the cellular composition for a MSC-based product (Mendicino, Bailey, Wonnacott, Puri, & Bauer, 2014).

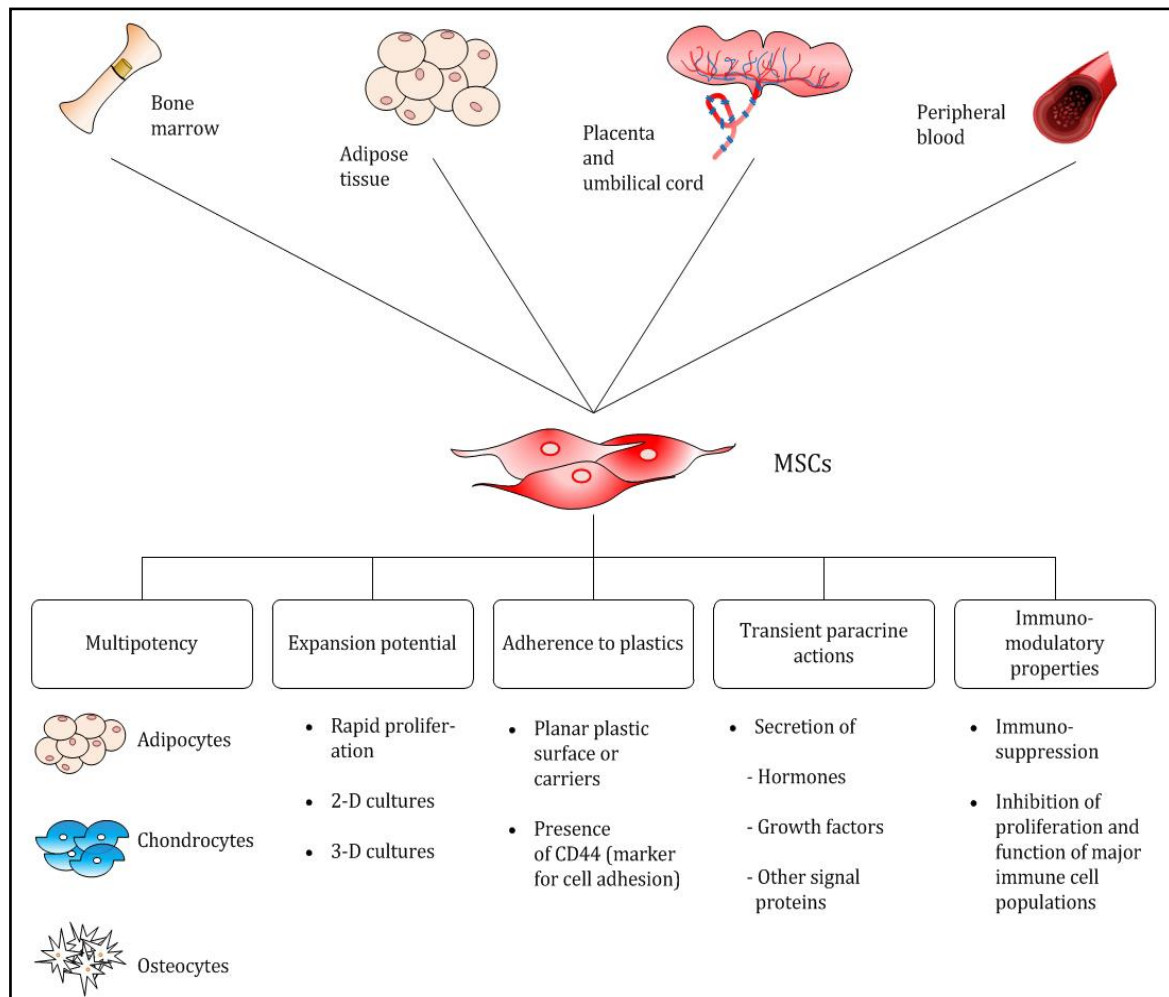


Fig.1.1 Schematic summarizing the main sources and properties of mesenchymal stem cells (modified from (Eberli et al., 2014)).

Clinical use of hMSC

The most commonly investigated source of hMSCs for clinical applications are bone marrow, adipose tissue and umbilical cord (clinicaltrials.gov).

hMSCs have the potential to home to and engraft at sites of injury where they can stimulate endogenous differentiation of resident cells towards tissue regeneration (Chamberlain, Fox, Ashton, & Middleton, 2007), or secrete a wide spectrum of bioactive molecules, such as cytokines, that will exert the therapeutic effect (Kinnaird et al., 2004). This second mechanism was also suggested by clinical trials where hMSCs lack long term homing and differentiation into the target tissue but showed that inflammation was reduced in disease models like myocardial infarction (Lee et al., 2009).

hMSCs can be administered either intravenously (IV) or directly implanted into the site. The former mechanism relies on the ability of the hMSCs to migrate across the endothelium and home to injured tissues in a manner similar to migration of leukocytes to sites of inflammation (Chamberlain et al., 2007). The latter is, however, preferred when there is a need to reduce the risk of cell migration to other sites in the body (Barbash et al., 2003).

Numerous pre-clinical and clinical studies are investigating the use of hMSC to induce bone regeneration, when the natural ability of bone to self-repair has been compromised by trauma or disease (X. Wang et al., 2013).

In addition to bone regeneration, hMSCs are also being used to target cartilage regeneration, which, unlike bone, has a very limited self-healing capacity (Steinert, Rackwitz, Gilbert, Noth, & Tuan, 2012). In most cases, hMSCs are used in combination with hydrogels that can be directly injected into the joint (Spiller, Maher, & Lowman, 2011).

hMSCs have also shown promising signs of clinical efficacy for cardiac regeneration (Mathiasen et al., 2015), (Bartunek et al., 2016).

Other applications include treatments for graft-versus-host-disease (GvHD) (Munneke et al., 2015) and Crohn's disease (Panés et al., 2016), (Carlsson, Schwarcz, Korsgren, & Le Blanc, 2015). Currently (August 2016) there are over 600 clinical trials using hMSCs for a wide range of disease (clinicaltrial.gov, results for "mesenchymal stem cells").

1.4 Manufacturing and delivery of cell based medicinal products

Despite the fact that cell therapy manufacturing shares some similarities with other biopharmaceuticals (such as monoclonal antibodies or vaccines), the use of human cells as therapeutic agents poses some challenges (Martin, Simmons, & Williams, 2014). Cell based therapies can be also divided into two broad groups: autologous (where the product is derived from the patient's own cell) and allogeneic (where the product is derived from one universal donor).

The differences between autologous and allogeneic products translate into two different manufacturing models. For autologous cell therapy products, the biopsy isolated from the patient needs to be processed and the cell expanded to a sufficient number to generate adequate patient doses and to allow quality tests. One batch of product will be used for one patient and to increase the number of batches produced in a given time, more culture devices can be run in parallel (Hourd, Ginty, Chandra, & Williams, 2014). In order to reduce the risk of cross-contamination, without having to dedicate one process room to processing one product for one patient, fully closed, automated and disposable processing systems should be used (Trainor, Pietak, & Smith, 2014). Allogeneic cell therapy manufacturing, on the other hand, is more similar to traditional biopharmaceutical manufacturing and production scale-up has been demonstrated (Heathman et al., 2015). The output is increased by increasing the volume of the

bioreactor, or the surface available for the cells to attach and grow so that more cells can be processed for each batch (Ma, Tsai, & Liu, 2016). Due to economy of scale, the latter is usually more cost-effective (Simaria et al., 2014). The need to scale up the production will increase along the clinical development of the product, as the cell therapy product approaches phase III and then the commercial stage, the demand will also increase. The difference in the whole bioprocessing of autologous and allogeneic products can be directly linked to the difference between these two types of therapies. Autologous cell therapies are patient specific and they carry a lower risk of immune reaction. On the other hand, they require two procedures (one for the biopsy harvest and the other for the administration of the therapy) and they are not suitable for emergency procedures as normally it takes two to three weeks after the biopsy for the cell product to be ready for implantation. The limited amount of “raw material” makes product, process and release tests development very difficult and expensive. Logistics is also more complicated due to the risk of mishandling or damage during transportation of both the biopsy from the hospital to the manufacturing site and the product back to the hospital. As one batch corresponds to one patient, autologous products can be also characterized by high batch to batch variability. Quality control assays have to be performed for every batch and, therefore, every patient dose. This will increase the costs of the therapy. Automation of some of the manufacturing steps is feasible but it can only be successfully achieved by adoption of a fully closed disposable system which enables parallel processing of multiple batches simultaneously, without the risk of cross-contamination (Trainor et al., 2014). Allogeneic cell-based therapies, on the other hand, are more similar to the traditional biopharma model where an “off-the-shelf” product is delivered to the hospital. Cells extracted from one universal donor are expanded and many patient doses are made from each donor. It is usually easier to develop robust, high quality manufacturing procedures for allogeneic products. There is also no need for painful harvesting procedures for the patient as the necessary cells are derived from one

universal donor. Historically, allogeneic cell therapies have been accompanied by the administration of immune suppressant drugs. However, the use of hMSCs, which show very low level of immunogenicity, negates the need for life-threatening immune-suppressant (Consentius, Reinke, & Volk, 2015).

Figure 1.2 compares the autologous and allogeneic bioprocessing of cell therapy. For allogeneic products, a “master cell bank” (MCB) needs to be developed from one universal donor and quality tested. From one lot of MCB, a “working cell bank” can be expanded and from this come all patient doses (Brandenberger et al., 2011).

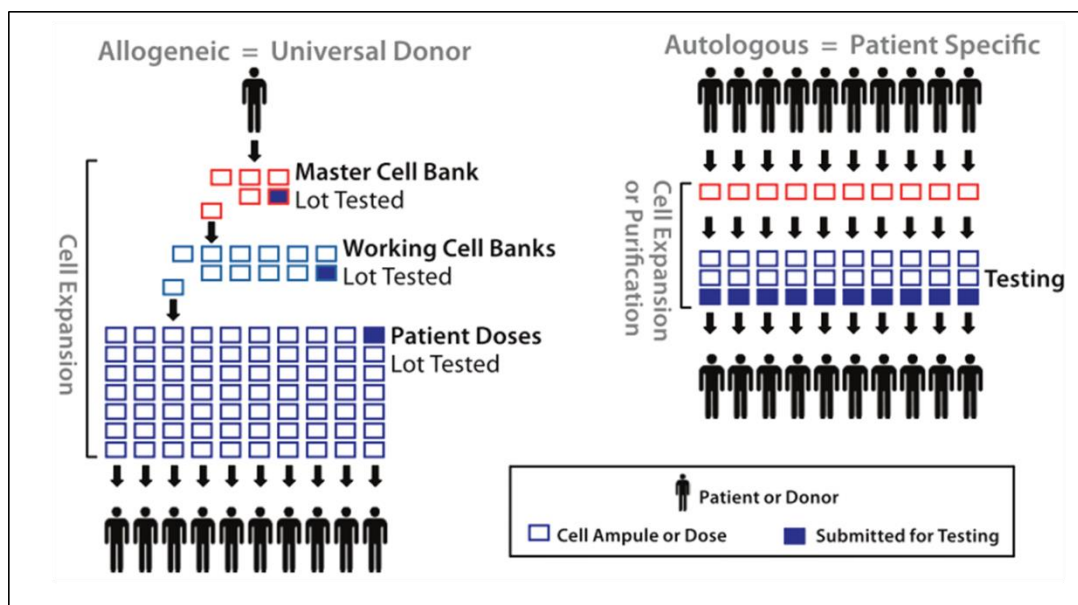


Fig. 1.2 Allogeneic versus autologous manufacturing models. Autologous products are patient specific; one batch will correspond to one patient. Starting from a biopsy isolated from the patients, cells will need to be processed to generate the number of doses required for that treatment and to allow quality testing. For allogeneic products, cells from one universal donor are isolated, validated and generate a master cell bank. This is further expanded into a working cell bank. When a production lot is required, patient doses will be generated from the working cell bank and will be used to treat multiple patients (modified from (Brandenberger et al., 2011)).

For both types of products, the biological function of the cells needs to be preserved across the entire supply chain. A validated potency assay should be in place to confirm that a product of consistent quality is manufactured and it is also necessary to establish the shelf-life of the product (C. A. Bravery et al., 2013).

1.5 Preservation methods for cell based medicinal products

The preservation of the viability and biological function of a cell-based product, also referred to as bio-preservation (Baust & Baust, 2007), is imperative for the delivery to the patients. This encompasses storage for transportation of the products from the manufacturing site to the clinic as well as storage for quality testing necessary for product release (Coopman & Medcalf, 2014). Autologous products are characterized by a circular distribution system as the “raw” materials are harvested from the patient, processed and then administered back to the same patient. Allogeneic products tend to have a more linear distribution system as doses are expanded from a donor and are then available for patients. Given their nature, allogeneic products normally require a longer shelf-life compared to autologous products; the former need to be used off-the-shelf while the latter are produced on demand for a specific patient. However, the need to treat a patient multiple times with the same batch of cells along with an increased flexibility in terms of scheduling of the treatment lead to a longer shelf life being preferable also for autologous product (Rayment & Williams, 2010) . Table 1.1 lists a number of marketed cell therapy products with their preservation method.

Table 3.1 List of selected marketed cell-based medicinal products with their final formulation, shelf-life and storage conditions. PAP-GM-CSF= prostatic acid phosphatase-granulocyte–macrophage-colony-stimulating factor, DMEM=Dulbecco’s modified eagles medium

Product	Company	Active ingredient	Final Formulation	Shelf life and storage conditions	Reference
Provenge® (Sipuleucel-T)	Dendreon	$\geq 50 \times 10^6$ autologous CD54 ⁺ cells/250 mL activated with PAP-GM-CSF	Lactated Ringer's solution (NaCl, NaC ₃ H ₅ O ₃ , KCl, CaCl ₂). Dispersion for infusion	18 hours at 2 °C-8°C	http://www.fda.gov/downloads/biologicsbloodvaccines/cellulargenetherapyproducts/approvedproducts/ucm214565.pdf
ChondroCelect®	Tigenix	4x10 ⁶ autologous human cartilage cells/ 0.4 ml	DMEM	48 hours at 15°C-25°C	http://www.ema.europa.eu/docs/en_GB/document_library/EPAR_-_Public_assessment_report/human/000878/WC500026035.pdf
MACI®	Vericel	0.5 x10 ⁶ -1x10 ⁶ autologous cultured chondrocytes/ cm ² porcine derived Type I/III collagen membrane	DMEM, HEPES adjusted for pH with HCl or NaOH and osmality with NaCl.	6 days at $\leq 37^\circ\text{C}$	http://www.ema.europa.eu/docs/en_GB/document_library/EPAR_-_Public_assessment_report/human/0

					02522/WC500145888.pdf
Carticel	Vericel	12 x 10 ⁶ chondrocytes	0.4 ml Buffered cell culture media (DMEM)	Viability up to 72 hours when vial is kept in secondary packaging at room temperature	http://www.fda.gov/downloads/BiologicsBloodVaccines/CellularGeneTherapyProducts/ApprovedProducts/UCM109339.pdf
Apligraf	Organogenesis	human fibroblasts (dermal cells) and human keratinocytes (epidermal cells)	supplied as a circular disk approximately 75 mm in diameter and 0.75 mm thick in agarose nutrient medium which contains agarose, L-glutamine, hydrocortisone, human recombinant insulin, ethanolamine, O-phosphorylethanolamine, adenine, selenious acid, DMEM powder, HAM's F-12 powder, sodium bicarbonate, calcium chloride, and water for injection	15 days from the packaging date, when stored within the closed shipper/storage box at a controlled room temperature 20°C - 23°C until use	http://www.apligraf.com/professionals/pdf/Apligraf_Storage_FAQs.pdf

Prochymal	Mesoblast	Liquid containing 100×10^6 hMSCs per 15 mL. The diluted product contains 2.5×10^6 hMSCs per mL	10% Dimethyl sulphoxide (DMSO) , 5% human serum albumin (HSA) in Plasma-Lyte A. Intravenous infusion	24-month shelf-life stored in liquid nitrogen (LN ₂) vapor phase temperature ($\leq -135^\circ\text{C}$)	http://www.sc.gc.ca/dhp-mps/prodpharma/sbd-smd/drug-med/sbd_smd_2012_prochymal_150026-eng.php
Holoclar	Chiesi Farmaceutici	300,000 to 1,200,000 viable <i>ex-vivo</i> expanded autologous human corneal epithelial cells including on average 3.5% (0.4% to 10%) limbal stem cells	physiological transport medium (containing DMEM), supplemented with L-glutamine	36 hours transport stable temperature (15°C - 25°C)	http://www.ema.europa.eu/docs/en_GB/document_library/EPAR_-_Public_assessment_report/human/002450/WC500183405.pdf
Dermagraft	Organogenesis	Human fibroblast-derived dermal substitute	Cryopreserved. Saline based cryoprotectant that contains 10% DMSO and bovine serum	Up to 6 months when stored at -80°C	http://www.dermagraft.com/quality/

Body temperature and hypothermic storage

Human cells are often preserved by lowering the temperature from 37 °C (body temperature) to 15°C-25 °C (controlled room temperature) and 2°C-8 °C (refrigerated)(Coopman & Medcalf, 2014). Evidence regarding the efficacy of storage and shipping at body temperature is limited and this range is not very widely adopted given the rather limited shelf life of the product when kept at 37 °C. Hypothermic preservation is widely used in surgical procedures, such as heart by-pass (Baos et al., 2015). By lowering the temperature, cell metabolism and cycle progression is slowed and cells are effectively ‘paused’(Robinson, Picken, & Coopman, 2014). This technique has been applied also to red blood cells and peripheral blood products that are often stored at 4 °C for 24-48 hours prior to infusion (Acker, 2013). However, cell injury post-hypothermia storage has also been documented (Corwin, Baust, Baust, & Van Buskirk, 2014). A number of studies have also investigated the production of heat shock proteins (HSP), which act as chaperon proteins to prevent cold-induced denaturation (Mahmood S Choudhery, Badowski, Muise, & Harris, 2015). In order to limit cell damage during hypothermic storage, and often extend the shelf life of the product, new formulations have been developed, such as intracellular-like HypoThermosol (HTS) (Mathew, Baust, Van Buskirk, & Baust, 2004). Another formulation is based on the encapsulation of the cells in alginate for storage at controlled room temperature and it has been successfully applied for adipose derived hMSCs (Swioklo, Constantinescu, & Connon, 2016).

Cryopreservation

The standard method for long-term stabilisation of biological cells is freezing at ultra-low temperatures (typically using liquid nitrogen). The process is known as cryopreservation and is a technique based on lowering the temperature in order to inhibit cellular metabolic and biochemical reactions (Baust & Baust, 2007). These are normally slowed down at -80 °C and completely halted at temperatures below -150 °C (which requires LN₂), which are normally used for long-term cell banking.

In order to prevent cell damage due to ice crystal formation during the cooling phase, the addition of cryoprotectants is required (Massie et al., 2014). The most commonly used cryoprotectants are dimethyl-sulfoxide (DMSO) and glycerol (Pogozhykh, Prokopyuk, Pogozhykh, & Mueller, 2015). However, these normally need to be removed prior to administration to the patient (Hunt, 2011).

While viability recovery post-cryopreservation has been documented for many cell types (Van Campenhout, Swinnen, Klykens, Devos, & Verhoef, 2014), evidence suggests that a number of cell types might not fully recover their biological function (Galipeau, 2013).

Lyophilisation

Another method to preserve the stability of the cells during storage is lyophilisation (dehydration), which is extensively used for protein-based drugs (Frokjaer & Otzen, 2005). For human cells, this method has so far been adopted for a very limited number of cell types, such as hematopoietic stem cells (Buchanan, Pyatt, & Carpenter, 2010) and red blood cells

(Han et al., 2005). Buchanan et al. demonstrated that hematopoietic stem cells could be lyophilized with the addition of a stabilizing sugar, trehalose, and preserved at 25 °C for 4 weeks and that they maintained their clonogenic and differentiation properties (Buchanan et al., 2010).

1.6 Statistical Design of Experiment (DoE) for cell therapy development

The concept of Quality by Design (QbD) was introduced by the International Conference on Harmonisation of Technical Requirements for Registration of Pharmaceuticals for human use and provides a modular and “systematic approach to product development that begins with predefined objectives and emphasizes product knowledge, process understanding and process control, based on sound science and quality risk management”

(<http://www.ich.org/products/guidelines/quality/article/quality-guidelines.html>).

The basic principle of QbD is that quality should be built in the products by design and only tested post manufacturing to confirm the pre-desired product attributes. Over the past decade, QbD programs have been developed mostly for small molecules but also for some biotechnology products, such as monoclonal antibodies and vaccines (Rathore & Winkle, 2009; Wurth et al., 2016). The adoption of the QbD framework for cell and gene based medicinal products has also been proposed (Lipsitz, Timmins, & Zandstra, 2016), although the complexity of these products limits its application and its successful implementation still needs to be demonstrated.

Statistical Design of Experiment (DoE) was developed and first used in the early 1920s by Sir Ronald Fisher (Montgomery, 2012) and is one of the key tools in the QbD framework.

While the common “One Factor at a Time” (OFAT) approach assumes a lack of statistical interaction of variables on the process response, DoE uses multivariate design to investigate multiple parameters in parallel experimental runs.

For many bioprocess systems it is common for variables to be interdependent and produce statistically and practically significant interactions. In practical terms, this means the response to a change in one factor level is often dependent on the level of one or two of the other variables. These effects will not be detected by OFAT experiments.

DoE is therefore an efficient way to identify a number of statistically significant main and interacting factor effects on one or more selected responses. It can also be used to determine input parameter ranges that maximize or minimize a selected response variable, whereas OFAT often leads to sub-optimal values (Lim et al., 2007).

The main advantages of DoE over the OFAT approach can therefore be summarized as follows:

1. It requires less resources (experiments, time, material, etc) for the amount of information obtained. This will reduce costs as experiments can be very expensive and time consuming.
2. The estimates of the effects of each factor are more precise. Using more observations to estimate an effect results in higher precision (reduced variability). For example, for full and fractional factorial designs, all the observations are used to estimate the effect of each factor and each interaction (property of hidden replication), while typically only two of the observations in a OFAT experiment are used to estimate the effect of each factor.
3. The interaction between factors can be estimated systematically. Interactions are not estimable from OFAT experiments.

4. There is experimental information in a larger region of the factor space. This improves the prediction of the response in the factor space by reducing the variability of the estimates of the response in the factor space, and makes process optimization more efficient because the optimal solution is searched for over the entire factor space.

1.7 Scope and aim of research

The development of successful bio-preservation strategies will play a key role in the supply chain of cell-based medicinal products (Salmikangas et al., 2015)(Coopman & Medcalf, 2014). Today, these products tend to be transported via solutions borrowed from biotech products, such as vaccines that are shipped at 2-8 °C, or cryopreserved. There is, however, increasing evidence that cryopreservation might alter the efficacy of the cell-based drug, as suggested by Galipeau et al.(2013) following the failure of a Phase III clinical trial of Prochymal for steroid-resistant GvHD to meet its primary clinical endpoint.

The limited, or lack of, knowledge of how cells will respond to chemical, mechanical and physical stimuli hinder the development of cost-effective standards for storage and transportation of these products.

The more complex nature of these ‘living’ drugs and the need to cope with large scale distribution supports a deeper investigation of the parameters that will ultimately affect the safety and efficacy of the product. As happened for protein-based drugs, which are sensitive to high temperature, shear, oxidative stress and pH changes (Frokjaer & Otzen, 2005), enhanced knowledge of the factors influencing the stability of the cell-based drug could pave the way to the development of innovative primary and secondary containers for the cost effective storage and transport of this new class of medicinal product.

hMSCs are currently considered one of the most promising 'living' pharmaceutical ingredients, given their broad therapeutic potential and limited risk of immune rejection (Consentius et al., 2015).

There is evidence that oxygen tension modulates the proliferation and differentiation potential of MSCs, although conflicting results can be found in the literature (Grayson, Zhao, Bunnell, & Ma, 2007a)(Holzwarth et al., 2010)(Wang, Fermor, Gimble, Awad, & Guilak, 2005). The effect of oxygen, however, has never been studied in combination with temperature.

A DoE based approach can be used as an investigation method to maximize the amount of information generated from experimental data and it is particularly useful for bioprocess systems as it is likely that process parameters interact (Montgomery, 2012). Moreover, DoE based models can be built and used as decision support tools, as previously shown in a number of industries (Montgomery, 2012). This would contribute to the development of the cell therapy product, in particular for autologous product, given the limited amount of 'raw materials' normally available for research and testing (Hourd et al., 2014).

The aims of this research project are the following:

- Investigate the combined effect of temperature, oxygen and storage duration for cartilage discs derived from hMSCs
- Investigate the combined effect of temperature and oxygen on undifferentiated hMSCs
- Demonstrate that statistical DoE can be successfully used as an investigational tool in cell therapy process development

- Develop predictive models that can be used in combination as a decision support tool for the development of robust storage and transportation solutions

1.8 Thesis overview

The subsequent thesis chapters are structured as follows:

Chapter 2: Describes the investigation of the storage properties of cartilage discs following a shelf-life of 5 and 7 days. Eight storage conditions were simulated by combining two levels (high and low) for each of the three factors (temperature, oxygen and storage duration) according to a 2^3 full factorial design. Viability, metabolite concentrations in the spent medium and chondrogenic markers were evaluated as response variables.

Chapter 3: Results described in Chapter 2 are further analysed using a system approach in order to highlight the effect of input parameters (temperature, oxygen and storage duration) on the response variables. The validity of the DoE based predictive models was assessed. Two case studies are also included, showcasing how the predictive models can be used as a decision support tool in the development of a storage and transportation solution for a cell therapy product.

Chapter 4: Describes the investigation of storage properties for undifferentiated hMSCs. Four storage conditions were simulated by combining two levels (high and low) for each of the two factors (temperature and oxygen) according to a 2^2 full factorial design. Metabolite

concentrations in the spent medium and the three differentiation lineages characteristic of hMSCs were evaluated as response models.

Chapter 5: Summarizes results, outlines challenges and provides suggestions for future work.

Chapter 2

Investigating storage properties of scaffold free bone marrow derived cartilage discs

Introduction

Cell therapies have the potential to treat a variety of unmet clinical needs (Kefalas, 2015; Trounson & DeWitt, 2016). Compared to traditional pharmaceutical products, cell based medicinal products are more complex and product characterization as well as manufacturing is very challenging (Kirouac & Zandstra, 2008; Salmikangas et al., 2015). In order to reach their full clinical potential, these cell-based medicinal products need to be delivered to the hospital preserving their biological properties. Storage and transportation to clinical site can be considered as the last manufacturing steps and they normally rely on passive containers which are designed to maintain and monitor the temperature within a set range during shipment (PDA technical report). As described in chapter 1, current storage and

transportation methods include controlled room temperature (CRT), hypothermic storage (2-8 °C) and cryopreservation (-80 °C, -196 °C). When cells are not cryopreserved and they are stored at CRT or hypothermic temperature, they will continue to metabolize glucose and glutamine to produce energy (Rafalski, Mancini, & Brunet, 2012). Waste products of these metabolic processes are lactate and ammonia (NH₃). These have known detrimental effects on biological properties of human mesenchymal stem cells (hMSCs) (Schop et al., 2009). To date, the effort of minimizing lactate and ammonia release has been focused on hMSCs growth and is normally achieved by media replenishment. While this is standard practice in a laboratory or production environment, it is not normally possible during storage and shipment of the product. It is, therefore, important to minimize the build-up of lactate and ammonia in the preservation medium containing the cell therapy product. Historically, temperature has been considered an important parameter which, if lowered, can reduce cellular metabolism (Reissis, Garcia-Gareta, Korda, Blunn, & Hua, 2013).

In this study, oxygen tension has also been considered and in combination with temperature and storage length. The hypothesis is that oxygen can also modulate viability as well as waste product release, which will affect the biological properties of the product. Apart from viability, preservation of the biological function of the cell therapy product is important to prove safety and efficacy of the medicinal product (Bravery et al., 2013; Martin et al., 2014).

A potential cell therapy product for cartilage regeneration has been selected to test different combinations of temperature, oxygen and storage duration as shown in Fig.1.

Hyaline articular cartilage is a specialized tissue which is characterized by low cell density, high matrix content, lack of vascularization and very limited repair capacity. Once damaged, progressive degradation can lead to disease such as osteoarthritis (OA) causing low-level inflammation and severe pain. Cell based therapies have been developed over the past

decades and are based on transplantation of *ex-vivo* expanded autologous chondrocytes harvested from a non-load bearing region of the same joint. The inability to expand a sufficient number of chondrocytes retaining their functional properties, limited clinical efficacy and high costs have led to investigations into alternatives. hMSCs, from bone marrow and adipose tissue, can differentiate into chondrocyte-like cells (Boeuf & Richter, 2010; Dabiri, Heiner, & Falanga, 2013) and could potentially be used to regenerate damaged articular cartilage. If proven clinically successful, MSC-based therapies could also limit the need for total joint replacement (arthroplasty).

Many cell culture methods have been developed to differentiate hMSCs towards chondrogenesis, such as: monolayer culture, pellet culture, micromass culture and seeding on a biomaterial based scaffold (Djouad et al., 2007; Im, Jung, & Tae, 2006; Mackay et al., 1998). It has been shown that transwell culture is the most efficient method to drive MSCs along the chondrogenic lineage since its cartilage-like matrix synthesis and deposition is greater than other established methods (Murdoch et al., 2007). Although cultured in static conditions, cells seeded on transwell inserts have access to nutrients and growth factors from above and below the permeable insert, which facilitates their chondrogenic differentiation into cartilage discs. In this study, it was assumed that the mechanism of action for this product would be engraftment and regeneration of cartilage. Ideally, an engineered tissue for cartilage regeneration should have high expression of the *COL2A1* and *ACAN* genes, which encode for collagen type II $\alpha 1$ and aggrecan respectively, while the expression of fibroblast genes such as *COL1A1*, which encodes for collagen type I $\alpha 1$, should be minimal (Chen, Duan, Zhu, Xiong, & Wang, 2014). The expression of these three genes is used as part of the potency assay to confirm the predicted biological function of ChondroCelect, a market-approved cell therapy product for cartilage regeneration (Bravery et al., 2013).

Gene expression was therefore considered a potential potency assay, linked to the biological property of the tissue.

Four tissue culture incubators were used to reproduce the storage conditions as shown in Fig. 2.1 and to investigate the storage properties of the scaffold free bone marrow derived cartilage discs. This method is preferred to a passive container based simulation given the inability of the latter to control both temperature and oxygen within the selected ranges. For temperature, the 26-37 °C range was selected for study. Although currently not very common, this temperature range is closer to physiological conditions and, if proven successful, could contribute to the preservation of the biological function. Oxygen tension range was selected to be between 20 % (ambient) and 3 %, which is the range of oxygen tension (estimated to be between 1 and 6 %) experienced by articular cartilage in the deep zone (Gibson, Milner, White, Fairfax, & Wilkins, 2008). As most commercially available cell based products do not have a shelf life longer than 6 days when stored in hypothermic conditions (Swioklo et al. 2016), 7 days was chosen as the storage length limit.

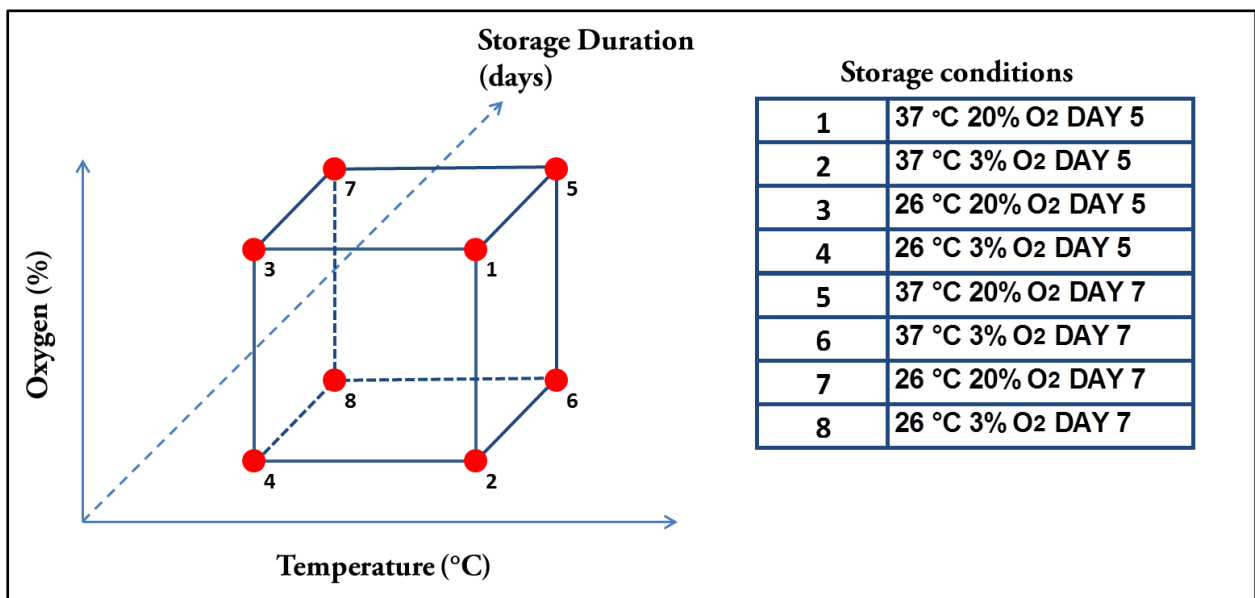


Figure 2.2 Multifactorial space under investigation. Eight storage conditions were defined by combining two levels (high and low) for the three factors: temperature, oxygen and storage duration.

2.1 Materials and methods

2.1.1 Human Bone Marrow derived MSCs culture

Human bone marrow derived MSCs (hMSCs) were isolated from human bone marrow mononuclear cells extracted from the posterior iliac crest of three healthy young Caucasian donors (Lonza Biosciences, Berkshire, UK) by adherence for 24 hours to 75 cm² tissue culture flasks (Corning) and were expanded in monolayer culture with mesenchymal stem cell growth medium (MSCGM BulletKit, Lonza) supplemented with 5 ng/ml fibroblast growth factor-2 (R&D Systems, Abingdon, UK). Cultures were maintained in a humid atmosphere of 5 % CO₂ / 95% air at 37 °C. Once cells reached confluence, they were washed with Ca²⁺ and Mg²⁺ free phosphate buffered saline (PBS, Sigma) and then incubated at 37 C 5% CO₂ with 2 ml Trypsin/EDTA (Sigma) for enzymatic harvesting. Cells were passaged at a split ratio of 1:3. Isolated MSCs were characterized by flow cytometry on a FACScanto II system (Becton Dickinson, Oxford, UK) using a human MSC Phenotyping Kit (Miltenyi Biotec, Bisley, UK) with positive staining for CD73, CD90 , and CD105 and negative staining for CD14, CD20, CD34, and CD45 according to ISCT guidelines (Dominici et al., 2006). Isolated MSCs from one additional healthy donor were also purchased from Lonza Biosciences. Donors details are provided in Appendix I. Experiments were performed using hMSCs between passages 4-5 (P4-P5).

2.1.2 Chondrogenic differentiation of hMSCs using the tranwell method

hMSCs were expanded in 75 cm² tissue culture flasks. Once the cells reached 80 % confluence, they were enzymatically detached by Trypsin/EDTA (Sigma) and centrifuged for 5 minutes at 1200 rpm. Supernatant was removed and the cell pellet was re-suspended in pre-warmed PBS (Sigma). Washed hMSCs were finally re-suspended in chondrogenic medium (Table 2.1).

Table 2.1 Chondrogenic medium composition.

Reagent	Supplier	Function
High Glucose (4.5 g/l) Dulbecco's Modified Eagle Medium (DMEM) with sodium pyruvate	(Lonza 12-614)	Enables cell growth and proliferation. (Z. Yang & Xiong, 2012)
Transforming Growth Factor (TGF) TGF-β_3 (10 ng/ml)	PeproTech, London, UK	Stimulates hMSCs to produce extracellular matrix rich in cartilage specific collagen type II and aggrecan (DeLise, Fischer, & Tuan, 2000)
Dexamethasone (100 nM)	Sigma-Aldrich, Poole, UK	Enhances chondrogenesis of MSCs induced by TGF- β_3 (Shintani & Hunziker, 2011)
Ascorbic acid -2-phosphate (50 μg/ml)	Sigma-Aldrich, Poole, UK	Stimulates secretion of collagen and glycosaminoglycan (Eslaminejad, Fani, & Shahhoseini, 2013)
Proline (40 μg/ml)	Sigma-Aldrich, Poole, UK	Essential amino acid which supports cells proliferation (Li, Sattler, & Pitot, 1995)
100X Insulin-Transferrin-Selenium (ITS+L) premix	ITS+L; BD Biosciences, Oxford, UK	ITS contains insulin, human transferrin and selenous acid. They stimulate cell proliferation under serum-reduced or serum free conditions (Kisiday, Kurz, DiMicco, & Grodzinsky, 2005)
L-Glutamine	Sigma-Aldrich, Poole, UK	Essential amino acid required for cell growth (Z. Yang & Xiong, 2012).
Penicillin/streptomycin (100 U/ml penicillin; 100 μg/ml streptomycin mix)	Sigma-Aldrich, Poole, UK	Used in culture media to mitigate risk of bacterial and fungal infections.

Four x 10⁵ hMSCs in 100 μ l chondrogenic medium were seeded onto a 6.5 mm diameter, 0.4 μ m pore size polycarbonate transwell insert (Merck Millipore, Watford, UK) and centrifuged in a 24-well plate (200g, 5 minutes). Five hundred μ l of chondrogenic medium were added to the lower well as described by Tew et al. (Tew, Murdoch, Rauchenberg, & Hardingham, 2008). The chondrogenic medium was replaced every 3 days up to 14 days. The consistency

of this chondrogenic differentiation protocol has been previously demonstrated by Murdoch et al. (Murdoch et al., 2007). However, it has been confirmed internally to ensure a consistent baseline of chondrogenic markers in the construct before performing storage experiments. This construct is referred to as scaffold-free bone marrow derived cartilage disc, henceforth cartilage disc.

2.1.3 Alamar blue assay for scaffold-free bone marrow derived cartilage disc

Metabolic assays such as Alamar blue, MTT (3-(4,5-dimethylthiazol-2-yl)-2,5-diphenyl tetrazolium bromide), MTS (3-(4,5-dimethylthiazol-2-yl)-5-(3-carboxymethoxyphenyl)-2-(4-sulfonyl)-2H-tetrazolium) and water-soluble tetrazolium salt (WST-1) (4-(3-(4-Iodophenyl)-2-(4-nitrophenyl)2H-5-tetrazolio)-1,3-benzene disulfonate) are commonly used to indirectly measure the viability of cells. MTT values have been found to closely correlate those from Alamar blue (Ng, Leong, & Hutmacher, 2005). The Alamar blue assay (ThermoFisher Scientific) was used to indirectly measure viability of cartilage discs. The assay is based on a redox reagent (resazurin) that fluoresces in response to the chemical reductions which occur during cellular metabolism and therefore provides an indirect measure of viable cell number (Rampersad, 2012). Resazurin is taken up by the cells where it is reduced to resorufin and then secreted into the medium, which results in a visible colour change from blue to pink and a fluorescent signal that can be measured (Back, Khan, Gan, Rosenberg, & Volpe, 1999). The assay can detect as few as 50 cells (ThermoFisher; <https://www.thermofisher.com/uk/en/home/references/protocols/cell-and-tissue-analysis/cell-proliferation-assay-protocols/cell-viability-with-Alamarblue.html>). Given the considerable overlap of the absorbance spectra for oxidised and reduced forms of the reagent,

fluorescence measurements are preferred (Back et al., 1999). The assay was performed according to the manufacturer's instructions. However, it has been validated to confirm its robustness for use with the cartilage discs. To this end, four scaffold-free bone marrow derived cartilage discs were prepared as described in 3.1.2. These were cut into 4 quarters using a scalpel blade and 3 quarters were used for the Alamar blue assay (Fig. 2.2). Samples were placed in a 96-well plate in triplicates before adding 100 μ l of chondrogenic medium and 10 μ l of pre-warmed Alamar blue reagent. Negative controls were included by adding 10 μ l of pre-warmed Alamar blue reagent to 100 μ l of chondrogenic medium not containing cells. A mix of chondrogenic medium and 10 % Alamar blue reagent was autoclaved in order to reduce the resazurin contained in the Alamar blue reagent. This represents the upper limit of resazurin reduction and was used as positive control. The plate was incubated at 37 °C and fluorescence values were measured every hour for 8 hours using a fluorescence spectrophotometer (Perkin Elmer LS50B) (excitation λ =560 nm, emission λ =590 nm). This experiment was also used to confirm the incubation time (4 h) suggested by the manufacturer as this is cell-dependent.

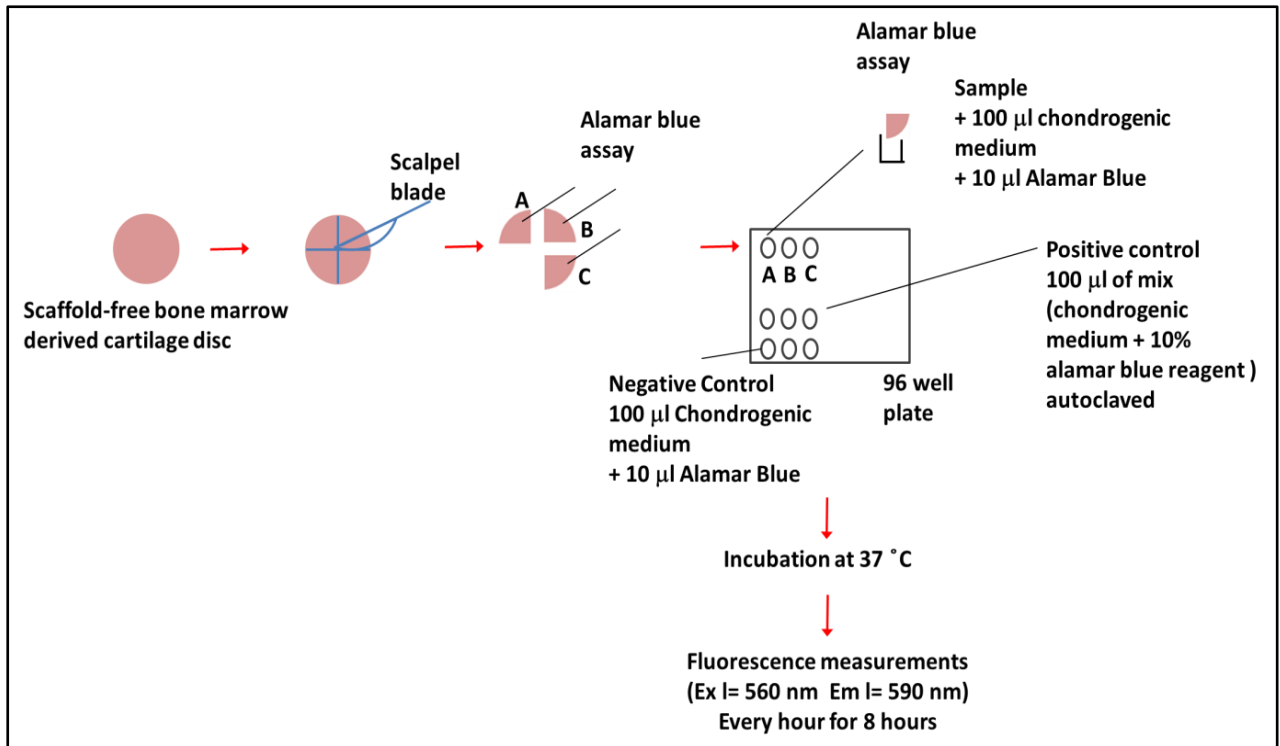


Figure 2.2 Schematic view of the Alamar blue assay cartilage disc. Three technical replicates are sampled by cutting the discs into four quarters with a scalpel blade. Three of the quarters are used for the Alamar blue assay. Each quarter was added to 100 µl chondrogenic medium and 10 µl Alamar blue reagent in a 96 well plate. Negative controls containing no cells were included. A mix of chondrogenic medium + 10% Alamar blue reagent was autoclaved and used as positive control as resazurin contained in the Alamar blue is completely reduced to resorufin. The plate was incubated at 37 °C and Alamar blue fluorescence values were measured every hour for eight hours. (Ex l= excitation wavelength; Em l= emission wavelength)

2.1.4 Quantitative viability indicator

As it was not possible to isolate the cells from the scaffold-free bone marrow derived cartilage disc and create a standard curve for the Alamar blue assay, a quantitative viability indicator was defined as follows:

$$\text{Viability indicator} = \frac{[\text{Alamar blue fluorescence value}]}{\text{DNA (ng)}}$$

Alamar blue fluorescence values were normalized by the amount of DNA contained in the sample, which was measured via the Picogreen Assay (Life Technologies). This assay has higher sensitivity than alternative options (such as Hoechst dyes or propidium iodide) and can detect as little as 25 pg/ml of double strand DNA (dsDNA) (ThermoFisher; <https://www.thermofisher.com/order/catalog/product/P11496>). As Picogreen dye cannot penetrate cell membranes, samples need to be lysed first to ensure that DNA is released. Extra cellular matrix proteins do not interfere with Picogreen fluorescence signals (Dragan et al., 2010). Scaffold-free bone marrow derived cartilage discs were cut into 4 quarters using a scalpel blade; 3 quarters were used for the Alamar blue and Picogreen assay (n=3) while 1 quarter was used for gene expression analysis (Fig 2.3). Samples were placed in a 96-well plate in triplicates before adding 100 µl of chondrogenic medium and 10 µl of pre-warmed Alamar blue reagent. Negative controls were also included by adding 10 µl of pre-warmed Alamar blue reagent to 100 µl of chondrogenic medium not containing cells. Fluorescence values were detected after 4 hours incubation at 37 °C using a fluorescence spectrophotometer (Perkin Elmer LS50B) (excitation λ=560 nm, emission λ=590 nm), according to manufacturer instructions. The incubation time had been verified as described in 3.1.4 to confirm that after 4 hours the fluorescence signal is still in its linear phase and does not reach a plateau. To compensate for phenol red fluorescence, negative controls were subtracted to fluorescence values for each sample. After Alamar blue fluorescence values have been measured, samples were then washed in PBS and transferred to 1.5 ml tubes (Eppendorfs). One ml of 1x Cyquant (ThermoFisher Scientific) lysis buffer was added to each sample before storage at – 80 °C. On the day the Picogreen assay was to be performed,

samples were thawed and homogenized with pestles. Three technical replicates were performed for each DNA sample. For each replicate, 100 μ l of DNA containing sample was added to 100 μ l of Picogreen Reagent (diluted 1:200). A standard curve was created using λ DNA (2 μ g/ml) provided in the kit. The plate was then covered with foil and incubated for 5 minutes at room temperature before reading fluorescence values using a spectrophotometer (excitation λ =480 nm, emission λ =520 nm). DNA amount per sample was calculated using the λ DNA standard curve.

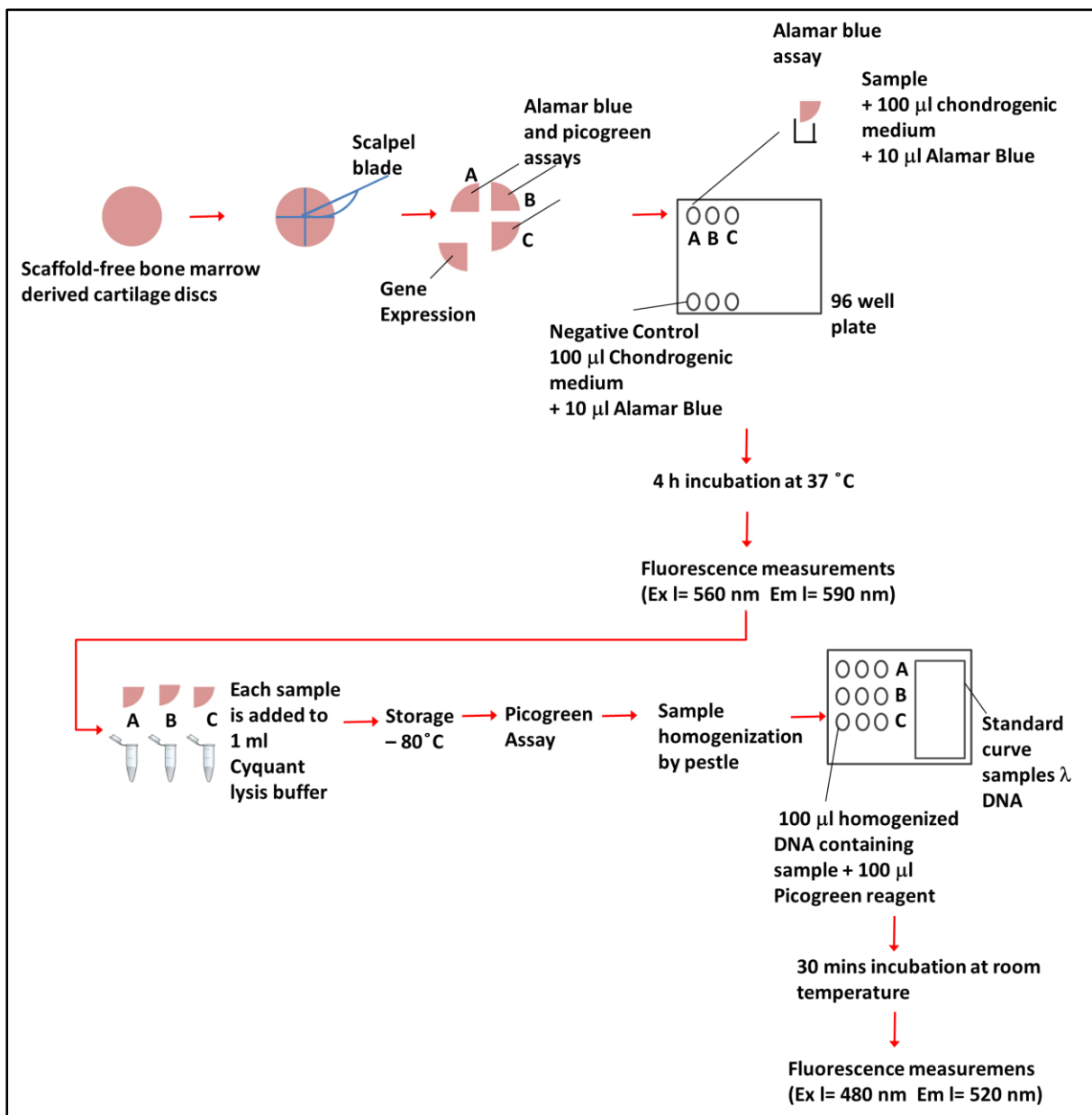


Figure 2.3. Schematic view of the quantitative viability indicator assay for scaffold-free bone

marrow derived cartilage discs. The assay is based on Alamar blue and Picogreen assays performed on the same sample. Each disc was cut into four quarters; three were used for Alamar blue and Picogreen assays and one was used for gene expression analysis. For each disc, three technical replicates were available (samples A, B, and C). Alamar blue fluorescence values were measured for each sample (Ex λ =560 nm, Em λ = 590 nm). For each sample, the amount of DNA was then quantified by Picogreen assay. Alamar blue fluorescence values were normalized by the amount of DNA per each sample. The resulting values were defined as viability indicator. (Ex λ = excitation wavelength; Em λ = emission wavelength).

2.1.5 Storage of cartilage discs

Nine scaffold-free bone marrow derived cartilage discs were prepared as described in 3.1.2. The storage experiment started on the day these discs were available (Fig.2.4). Each disc was transferred to a new 24-well plate in its transwell insert. Fresh chondrogenic medium (2.4 ml) was added to each disc before the storage period. Plates were then placed in tissue culture incubators according to the storage conditions shown in Table 2.2. One disc was used as control (storage start-day 0). After storage, discs were harvested, washed in pre-warmed PBS and spent medium aspirated for further analysis as described in 3.1.6. For each disc, the total amount of DNA contained in the three quarters of the disc used for the quantitative viability indicator (2.1.4) was used to identify potential significant differences in the cell number between different discs used for the storage experiment. The experiment was performed for three healthy donors.

Table 2.2 Storage conditions. Two levels (low and high) were selected for each of the three parameters under investigation: Temperature, oxygen partial pressure (pO₂) and storage

duration. Eight combinations were defined by combining low (-) and high (+) values for the three parameters.

Run #	Pattern	Temperature (°C)	pO2 (%)	Storage duration (days)
1	++-	37	20	5
2	+--	37	3	5
3	-+-	26	20	5
4	---	26	3	5
5	+++	37	20	7
6	+++	37	3	7
7	-++	26	20	7
8	--+	26	3	7

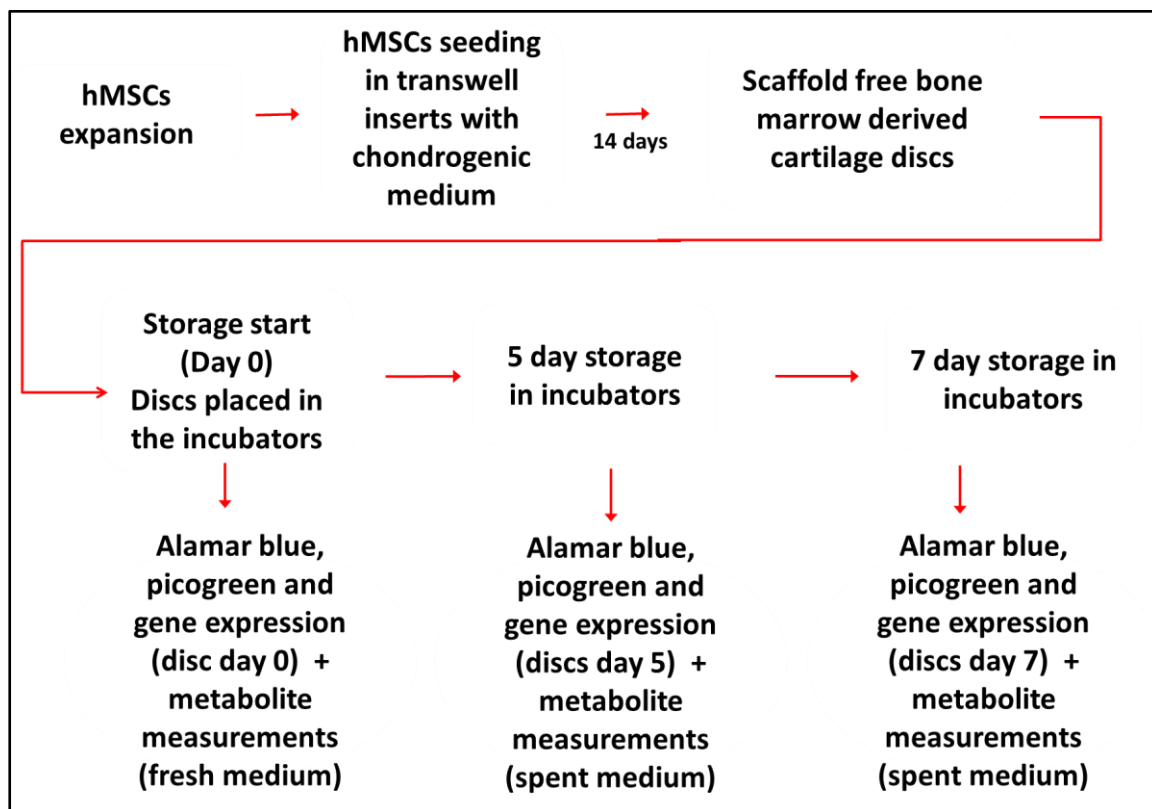


Figure 2.4 Schematic view of the storage experiment of scaffold-free bone marrow derived cartilage discs.

2.1.6 Spent medium analysis

To quantify the metabolite concentration of scaffold free bone marrow derived discs after storage, spent medium was aseptically removed from the wells after the storage period and stored at -80 °C in 1.5 ml tubes (Eppendorfs). Fresh medium samples were also included as control. Stored samples were thawed and run on the Bioprofile FLEX bioanalyzer (Nova Biomedical) for measurement of glucose [g/l], lactate [g/l], glutamine [mM] and ammonium [mM]. The bioanalyzer consists of biosensors which, once in contact with glucose, lactate, glutamine and ammonium, will convert the concentration into an electrical signal. The machine is automatically calibrated every hour. For each storage condition and each disc, only 2 ml of spent medium were available. As each measurement requires 1 ml of spent medium, only two technical repeats were possible for each storage condition.

2.1.7 Extraction of total RNA

RNA was extracted using the Trizol/chloroform method. Molecular grinding resin (G-Biosciences, St. Louis, USA) was added to each tube containing the samples, which were re-suspended in 250 µl Trizol (LifeTechnologies, USA). The samples were homogenized with pestles and incubated at room temperature for 5 minutes. Phase separation was achieved by addition of 50 µl of chloroform (Fisher Scientific), vigorous shaking of the tubes, incubation at room temperature for 2 minutes and centrifugation at 4 °C at 13000 rpm for 15 minutes. The aqueous phase was transferred to a fresh 1.5 ml tube and mixed with 125 µl of

isopropanol (LifeTechnologies, USA) to precipitate the RNA. The tubes were then vortexed, incubated at room temperature for 10 minutes and centrifuged at 4 °C at 13000 rpm for 10 minutes. The RNA pellets in each tube were washed in a 250 µl solution of 75 % ethanol-25 % DEPC-treated water (Invitrogen). The tubes were centrifuged at 4 °C at 13000 rpm for 5 minutes. The ethanol was discarded and the pellets left to air dry for 10 minutes before being re-suspended in 30 µl of DEPC-treated water. The RNA was quantified using a Nanodrop 1000 spectrophotometer and the RNA samples were stored at – 80 °C.

2.1.8 Gene Expression analysis

2.1.8.1 cDNA synthesis

cDNA was synthesised from 1 µg of RNA. RNase-free pipettes and tubes were used throughout to ensure that the RNA did not degrade. To remove genomic DNA (gDNA) contamination, 4 µl of 250 ng/µl RNA was incubated at 37 °C for 30 minutes with 1 µl of Turbo DNase (2 units; Ambion), 1 µl of DNase buffer (10X; Ambion) and 4 µl of DEPC-treated water (Invitrogen). DNase was inactivated by adding 1.8 ml of 100mM Ethylenediaminetetraacetic acid (EDTA; Sigma-Aldrich, Poole, UK) and then incubating at 75 °C for 10 minutes. The DNase treated RNA was incubated with 1µl random primers (50 ng/µl), 1µl of 10mM dNTP mix, 2 µl DEPC water for 5 mins at 65°C (all from Invitrogen). Reaction tubes containing RNA samples were then placed on ice for 1 minute. A reaction mix of 4 ml of 5X RT Buffer , 4 µl of 25mM MgCl₂ (Applied Biosystems, ABI, Life Technologies), 2 µl of 10mM DTT and 1 µl RNaseOUT inhibitor (Invitrogen) was added to each tube and reactions were incubated at 25 °C for 1 minute. SuperScript II RT enzyme (200 U/µl; Invitrogen) was diluted four times using DEPC water and 1 µl (50 U) of this was

added to the reaction and mixed by pipetting. The reverse transcriptase (RT) reaction was carried out by incubating at 25 °C for 10 minutes, 42 °C for 50 minutes and 70 °C for 15 minutes. cDNA samples were then stored at -20 °C.

2.1.8.2 Quantitative real-time PCR

Taqman assays used primers and probes commercially available (IDT, Glasgow, UK) to analyse gene expression changes in a panel of selected genes (Table 2.3). Two and a half microliters of 1:20 diluted cDNA were added to 7.5 µl of assay master mix in wells of a MicroAmpr fast optical 96 well reaction plate (ABI, Life Technologies). The components of the master mix are shown in Table 2.4. Three technical repeats were performed for each sample. Quantitative real time PCR was performed using an ABI PRISM 7900HT Sequence Detection System, setting the following cycle conditions: 40 cycles of 95 °C for 15 seconds and 60 °C for 20 seconds. The gene expression was analysed using the comparative cycle threshold (Ct) method using SDS 2.3 software (Applied Biosystems). For each gene, Ct values were calculated using the delta Ct method and relative to the average of the housekeeping genes *18S*, *HPRT1* and *GAPDH* ($2^{-(Ct \text{ test gene} - Ct \text{ mean of housekeepers})}$).

Table 2.3 Primers used for quantitative real time PCR

Gene	Primer type	Sequence (5'-3')
<i>GAPDH</i>	Forward	ACATCGCTCAGACACCATG
	Reverse	TGTAGTTGAGGTCAATGAAGGG
	Probe	AAGGTCGGAGTCAACGGATTGGTC
<i>HPRT1</i>	Forward	TGCTGAGGATTGGAAAGGG
	Reverse	ACAGAGGGCTACAATGTGATG
	Probe	AGGACTGAACGTCTTGCTCGAGATG
<i>18s</i>	Forward	CGAATGGCTCATTAAATCAGTTATGG
	Reverse	TATTAGCTCTAGAATTACCACAGTTATCC
	Probe	TCCTTTGGTCGCTCGCTCCTCTCCC
<i>COL2A1</i>	Forward	ACCTTCATGGCGTCCAAG
	Reverse	AACCAGATTGAGAGCATCCG

	Probe	AGACCTGAAACTCTGCCACCCTG
<i>ACAN</i>	Forward	TGTGGGACTGAAGTTCTTGG
	Reverse	AGCGAGTTGTCATGGTCTG
	Probe	CTGGGTTTTTCGTGACTCTGAGGGT
<i>COL1A1</i>	Forward	CCCCTGGAAAGAATGGAGATG
	Reverse	TCCAAACCACTGAAACCTCTG
	Probe	TTCCGGGCA ATCCTCGAGCA

Table 2.4: Reaction mix for TaqMan assays. TFU: TaqMan Fast Universal PCR Master Mix (Applied Biosystems). Primer probe mix contains forward primer, reverse primer and probe.

Master mix for 18S	Master mix for <i>HPRT1</i>, <i>GAPDH</i>, <i>COL2A1</i>, <i>ACAN</i>, <i>COL1A1</i>
TFU 5 µl Forward primer 0.2 µl Reverse primer 0.2 µl Probe 0.4 µl Water 2 µl	TFU 5 µl Primer probe mix 1 µl Water 1.5 µl

2.1.9 Statistical analysis

As raw data were affected by donor to donor variability, different storage conditions were compared using the least-squares means (LS-means) method (Montgomery, 2012). LS-means were estimated from raw data for each response variable (Viability indicator, glucose, lactate, glutamine, ammonia, *COL2A1*, *ACAN*, *COL1A1*) using JMP SAS software (http://www.jmp.com/en_us/home.html). This method compensates for donor to donor variability by considering all storage conditions as part of three sets of data: donor #1, donor #2, donor #3 (Montgomery, 2012). Statistical significance was assessed by graphically comparing confidence intervals (95%) of the different storage conditions listed in Table 2.2. Non-overlapping confidence intervals indicate statistically different storage conditions. This identifies sets of storage conditions which are consistently different across all three donors. It also allows identification of overall statistical difference between the three donors.

2.2 Results

2.2.1 Alamar blue assay for cartilage discs

Murdoch et al. (Murdoch et al. 2007) demonstrated that hMSCs, when cultured in transwell insert with TGF- β_3 and dexamethasone, will proliferate mainly in the first 7 days and will then form a cartilage matrix that stains strongly and uniformly with Safranin O, which stains glycosaminoglycans (Kiviranta, Jurvelin, Säämänen, & Helminen, 1985). Compared to the well-established pellet culture protocols, it was possible to obtain uniform cartilage discs 20-fold bigger in wet mass with the same amount of cells and identical chondrogenic medium. They also showed increased collagen II and aggrecan expression.

In this study hMSCs were differentiated via the transwell insert method in the presence of chondrogenic medium (Fig. 2.5) and formed cartilage discs. These were used as a cell

therapy model for storage experiments. In order to measure the viability of the discs following storage experiments, the Alamar blue assay was preliminarily tested on four discs. Results are shown in Fig. 2.6.

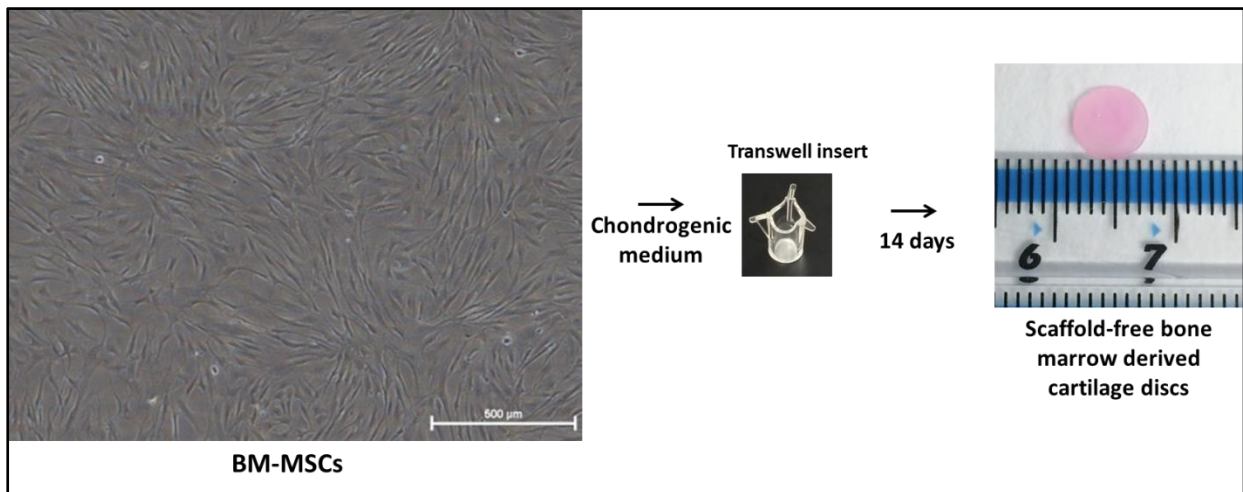


Figure 2.5 Chondrogenic differentiation of hMSCs into cartilage discs. Cells were cultured for 14 days in a transwell with chondrogenic medium (Table 1) forming a 7 mm diameter disc which has been used as cell therapy product model for subsequent experiments. Scale bar= 500 µm).

Alamar blue fluorescence values consistently increased for all 4 discs over 8 hour incubation time and between the negative control and positive control values. These results also confirm that after 4 h incubation (as per manufacturer's instruction), the Alamar blue curve is still in its linear phase and has not reached its plateau. A 4 hour incubation can therefore be used to measure the viability via the Alamar blue assay for this specific cell therapy product. For each time point, Alamar blue fluorescence values for the four discs did not show a significant spread between discs demonstrating the reproducibility of this assay.

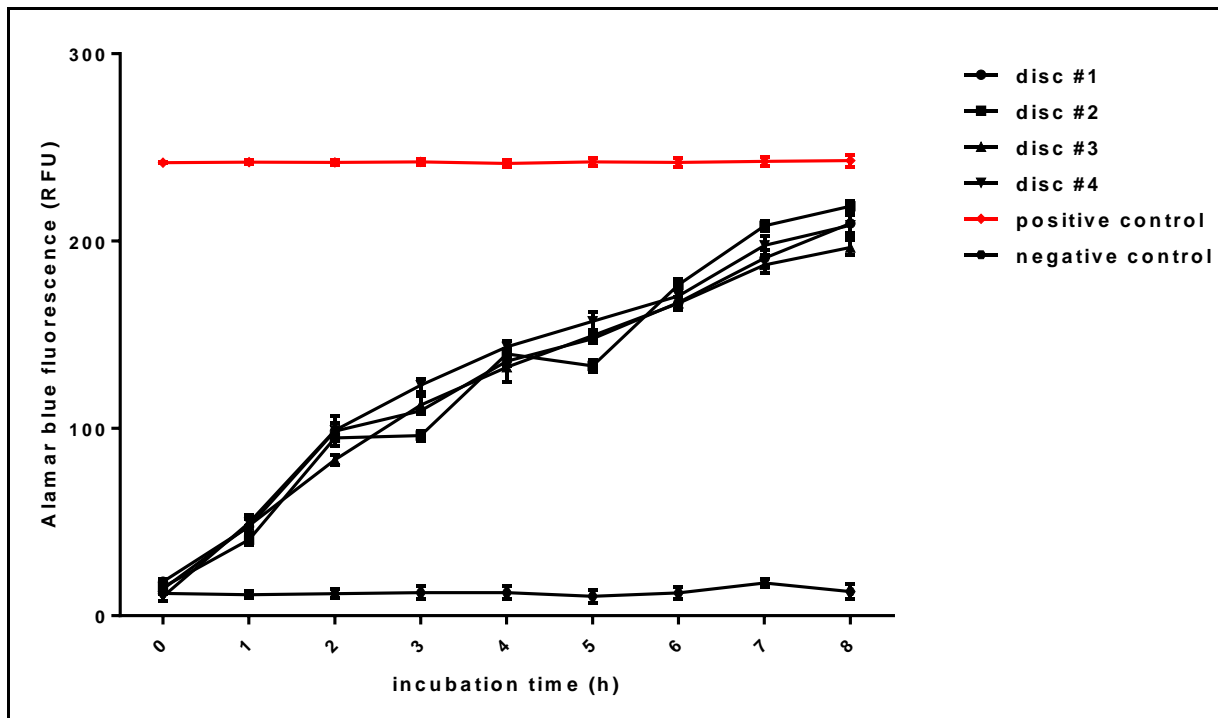


Fig 2.6 Alamar blue fluorescence (Relative fluorescence units, RFU) of four cartilage discs during 8 h incubation at 37 °C. Each disc was prepared as described in 3.1.2 using hMSCs isolated from 1 healthy donor. For each time point, results are represented as mean \pm standard deviation for three technical replicates. These were sampled by cutting each disc into four quarters and using three for the Alamar blue assay. Negative control samples were included (chondrogenic medium plus Alamar blue reagent only). Positive control was created by preliminary autoclaving chondrogenic medium and Alamar blue reagent. Resazurin contained in the Alamar blue reagent is reduced and changes color from blue to pink.

2.2.2 Post storage viability of scaffold-free bone marrow derived cartilage discs

In order to investigate the stability of the cell product post storage, eight scaffold-free bone marrow derived cartilage discs were prepared.

Discs were stored in 4 tissue culture incubators simulating 8 different storage conditions (Table 2.2). Discs were then characterized in terms of viability, spent medium metabolites and gene expression (Fig 2.4). The experiment was undertaken for the three healthy young Caucasian donors.

The Alamar blue and Picogreen assay were used to indirectly measure cell viability of the cartilage discs after storage, as described in 3.1.4. Viability indicator values relative to day 0 (storage start) for each storage condition and for the three healthy donors are shown in Fig. 2.7. For all three donors, storage at 26 °C led to a better viability than storage at 37 °C after both 5 and 7 days. After 5 days at 26 °C, viability is even higher than at day 0 (storage start) for both oxygen levels (20 % and 3 %). This could be due to the proliferation of cells over 5 day storage. A similar trend can be seen after 7 day storage. For all storage conditions, viability decreased at day 7 reaching the lowest value (57.7%) at 37 °C and 20% O₂ for donor #2. Oxygen tension did not have a large effect on modulating viability post-storage, although differences in viability indicator can be noticed for donor #3 both at day 5 and day 7 when stored at 26 °C.

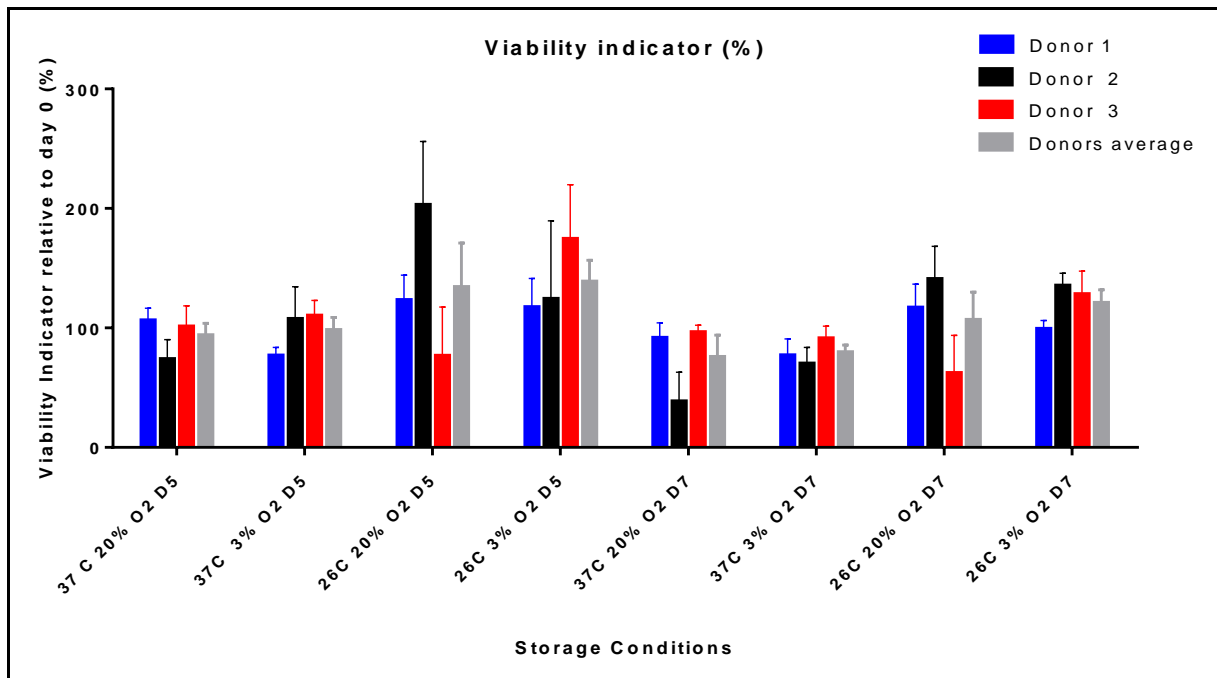


Figure 2.7 Post-storage viability indicator of cartilage discs measured via Alamar blue and Picogreen assays. Discs were prepared using bone marrow derived hMSCs isolated from three healthy donors. Discs were exposed to storage conditions listed in Table 2.2. For each disc, Alamar blue fluorescence was measured by cutting the disc into four quarters (three quarters were used for Alamar Blue and Picogreen Assay). For each quarter, Alamar blue fluorescence was normalized by the amount of DNA measured via Picogreen assay. This was defined as the viability indicator. Viability indicator values for all storage conditions and all three donors are plotted relative to a disc not exposed to storage conditions (storage start, day 0). Values are plotted as mean and standard error of the mean (n=3). (37 C=37 °C, O₂=pO₂ oxygen tension, D5= day 5, D7= day 7).

Figure 2.8 shows that although the estimated least square means (LS-means) of viability indicator for each storage condition are different between donors, these are not statistically different. It is possible to notice a consistent trend in the viability indicator for all three donors, with lower values corresponding to higher temperature and longer storage period.

Viability following 5 day storage at 26 °C and 3 % O₂ was statistically different across all three donors than viability following 7 day storage at 37 °C and 20 % oxygen and 37 °C and 3 % oxygen.

The amount of DNA per disc was also analysed to detect possible variations that could affect the above mentioned considerations on variability indicators. For each disc, the total amount of DNA was calculated by adding the DNA contained in the three quarters used to normalize the Alamar blue fluorescence values. Fig. 2.9 shows that for all three donors, the total amount of DNA contained in each disc was within an average value and two standard deviations (mean \pm SD, upper control limit and lower control limit).

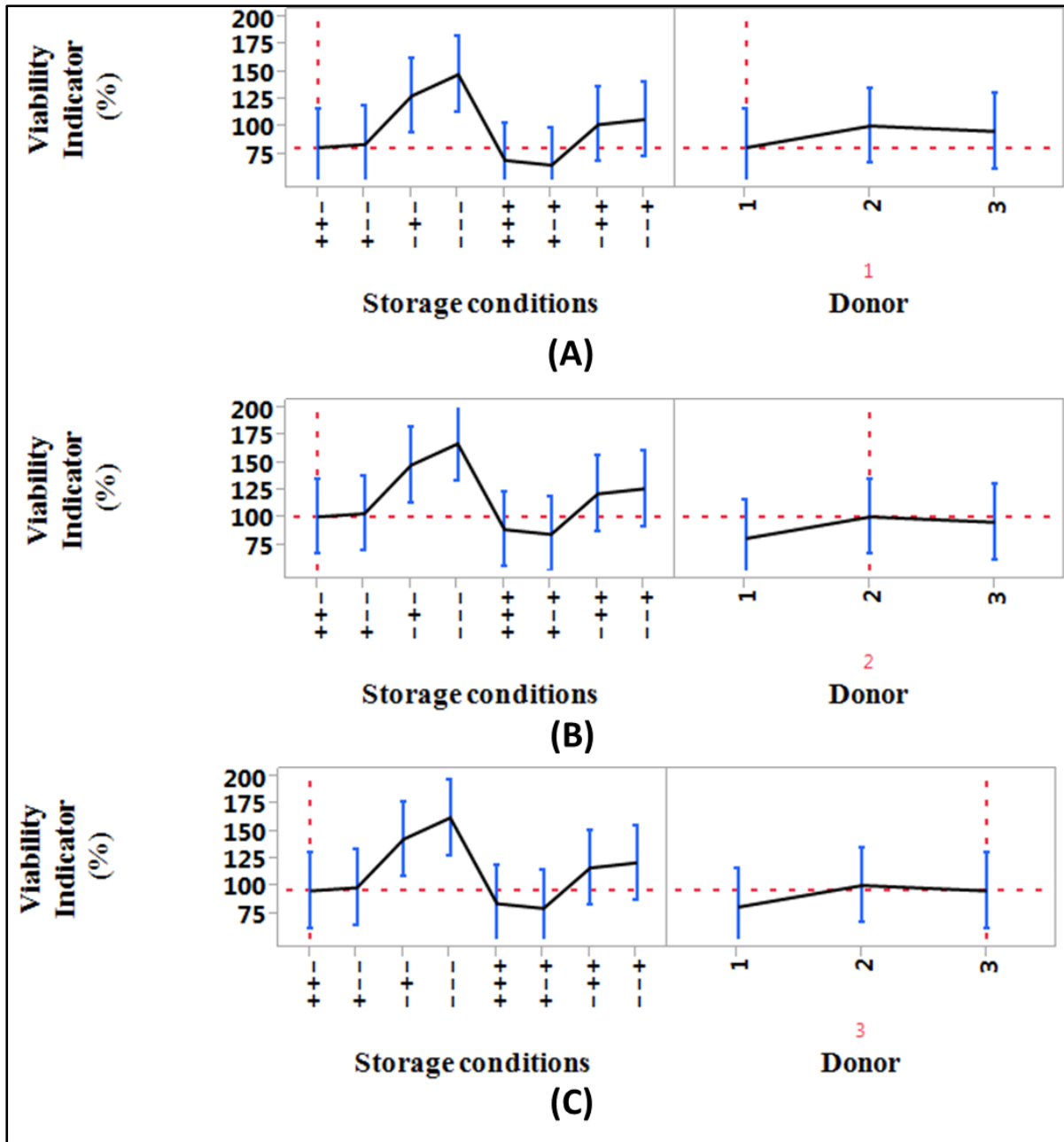
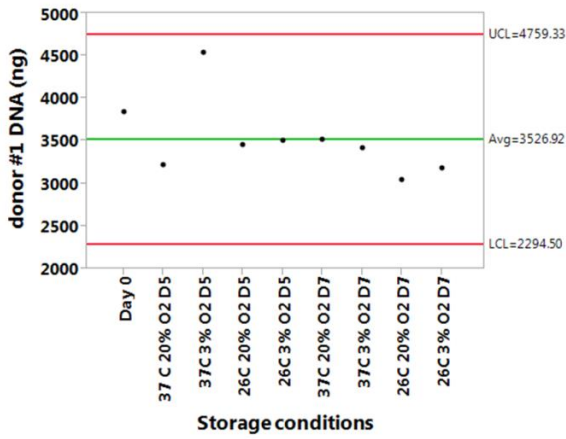
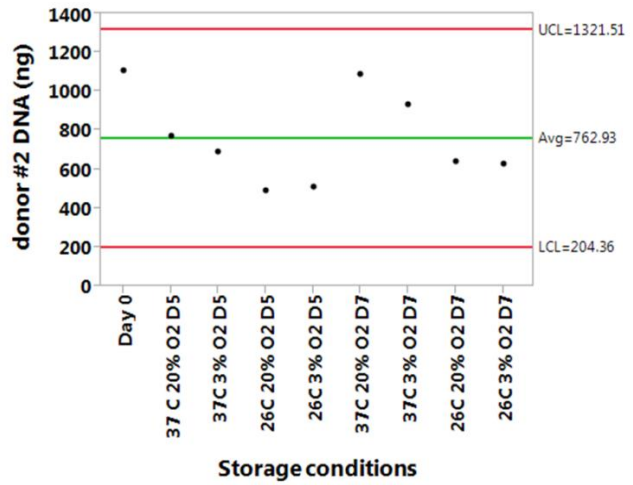


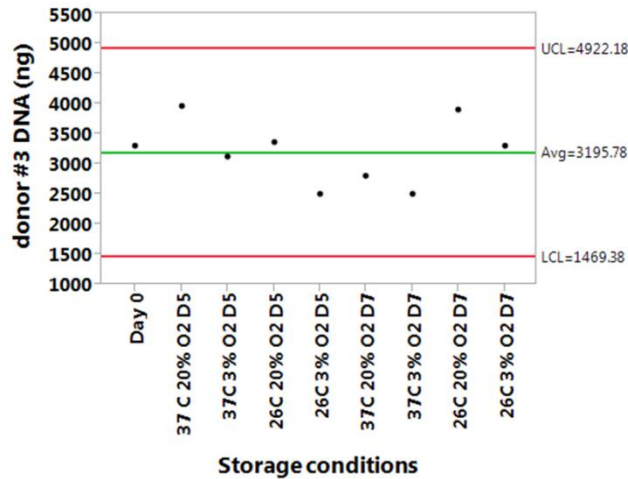
Figure 2.8 Least square means for viability indicator for cartilage discs following storage conditions listed in table 2 for donor 1 (A), 2 (B) and 3(C) respectively. Least square means (LS-means) were estimated using JMP SAS software. Viability indicator raw data used to estimate the LS-means were expressed as % relative to untreated samples which were not exposed to any storage condition. Storage conditions were defined by combining high (+) and low(-) levels of the three parameters under investigation: temperature (37 -26 °C), oxygen (3-20 % O₂) and storage duration (5-7 days). This method allows to compare by compensating for donor to donor variability. Left (A,B,C), least square means for viability indicator (%) for each storage condition. Right (A,B,C), least square means for each donor calculated across all storage conditions. Error bars represent 95% CI. Confidence intervals that do not overlap represent storage conditions which were consistently different across the three donors. Statistically different storage conditions or donors can be identified by non-overlapping CIs.



A



B



C

Figure 2.9 Control charts for total DNA (ng) contained in three quarters of scaffold-free bone marrow derived cartilage disc measured via Picogreen assay. Each control chart (A, B and C) shows the average amount of DNA (Avg) for the three quarters for all discs used in the storage experiment for donor 1, 2 and 3 respectively. For each donor, day 0 corresponds to the disc used as control (storage start). Avg (green line) is the center line. Upper control limit (UCL) and lower control limit (LCL) represent +3 SD and - 3 SD respectively. All points are between the control limits.

It is possible that differences in the amount of DNA are due to variations in cutting the discs into quarters. Moreover, even if hMSCs are likely to distribute evenly on the surface of the transwell insert during seeding, heterogeneity of cell population might result in uneven proliferation within the transwell. This might lead to areas of the disc that are densely populated, explaining the small difference in DNA amount per disc. Discs from donor #2 were visibly thinner than discs from donor #1 and #3 and this is confirmed by the lower average amount of DNA in discs from donor#2 (825.35 ng) compared to donor#1 (3438.57 ng) and donor#3 (3220.43 ng). The reduced matrix formation might be explained by the limited proliferation of the cells in the transwell insert which was detected by measuring the amount of DNA (Fig. 2.9).

2.2.2 Post storage metabolites concentration

Glucose is the primary source of energy for cells. It can be metabolized to produce adenosine triphosphate (ATP) both in the presence of oxygen (aerobically) and in its absence (anaerobically). These reactions occur in the presence of temperature-dependent enzymes. Temperatures below 37 °C will lead to a slower reaction rate while higher temperature will cause enzyme denaturation (Berg, Tymoczko, & Stryer, 2012). The anaerobic pathway is coupled with the production of lactate. Accumulation of lactate also causes a reduction in intracellular pH, which can have detrimental effects on the viability of the cells (Schop et al., 2009). Glutamine is a non essential amino acid which is hydrolysed by glutaminase yielding glutamate and ammonia as waste products. In addition to glucose, glutamine can also be used to generate cellular energy. Spent medium was aseptically isolated after 5 and 7 days of

storage and the concentration of glucose, lactate, glutamine and ammonia were measured.

This was undertaken for all three donors.

2.2.2.1 Glucose and lactate

It was possible to determine which storage condition led to the lowest amount of glucose in the spent medium (Fig 2.10).

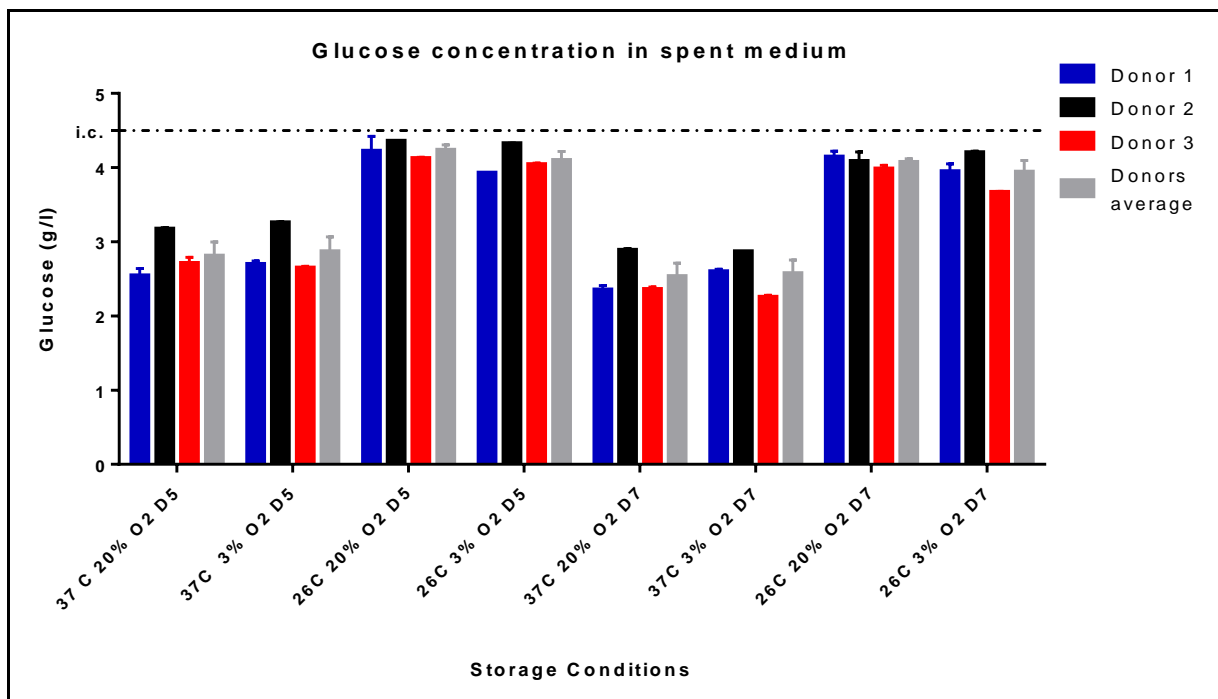


Figure 2.10 Post-storage glucose concentrations (g/l) in spent medium. Scaffold-free bone marrow derived cartilage discs were prepared using bone marrow hMSCs isolated from three healthy donors. Discs were exposed to storage conditions listed in Table 2.2. Dotted line represents initial glucose concentration in fresh medium (i.c.) (4.5 g/l). Each measurement requires 1 ml of spent medium. As only 2 ml of spent medium were available for each storage condition, two technical replicates only were possible. Values are plotted as mean and standard error of the mean (n=2). (37 C=37 °C, O2=pO₂ oxygen tension, D5= day 5, D7= day 7).

Five day storage at 26 °C and 20 % oxygen resulted in 34 % less glucose metabolized compared to discs stored at 37 °C and 20 % oxygen. Lower oxygen tension less markedly

affected the amount of glucose metabolized. At 37 °C, it decreased by 2 % at day 5 and 1.5 % at day 7. It can be noticed that at 26 °C, glucose consumption increased at 3% oxygen tension by 3.2 % both at day 5 and day 7. Discs from donor #2 metabolized less glucose in all storage conditions and this is consistent with the reduced number of cells per disc described in 3.2.1. Figure 2.11 shows a consistent trend in consumption of glucose for all three donors. Unlike viability indicator where LS-means were different despite the consistent trend, glucose consumption was very similar for donor #1 and #3.

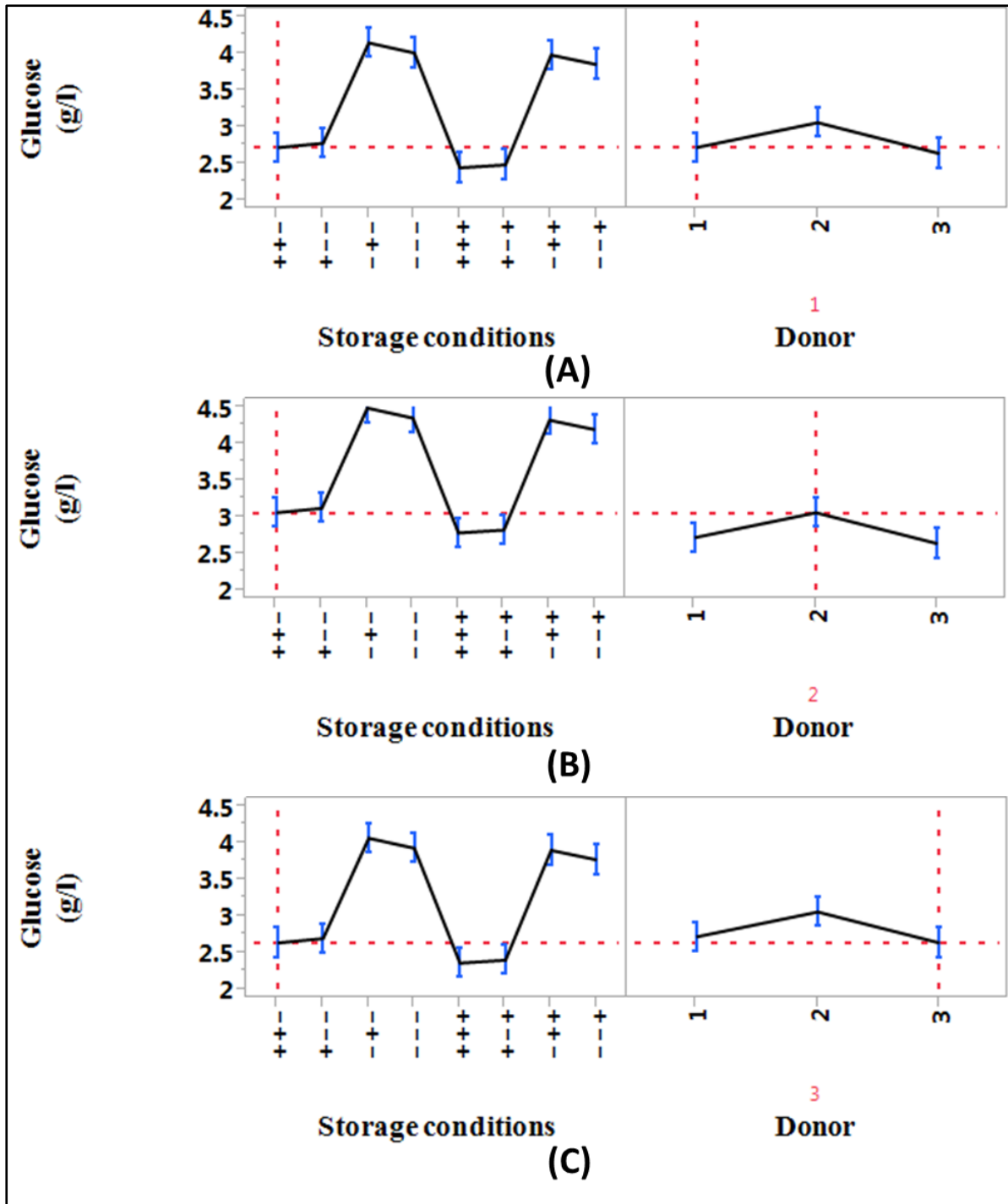


Figure 2.11 Least square means for glucose for scaffold-free bone marrow derived cartilage discs following storage conditions listed in table 2 for donor 1 (A), 2 (B) and 3(C) respectively. Least square means (LS-means) were estimated using JMP SAS software. Storage conditions were defined by combining high (+) and low(-) levels of the three parameters under investigation: temperature (37 -26 °C), oxygen (3-20 % O₂) and storage duration (5-7 days). This method allows to compare by compensating for donor to donor variability. Left (A,B,C), least square means for glucose for each storage condition. Right (A,B,C), least square means for each donor calculated across all storage conditions. Error bars represent 95% CI. Confidence intervals that do not overlap represent storage conditions which were consistently different across the three donors. Statistically different storage conditions or donors can be identified by non-overlapping CIs.

Similarly to glucose, it was possible to determine which condition led to the minimum amount of lactate released by the discs during storage (Fig 2.12). For all the three donors, the highest amount of lactate was produced when the discs were stored at 37 °C as opposed to 26 °C. This can be explained by the reduced metabolism of cells at 26 °C and it is consistent with the amount of glucose which was metabolised (Fig 2.10). Lactate production was 87 % higher at 37 °C compared to 26 °C after 5 days and 82 % after 7 days. While lower oxygen tension at 37 °C only led to a 1 % decrease in lactate release after 5 days, the effect was greater and resulted in a 4 % decrease after 7 day storage.

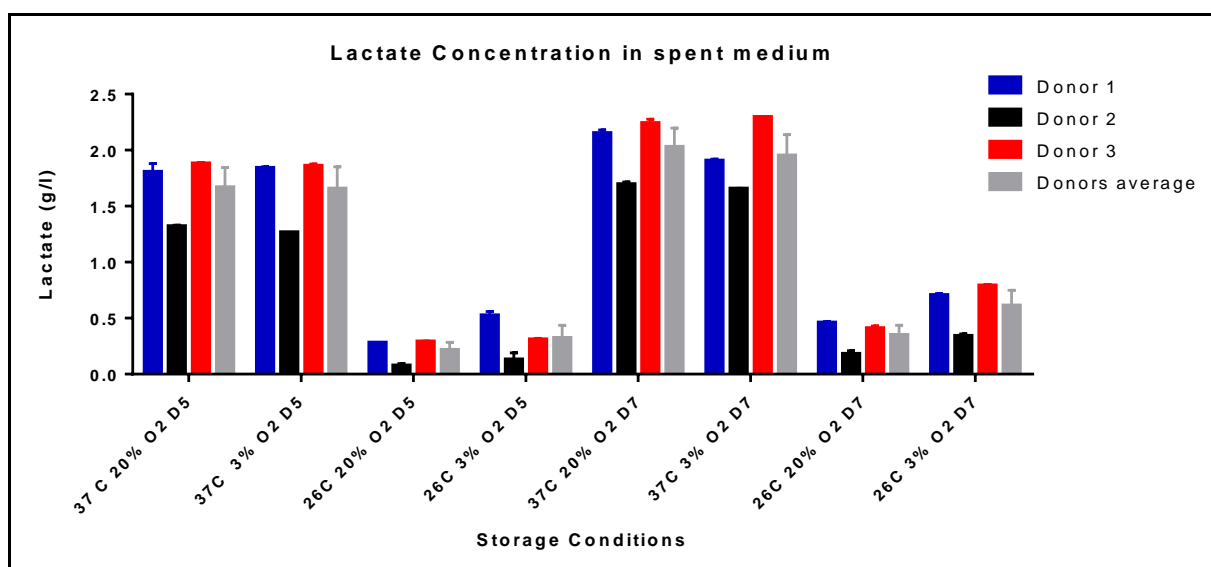


Figure 2.12 Post-storage lactate concentrations (g/l) in spent medium. Initial concentration is 0 g/l. Scaffold-free bone marrow derived cartilage discs were prepared using bone marrow hMSCs isolated from three healthy donors. Discs were exposed to storage conditions listed in Table 2.2. Each measurement requires 1 ml of spent medium. As only 2 ml of spent medium were available for each storage condition, two technical replicates only were possible. Values are plotted as mean and standard error of the mean (n=2). (37 C=37 °C, O2=pO₂ oxygen tension, D5= day 5, D7= day 7).

As with glucose, it is apparent that when the discs were stored at 26 °C and 3 % oxygen the production of lactate (and the metabolism of glucose) increased compared to when stored at 26 °C and 20 % oxygen. This effect tends to be greater after day 7 (43 % increase) than after

day 5 (33 % increase) day storage. Lactate release inversely matched glucose concentration with higher values for longer storage at higher temperature (Fig.2.12).

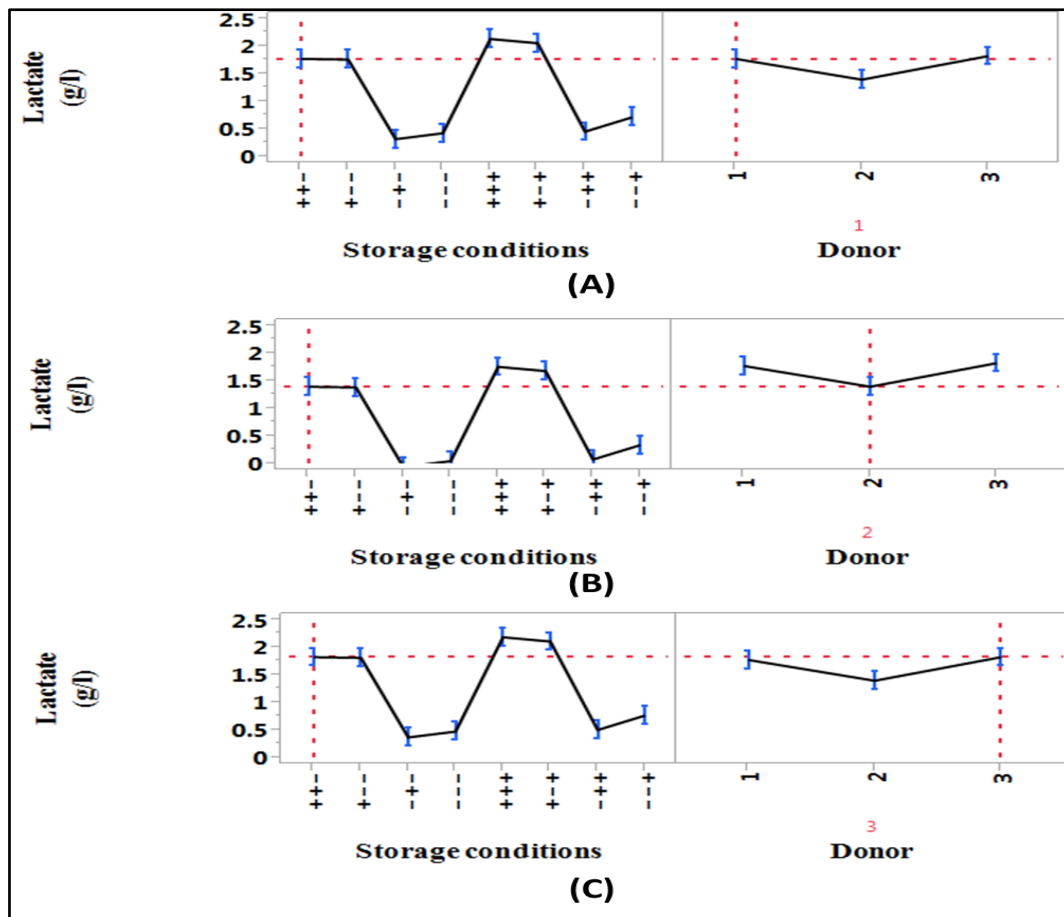


Figure 2.13 Least square means for lactate for scaffold-free bone marrow derived cartilage discs following storage conditions listed in table 2 for donor 1 (A), 2 (B) and 3(C) respectively. Least square means (LS-means) were estimated using JMP SAS software. Storage conditions were defined by combining high (+) and low(-) levels of the three parameters under investigation: temperature (37 -26 °C), oxygen (3-20 % O₂) and storage duration (5-7 days). This method allows to compare by compensating for donor to donor variability. Left (A,B,C), least square means for lactate (%) for each storage condition. Right (A,B,C), least square means for each donor calculated across all storage conditions. Error bars represent 95% CI. Confidence intervals that do not overlap represent storage conditions which were consistently different across the three donors. Statistically different storage conditions or donors can be identified by non-overlapping CIs.

Lactate release from donor #2 was statistically different than donor #1 and #3 (Fig. 2.13).

Discs prepared using hMSCs from these two donors showed a very similar metabolism during storage both in terms of glucose consumption and lactate release, suggesting a strong effect of cell number on tissue metabolism rate.

2.2.2.2 Glutamine and ammonia

Glutamine concentration (mM) in spent medium after 5 and 7 day storage was measured and the results are shown in Fig.2.14.

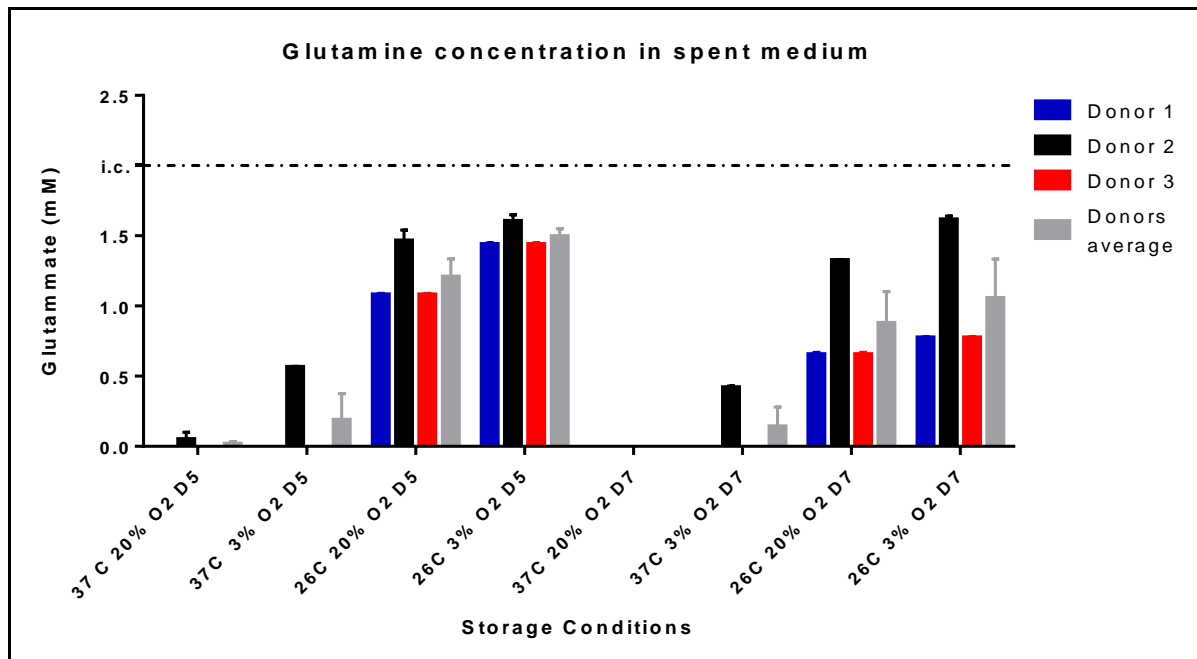


Figure 2.14 Post-storage glutamine concentrations (mM) in spent medium. Scaffold-free bone marrow derived cartilage discs were prepared using bone marrow hMSCs isolated from three healthy donors. Discs were exposed to storage conditions listed in Table 2.2. Dotted line represents initial glutamine concentration in fresh medium (i.c.) (2 mM). Each measurement requires 1 ml of spent medium. As only 2 ml of spent medium were available for each storage condition, two technical replicates only were possible. Values are plotted as mean and standard error of the mean (n=2). (37 C=37 °C, O₂=pO₂ oxygen tension, D5= day 5, D7= day 7).

It was possible to notice that different temperature and oxygen tension levels can trigger different metabolic pathways. When stored at 37 °C, discs metabolise all glutamine available. At a lower temperature, glutamine metabolism was greatly reduced. This further decreased at lower oxygen tension level (3%). This suggests that storage at lower temperature and hypoxic condition also reduces glutamine metabolism. Glutamine concentration in the spent medium post-storage ranged from 1% of the initial glutamine concentration (2 mM) after 5 day

storage at 37 °C and 20 % oxygen to 76 % after 5 days storage at 26 °C and 3 % oxygen. All three donors consistently responded to changes in temperature and oxygen tension levels during storage (Fig. 2.15). Glutamine metabolism was lower for discs from donor #2, although this was not statistically significant.

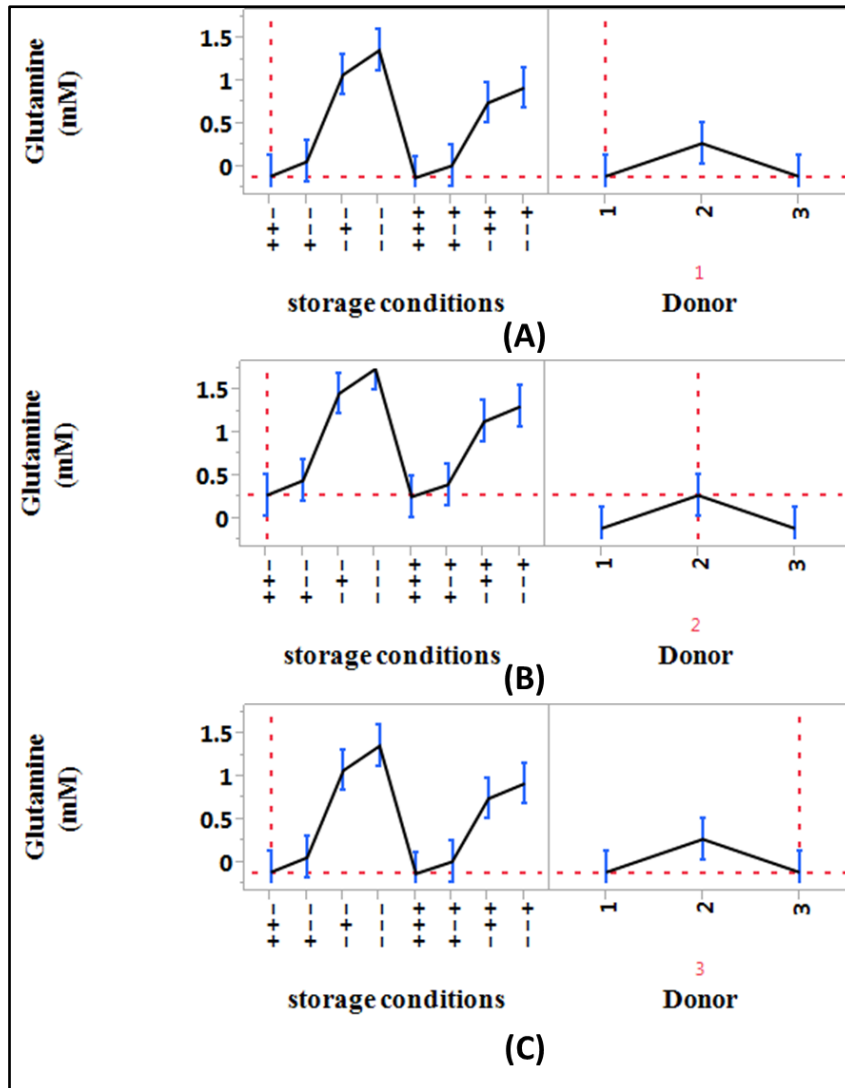


Figure 2.15 Least square means for glutamine for scaffold-free bone marrow derived cartilage discs following storage conditions listed in table 2 for donor 1 (A), 2 (B) and 3(C) respectively. Least square means (LS-means) were estimated using JMP SAS software. Storage conditions were defined by combining high (+) and low(-) levels of the three parameters under investigation: temperature (37 -26 °C), oxygen (3-20 % O₂) and storage duration (5-7 days). This method allows to compare by compensating for donor to donor variability. Left (A,B,C), least square means for glutamine for each storage condition. Right (A,B,C), least square means for each donor calculated across all storage conditions. Error bars represent 95% CI. Confidence intervals that do not overlap represent storage conditions which were consistently different across the three donors. Statistically different storage conditions or donors can be identified by non-overlapping CIs.

Closely linked to glutamine metabolism, ammonia concentration in spent medium post-storage was also measured in order to assess which storage conditions would be less detrimental for the cell based product. Results are shown in Fig. 2.16.

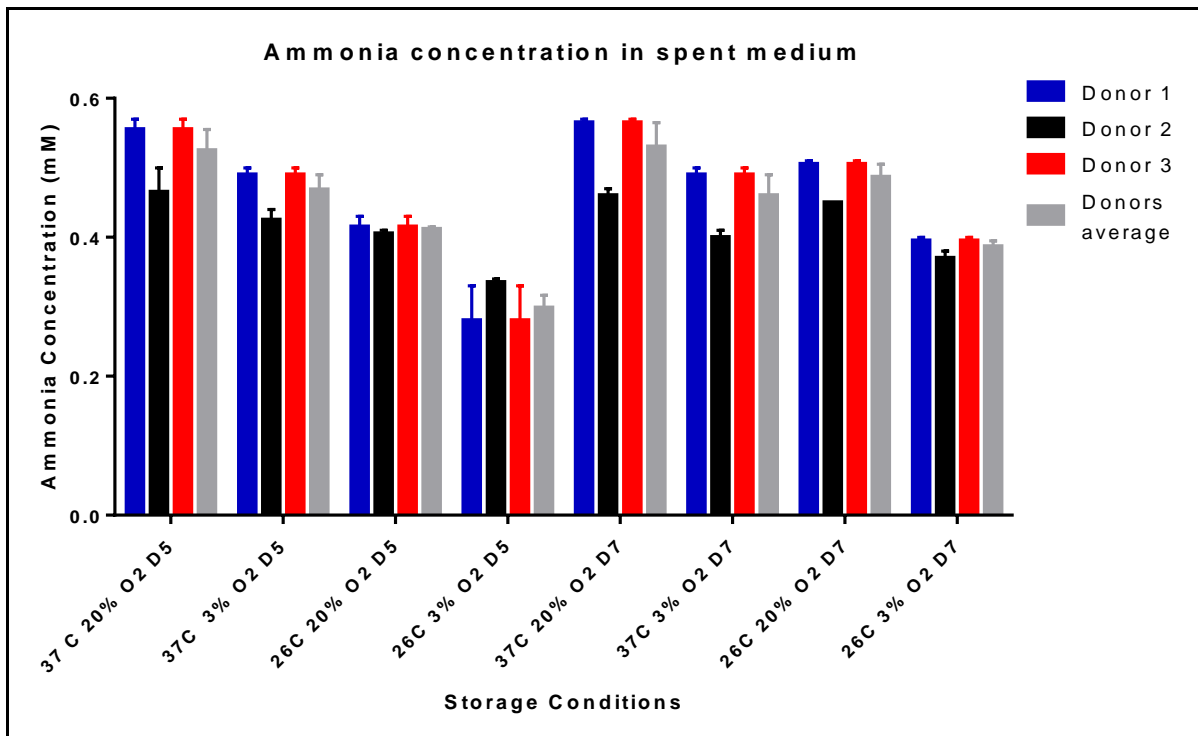


Figure 2.16 Post-storage NH_3 concentrations (mM) in spent medium. Scaffold-free bone marrow derived cartilage discs were prepared using bone marrow hMSCs isolated from three healthy donors. Discs were exposed to storage conditions listed in Table 2.2. Initial NH_3 concentration was 0 mM. Each measurement requires 1 ml of spent medium. As only 2 ml of spent medium were available for each storage condition, two technical replicates only were possible. Values are plotted as mean and standard error of the mean (n=2). (37 C=37 °C, O2=pO₂ oxygen tension, D5= day 5, D7= day 7).

Consistently with glutamine metabolism, lower temperature and oxygen levels led to a reduced amount of ammonia produced both after 5 and 7 days of storage. Ammonia concentration in spent medium was as high as 0.525 mM (n=3) after 5 days (37 °C and 20 % oxygen) and as low as 0.29 mM (n=3) at 5 days (26 °C and 3 % oxygen). Fig. 2.17 shows that the amount of NH_3 released at 26 °C and 20 % oxygen is statistically different from the amount released when the discs were stored at 26 °C and 3 % Oxygen, both after 5 and 7 days and for all three donors.

This suggests that both glucose and glutamine metabolism could be potentially modulated by physical parameters like temperature and oxygen tension in order to minimize detrimental effect of waste products, such as lactate and ammonia.

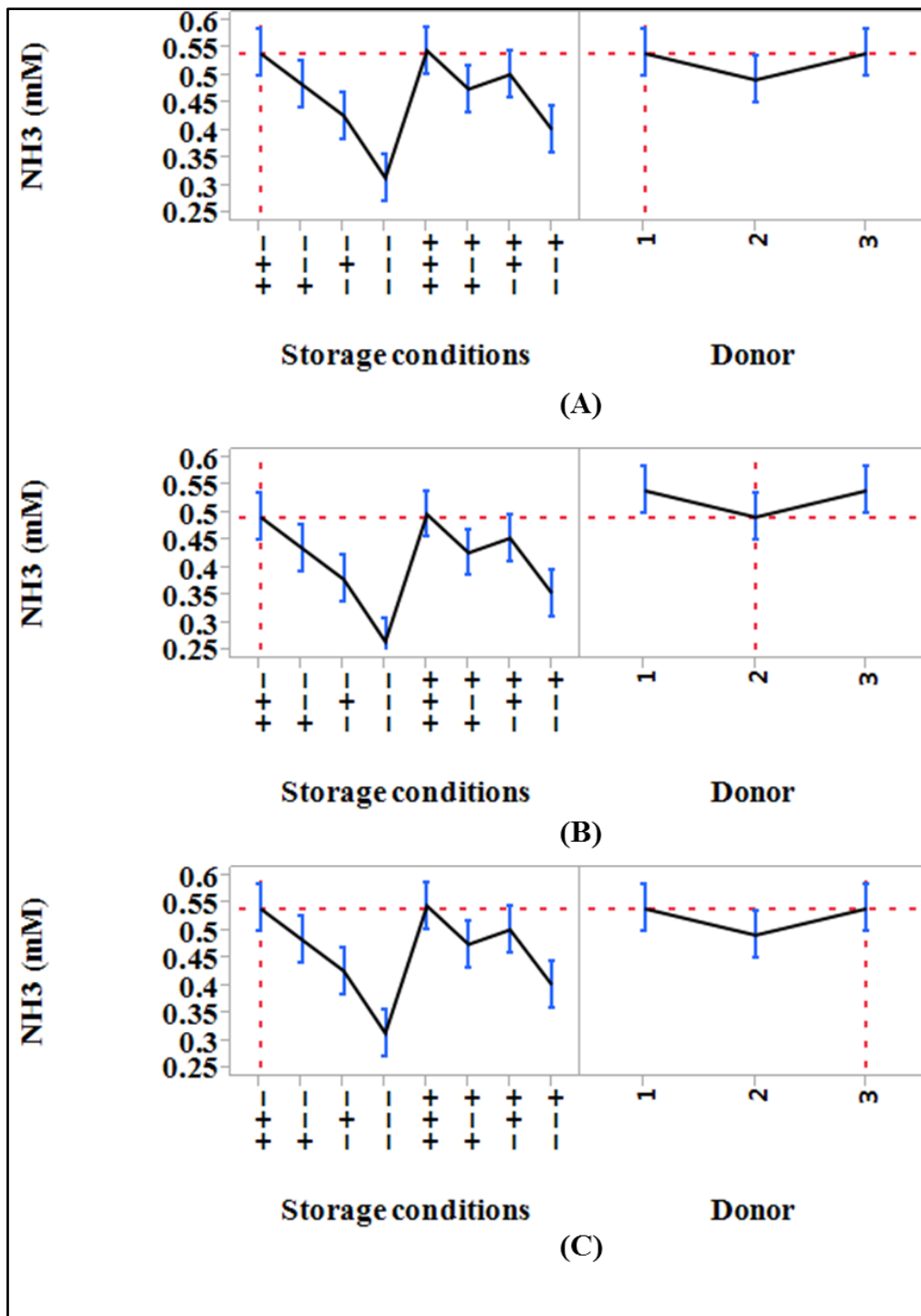


Figure 2.17 Least square means for NH_3 for scaffold-free bone marrow derived cartilage discs following storage conditions listed in table 2 for donor 1 (A), 2 (B) and 3(C) respectively. Least square means (LS-means) were estimated using JMP SAS software. Storage conditions were defined by combining high (+) and low(-) levels of the three parameters under investigation: temperature ($37 - 26^\circ\text{C}$), oxygen (3-20 % O_2) and storage duration (5-7 days). This method allows to compare by compensating for donor to donor variability. Left (A,B,C), least square means for viability indicator (%) for each storage condition. Right (A,B,C), least square means for each donor calculated across all storage conditions. Error bars represent 95% CI. Confidence intervals that do not overlap represent storage conditions which were consistently different across the three donors. Statistically different storage conditions or donors can be identified by non-overlapping CIs.

2.2.3 Post storage gene expression analysis

In order to assess if gene expression would change in response to different storage conditions, (for example, changing temperature and oxygen tension level at which discs were stored) RNA was extracted from discs post-storage and variation in gene expression quantified using quantitative real-time PCR. *COL2A1* expression, which encodes for collagen type II α 1, in terms of fold change relative to day 0 (storage start) are shown in Fig 2.18.

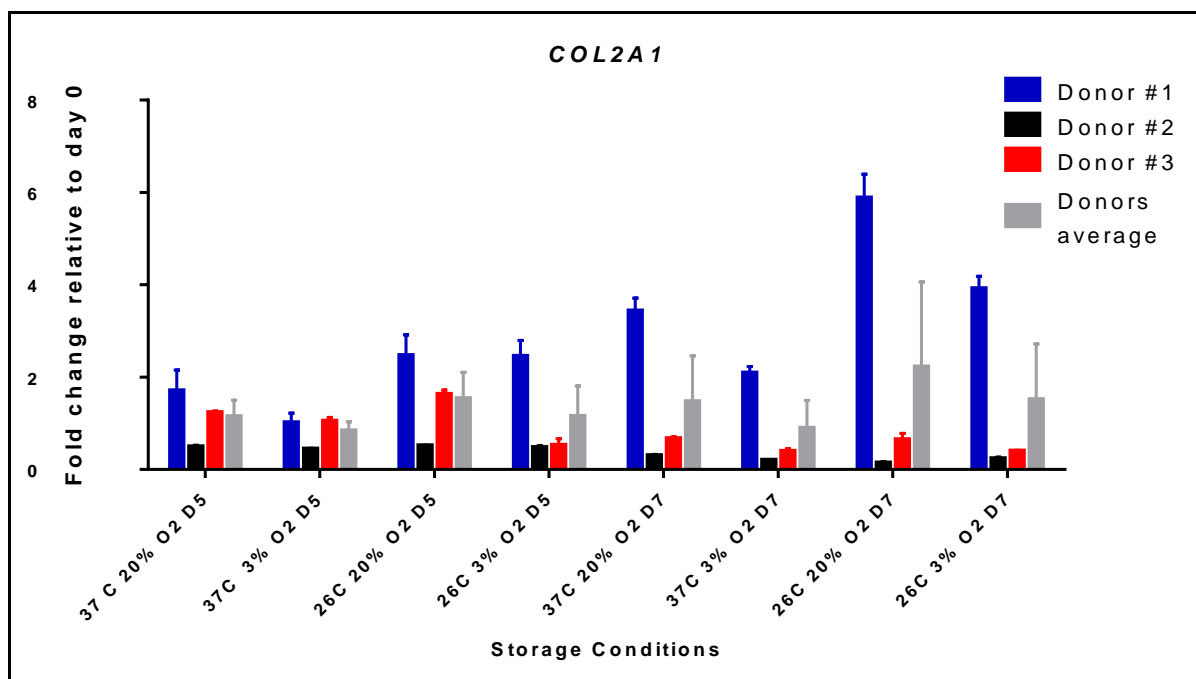


Figure 2.18 Fold change in *COL2A1* gene expression in response to storage. Scaffold-free bone marrow derived cartilage discs were prepared using bone marrow hMSCs isolated from three healthy donors. Discs were exposed to storage conditions listed in Table 2.2. Fold change values are relative to an unstored disc and plotted as mean and standard error of the mean for three technical replicates for each donor. (37 C=37 °C, O2=pO₂ oxygen tension, D5= day 5, D7= day 7).

COL2A1 was more abundantly expressed in discs from donor #1 compared to discs from donor #2 and #3. It is reasonable to assume that the chondrogenic stimulation induced by TGF- β_3 continued during the storage period for donor #1, with higher fold changes relative to day 0 (storage start) at 7 days. For both storage length (5 and 7 days), a similar trend can be observed where lower temperature and higher oxygen tension correspond to higher fold change relative to day 0 (storage start). The fact that higher oxygen tension leads to upregulation of *COL2A1* could be linked to *in-vivo* cartilage homeostasis. When stored at 37°C and 3% oxygen, which closely mimic the environment experienced by the hMSCs *in-vivo* in absence of injuries (Zhou, Cui, & Urban, 2004), *COL2A1* was under regulated in discs from all three donors both after 5 and 7 day storage. As shown in Fig.2.19, discs from the 3 donors showed a consistent trend although *COL2A1* was expressed less in discs from donor #2 and even less in discs from donor #3. The three patterns were not statistically different. Moreover, no statistically significant difference was found between all 8 storage conditions.

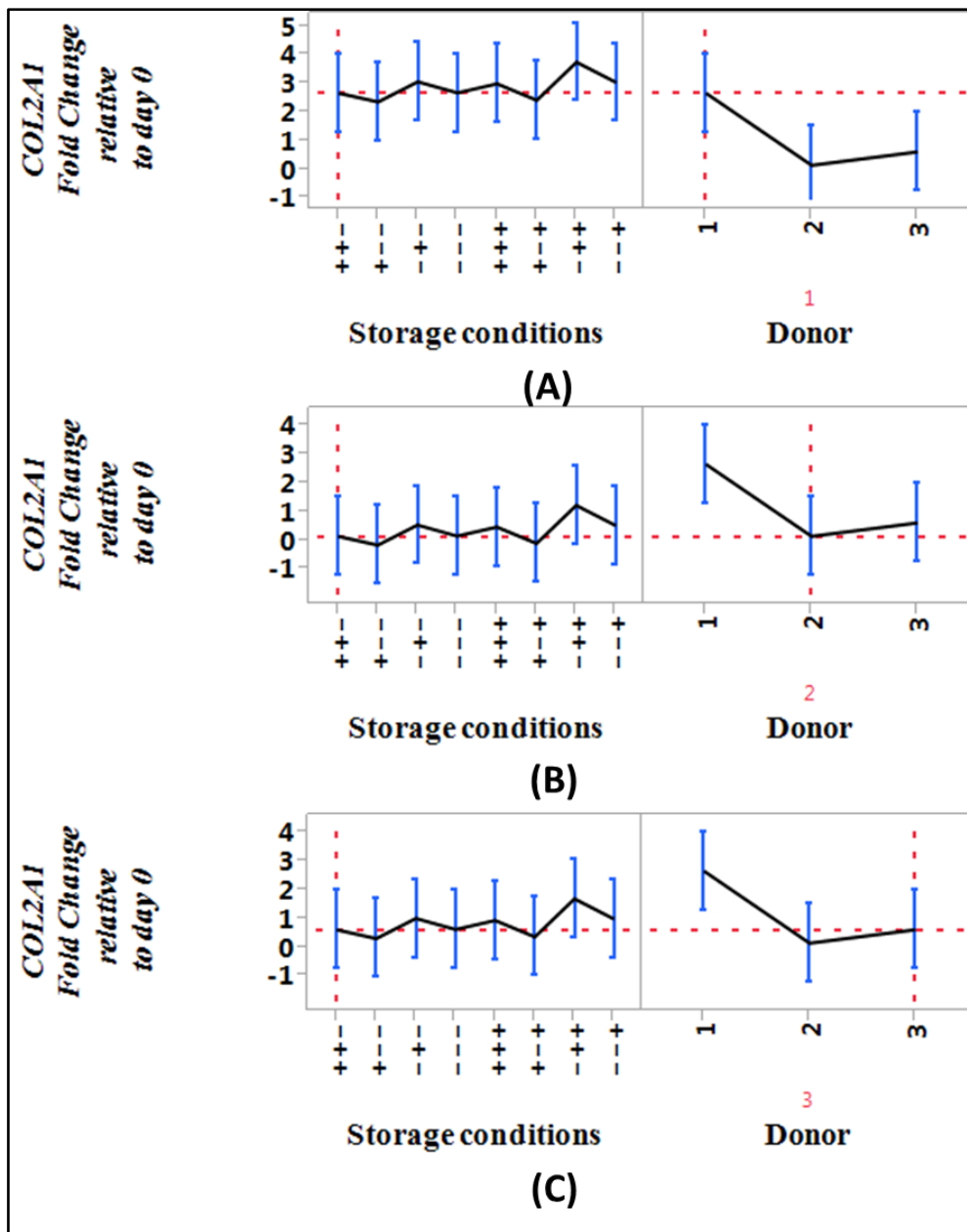


Figure 2.19 Least square means for *COL2A1* fold change for scaffold-free bone marrow derived cartilage discs following storage conditions listed in table 2 for donor 1 (A), 2 (B) and 3(C) respectively. Least square means (LS-means) were estimated using JMP SAS software. Fold changes are relative to untreated samples which were not exposed to any storage condition. Storage conditions were defined by combining high (+) and low(-) levels of the three parameters under investigation: temperature (37 -26 °C), oxygen (3-20 % O₂) and storage duration (5-7 days). This method allows to compare by compensating for donor to donor variability. Left (A,B,C), least square means for *COL2A1* fold change for each storage condition. Right (A,B,C), least square means for each donor calculated across all storage conditions. Error bars represent 95% CI. Confidence intervals that do not overlap represent storage conditions which were consistently different across the three donors. Statistically different storage conditions or donors can be identified by non-overlapping CIs.

Similarly to *COL2A1*, fold changes relative to day 0 (storage start) for *ACAN*, which codes for the major proteoglycan in hyaline cartilage, were higher for donor #1 compared to donor

#2 or #3 (Fig. 2.20) and this can be linked to the different proliferation of cells in the transwell. It has been reported that, other than chondrogenic medium, high cell density is key in inducing chondrogenic differentiation (Murdoch et al., 2007). Differences in fold change can be noticed for different oxygen tensions only for storage at 37 °C. At this temperature, *ACAN* was more abundantly expressed at 20 % oxygen compared to discs stored at 3 % oxygen for donor #1 and #3 after 5 day storage. For these two donors, the trend can be also noticed after 7 day storage, although fold change values were smaller. When storage at 26 °C, oxygen tension only leads to an increased fold change after 7 day storage. Differences in *COL2A1* fold change values were consistent to those found for *ACAN* and they are probably due to the different chondrogenic process taking place in the discs from different donors as result of inter donor variability rather than storage conditions.

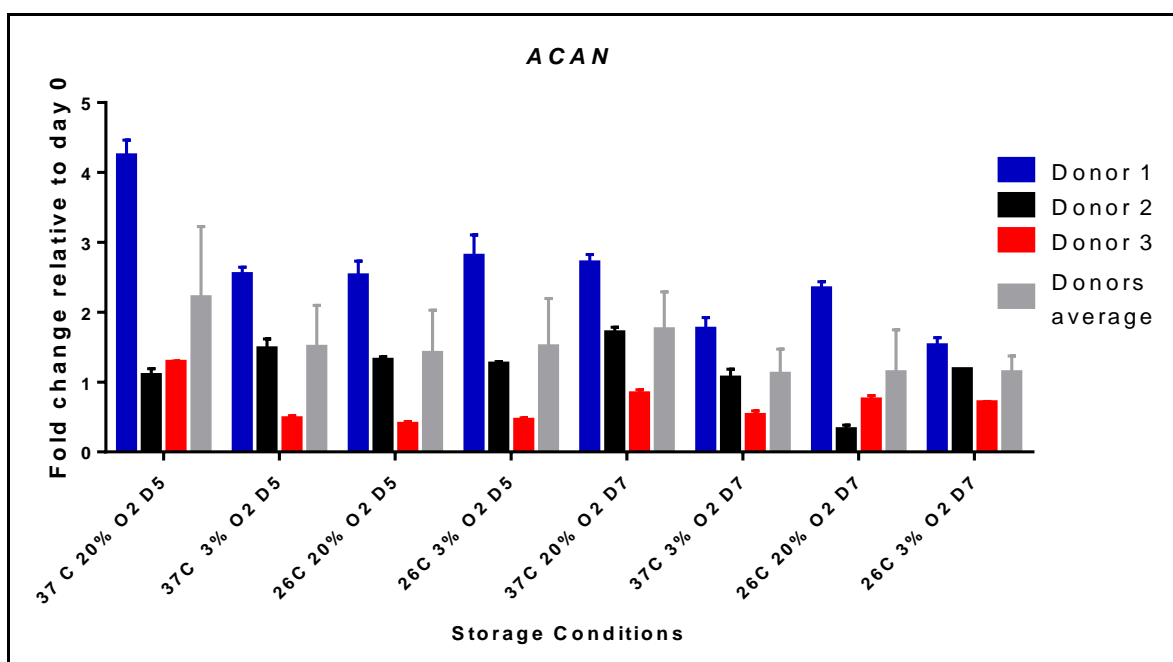


Figure 2.20 Fold change in *ACAN* gene expression in response to storage. Scaffold-free bone marrow derived cartilage discs were prepared using bone marrow hMSCs isolated from three healthy donors. Discs were exposed to storage conditions listed in Table 2.2. Fold change values are relative to an unstored disc and plotted as mean and standard error of the mean for three technical replicates for each donor. (37 C=37 °C, O2=pO₂ oxygen tension, D5= day 5, D7= day 7).

Figure 2.21 shows that mean fold change values for donor #1 are statistically different than mean fold change values for donor #3. No significant differences were found between storage conditions.

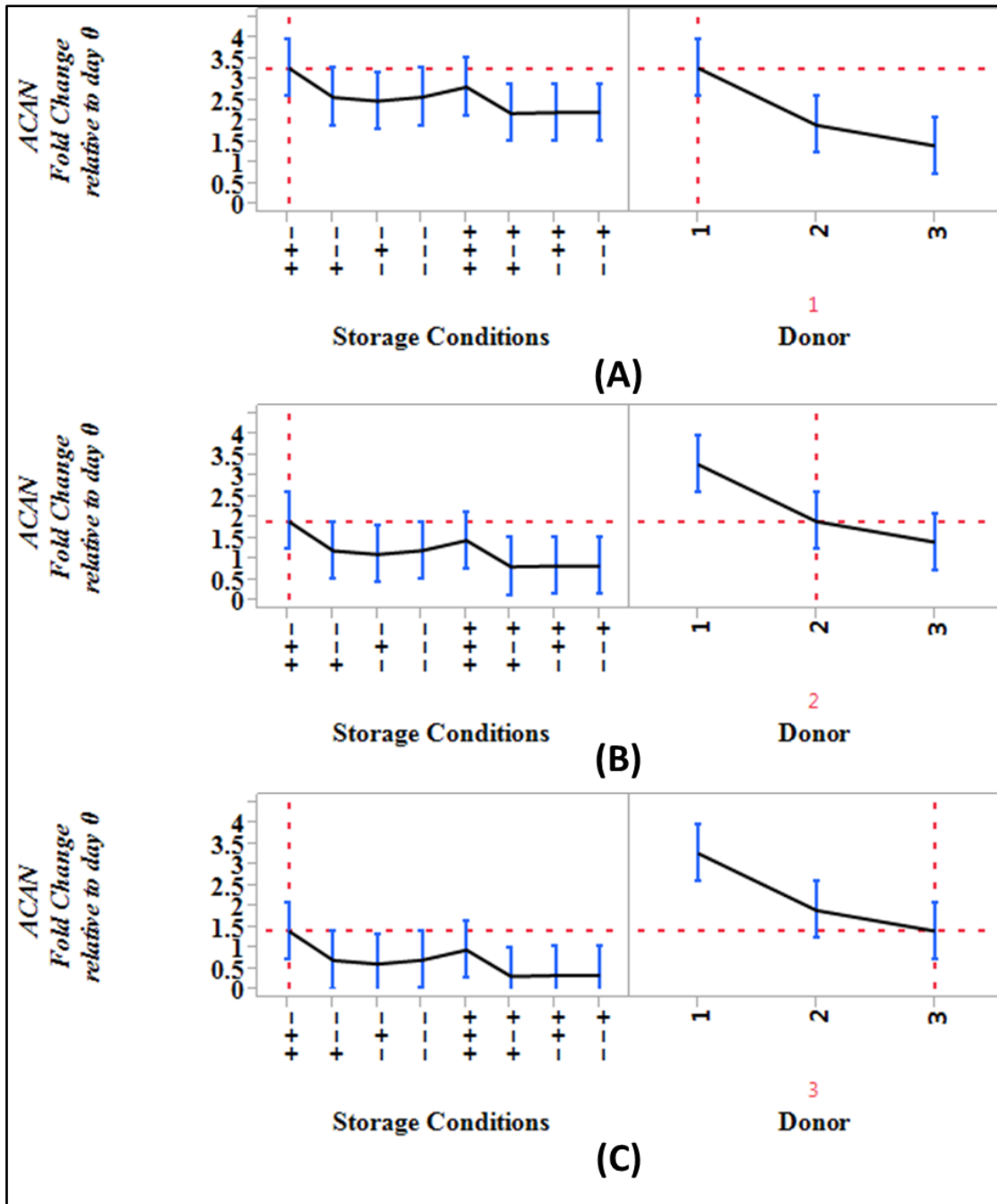


Figure 2.21 Least square means for ACAN fold change for scaffold-free bone marrow derived cartilage discs following storage conditions listed in table 2 for donor 1 (A), 2 (B) and 3(C) respectively. Least square means (LS-means) were estimated using JMP SAS software. Fold changes are relative to untreated samples which were not exposed to any storage condition. Storage conditions were defined by combining high (+) and low(-) levels of the three parameters under investigation: temperature (37 -26 °C), oxygen (3-20 % O₂) and storage duration (5-7 days). This method allows to compare by compensating for donor to donor variability. Left (A,B,C), least square means for ACAN fold change for each storage condition. Right (A,B,C), least square means for each donor calculated across all storage conditions. Error bars represent 95% CI. Confidence intervals that do not overlap represent storage conditions which were consistently different across the three donors. Statistically different storage conditions or donors can be identified by non-overlapping CIs.

The expression of *COL1A1*, which encodes for collagen type I $\alpha 1$, in response to different storage conditions was also analysed (Fig. 2.22). *COL1A1* was also down regulated for donor #1 compared to the other donors. This can be explained by the lower proliferation of the cells in the transwell for donor #3 compared to donor #1 and #2. As higher cell density induce better chondrogenesis as confirmed by *COL2A1* and *ACAN* expression, lower cell density, on the other hand, correlates to an increased expression of *COL1A1*.

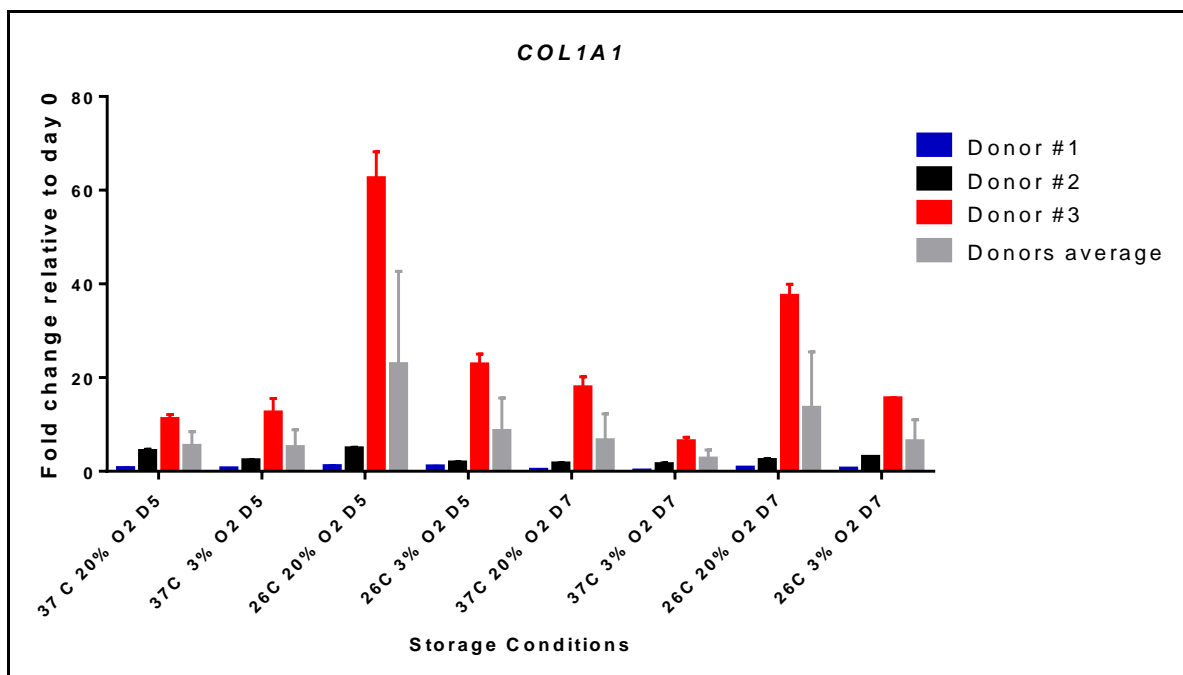


Figure 2.22 Fold change in *COL1A1* gene expression in response to storage. Scaffold-free bone marrow derived cartilage discs were prepared using bone marrow hMSCs isolated from three healthy donors. Discs were exposed to storage conditions listed in Table 2.2. Fold change values are relative to an unstored disc and plotted as mean and standard error of the mean for three technical replicates for each donor. (37 C=37 °C, O2=pO₂ oxygen tension, D5= day 5, D7= day 7).

Discs from donor #3 which showed a lower *COL2A1* and *ACAN* expression in all storage conditions, showed higher *COL1A1* expression relative to day 0 (storage start). For this donor, lower temperature and higher oxygen tension lead to an increase in *COL1A1* fold

change after 5 and, although less marked, after 7 day storage. Figure 2.23 shows that a similar pattern can be noticed among the three donors but the mean values are statistically different. Three statistical differences can also be found between storage conditions for all the three donors; storage at 26° C 20% oxygen for 5 days was significantly different than storage at 37° C 20 % or 3 % oxygen for 7 days. *COLIA1* fold changes were also statistically different between discs stored at 37° C and 3 % oxygen and discs stored at 26° C 20 % oxygen for 7 days.

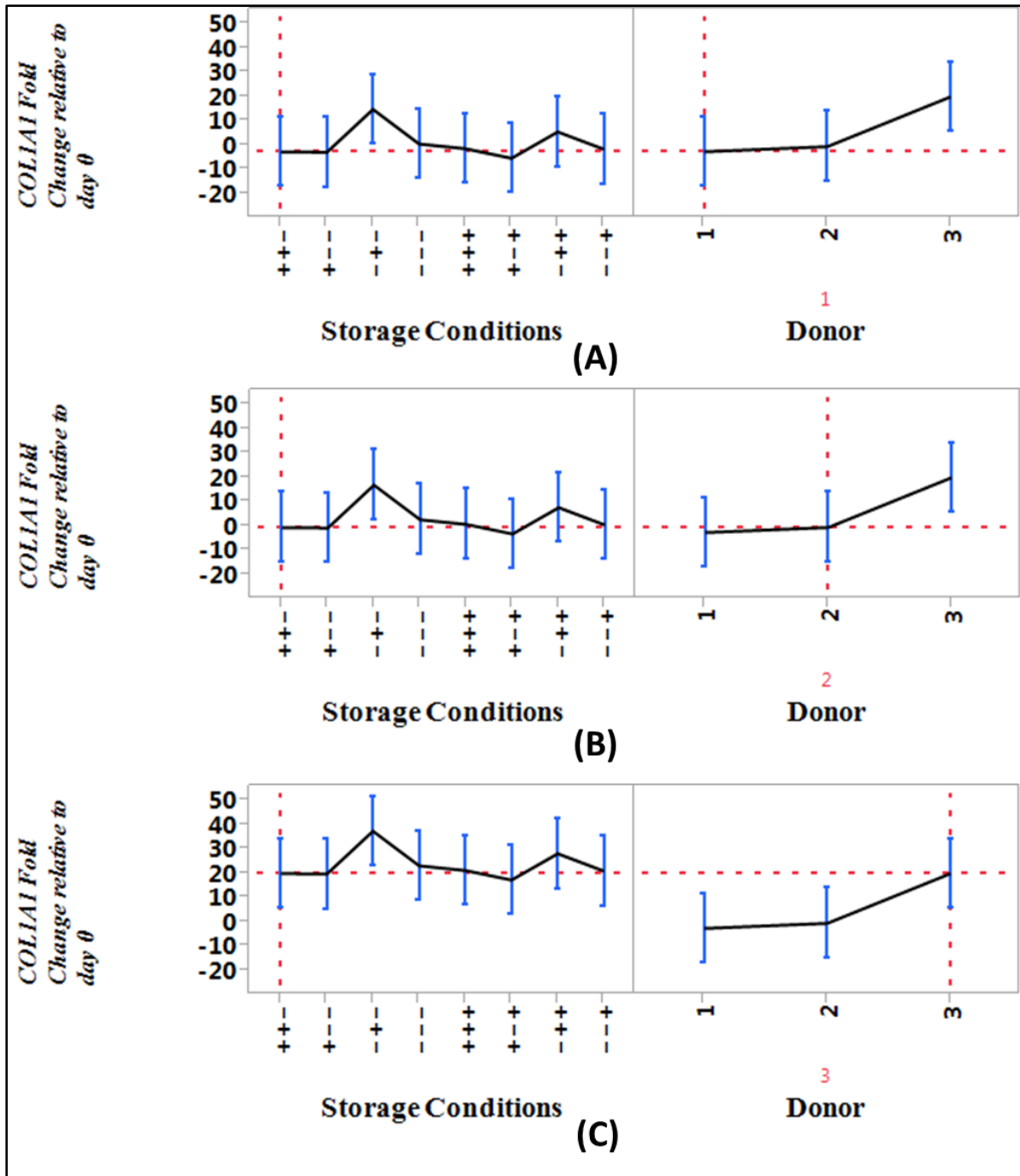


Figure 2.23 Least square means for *COL1A1* fold changes for scaffold-free bone marrow derived cartilage discs following storage conditions listed in table 2 for donor 1 (A), 2 (B) and 3(C) respectively. Least square means (LS-means) were estimated using JMP SAS software. Fold changes are relative to untreated samples which were not exposed to any storage condition. Storage conditions were defined by combining high (+) and low(-) levels of the three parameters under investigation: temperature (37 -26 °C), oxygen (3-20 % O₂) and storage duration (5-7 days). This method allows to compare by compensating for donor to donor variability. Left (A,B,C), least square means for *COL1A1* fold changes for each storage condition. Right (A,B,C), least square means for each donor calculated across all storage conditions. Error bars represent 95% CI. Confidence intervals that do not overlap represent storage conditions which were consistently different across the three donors. Statistically different storage conditions or donors can be identified by non-overlapping CIs.

2.3 Brief summary of data described

In this chapter, the storage of cartilage discs from three healthy donors has been studied.

Table 2.5 summarizes the key findings.

Table 2.5 Brief summary of key findings for the storage of cartilage discs in a controlled environment for 5 and 7 days.

	Key finding
Viability	Storage at 26 °C led to a better viability than storage at 37 °C both at 5 and 7 days. Oxygen did not have a large effect on modulate viability.
Metabolites	
Glucose	Glucose concentration in spent medium increased as storage temperature decreased from 37 to 26 °C and less remarkably when oxygen tension increased from 3 to 20 %.
Lactate	The highest amount of lactate was produced when the discs were stored at 37 °C, consistently with glucose metabolism.
Glutamine	Storage at lower temperature and hypoxic conditions reduced glutamine metabolism
Ammonia	Consistently with glutamine metabolism, lower temperature and oxygen levels led to a reduced amount of ammonia produced both after 5 and 7 days of storage.
Chodrogenic potential	
<i>COL2A1</i>	For both storage lengths, lower temperature and higher oxygen correspond to higher fold change relative to day 0 (storage start)
<i>ACAN</i>	Storage at higher temperature led to higher fold changes after 5 and 7 days. <i>ACAN</i> was also upregulated for storage at higher oxygen but only at 37 °C.
<i>COL1A1</i>	<i>COL1A1</i> was upregulated for lower storage conditions at higher oxygen level both after 5 and 7 days.

2.4 Discussion

The aim of this chapter was to investigate the storage properties of cartilage discs which have been used as engineered tissue model. These discs were prepared using the method developed by *Murdoch et al. (2007)*. The effect of temperature was investigated in combination with oxygen tension over a period of 5 and 7 day storage. A number of research groups have investigated such parameters separately and mainly in order to optimize the expansion of cells in bioreactors for therapeutic purposes (*Panchalingam et al., 2015; Schnitzler et al., 2015*). As cells are normally exposed to variation in temperature as well as oxygen tension when stored and transported to the clinical site, it is important to better understand their behaviour when exposed to different storage conditions. It can be noticed that preferential storage conditions in terms of viability, lactate and ammonia production, *COL2A1* and *ACAN* production are the ones that led to upregulation of *COL1A1*, which should be minimal for cartilage-like tissue as collagen type I is abundant in bone ECM but nearly absent in hyaline cartilage (*Brian Johnstone et al., 2013*)

Viability is considered the first step towards establishing the shelf life of the cell based product and is part of more complex, yet mandatory, stability studies (*ICH Q5C*, <http://www.ich.org/products/guidelines/quality/article/quality-guidelines.html>). This is because it is not normally enough to prove that cells are alive but it is important that they maintain the relevant biological function once delivered to the patient. As described in chapter 1, the shelf life of commercially available products spans from a minimum of 18 h (*Provenge, Dendreon*) to a maximum of 15 days (*Apligraf, Organogenesis*). The former is a suspension of 50×10^6 autologous $CD54^+$ cells activated with PAP-GM-CSF, while the latter

is an engineered tissue (75 mm in diameter and 0.75 mm thick) comprised of human fibroblasts and keratinocytes. This suggests that tissue engineered products might have longer shelf life compared to cells stored in suspension. The presence of extra cellular matrix might exert a protective effect to the cells enabling them to preserve their viability for longer. This hypothesis inspired the use of polymeric materials, like bioactive polymer fibrin (Janmey, Winer, & Weisel, 2009) and inert semi-permeable polymer alginate (Swioklo et al., 2016) to improve the preservation of cells during storage and transport. The approval of Holoclar (EPAR-EMA), which is the first advanced therapy medicinal product (ATMP) containing stem cells, demonstrate that cell type might, more than the formulation, dictate the extent of shelf life. This product, used for severe limbal stem cell deficiency due to chemical burn to the eye, consists of autologous human corneal epithelial cells on a fibril gel but its shelf life is limited to 36 hours. It should also be considered that many of the assays used for the viability assessment of tissues might hide cell loss as they discern dead cells on the basis of membrane integrity, which could be maintained due to the ECM even if the cells are actually dead or apoptotic. For this reason, Alamar blue assay has been increasingly being used to indirectly measure the viability of cells, aggregates, spheroids and tissue (Bayoussef, Dixon, Stolnik, & Shakesheff, 2012; Rampersad, 2012). Another consideration about the enhanced maintenance of cells when embedded in matrix is that the ECM might allow for some regeneration when cells are lost, which does not normally happen when cells are stored in suspension, as opposed to complete maintenance of the starting cell population. This could explain why in the storage experiments described in this chapter, viability indicator (%) was on average no lower than 75.5 % after 7 day storage at 37°C and 20 % oxygen (the worst condition in terms of viability). The use of chondrogenic medium, as opposed to commercially available storage medium, might also play a role in preserving good cell viability even after 7 days. The presence of waste products such as lactate and NH₃ have a toxic effect on cell growth and can

even inhibit proliferation (Hassell, Gleave, & Butler, 1991; Schop et al., 2009). Inhibiting values vary depending on the cell type and span from 10 mM to 40 mM for lactate and from 0.5 mM to 40 mM for ammonia.

Therefore the importance of finding a storage condition that would minimize their concentration in the spent medium after 7 day storage. Results described in this chapter showed that storage of scaffold free bone marrow derived cartilage discs for 7 days at 26 °C and 3 % oxygen led to lower NH₃ release. This informative finding suggests that temperature is not the only parameter that should be controlled to enable successful storage of cell based medicinal products.

A number of studies investigating factors influencing chondrogenic differentiation of hMSCs have also considered oxygen (Boregowda et al., 2012; dos Santos et al., 2009; Panchalingam et al., 2015) and temperature (Mahmood S Choudhery et al., 2015; Schnitzler et al., 2015) separately but little to no evidence is available regarding the stability of these products once the differentiation process has taken place and without medium replenishment. Results described in this chapter show that *COL2A1* and *ACAN* expression was not statistically different after 5 and 7 day storage in all storage conditions investigated. Inter-donor variability was observed and this might be linked to incorrect criteria to select healthy donors to extract bone marrow and isolate hMSCs from. While the use of cells or starting material from “healthy” donors as opposed to patients is common practice in research, it is important to add further selection criteria in order to limit biological variability. This will impact on the properties of the cell therapy product by affecting proliferation and, therefore, chondrogenic differentiation. This has been also shown in this study as the expression of *COL1A1* was statistically different between the three donors and this might be also due to the differences in

proliferation of the cells. It has been demonstrated that chondrogenic differentiation of hMSCs is enhanced by high cell density (Murdoch et al., 2007). It is possible to use the data shown in this chapter to build models that will predict how viability, metabolites and gene expression will change in response to variations in temperature, oxygen and storage duration. This is the focus of chapter 3.

Chapter 3

Factorial experimental design as an investigational and decision support tool for cell therapy product development

Introduction

In the previous chapter, the results of storage experiments for scaffold free bone marrow derived cartilage discs were presented. Eight different storage conditions were created by combining two levels of each factor under investigation: temperature (26,37°C), oxygen (3,20%) and storage duration (5-7 days). These combinations correspond to the runs of a 2^k full factorial design, where k is the number of factors under investigation (Montgomery, 2012).

The storage experiments were repeated for three healthy donors. While in chapter 2 each combination was considered as a separate treatment, here a system approach is used to investigate the effect of the input parameters (temperature, oxygen tension and storage duration) and system responses (viability, glucose, lactate, glutamine, ammonia). Eight response models were built by using data from three healthy donors presented in chapter 2 (Fig.3.1). As raw data showed inter donor variability, donor number (donor #) was introduced in the model as an additional variable to mitigate the effect of biological variability. This technique is known as blocking (Montgomery, 2012) and increases the precision by which main effects and statistical significant interactions between factors are identified.

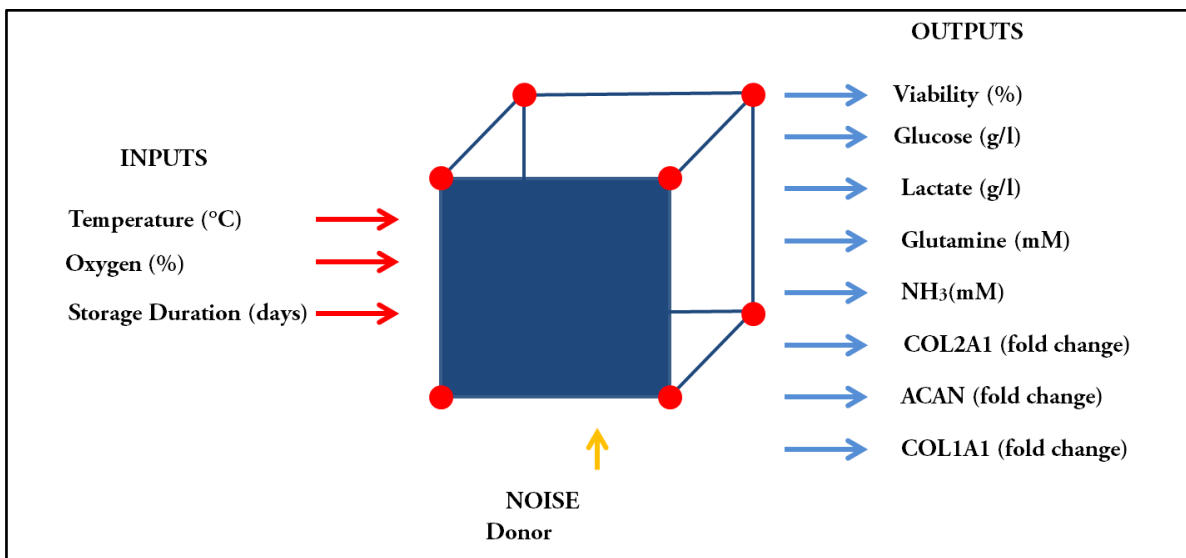


Fig. 3.1 Statistical design of experiment schematic showing input and output factors selected. This system represents the storage of a cartilage disc, used as cell therapy model. For each input factor, two levels (high and low) have been selected creating eight combinations. Output values were measured for each sample as described in chapter 3. The experiment was performed for three healthy donors. As output data showed inter donor variability, one additional nominal variable, donor, has been introduced in the design to account for known variability introduced by noise (donor number) on the output factors.

Multifactorial design of experiment (DoE) is an important tool to identify main factors and interactions that would not be otherwise detectable using one-factor-at-a-time (OFAT) approach. It is widely used in the process industry, including the pharmaceutical industry (Rathore & Winkle, 2009).

Applications of such a tool for investigation purposes, as in this study, have been rather limited (Chen et al., 2011; Lim, Shunjie, Panoskaltsis, & Mantalaris, 2012). As adequate cell product characterization is a requirement in order to deliver market authorization (EMA website, <http://www.ema.europa.eu/ema/>), DoE could be introduced to gather more data about the product which will facilitate, in turn, the path towards market authorization.

The response models generated can also be used to predict the value of system response parameters within the multidimensional space (Montgomery, 2012). While this cannot replace necessary data, it could be used to significantly reduce the number of experiments when limited resources are available, such as limited cell biopsy from the patient (Hourd et al., 2014). Two case studies are described in this chapter.

3.1 Material and methods

3.1.1 Factorial Design of Experiment

A full factorial three factor with two level design (2^3) has been implemented to study the effect of temperature, oxygen tension and storage duration on the preservation of cartilage discs used as cell therapy product model. For each factor, two levels (high and low) have been selected, namely 26 °C and 37 °C for temperature, 3% and 20% for oxygen and 5 and 7 days for storage duration. The experiments were repeated for three healthy donors as described in chapter 2. Data showed donor to donor variability. In order to improve the precision with which comparisons among factors of interest are made, one additional variable (donor number) was added to the design. This technique, referred to as blocking (Montgomery, 2012), reduces the variability introduced by known sources that are not of interest to the particular study. This study focused on the effect of temperature, oxygen level and storage duration rather than the difference between donors. Donor number becomes a nuisance factor and each level becomes a block: block 1 (donor #1), block 2 (donor #2) and block 3 (donor #3). All storage conditions created by combining different levels of the three factors under investigation, as described in table 3.2, are divided into these three blocks. Response variables have been selected on the basis of their biological properties, which are representative for this cell therapy model. Each response was an average value of triplicate measurements on the cartilage discs. JMP SAS software (http://www.jmp.com/en_gb/home.html) was used for all statistical analysis and data transformation. The software used multiple regression to fit a linear model for each response variable and parameter estimation was performed by least squares estimation. ANOVA was

used to identify main effects (factors which have a statistical significant effect on the response) and interactions between factors. Main effects on every response variable and interactions were evaluated by establishing statistical significance at $p < 0.05$.

3.1.2 Model adequacy checking

The validity of the response models to identify the main effect and interactions was tested by the examination of residuals. A residual is defined as the difference between the experimentally observed value and the value predicted by the model (Montgomery, 2012). For a model to be valid, residuals need to have constant variance across the experimental range and not be systematically affected by the experimental order (Montgomery, 2012). This requirement can be tested by plotting the residuals versus the experimental run order and the residuals versus predicted values for that response variable. For the condition of constant variance, the former has to show no positive correlation, while the latter has to show no obvious pattern. If the variance of the observations increases as the magnitude of the observation increases, residuals in the plot would appear like an outward-opening funnel. Non constant variance would also indicate data are not normally distributed (Montgomery, 2012). In case the variance is not constant across the experimental range, response can be transformed and the newly obtained variable modelled. One of the most commonly used transformations is the logarithmic transformation, where each data point is replaced by its \log_{10} (Montgomery, 2012). For each response model, r^2 , which is the proportion of the variability in the data explained by the models, was also calculated by the JMP SAS software.

Response models were used for prediction. Function Profiler on JMP SAS software enables one to predict the value of each response variable within the space defined by temperature, oxygen and storage duration.

3.1.3 Centre points and linearity assumption

Response models estimated as described in 3.1.1 assume a linear relationship between input (temperature, oxygen tension, storage duration) and output factors (viability, glucose, lactate, glutamine, ammonia, *COL2A1*, *ACAN*, *COL1A1*). In order to confirm the linear relationship, three cartilage discs were prepared as described in 2.3. One disc was used as control (day 0, storage start) and the other two were stored at 31.5 °C, 11.5 % O₂ for 6 days. This storage condition is in the middle of the investigational space defined by temperature range (26- 37 °C), oxygen (3-20 % O₂), storage duration (5-7 days). These data points are referred to as centre points and can be added to the 2³ full factorial design described in 4.1.1 (Montgomery, 2012). Viability, glucose, lactate, glutamine, ammonia, *COL2A1*, *ACAN*, *COL1A1* were measured relative to the control disc not exposed to storage as described in chapter 3. These values were included in the response models and linearity assumption was tested by analysing goodness of fit and residuals plots.

3.1.4 Case study 1

This case study describes how the eight response models presented in this chapter can be combined together and used to support the assessment of a storage container for cartilage discs. In this hypothetical scenario, two storage containers are available and two storage conditions (A and B) are simulated, as shown in Table 3.4. These sets of input parameters are within the investigated space which is described by the response models and, therefore, the values of viability, glucose, lactate, glutamine and ammonia in the spent medium and gene expression changes (*COL2A1*, *ACAN* and *COL1A1*) can be predicted selecting donor 1 as representative donor in the profiler function on JMP SAS software.

Table 3.4 Simulated storage conditions (A and B) for cartilage discs (Case study 1).

Storage Conditions	Temperature (°C)	Oxygen (%)	Storage duration (days)
A	32	20	6
B	28	5	7

Predicted values can be compared to acceptance thresholds which have been established for the cell therapy product based on clinical data.

3.1.5 Case study 2

This case study describes another hypothetical scenario where the response models are used to inform the design of a customized storage container. The aim is to define a range for the three input parameters considered (temperature, oxygen and storage duration), which will lead to a cell therapy product that will meet set specifications of the output variables following storage. These specifications are linked to the quality attributes of the cell therapy product that can be defined during clinical development and are listed in Table 3.2.

Table 3.2: Hypothetical list of quality attributes and specifications which need to be satisfied by the cartilage disc following storage.

Quality attribute	Specifications
Viability	$\geq 80\%$
Lactate	0-1.5 g/l
NH₃	0-0.5 mM
Log₁₀ COL2A1	0.4-0.55
Log₁₀ ACAN	0.40-0.60
Log₁₀ COL1A1	0.25-0.35

By selecting donor 1 as representative donor and storage duration of 7 days, contour plots were created using JMP SAS software. These are a graphical representation of predicted output values versus two inputs modelled by the DoE (Tye, 2004). By overlaying the contour plots for viability, lactate, ammonia, log₁₀COL2A1, log₁₀ACAN, log₁₀COL1A1, an area is defined which includes all combinations of temperature and oxygen that ensure specifications are satisfied.

3.2 Results

3.2.1 Analysis of post-storage viability response model

Cartilage discs were stored as described in Chapter 2. The eight storage conditions were created according to a 2^3 full factorial design and represent the combinations of two levels (high and low) of the three input parameters investigated: temperature, oxygen and storage duration. Response variables were viability, glucose, lactate, glutamine, ammonia, gene expression changes (Fig.3.1). The storage experiments were repeated for three healthy donors. As donor to donor variability was observed, one additional categorical variable “donor” was introduced to account for the effect introduced by the donor number on the response variables. Each response variable was analysed separately to identify factors (and interactions) which have a statistically significant effect. In order to identify statistically significant factors and interactions for the viability, the validity of the response model was tested by analysis of residuals (Fig. 3.2). Residuals show no outliers and no pattern, hence the validity of the viability response model was confirmed.

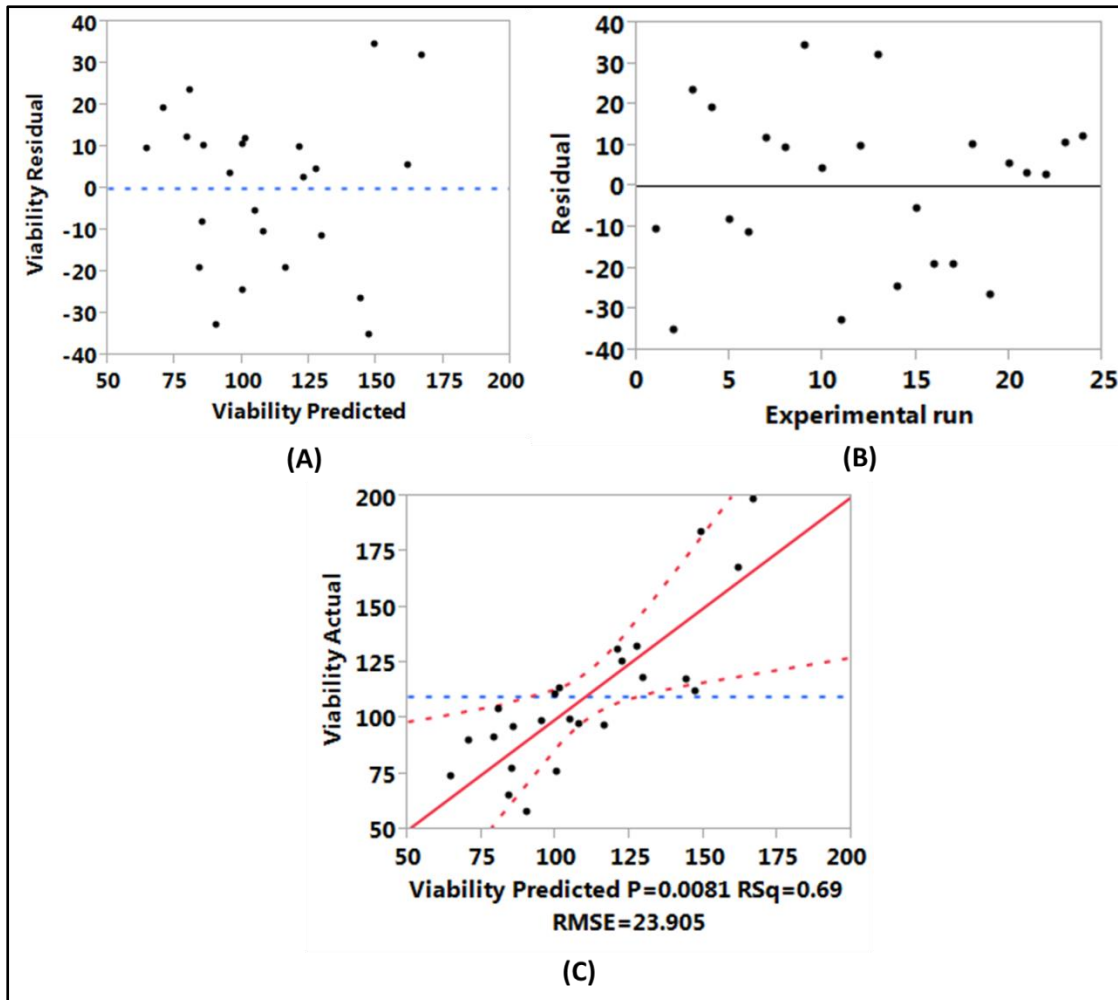


Fig. 3.2 Analysis of residuals for viability model. Residuals are plotted versus viability predicted values (A) and versus experimental run number (B) to confirm the hypothesis of constant variance. As no trend nor pattern is shown in (A) and (B) the model is valid. (C) shows goodness of fit by plotting viability actual values versus viability predicted values. $RSq=r^2$, $RMSE$ =root mean square error.

Fig. 3.3 shows how viability is predicted to vary when temperature, oxygen and storage duration vary within the investigated ranges for each donor. For all three donors, viability decreases as storage temperature or storage duration increases.

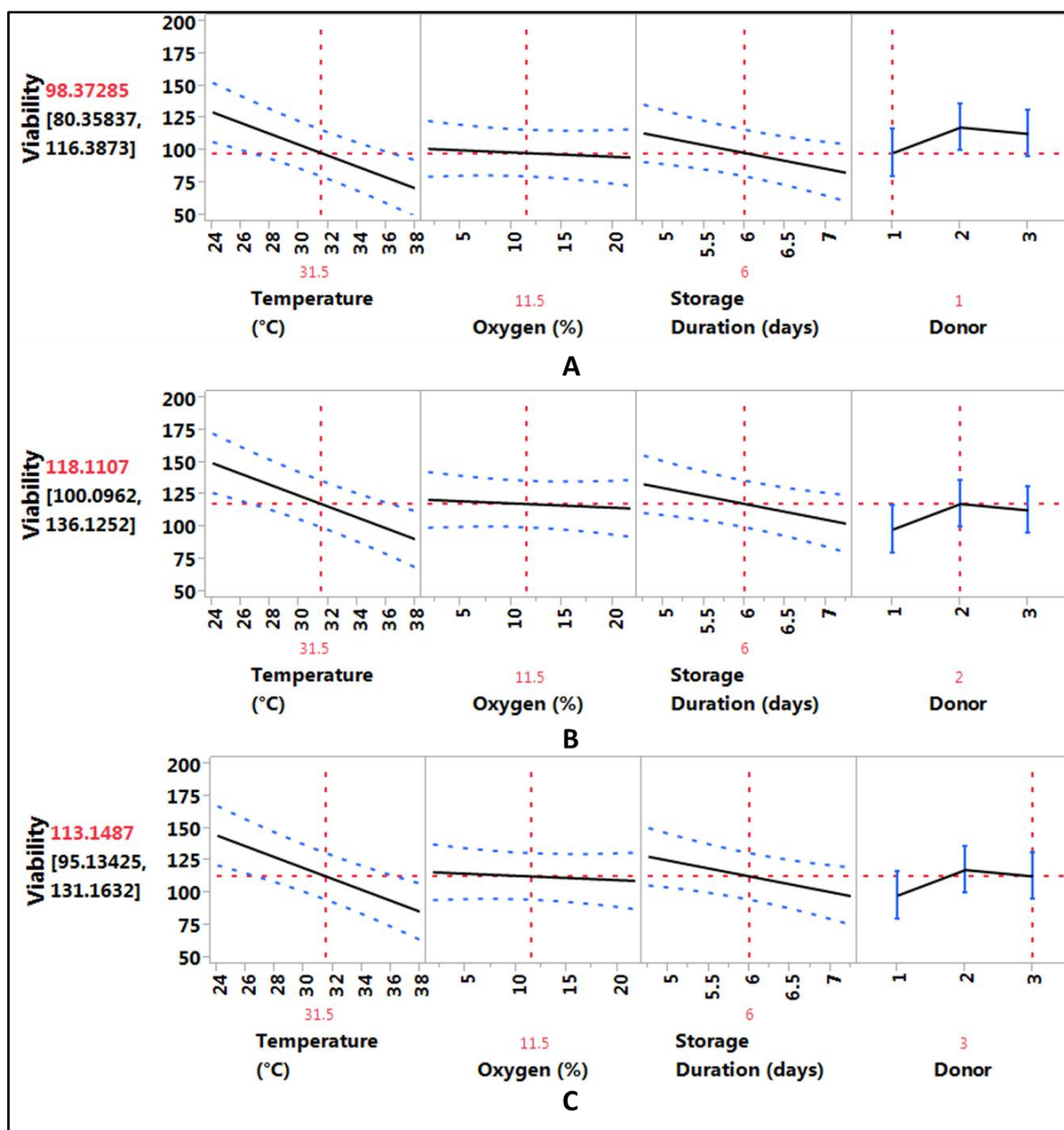


Fig. 3.3 Post-storage viability models for the process space under investigation. Models' parameters estimation performed via least square estimation. Variability values are predicted for temperature range (26-37 °C), oxygen range (3-20%), storage duration 5-7 days and for donor 1 (A), 2 (B) and 3 (C) respectively. In red, viability predicted values for T= 31.5 °C, oxygen= 11.5 % and 6 day storage. Blue dashed lines and blue error bars represent 95 % confidence intervals. Temperature and storage duration have a statistical significant effect on viability, although the former is greater than the latter. Viability decreases as temperature and storage duration increase, while oxygen tension show no significant effect. Samples from the three donors studied showed consistent trends and inter-donor variability was not significant.

Consistently for all three donors, temperature and storage duration have a statistically significant effect on viability ($p=0.0003$ and $p=0.0243$ respectively). Temperature has a greater effect on viability; lowering the temperature will improve the viability of the construct following storage. This is consistent with findings reported by Robinson, Picken & Coopman(2014). Lower temperature reduces cell metabolism as well as nutrient and oxygen demand and the tissue can be preserved 'healthy' for longer. Oxygen does not have a statistically significant effect on viability. It can be hypothesed that, as lowering the temperature reduces cellular metabolism, oxygen demand will also diminish and therefore its value does not impact cell viability after 5 or 7 days storage. The storage length (time) also has an effect on viability but not as strong as temperature (Fig. 3.3a). Viability of cell therapy products tend to diminish with shelf life (Reissis, García-Gareta, Korda, Blunn, & Hua, 2013). As no interactions were statistically significant, temperature effect is independent of time. This translate in two important findings: temperature affects viability over storage period and, regardless of the temperature, viability will diminish with the shelf life of the product. As donor number has no significant effect on the response, it is possible to confirm that all three donors behaved in a consistent manner (Fig.3.3a,3.3b,3.3c).

3.2.2 Analysis of post-storage glucose and lactate response models

Glucose and lactate response models were created using data described in chapter 2. The validity of the glucose response model was checked by analysis of residuals (Fig 3.4).

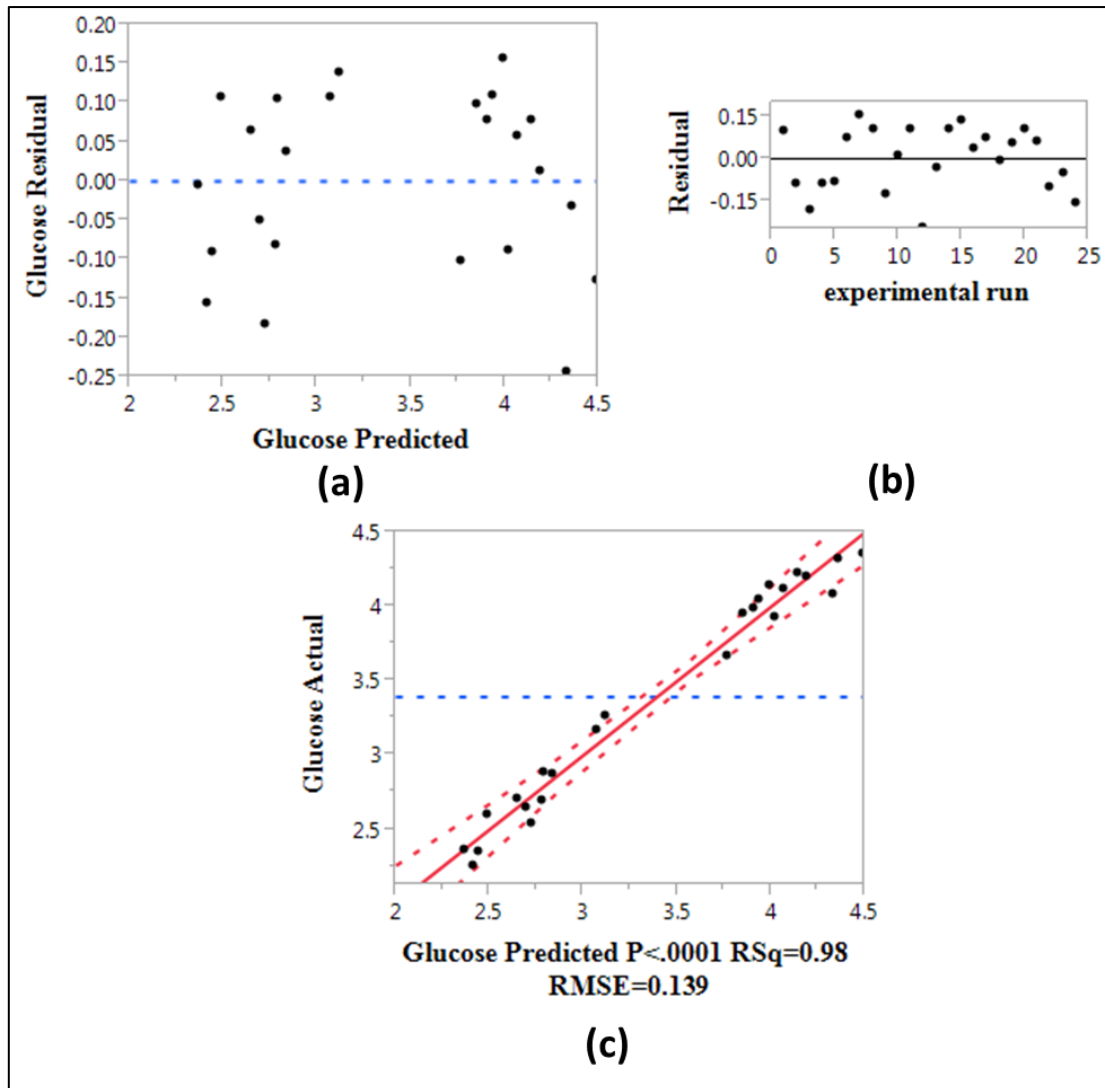


Fig.3.4 Analysis of residuals for glucose model. Residuals are plotted vs glucose predicted values (A) and versus experimental run number (B) to confirm the hypothesis of constant variance. As no trend nor pattern is shown in (A) and (B) the model is valid. (C) shows goodness of fit by plotting glucose actual values versus glucose predicted values. $RSq = r^2$, $RMSE =$ root mean square error.

Once the validity of the model has been confirmed, glucose concentration in spent medium when temperature, oxygen tension and storage duration vary within the investigated ranges can be predicted (Fig. 3.5). Final glucose concentration in spent medium decreases as temperature increases.

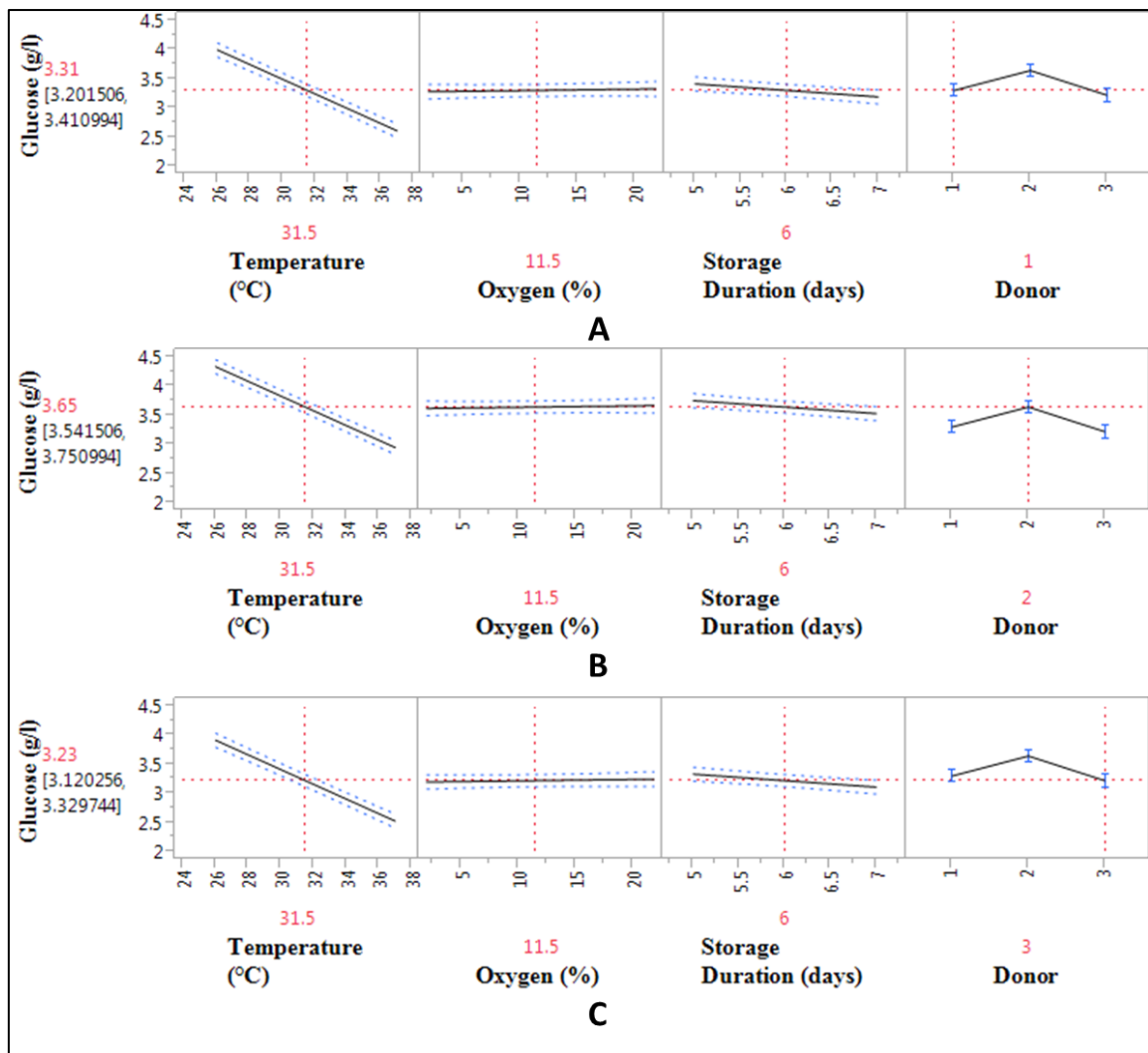


Fig. 3.5 Post-storage glucose concentration models for the process space under investigation. Models' parameters estimation performed via least square estimation. Glucose values are predicted for temperature range (26-37 °C), oxygen range (3-20%), storage duration 5-7 days and for donor 1 (A), 2 (B) and 3 (C) respectively. In red, glucose predicted values for T= 31.5 °C, oxygen= 11.5 % and 6 day storage. Blue dashed lines and blue error bars represent confidence intervals. Temperature and storage duration have a statistical significant effect on glucose consumption, although the former is greater than the latter. Final glucose concentration decreases as temperature and storage duration increase, while oxygen tension did not show significant effect. Samples from the three donors studied showed consistent trends but donor 2 was statistically different.

Consistently for all three donors, temperature and storage duration have a statistically significant effect on glucose metabolism ($p < 0.0001$ and $p = 0.0013$ respectively). Temperature has a greater effect than time. Although glucose concentration will diminish over the storage

duration, temperature at which the cell product is stored is much more important in lowering its consumption. Oxygen has not a strong effect on glucose concentration at the end of the 5 and 7 day storage. This is consistent with the fact that at lower temperature, oxygen demand will also decrease (Corwin et al., 2014). As the difference between donor numbers is statistically significant, it is possible to conclude that all three donors have not consistently metabolized glucose present in the culture medium during storage. No interactions had a statistically significant effect on glucose and, therefore, temperature and storage duration will independently affect glucose concentration in the spent medium.

Similarly to glucose, lactate concentration variation can also be predicted. The validity of the model was checked by residuals analysis (Fig. 3.6).

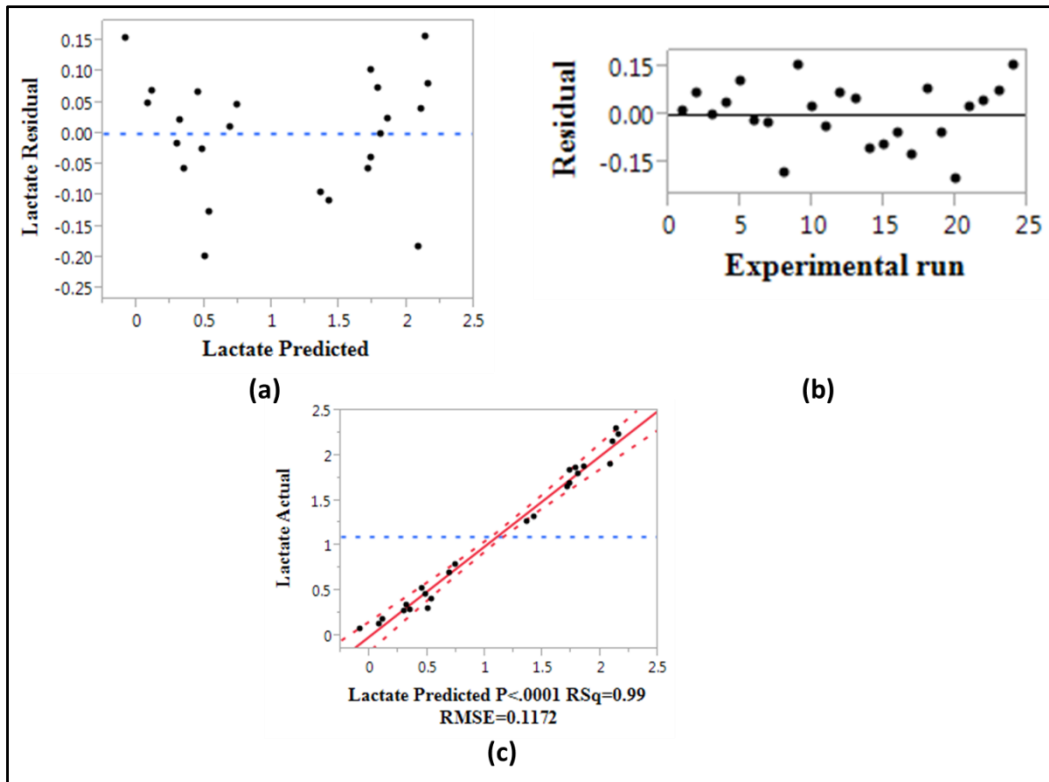


Fig.3.6 Analysis of residuals for lactate model. Residuals are plotted versus lactate predicted values (a) and versus experimental run number (b) to confirm the hypothesis of constant variance. As no trend nor pattern is shown in (a) and (b) the model is valid. (c) shows goodness of fit by plotting lactate actual values versus lactate predicted values. $RSq = r^2$, $RMSE = \text{root mean square error}$.

Once the validity of the model has been confirmed, lactate concentration in spent medium within the investigated range was predicted (Fig. 3.7). Consistently with glucose variation, lactate concentration increased with temperature and storage length.

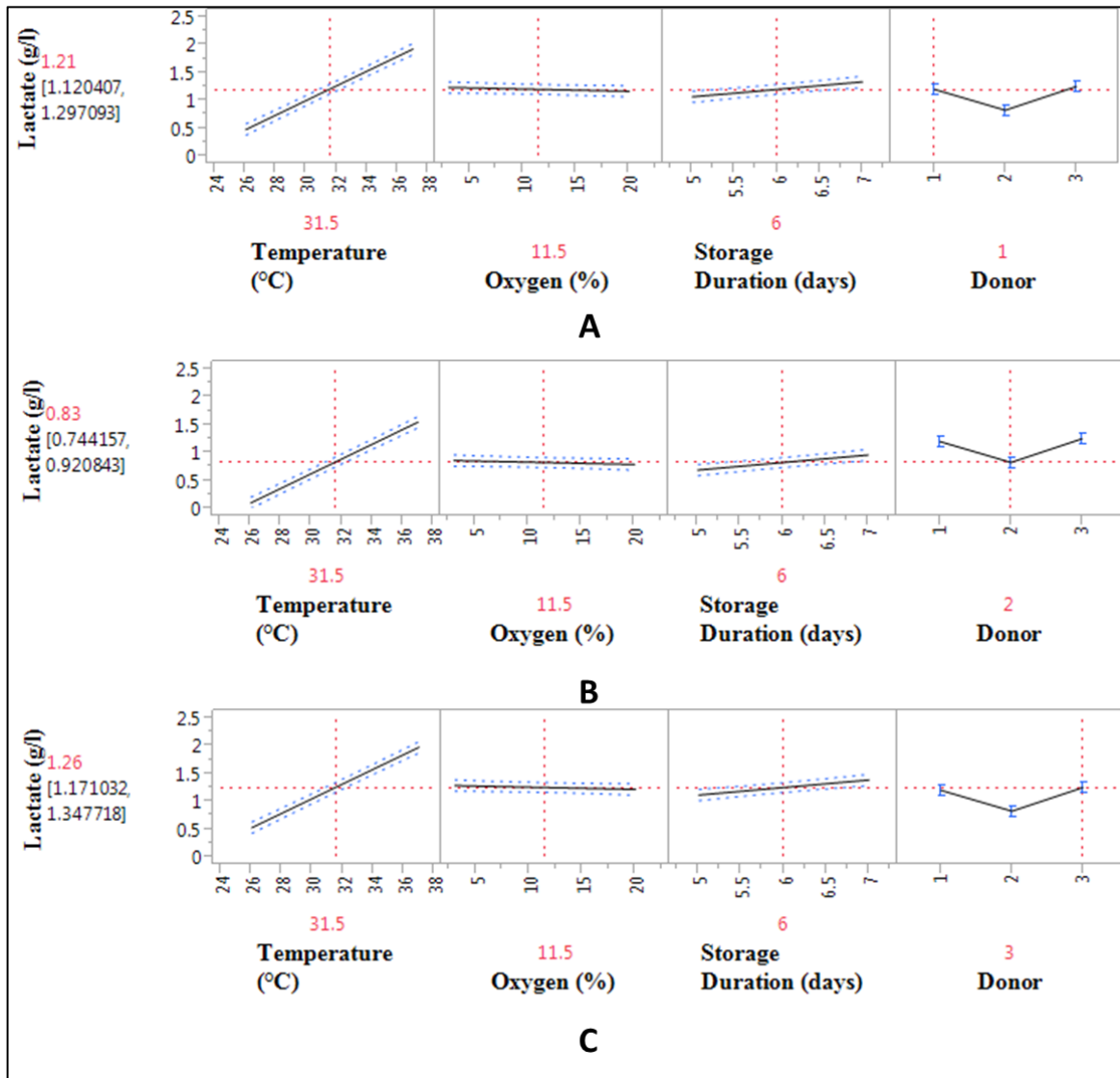


Fig.3.7 Post-storage lactate concentration models for the process space under investigation. Models' parameters estimation performed via least square estimation. Lactate values are predicted for temperature range (26-37 °C), oxygen range (3-20%), storage duration 5-7 days and for donor 1 (A), 2 (B) and 3 (C) respectively. In red, lactate predicted values for T= 31.5 °C, oxygen= 3-20 % and 6 day storage. Blue dashed lines and blue error bars represent confidence intervals. Temperature and storage duration have a statistical significant effect on lactate release, although the former is greater than the latter. Post storage concentration increases as temperature and storage duration increase, while oxygen tension did not show significant effect. Samples from the three donors studied showed consistent trends but donor 2 was statistically different.

Consistently for all three donors, temperature ($p < 0.0001$) and storage duration ($p < 0.0001$) had a statistically significant effect on lactate production (Fig. 3.7). This is consistent with the observed glucose metabolism. Temperature has a much greater effect than time. While oxygen does not have a significant effect on lactate production, its interaction with temperature is statistically significant ($p = 0.03$) (Fig. 3.8). This translates in the fact that oxygen will have an impact on lactate production which is dependent on the temperature; decreasing the oxygen tension from 20 % to 3 % during storage leads to an increased lactate production both at 5 and at 7 day storage.

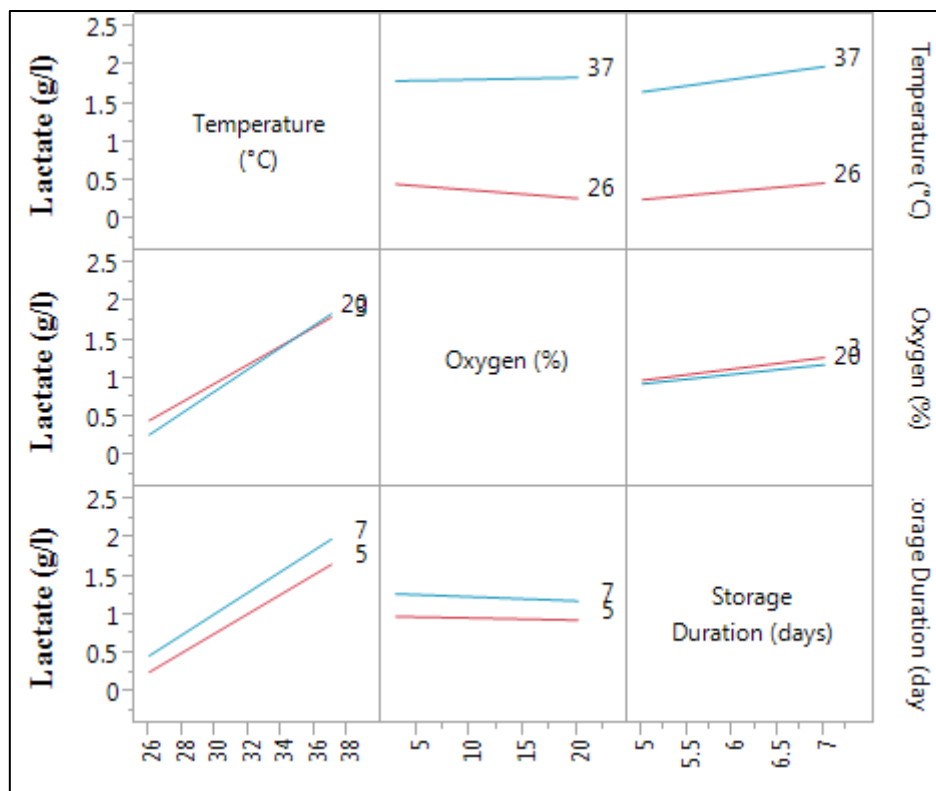


Fig. 3.8 Interaction plots for post storage lactate concentration model. All possible combinations of input variables (temperature, oxygen and storage duration) are shown. For each variable, red line represents low levels while blue line represents high levels. Statistically significant interactions towards post storage lactate concentration are represented by crossing lines. Oxygen and temperature interaction was statistically significant.

3.2.3 Analysis of post-storage glutamine and ammonia response models

Glutamine is a non essential amino acid which is hydrolysed by glutaminase yielding glutamate and ammonia as waste products (Schop et al., 2009). In addition to glucose, glutamine can also be used to generate cellular energy. Glutamine concentration (mM) in spent medium was modelled using data described in chapter 2.

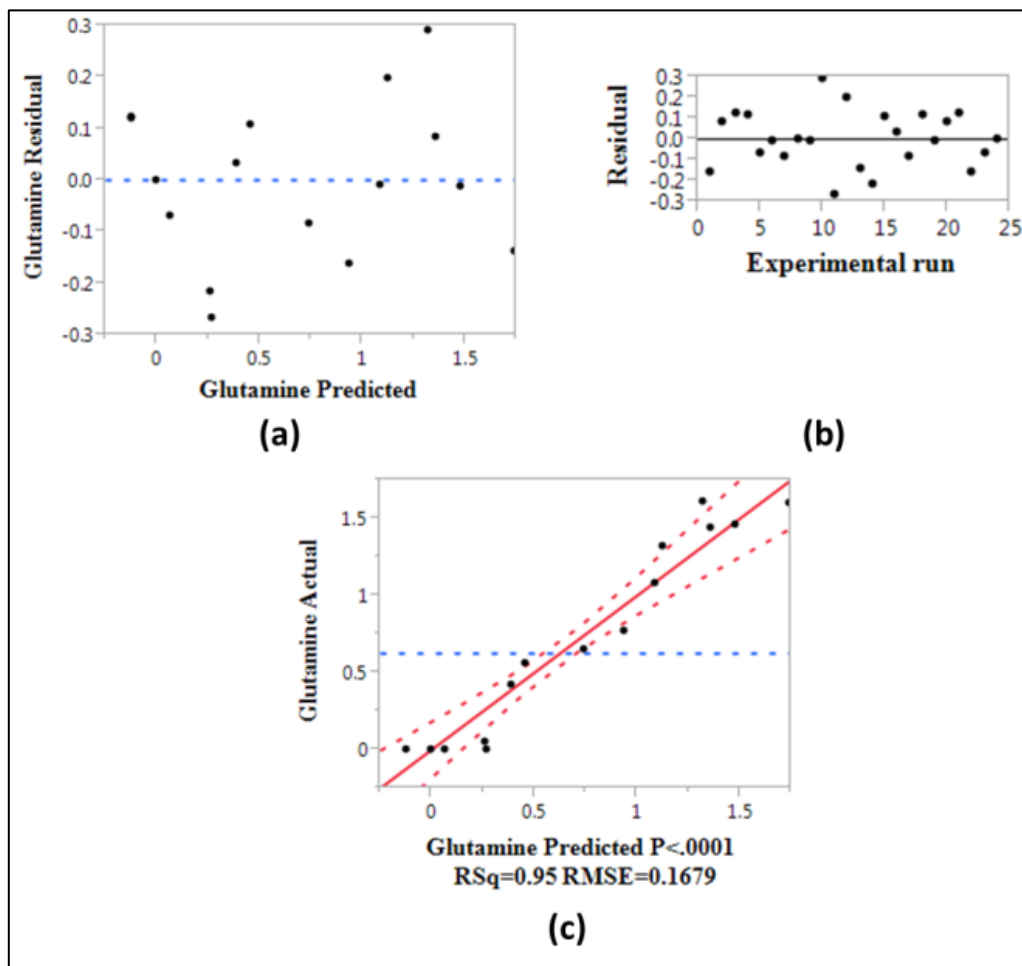


Fig 3.9 Analysis of residuals for glutamine model. Residuals are plotted vs glutamine predicted values (a) and versus experimental run number (b) to confirm the hypothesis of constant variance. As no trend nor pattern is shown in (a) and (b) the model is valid. (c) shows goodness of fit by plotting glutamine actual values versus glutamine predicted values. $RSq = r^2$, $RMSE = \text{root mean square error}$.

Once the validity of the model has been confirmed, it was possible to evaluate main effect and potential interactions which have a statistically significant effect on glutamine (Fig. 3.10).

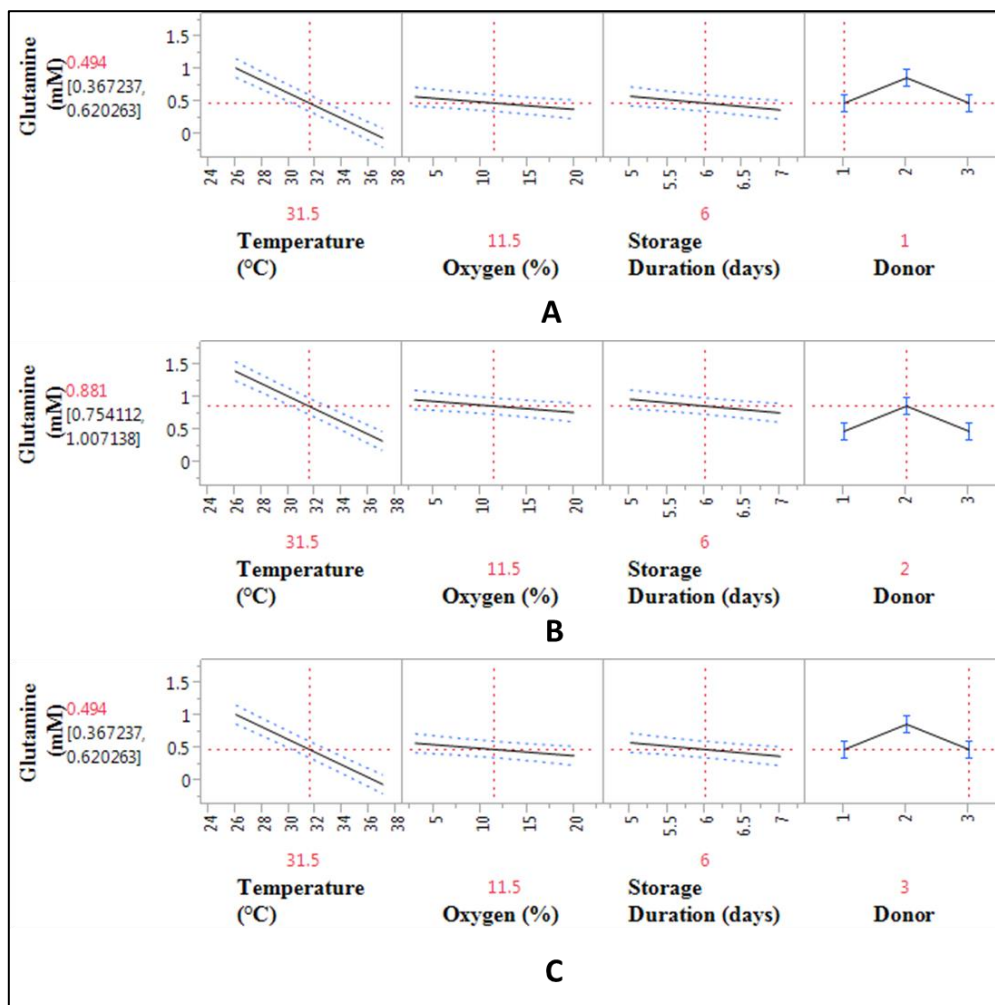


Fig. 3.10 Post-storage glutamine concentration models for the process space under investigation. Models' parameters estimation performed via least square estimation. Glutamine values are predicted for temperature range (26-37 °C), oxygen range (3-20%), storage duration 5-7 days and for donor 1 (A), 2 (B) and 3 (C) respectively. In red, glutamine predicted values for T= 31.5 °C, oxygen= 3-20 % and 6 day storage. Blue dashed lines and blue error bars represent confidence intervals. Temperature, oxygen and storage duration have a statistical significant effect on glutamine consumption, although the former is much greater. Post storage glutamine concentration decreases as temperature, oxygen and storage duration increase. Samples from the three donors studied showed consistent trends but donor 2 was statistically different.

Consistently for all three donors, temperature ($p < 0.0001$), oxygen ($p < 0.0127$) and storage length ($p = 0.0082$) have significant effect on glutamine metabolism (Fig 3.10). As temperature and time interaction was also significant ($p = 0.0213$), the effect of temperature on glutamine metabolism will depend on the storage length and in particular it will be greater for longer storage period. As shown in Fig. 3.10, temperature has a much greater impact than time and oxygen decreasing glutamine. As it can be also noticed in Fig 3.10, donor #2 shows a statistically significant difference compared to donor #1 and donor #3 which is probably due to the difference in terms of number of cells per disc. Closely linked to glutamine metabolism, post-storage ammonia concentration in spent medium was also analysed.

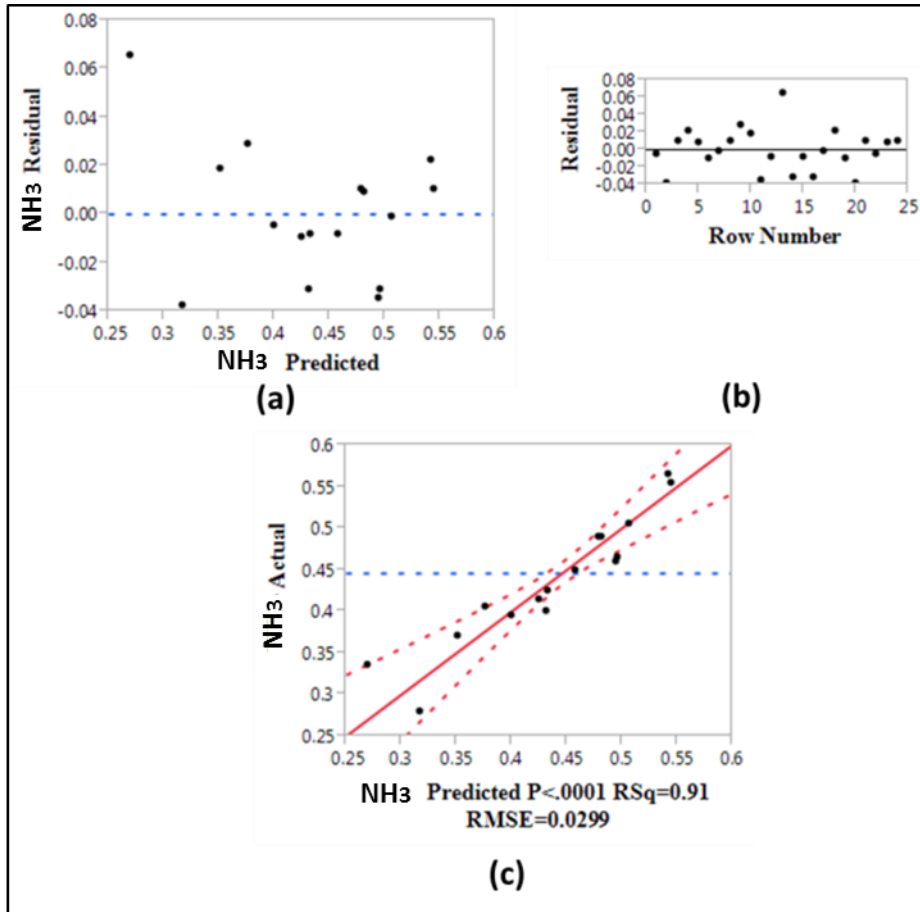


Fig. 3.11 Analysis of residuals for NH₃ model. Residuals are plotted vs ammonia predicted values (a) and versus experimental run number (b) to confirm the hypothesis of constant variance. As no trend nor pattern is shown in (a) and (b) the model is valid. (c) shows goodness of fit by plotting ammonia actual values versus ammonia predicted values. $RSq = r^2$, $RMSE = \text{root mean square error}$.

Once the validity of the model has been checked, the concentration of ammonia in the spent medium was predicted (Fig. 3.12).

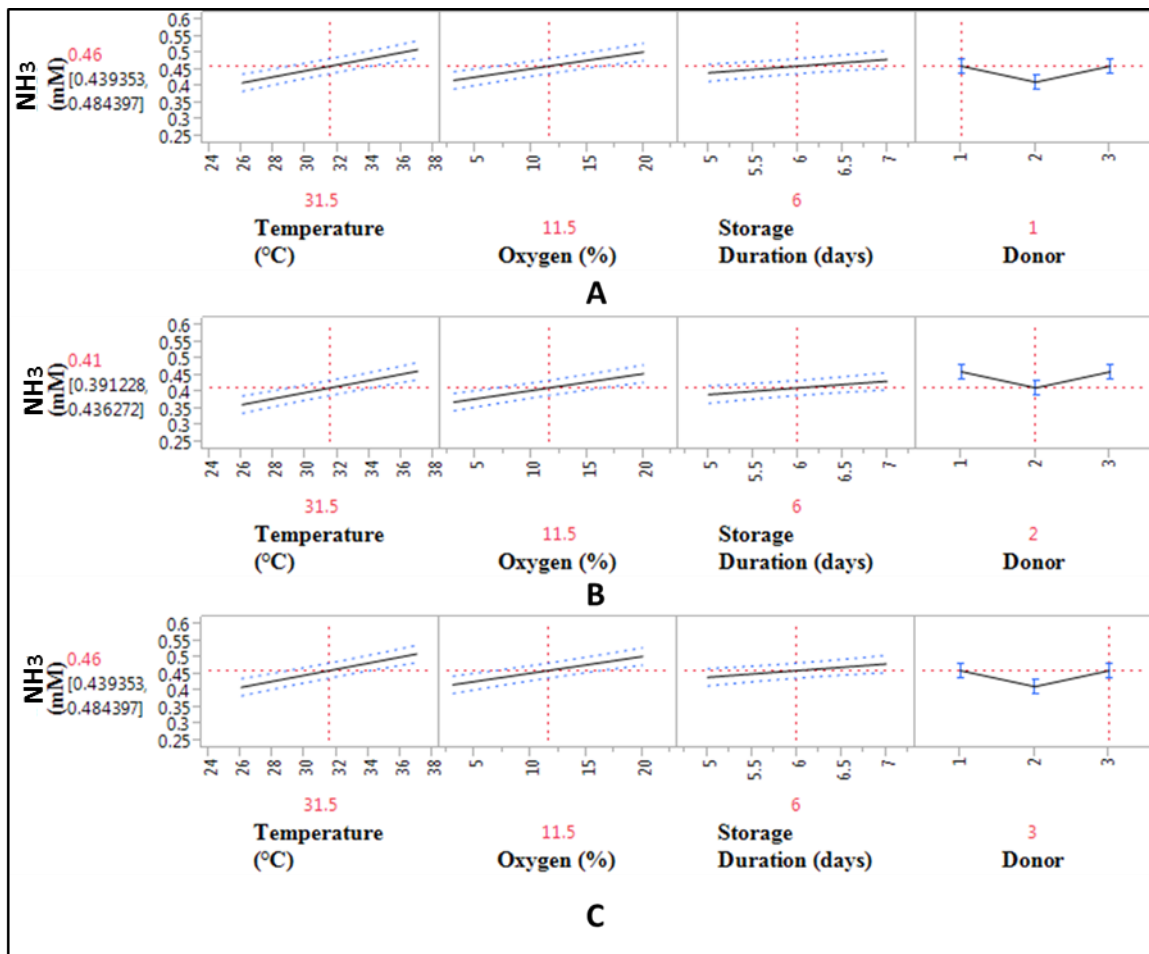


Fig.3.12 Post-storage NH₃ concentration models for the process space under investigation. Models' parameters estimation performed via least square estimation. NH₄⁺ values are predicted for temperature range (26-37 °C), oxygen range (3-20%), storage duration 5-7 days and for donor 1 (A), 2 (B) and 3 (C) respectively. In red, NH₄⁺ predicted values for T= 31.5 °C, oxygen= 3-20 % and 6 day storage. Blue dashed lines and blue error bars represent confidence intervals. Temperature, oxygen and storage duration have a statistical significant effect on ammonia release, although the former is greater. Post storage ammonia concentration increases as temperature, oxygen and storage duration increase, while oxygen tension did not show significant effect. Samples from the three donors studied showed consistent trends but donor 2 was statistically different.

Consistently for all three donors, temperature ($p < 0.0001$), oxygen ($p < 0.0001$) and storage length ($p = 0.0051$) significantly affected ammonia production. The interaction temperature-time was also statistically significant, consistently with glutamine (Fig. 3.13).

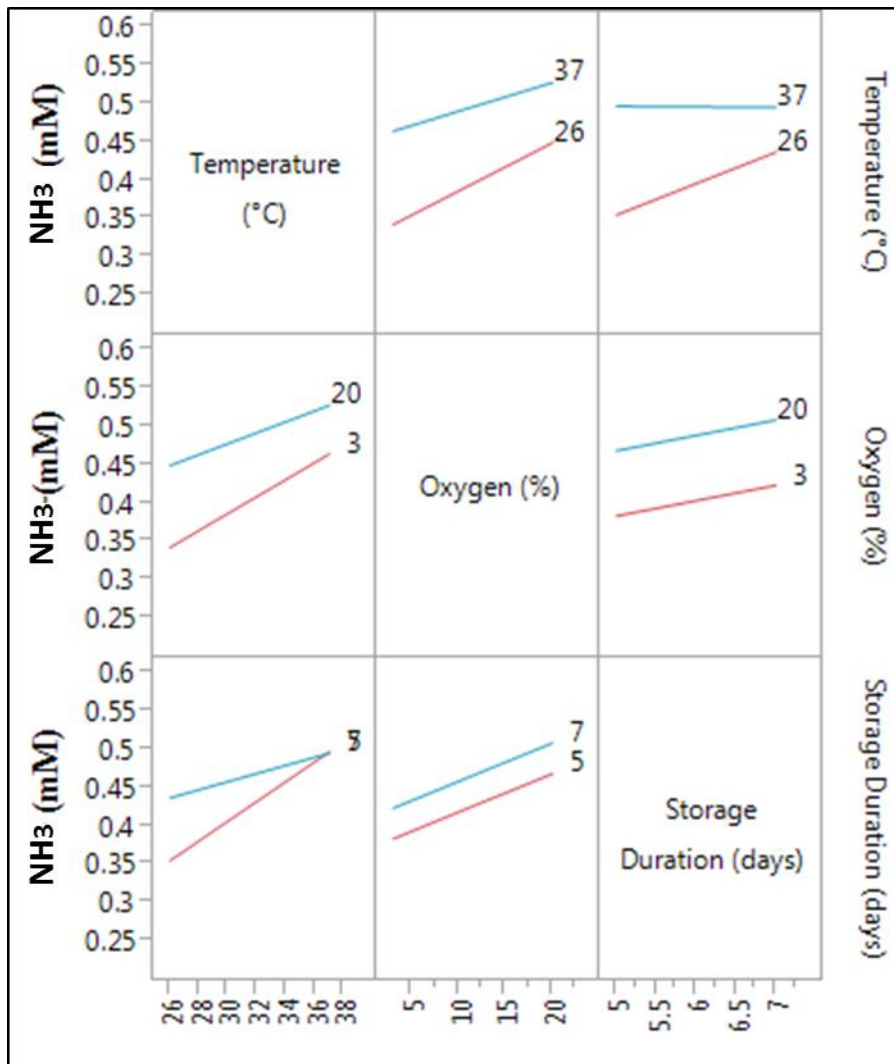


Fig. 3.13 Interaction plots for post storage NH₃ concentration model. All possible combinations of input variables (temperature, oxygen and storage duration) are shown. For each variable, red line represents low levels while blue line represents high levels. Statistically significant interactions towards post storage lactate concentration are represented by crossing lines. Oxygen and temperature interaction was statistically significant.

Interestingly, Fig. 3.12 shows that the effect of temperature and oxygen on ammonia production is greater than the storage duration, unlike for glutamine. For both glutamine and NH₃, all three input variables (temperature, oxygen tension and storage length) are statistically significant as well as temperature and time interaction. This suggests that storage parameters can be engineered in order to guide cells towards a specific metabolic pathway

(glucose or glutamine metabolism), minimize waste product release and improve cell product preservation during storage.

3.2.4 Analysis of post-storage gene expressions response models

Other than viability, preservation of biological function of cell therapy product is important to prove safety and efficacy of the medicinal product. In this study, it has been assumed that the mechanism of action for this product would be to engraft and stimulate regeneration of cartilage. Gene expression was therefore considered a potential potency assay, linked to the biological property of the tissue. For cartilage tissue, it is important to retain *COL2A1* and *ACAN* expression, while the expression of fibroblast genes like *COL1A1* should be minimal. Initially, the validity of the *COL2A1* response model was checked by residual analysis (Fig.3.14).

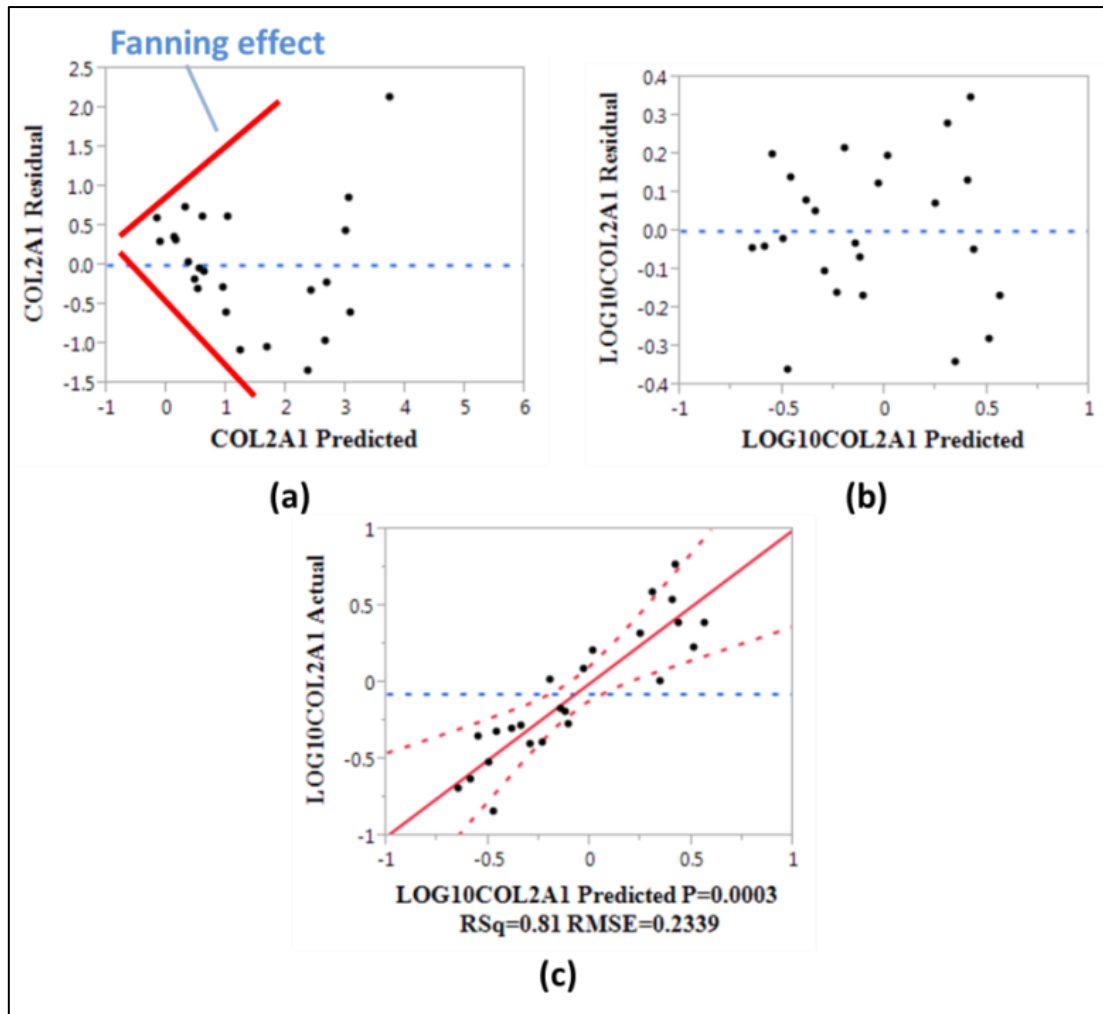


Fig. 3.14 Analysis of residuals for *COL2A1* model. Residuals are plotted vs *COL2A1* predicted values (a). Residuals showed uneven spreading (fanning effect) which violates the assumption of constant variance. *COL2A1* values were transformed by \log_{10} . Residuals for the transformed *COL2A1* values ($\text{LOG}_{10}\text{COL2A1}$) are plotted versus predicted $\text{LOG}_{10}\text{COL2A1}$ (b). No fanning is shown in (b) and the model can therefore be considered valid. (c) shows goodness of fit by plotting $\text{LOG}_{10}\text{COL2A1}$ actual values versus predicted values. $\text{RSq} = r^2$, $\text{RMSE} = \text{root mean square error}$.

At first, residuals showed a pattern, known as “fanning” where the variance increases with the predicted values (Fig 3.14a). This effect highlights that the variance is not constant within residuals (Montgomery, 2012). *COL2A1* values were then transformed by \log_{10} . The fanning effect was removed and residuals showed no trends (Fig.3.14b).

Fig. 3.15 shows the variation of $\text{Log}_{10}\text{COL2A1}$ within the range of temperature, oxygen and storage duration considered. Temperature, oxygen and storage duration did not have a statistically significant effect on the expression of *COL2A1*. Furthermore, *COL2A1* variation was characterized by very high donor to donor variability.

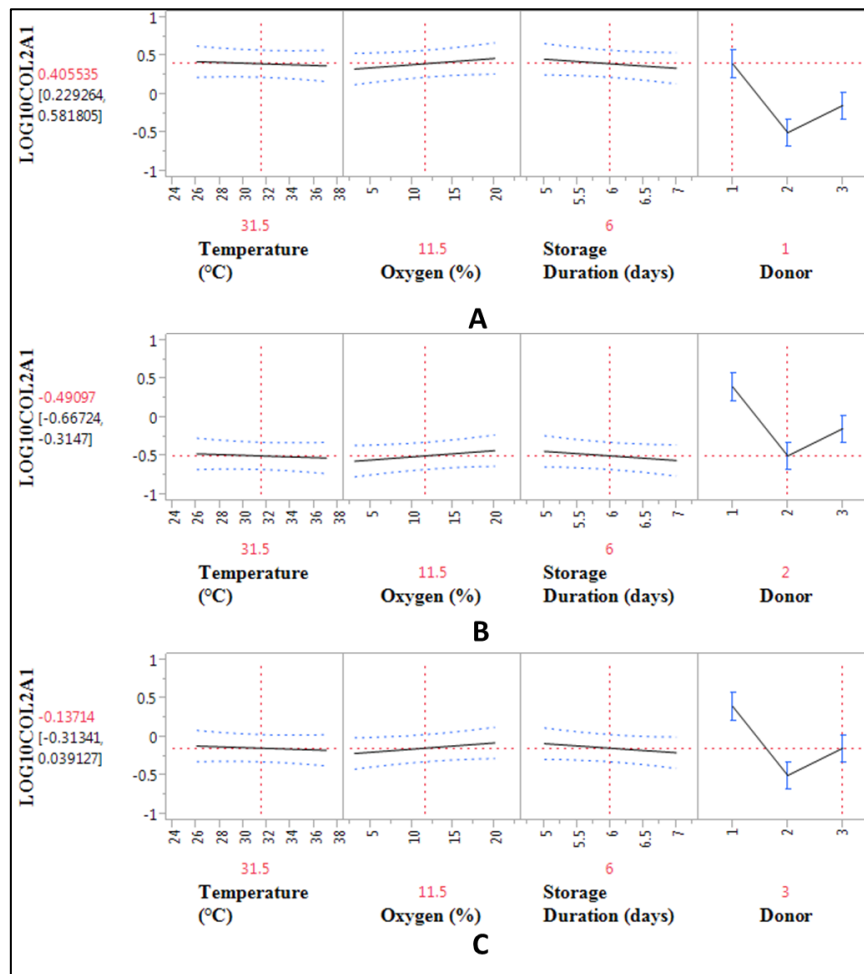


Fig. 3.15 Post storage *COL2A1* expression fold change relative to non-stored samples models for the process space under investigation. Fold change values were transformed by log_{10} . Models' parameters estimation performed via least square estimation. Log_{10} of *COL2A1* fold change values are predicted for temperature range (26-37 °C), oxygen range (3-20%), storage duration 5-7 days and for donor 1 (A), 2 (B) and 3 (C) respectively. In red, log_{10} fold changes *COL2A1* predicted values for T= 31.5 °C, oxygen= 3-20 % and 6 day storage. Blue dashed lines and blue error bars represent confidence intervals. Temperature, oxygen tension and storage duration did not have a statistical significant effect on *COL2A1* expression. Samples from the three donors studied showed consistent trends but donor 1 expressed higher *COL2A1* values compared to donor 2 and 3.

Similarly to *COL2A1*, *ACAN* variation was also modelled. To test the validity of the model, residuals have been plotted and analysed (Fig 3.16a). Fanning was also present here as in *COL2A1* and data were then transformed by log₁₀. Fanning effect was removed and residuals were randomly distributed (Fig. 3.16b).

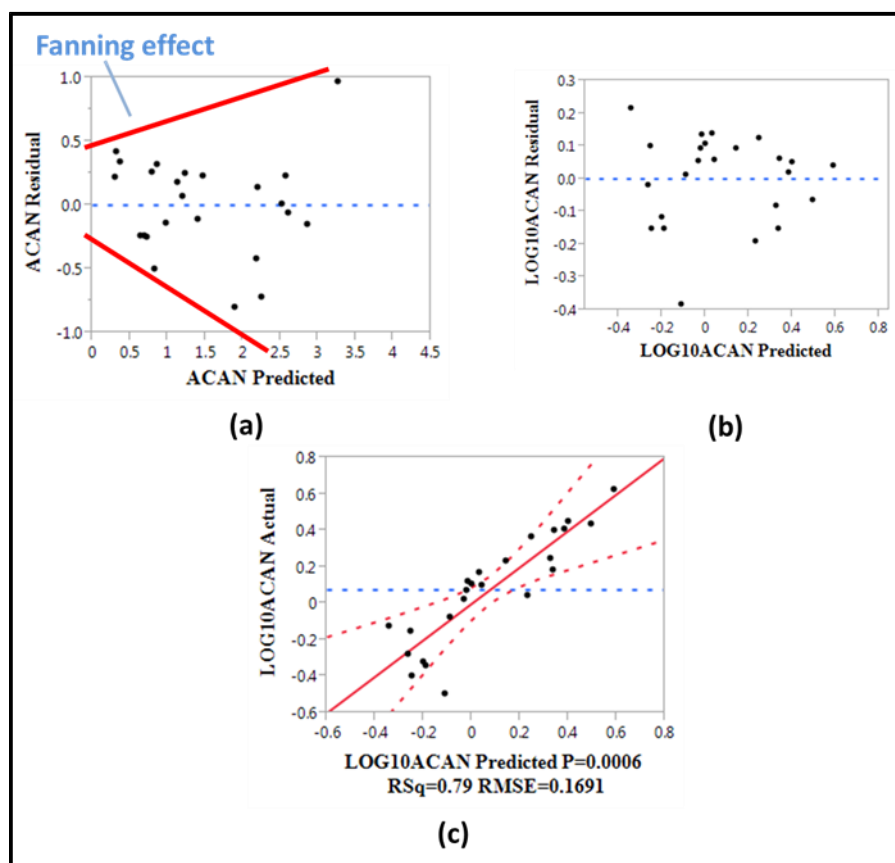


Fig. 3.16 Analysis of residuals for *ACAN* model. Residuals are plotted vs *ACAN* predicted values (a). Residuals showed uneven spreading (fanning effect) which violates the assumption of constant variance. *ACAN* values were transformed by log₁₀. Residuals for the transformed *ACAN* values (LOG10ACAN) are plotted versus predicted LOG10ACAN (b). No fanning is shown in (b) and the model can therefore be considered valid. (c) shows goodness of fit by plotting LOG10ACAN actual values versus predicted values. RSq= r², RMSE=root mean square error.

The expression of *ACAN* increased with temperature and oxygen while it decreases with storage duration but none of these factors were statistically significant (Fig. 3.18).

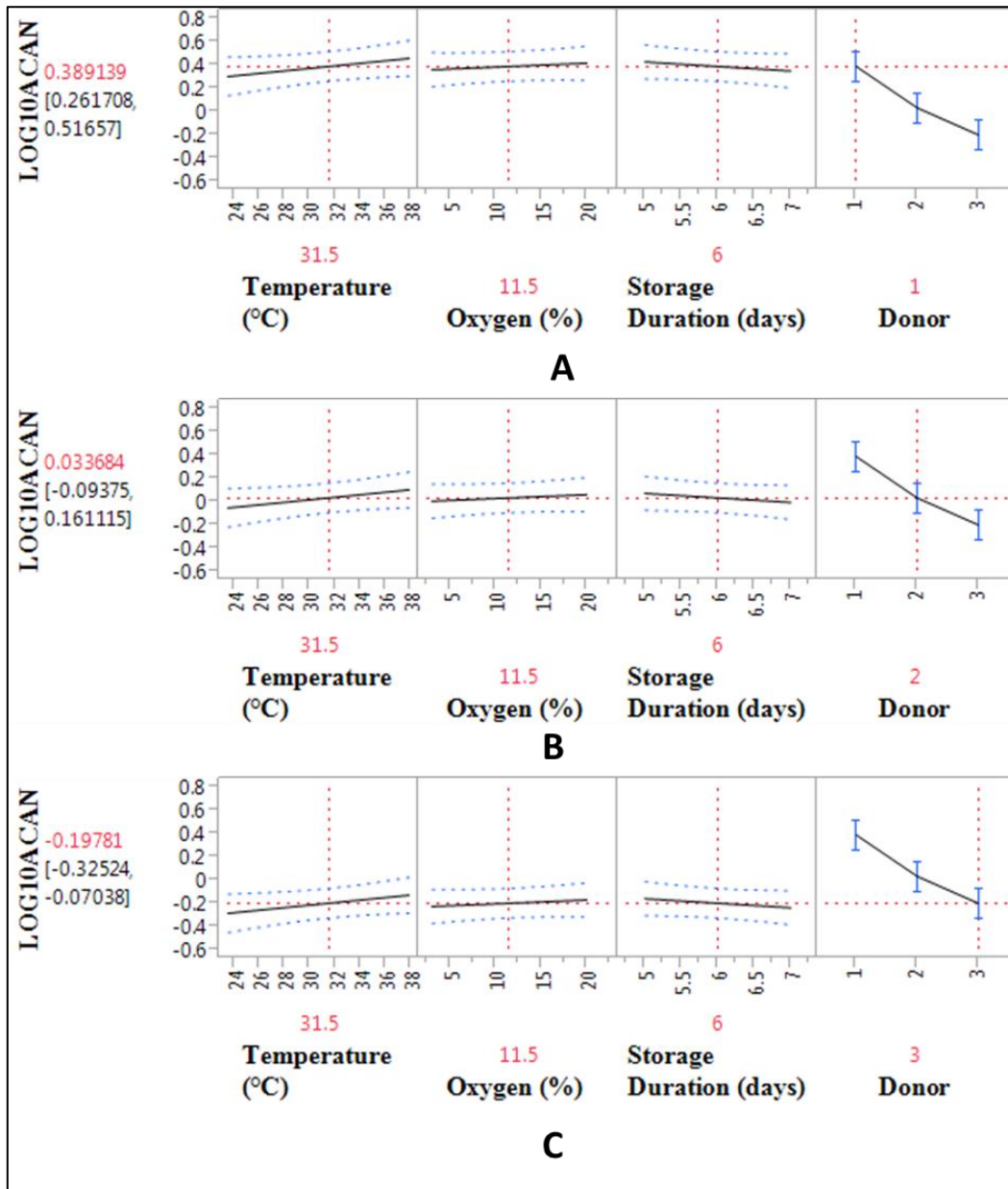


Fig. 3.17 Post storage ACAN expression fold change relative to non-stored samples models for the process space under investigation. Fold change values were transformed by log10. Models' parameters estimation performed via least square estimation. Log10 of ACAN fold change values are predicted for temperature range (26-37 °C), oxygen range (3-20%), storage duration 5-7 days and for donor 1 (A), 2 (B) and 3 (C) respectively. In red, log10 fold changes ACAN predicted values for T= 31.5 °C, oxygen= 3-20 % and 6 day storage. Blue dashed lines and blue error bars represent confidence intervals. Temperature, oxygen tension and storage duration did not have a statistical significant effect on ACAN expression. Samples from the three donors studied showed consistent trends but donor 1 was statistically different.

COLIA1 model was also analysed (Fig. 3.18a). Due to the presence of fanning in the residuals, *COLIA1* data points were transformed by \log_{10} ($\text{LOG}_{10}\text{COLIA1}$) (Fig.3.18b).

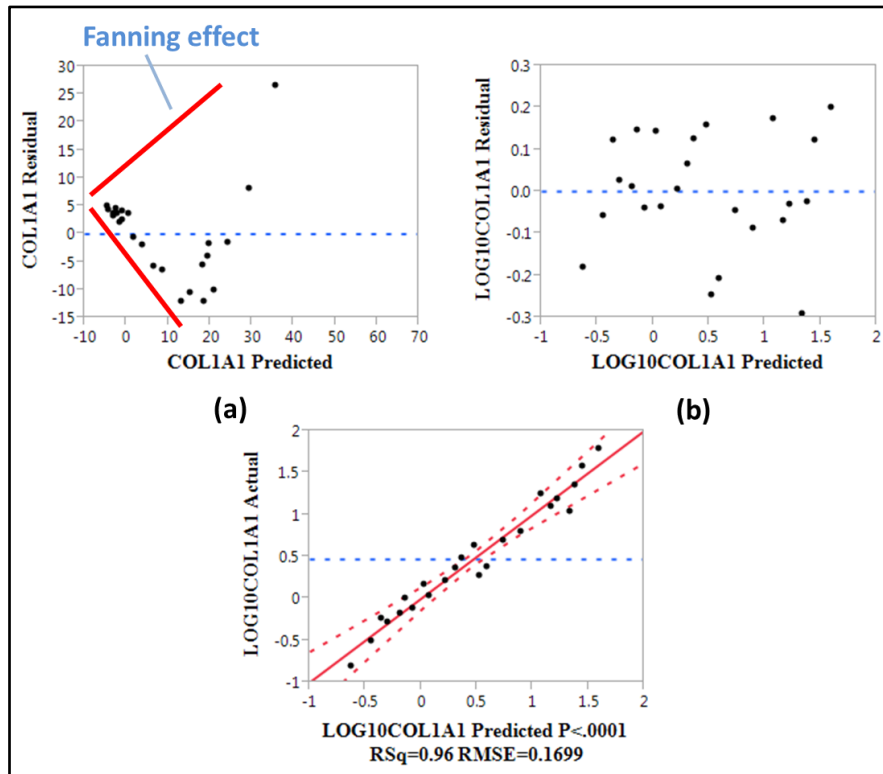


Fig. 3.18 Analysis of residuals for *COLIA1* model. Residuals are plotted vs *COLIA1* predicted values (a). Residuals showed uneven spreading (fanning effect) which violetes the assumption of constant variance. *COLIA1* values were transformed by \log_{10} . Residuals for the transformed *COLIA1* values ($\text{LOG}_{10}\text{COLIA1}$) are plotted versus predicted $\text{LOG}_{10}\text{COLIA1}$ (b). No fanning is shown in (b) and the model can therefore be considered valid. (c) shows goodnees of fit by plotting $\text{LOG}_{10}\text{COLIA1}$ actual values versus predicted values. $\text{RSq} = r^2$, $\text{RMSE} = \text{root mean square error}$.

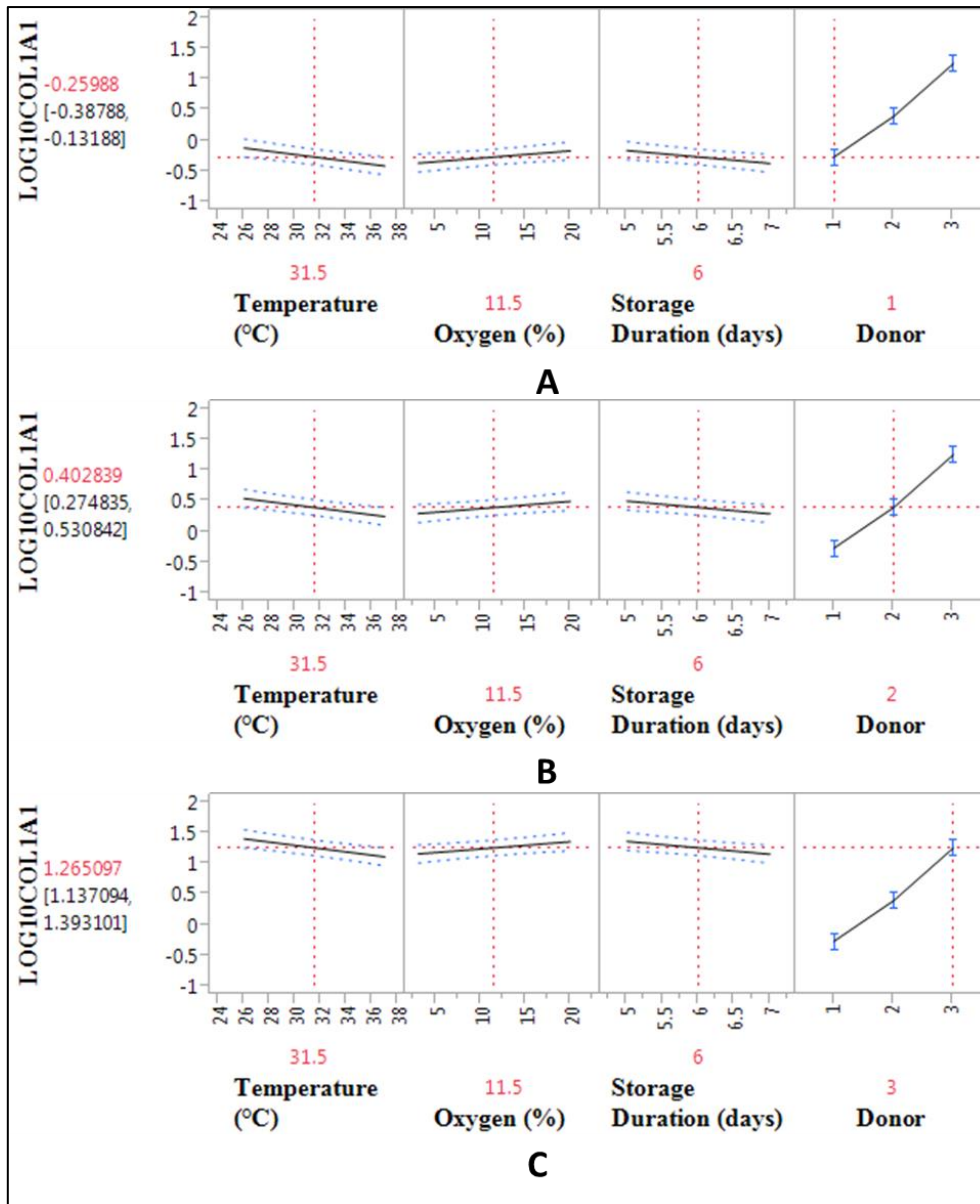


Fig. 3.19 Post storage COL1A1 expression fold change relative to non-stored samples models for the process space under investigation. Fold change values were transformed by log₁₀. Models' parameters estimation performed via least square estimation. Log₁₀ of COL1A1 fold change values are predicted for temperature range (26-37 °C), oxygen range (3-20%), storage duration 5-7 days and for donor 1 (A), 2 (B) and 3 (C) respectively. In red, log₁₀ fold changes COL1A1 predicted values for T= 31.5 °C, oxygen= 3-20 % and 6 day storage. Blue dashed lines and blue error bars represent confidence intervals. Temperature, oxygen tension and storage duration did not have a statistical significant effect on COL2A1 expression. Samples from the three donors studied showed consistent trends but were statistically different.

Temperature ($p < 0.0007$), storage duration ($p = 0.0086$) and oxygen (0.0114) were all statistically significant. Unlike *COL2A1* and *ACAN* which were upregulated, *COL1A1* was also down regulated for donor #1 compared to the other donors. This can be explained by the highest proliferation of the cells in the transwell which correlates to better chondrogenesis and, therefore, reduced expression of *COL1A1*. Storage conditions can therefore be engineered to preserve a chondrogenic-like phenotype and minimize the expression of fibroblastic genes like *COL1A1*.

It was interesting to notice that preferential storage conditions in terms of viability, lactate and ammonia production, *COL2A1* and *ACAN* production are the ones that lead to upregulation of *COL1A1*, which should be minimal for cartilage-like tissue. This suggests that multiple factors should not be analysed nor controlled independently as the preferred outcome might only be achieved by adequately combining input factors. This concept is the basis for the following case studies.

3.3 Linearity testing and centre points

Response models described in this chapter assume the presence of a linear relationship between input and output factors. In order to further investigate this linearity, two additional cartilage discs, cultured as described in 3.1.3, were stored at 31.5 °C, 11.5 % oxygen for 6 days (centre points storage conditions). Viability, glucose, lactate, glutamine, ammonia and gene expression changes were measured following storage under these centre point conditions. Results are shown in table 3.3.

Table 3.3 Centre points response values. CP1 (centre point 1), CP2 (centre point 2). Values are expressed as mean \pm SEM for three technical replicates from one healthy donor

	Viability	Glucose	Lactate	Glutamine	Ammonia	<i>COL2A1</i>	<i>ACAN</i>	<i>COL1A1</i>
CP1	0.05 \pm 0.006	3.36 \pm 0.075	1.11 \pm 0.035	0.445 \pm 0.045	0.73 \pm 0.41	8.10 \pm 0.44	0.41 \pm 0.29	1.69 \pm 0.33
CP2	0.04 \pm 0.002	3.34 \pm 0.053	1.18 \pm 0.045	0.34 \pm 0.061	0.75 \pm 0.032	7.15 \pm 0.33	0.47 \pm 0.43	1.72 \pm 0.41

These center points were added to the 2³ full factorial design. Response models were checked again to identify potential lack of fit due to the centre points. Fig. 3.20 compares viability response models with and without centre points.

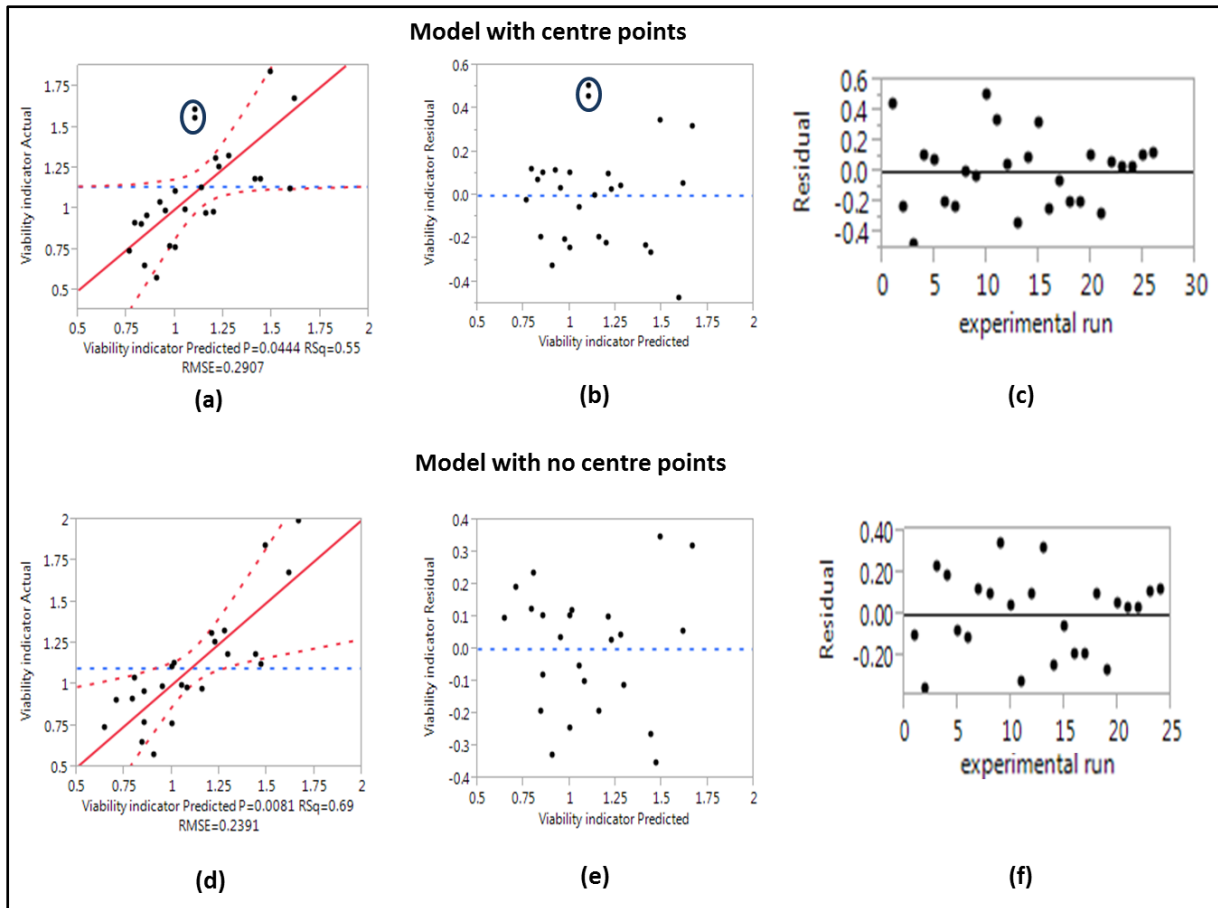


Fig. 3.20 Center points analysis on viability model. (Top) Viability model with center points. Viability values measured plotted versus predicted values showing the presence of two outliers which correspond to center points (blue circle) (a) Lack of fit due to center points was observed. Residuals are plotted versus predicted values (b) and versus experimental run (c), confirming the presence of outliers (centre points). (Bottom) Viability model after center points removal (d). No lack of fit was observed. Residuals plotted versus predicted values (e) and experimental run (f) showed no correlations and no trends confirming the hypothesis of constant variance.

Lack of fit due to centre points was observed. The presence of lack of fit due to center points leads to hypothesis of curvature in the system (i.e. non linear relationship between input and output parameters). However, this would require additional data points. As this was not possible in this study, linearity was assumed correct and lack of fit introduced by centre points due to time-dependent variation not captured by the model. This could be explained by the fact that these centre points were performed at a later time.

3.4 Case study 1

The eight response models described in this chapter highlight that parameters have a contrasting effect on the biological properties of the cell product following storage. When used in combinations, these models can provide useful information about the biological properties of the product while reducing the number of experiments. Assuming the storage of the cell therapy product under investigation in two simulated storage conditions (A and B), the response models were used to predict the output values given these combinations of input factors. Results are shown in Fig. 3.21 for storage condition A and Fig.3.22 for storage condition B.

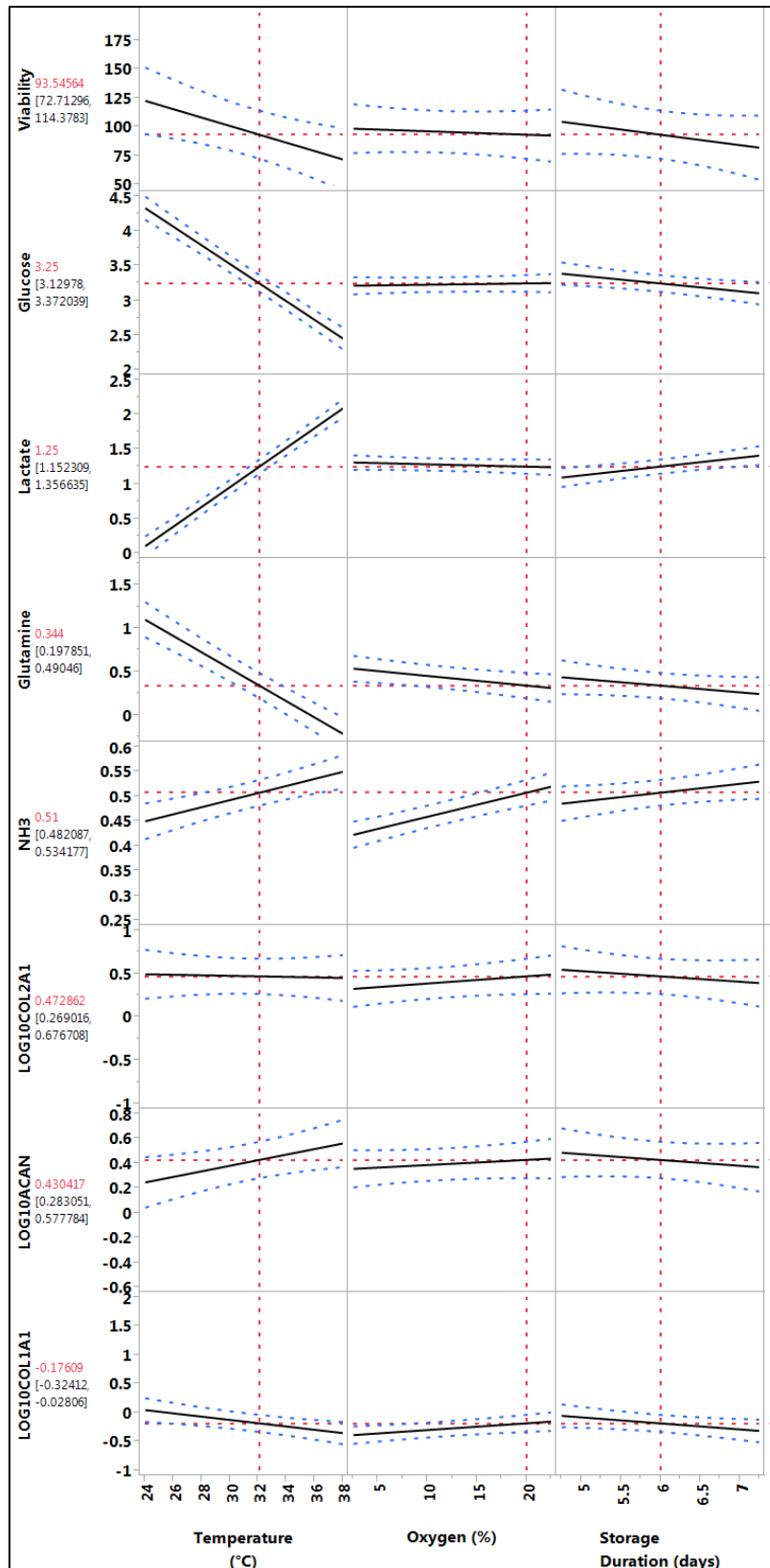


Fig. 3.21 Output values prediction for simulated storage condition A ($T = 32\text{ }^{\circ}\text{C}$, oxygen = 20 %, storage duration= 6 days). Vertical red dashed lines indicate selected input values in the Profiler function in JMP SAS software. Horizontal red dashed lines represent output predicted values for each response variable. Predicted values are also indicated in red for each response variable with 95 % confidence intervals (CIs). Blue dashed lines represent 95 % CIs for the predicted values within the investigated range of input factors.

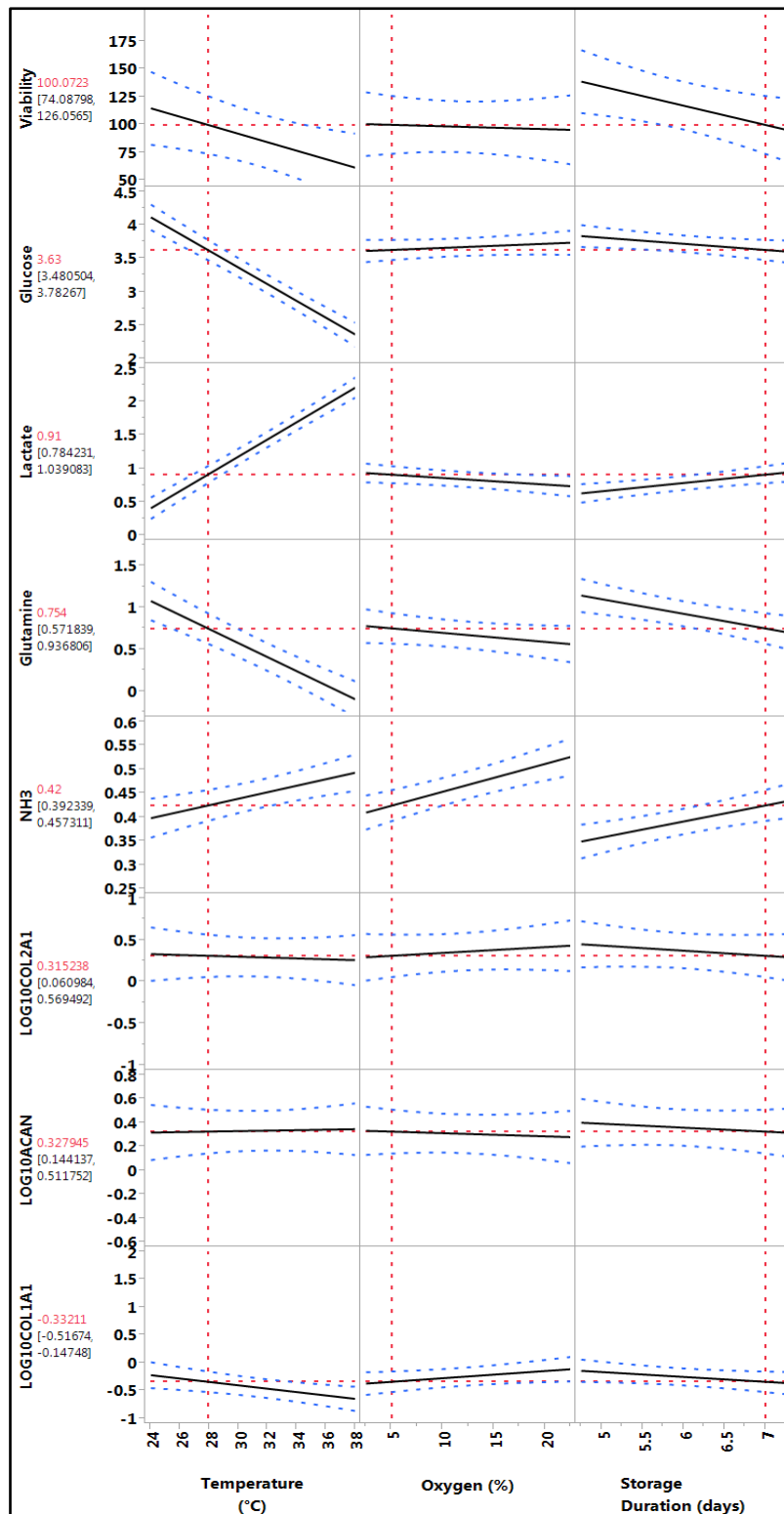


Fig. 3.22 Output values prediction for simulated storage condition B (T=28 °C, oxygen = 5 %, storage duration= 7 days). Vertical red dashed lines indicate selected input values in the Profiler function in JMP SAS software. Horizontal red dashed lines represent output predicted values for each response variable. Predicted values are also indicated in red for each response variable with 95 % confidence intervals (CIs). Blue dashed lines represent 95 % CIs for the predicted values within the investigated range of input factors.

These predicted values can then be compared to acceptance criteria established for that product during clinical development and support the establishment of a successful storage solution. Although confirmatory and validation experiments will be necessary, this will considerably reduce the number of experiments needed during the procurement phase of the container.

3.5 Case study 2

Similarly to what was described in 3.2.5, the response models can be used to identify the optimal input parameter settings that will lead to the desired outcome. This data can then inform the design of an *ad hoc* storage or transport container. As discussed in chapter 1, storage and transportation of a cell based medicinal product can be considered the last manufacturing step. Results described in this chapter showed that within the process space under investigation (temperature=26-37 °C, oxygen tension= 3-20% and storage duration=5-7 days), process parameters affect response variables in contrasting ways. In order to define an optimal set of input parameters (process parameters) for a storage container within the defined process space, response models can be combined. Specifications can be selected for all the relevant quality attributes of the product: viability, lactate and NH₃ maximum acceptable release and log₁₀ of *COL2A1*, *ACAN* and *COL1A1* fold changes relative to non-stored discs. Assuming a storage duration of 7 days, for each response variable all possible combinations of temperature and oxygen which meet the set specification have been defined. These are represented by contour plots (Fig.3.23). By overlaying contour plots for all response variables

considered, an optimal process space was identified. This is represented as a white area in a graph of temperature versus oxygen (Fig.3.23,H) .

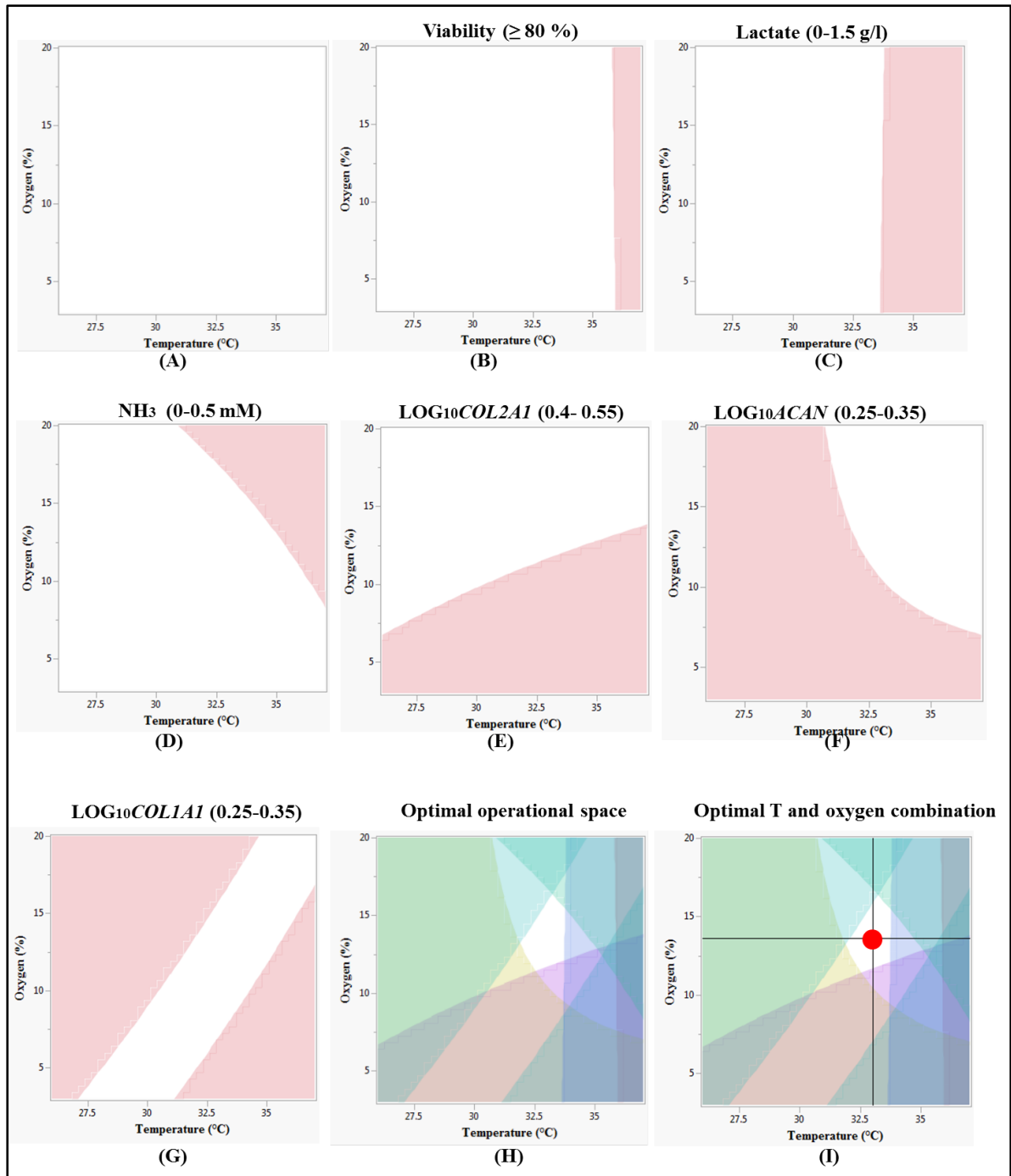


Fig.3. 23 Contour plots 7 day storage of cartilage disc. The set specifications were (B) viability $\geq 80\%$, (C) lactate concentration in spent medium after storage 0-1.5 g/l, (D) NH_3 concentration 0-0.5 mM, (E) \log_{10} of COL2A1 fold change relative to non-stored discs 0.4-0.55, (F) \log_{10} of ACAN fold change relative to non-stored discs 0.40-0.6 (G) \log_{10} of COL1A1 fold change relative to non-stored discs -0.35 to -0.25 (H) Design space for the process space under investigation. White areas represent combinations of temperature and oxygen which would meet the set specifications (B-G). Design space shown in H is given by overlapping colored areas B-G. Each point within the white area in H will meet all specifications. A point can be selected within the design space to test the robustness of the system (I).

3.6 Discussion

Statistical design of experiment (DoE) has been successfully used in many industries, such as automotive (Valles & Sanchez, 2009), medical device (Eatock, Dixon, & Young, 2009), semiconductor (Joshi, 1991) and pharmaceutical (Rathore & Winkle, 2009). More recently, it has been applied as a tool to investigate the simultaneous involvement of factors and their interactions during *in vitro* differentiation of stem cells (Sotiropoulou, Perez, Salagianni, Baxevanis, & Papamichail, 2006), osteogenic differentiation (Decaris & Leach, 2011) and the culture of human embryonic stem cells in stirred tank bioreactors (M., MengGuoliang, E., D., & S., 2013).

In this chapter, DoE has been applied to investigate the simultaneous effects of temperature, oxygen and storage duration on the biological properties of cartilage discs used as a cell therapy model.

Temperature is the most commonly studied parameter modulating the biopreservation of cell therapy products (Garrity, Stoker, Sims, & Cook, 2012)(Stolzing & Scutt, 2006)(Stolzing, Sethe, & Scutt, 2006). For the cell therapy product described here, temperature had a statistically significant effect on viability, glucose, lactate, glutamine, ammonia and *COL1A1* expression. Oxygen had a statistically significant effect on glutamine and NH_3 concentration and on *COL1A1* expression. Oxygen and temperature interaction showed a statistically significant effect on lactate metabolism, which could not have been detected by a traditional one-factor-at-a-time approach (Montgomery, 2012). This finding implies that the temperature mediated decrease in lactate released by the cell therapy product in the medium will be depended on the oxygen tension present in the medium.

Storage duration showed a statistically significant effect on viability, glucose, lactate, glutamine, ammonia and *COL1A1*.

The analysis of these models showed the input factors investigated have a contrasting effect on some of the biological properties of the product following storage. In particular, preferential storage conditions in terms of viability, lactate and ammonia production, *COL2A1* and *ACAN* production are the ones that lead to upregulation of *COL1A1*, which should be minimal for cartilage-like tissue.

Other than investigational purposes, this system approach can be also used as a decision support tool for process development by combining the response models. As demonstrated in case study 1, response values for simulated storage conditions can be predicted. This can limit the number of experiments needed to evaluate a new container for storage of a cell therapy product, like the one described in this chapter. This application can be particularly useful for autologous product development, where the amount of biological material available is rather limited (I. Martin et al., 2014).

An additional application is the use of these response models to identify optimal set of input parameters which will enable a product within specifications (case study 2).

The response models described in this chapter suffer from one main limitation: assumption of linearity that could not be verified with the presence of centre points. This study could be further expanded with the addition of axial point, a method referred to as central composite design (Montgomery, 2012).

The addition of points to confirm the presence of curvature and other factors which might have an effect, can improve the accuracy of these models in predicting response values. This is out of the scope of this thesis, as described in chapter 5.

Once optimal input values have been determined, Monte Carlo simulations can be performed to account for uncertainty in input values (W. Schneider, Bortfeld, & Schlegel, 2000).

If these response models were to be used as decision support tools for designing a container for storage and transportation of the cell therapy product, it would be useful to determine the probability of the output parameters (quality attributes) to be off specifications.

Chapter 4

Investigating storage properties of hMSCs prior to their differentiation

Introduction

As discussed in chapter 1, hMSCs have been advocated as a useful “living” active pharmaceutical ingredient for cell therapy applications with over 400 clinical trials currently ongoing (clinicaltrials.gov). These cells can be isolated from a number of tissues including bone marrow (Capelli et al., 2015), adipose tissue (Rasini et al., 2013), cord tissue (M S Choudhery, Badowski, Muise, & Harris, 2013).

The effect of low oxygen tension (hypoxia) on hMSCs expansion has been investigated mainly in order to improve cell expansion yields (Dos Santos et al., 2010). However, little is known as to whether temperature and oxygen can orchestrate a stimulation pattern which enhances or inhibits the biological properties of hMSCs. A deeper understanding of temperature and oxygen effect on hMSCs could facilitate the design of innovative solutions for storage and transportation solutions for cell therapy medicinal products. Moreover,

hypoxic pre-conditioning have been shown to enhance the therapeutic potential for hMSCs (Chang et al., 2013). In this study, only the ability of hMSCs to differentiate into the three lineages (chondrogenic, osteogenic and adipogenic) has been investigated along with the metabolic activity over the 5 day storage period.

Similarly to what was described in chapters 2 and 3, the combined effect of temperature and oxygen was studied for hMSCs when stored in the controlled environment provided by four tissue culture incubators. The same ranges were selected for temperature (26-37 °C) and oxygen (3-20 %). Storage duration was limited to five days (Fig. 4.1).

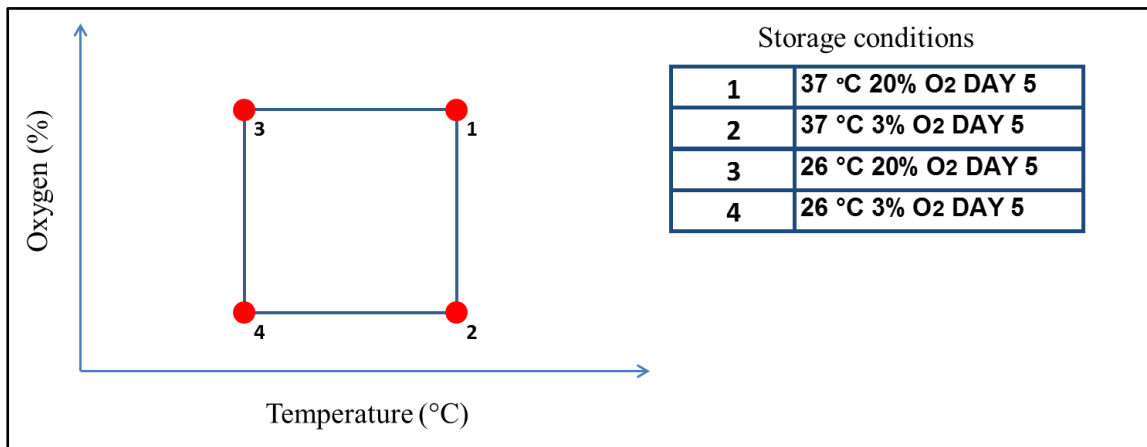


Fig. 4.1 Multifactorial space under investigation for hMSCs. Four storage conditions were defined by combining two levels (high and low) for the two factors: temperature and oxygen

4.1 Materials and methods

4.1.1 Storage of hMSCs in tissue culture flasks and plates

hMSCs from three healthy donors (Lonza Biosciences) were isolated from bone marrow as described in Chapter 2 paragraph 1.1. hMSCs were expanded in T-75 flasks with Mesenchymal Stem Cell Growth Medium (Lonza, cat. No. PT-3001) supplemented with 5 ng/ml fibroblast growth factor-2 (FGF2, R&D Systems). Upon reaching passage 4 (P4), cells were seeded into T-25 flasks at a seeding density of 10^4 cells/cm². Each flask corresponded to a different storage condition. The flasks were then placed in 4 incubators providing 4 different storage conditions as shown in Table 4.1. After 5 day storage, cells were differentiated towards chondrogenic, osteogenic and adipogenic lineage and spent medium metabolites measured (Fig. 4.1). Three flasks which have not been exposed to any storage period were also differentiated towards the three lineages and used as controls (one for each donor). Additionally, hMSCs from one healthy donor were also seeded in 24-well plates at the same seeding density and stored under the same conditions as the flasks (Table 4.1) and after 5 days these cells were differentiated towards osteogenic and adipogenic lineages. Each plate corresponds to a different storage condition and lineage differentiation. For each plate, 3 wells were seeded. Two plates were not exposed to any storage conditions and the hMSCs were differentiated towards osteogenic and adipogenic lineage on the same day the storage period started. These plates were used as control.

Table 4.1. Storage conditions for hMSCs seeded in T25 flasks and 24 well plates. Storage duration was 5 days.

Run	Temperature (°C)	Oxygen (%)
1	37	20
2	37	3
3	26	20
4	26	3

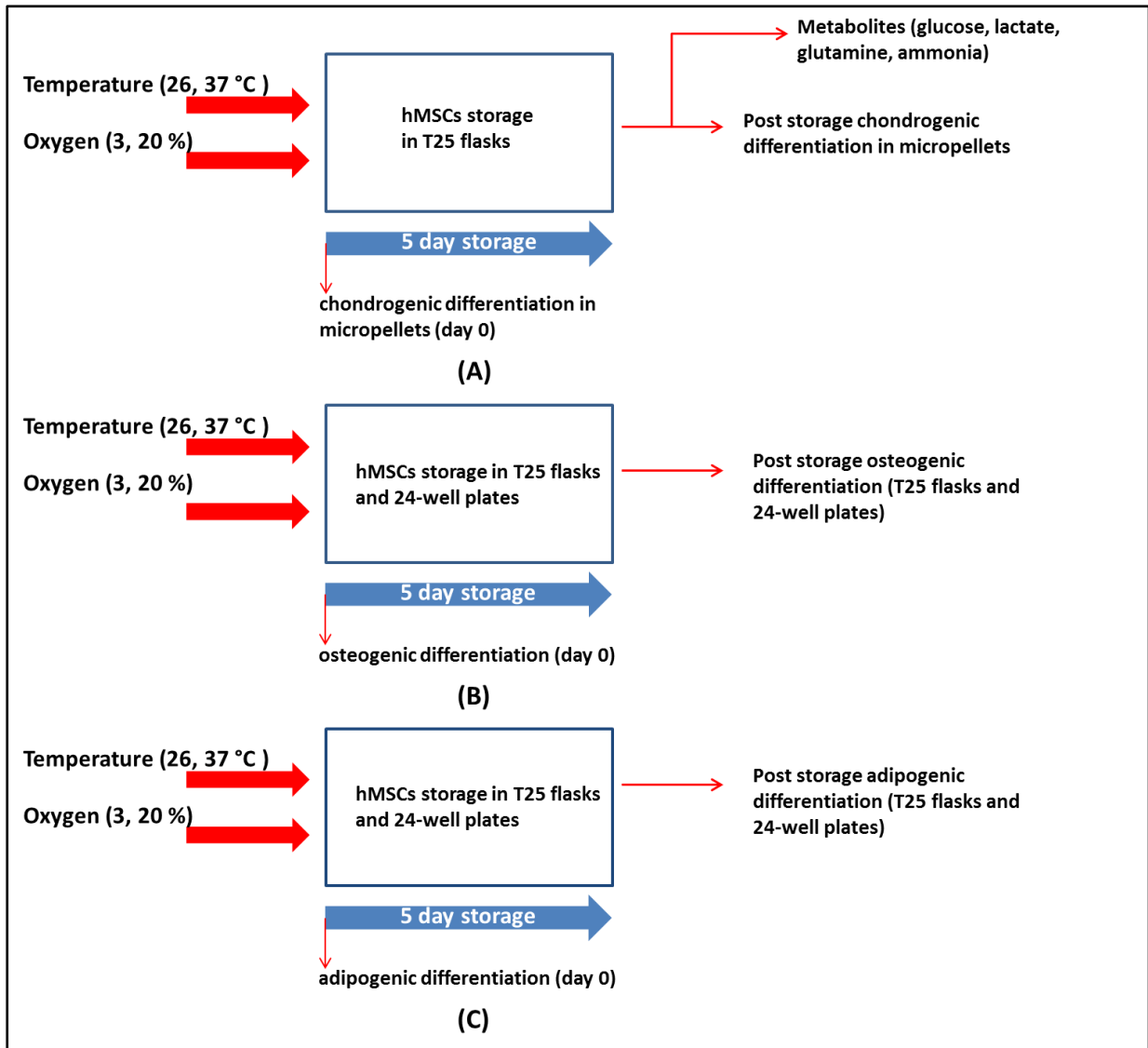


Fig. 4.2 Storage experiments schematic. hMSCs from three healthy donors were seeded in T25 flasks and exposed to different combinations of temperature and oxygen for 5 days (Table 4.1). Stored hMSCs were then differentiated towards chondrogenic (A), osteogenic (B) and adipogenic (C) lineages. Non stored hMSCs were also differentiated towards the three lineages on the day the storage period started (day 0) and used as control. Spent medium was also analysed for glucose, lactate, glutamine and NH_3 concentrations. For osteogenic (B) and adipogenic (C) lineages hMSCs were also seeded, stored and differentiated in 24 well plates.

4.1.2 Spent medium analysis

To quantify the metabolite concentration of hMSCs after storage, spent medium was aseptically removed from the T-25 flasks after the storage period and stored at -80 °C in plastic tubes (Eppendorfs). Fresh Mesenchymal Stem Cell Growth Medium (Lonza, cat. No. PT-3001) samples were also included as control. Stored samples were then thawed and run on the Bioprofile FLEX bioanalyser (Nova Biomedical) for analysis of glucose [g/l], lactate [g/l], glutamine [mM] and ammonium [mM] concentrations. As 3 ml of spent medium were available for each storage condition and 1ml if required for each measurement, three technical repeats were performed.

4.1.3 Post-storage chondrogenic differentiation in micropellets

Following 5 day storage under the conditions shown in Table 4.1, hMSCs were washed with pre-warmed PBS (Sigma) before being detached from the T25 flasks via 1 ml trypsin digestion. For each storage condition, three flasks were studied corresponding to three healthy donors. hMSCs from each flask were centrifuged in 15 ml falcon tubes at 240 x g for 5 minutes. Supernatant was discarded and 5 ml of pre-warmed PBS was added to each falcon tube. Cells were then centrifuged again at 240 x g for 5 minutes. Supernatant was discarded and the cells were re-suspended in 1 ml of chondrogenic medium (Table 2.1, chapter 2). Three micropellets were prepared for each storage condition and each donor by seeding 150000 hMSCs per well in a non-treated V-bottom 96 well plate (Greiner) which had been previously UV-irradiated for 30 minutes. Following seeding, chondrogenic medium was

added to a final volume of 200 μ l per well. The plate was then centrifuged at 500 g for 5 minutes. PBS was added to border wells to prevent evaporation loss. Chondrogenic medium was replenished every 3 days for 14 days. The same procedure was used to prepare micropellets from flasks not exposed to storage (one for each donor). Chondrogenic differentiation of micropellets was compared to micropellets not exposed to storage.

4.1.4 Post-Storage osteogenic differentiation

Following 5 day storage under the conditions shown in Table 4.1, hMSCs in flasks and plates were washed with pre-warmed PBS (Sigma) before adding 3 ml per flask and 500 μ l per well of osteogenic medium respectively (Table 4.2). Osteogenic medium was replenished every 3 days for 14 days. Light microscopy images were also taken to confirm osteogenic differentiation.

Table 4.2 Osteogenic medium

Reagent	Supplier	Function
Low glucose DMEM	Gibco –Life technologies	Enables cell growth and proliferation. (Z. Yang & Xiong, 2012)
2 mM L-glutamine	Sigma-Aldrich, Poole, UK	Essential amino acid required for cell growth (Z. Yang & Xiong, 2012).
10 % v/v foetal bovine serum	Sigma-Aldrich, Poole, UK	Enables cell attachment to surface and growth (Z. Yang & Xiong, 2012)
0.1 μM Dexamethasone	Sigma-Aldrich, Poole, UK	Enhances the osteoblastic differentiation of hMSCs(Sun, Wu, Dai, Chang, & Tang, 2006)
10 mM β-glycerophosphate	Sigma-Aldrich, Poole, UK	Promotes mineralization of hMSCs (Schäck et al., 2013)
50 μM ascorbic acid	Sigma-Aldrich, Poole, UK	Stimulates secretion of collagen and glycosaminoglycan (Eslaminejad et al., 2013)
100 U/ml penicillin, 100 μg/ml streptomycin	Gibco –Life technologies	Used in culture media to mitigate risk of bacterial and fungal infections.

4.1.5 Post storage adipogenic differentiation

Following 5 day storage under the conditions shown in Table 1, hMSCs from flasks and plates were preliminary washed with pre-warmed PBS (Sigma) before adding 3 ml per flask and 500 μ l per well of adipogenic induction medium respectively (Table 4.3). Adipogenic induction medium was removed at day 3 and replaced with adipogenic maintenance medium (Table 4.4) which was replenished two days later. On day 7, this cycle was repeated for a total adipogenic differentiation period of 14 days. Light microscopy images were also taken to confirm adipogenic differentiation.

Table 4.3 Adipogenic induction medium

Reagent	Supplier	Function
4g/L DMEM	Gibco –Life technologies	Enables cell growth and proliferation. (Z. Yang & Xiong, 2012)
10% (v/v) FBS	Sigma-Aldrich, Poole, UK	Enables cell attachment to surface and growth (Yang & Xiong, 2012)
1μM dexamethasone	Sigma-Aldrich, Poole, UK	Contributes to hMSCs differentiation (Scott, Nguyen, Levi, & James, 2011)
100U/ml penicillin 100μg/ml streptomycin	Gibco –Life technologies	Used in culture media to mitigate risk of bacterial and fungal infections.
0.65 mM 3-isobutyl-1-methylxanthine (IBMX)	Gibco –Life technologies	Stimulates adipogenic differentiation in hMSCs (Scott et al., 2011)
Insulin growth factor (IGF-1) 20 nM	Gibco –Life technologies	Induces adipogenic differentiation (Scott et al., 2011)
Rosiglitazone 20mM	Gibco –Life technologies	Stimulates adipogenesis in hMSCs (Rosen & MacDougald, 2006)
10μg/ml insulin	Gibco –Life technologies	Stimulates glucose metabolism and lipid uptake (Rosen & MacDougald, 2006)

Table 4.4 Adipogenic maintenance medium

Reagent	Supplier	Function
4g/L DMEM	Gibco –Life technologies	Enables cell growth and proliferation. (Yang & Xiong, 2012)
10% (v/v) FBS	Sigma-Aldrich, Poole, UK	Enables cell attachment to surface and growth (Yang & Xiong, 2012)
100U/ml penicillin 100µg/ml streptomycin	Gibco –Life technologies	Used in culture media to mitigate risk of bacterial and fungal infections.
10µg/ml insulin	Gibco –Life technologies	Stimulates glucose metabolism and lipid uptake (Rosen & MacDougald, 2006)

4.1.6 Post storage GAGs assay

Following storage, hMSCs were differentiated towards the chondrogenic lineage as described in 4.3. Sulfated glycosaminoglycan production was quantified via the dimethylmethylene blue (DMB) assay as described by Kafienah and Sims (Kafienah & Sims, 2004). Micropellets were collected and washed with PBS (Sigma) before being stored at -80 °C. On the day the assay was performed, samples were thawed and placed into 1.5 ml tubes (Sarstedt). Micropellets were then digested by adding 70 µl of phosphate buffer (0.1 M pH 6.5, Sigma Aldrich), and 40 µl of the digestion solution (Table 4.5).

Table 4.5 Micropellet digestion solution

Reagent	Concentration	Supplier
Papain	20 µl (0.25 g in 10 ml 0.1M phosphate buffer pH 6.5)	Sigma-Aldrich, Poole, UK
Cystein-HCl	10 µl (0.078 g in 10 ml 0.1M phosphate buffer pH 6.5)	Sigma-Aldrich, Poole, UK
EDTA	10 µl (0.19g in 10 ml 0.1 M phosphate buffer pH 6.5)	Sigma-Aldrich, Poole, UK

Tubes were then incubated overnight at 65 °C. DMB stock solution was prepared by dissolving 16 mg DMB powder (Sigma-Aldrich, cat. No. 34088) in 900 ml double distilled water in a glass bottle covered with aluminium foil containing 3.04 g glycine (sigma-Aldrich) and 2.73 g of NaCl (Sigma-Aldrich). This was mixed for 2 hours and the pH adjusted to 3.0 with HCl (Sigma) to a final volume of 1 L. The solution was stored at room temperature in the glass bottle covered with aluminium foil. In order to make a standard curve, chondroitin sulphate (Sigma-Aldrich) was prepared in water in a 1 mg/ml stock solution and kept refrigerated. Nine tubes were prepared with known concentration of chondroitin sulphate as described in Table 4.6.

Table 4.6 Chondroitin sulphate calibration curve

Standard (µg/ml)	Phosphate Buffer (µl)	Chondroitin sulphate (µl)
0	200	0
5	199	1
10	198	2
15	197	3
20	196	4
25	195	5
30	194	6
35	193	7
40	192	8

Overnight digested samples were diluted (1:4) and for each sample 40 µl were added to a 96 well plate (Grainer) in triplicates. For each standard (Table 4.6), 40 µl were also added to the plate in triplicates. Two hundred and fifty µl of DMB stock solution were then added to each well and absorbance was read at 530 nm using a TECAN plate reader and Xflor 4 software. GAG values in µg/ml were then normalized with the amount of DNA per micropellet measured via Picogreen assay as described in chapter 2 paragraph 1.4. From each digested sample, three technical repeats were performed by adding 25 µl of DNA containing sample to

75 µl of Tris-EDTA buffer. The amount of DNA per micropellet was calculated as the average of the three values.

4.1.7 Post-storage alkaline phosphatase assay and osteogenic staining

Following storage in 24 well culture plates (Table 4.1), hMSCs were induced to differentiate into the osteogenic lineage as described in 4.4. The osteogenic differentiation potential was tested by alkaline phosphatase (ALP) assay. ALP is a membrane bound enzyme that is used as a marker for osteogenic differentiation (Müller et al., 2007). This can be indirectly measured by the amount of para-nitrophenol, which is yellow when hydrolysed by alkaline phosphatase. P-nitrophenol (pNPP) is formed by its substrate (p-nitrophenyl phosphate) in presence of ALP. Absorbance can be measured at 405 nm and the amount of p-nitrophenol can be correlated to the amount of ALP (Matsubara et al., 2004). After 14 days osteogenic differentiation, hMSCs were washed with warm PBS and fixed with 4% (w/v) paraformaldehyde for 5-10 min. This was removed and fixed cells were washed in PBS Tris buffer pH 8.3 for 5 minutes. Three hundred µl of alkaline phosphate yellow liquid substrate for ELISA (Sigma Aldrich) was added to each well. Plates were covered with aluminium foil and incubated at room temperature for 30 minutes. After incubation, yellow substrates from each well were transferred to a 96 well plate in triplicates and absorbance measured at 405nm, using a TECAN plate reader and Xflor 4 software. A standard curve was prepared by adding 20 µl of 10 mM p-nitrophenol standard (Sigma) in 1 ml of PBS Tris buffer pH 8.3 and creating serial dilutions to give a concentration range of 200, 100, 50, 25, 12.5 and 6.25 µM.

Following enzymatic reaction, cells were washed with PBS Tris buffer pH 8.3 for 5 minutes before being incubated with the osteogenic staining solution (Table 4.7) for 20 minutes.

Table 4.7 Osteogenic staining solution

Reagent	Quantity	Supplier
Naphthol AS phosphate	0.005 g in 200 μ l of NN-Dimethylformaldehyde (DMF)	Sigma Aldrich
Fast Blue Salt	0.03 g in 50 ml PBS Tris Buffer pH 8.3	Sigma Aldrich

Stained cells were washed with PBS and then visualized by brightfield microscopy (Zeiss Axio Imager 2 microscope).

4.1.8 Post storage adipogenic staining of hMSCs

The adipogenic differentiation of hMSCs is accompanied by the formation of lipid vacuoles (Cai, Nakamoto, Hoshihara, Kawazoe, & Chen, 2014). These are formed by accumulation of intracellular droplets of triglycerides and can be used as a marker of adipogenic differentiation. To identify lipid vacuoles generated in hMSCs following storage, the AdiporeRed assay (LONZA) was performed. The assay is based on Nile red which fluoresces in the presence of droplets of triglyceride. Following adipogenic differentiation as described in 4.1.5, culture medium was removed and 1 ml of pre-warmed PBS was added

to each well. Lipidic vacuoles were stained by adding 200 μ l of AdipoRed reagent and incubated for 10 minutes, according to manufacturer instructions. Lipidic vacuoles (in red) were visualized by fluorescence microscopy (Zeiss Axio Imager II microscope) (excitation λ =485 nm; emission λ =535 nm) and counted by IMARIS software (BITPLANE, <http://www.bitplane.com/>).

4.1.9 Gene expression analysis from micropellets and hMSCs

RNA was extracted via the Trizol/chloroform method from micropellets as described in chapter 2.1.7. From cells seeded in T25 flasks, the following modifications were applied: the amount of Trizol, chlorophorm, isopropanol and 75 % ethanol-25 % DEPC-treated water used were 1 ml, 200 μ l, 500 μ l, 1 ml. cDNA was synthesised as described in 2.1.8.1 and quantitative real-time PCR performed as described in 2.1.8.2 using the primers shown in table 4.8.

Table 4.8 Primers used for quantitative real-time PCR

Gene	Primer type	Sequence (5'-3')
<i>GAPDH</i>	Forward	ACATCGCTCAGACACCATG
	Reverse	TGTAGTTGAGGTCAATGAAGGG
	Probe	AAGGTCGGAGTCAACGGATTTGGTC
<i>HPRT1</i>	Forward	TGCTGAGGATTTGGAAAGGG
	Reverse	ACAGAGGGCTACAATGTGATG
	Probe	AGGACTGAACGTCTTGCTCGAGATG
<i>18s</i>	Forward	CGAATGGCTCATTAAATCAGTTATGG
	Reverse	TATTAGCTCTAGAATTACCACAGTTATCC
	Probe	TCCTTTGGTCGCTCGCTCCTCTCCC
<i>COL2A1</i>	Forward	ACCTTCATGGCGTCCAAG
	Reverse	AACCAGATTGAGAGCATCCG
	Probe	AGACCTGAAACTCTGCCACCCTG
<i>ACAN</i>	Forward	TGTGGGACTGAAGTTCTTGG
	Reverse	AGCGAGTTGTCATGGTCTG

	Probe	CTGGGTTTTTCGTGACTCTGAGGGT
<i>COL1A1</i>	Forward	CCCCTGGAAAGAATGGAGATG
	Reverse	TCCAAACCACTGAAACCTCTG
	Probe	TTCCGGGCAATCCTCGAGCA
<i>RUNX2</i>	Forward	TGTTTGATGCCATAGTCCCTC
	Reverse	AATGGTTAATCTCCGCAGGTC
	Probe	CTGTTGGTCTCGGTGGCTGGTAG
<i>ALPL</i>	Forward	GACCCTTGACCCCCACAAT
	Reverse	GCTCGTACTGCATGTCCCCT
	Probe	TGGACTACCTATTGGGTCTCTTCGAGCCA
PPARG	Forward	GAGCCCAAGTTTGAGTTTGC
	Reverse	GCAGGTTGTCTTGAATGTCTTC
	Probe	CGCCCAGGTTTGCTGAATGTGAAG
<i>FABP4</i>	Forward	CATGTGCAGAAATGGGATGG
	Reverse	AACTTCAGTCCAGGTCAACG
	Probe	CGCCCAGGTTTGCTGAATGTGAAG

4.1.10 Factorial design of experiment for hMSCs storage

A full factorial two factor with two level design (2^2) was implemented to study the effect of temperature and oxygen tension on the hMSCs chondrogenic, osteogenic and adipogenic potential as well as metabolism over 5 day storage. For each factor, two levels (high and low) were selected, namely 26 °C and 37 °C for temperature and 3 % and 20 % for oxygen. The experiment was repeated for three healthy donors. One nuisance factor was introduced to account for the inter donor variability. Response variables were selected on the basis of the biological property under investigation for the hMSCs and are listed in Table 4.8. Each response was an average value of triplicated measurements. JMP SAS software (http://www.jmp.com/en_gm/home.html) was used for all statistical analysis and data transformation. ANOVA was used to identify main effects and interaction between factors.

Table 4.8 Input and output variables for the hMSCs storage system. Input and output variables of the full factorial design of experiments are presented.

Input variables	Output variables
Temperature	Glucose
Oxygen	Lactate
	Glutamine
	Ammonia
	<i>COL2A1</i>
	<i>ACAN</i>
	<i>COL1A1</i>
	<i>RUNX2</i>
	<i>ALPL</i>
	<i>PPARG</i>
	<i>FABP4</i>

To further investigate the osteogenic and adipogenic potential of hMSCs following storage, one additional full factorial 2² design of experiment was created with data from just one donor. Input variables were temperature and oxygen while output variables were ALP activity and number of adipocytes.

4.2 Results

4.2.1 Post storage metabolites concentration for undifferentiated hMSCs

The concentrations of glucose, lactate, glutamine and ammonia in spent medium were measured following 5 day storage in T25 flasks as described in table 4.1. This permitted the evaluation of the effect of temperature and oxygen on the modulation of hMSCs metabolism and for the identification of the storage conditions which might be detrimental to hMSCs biological properties.

When stored at 20 % oxygen and 37 °C, 94 % of glucose available was metabolized (Fig. 4.3).

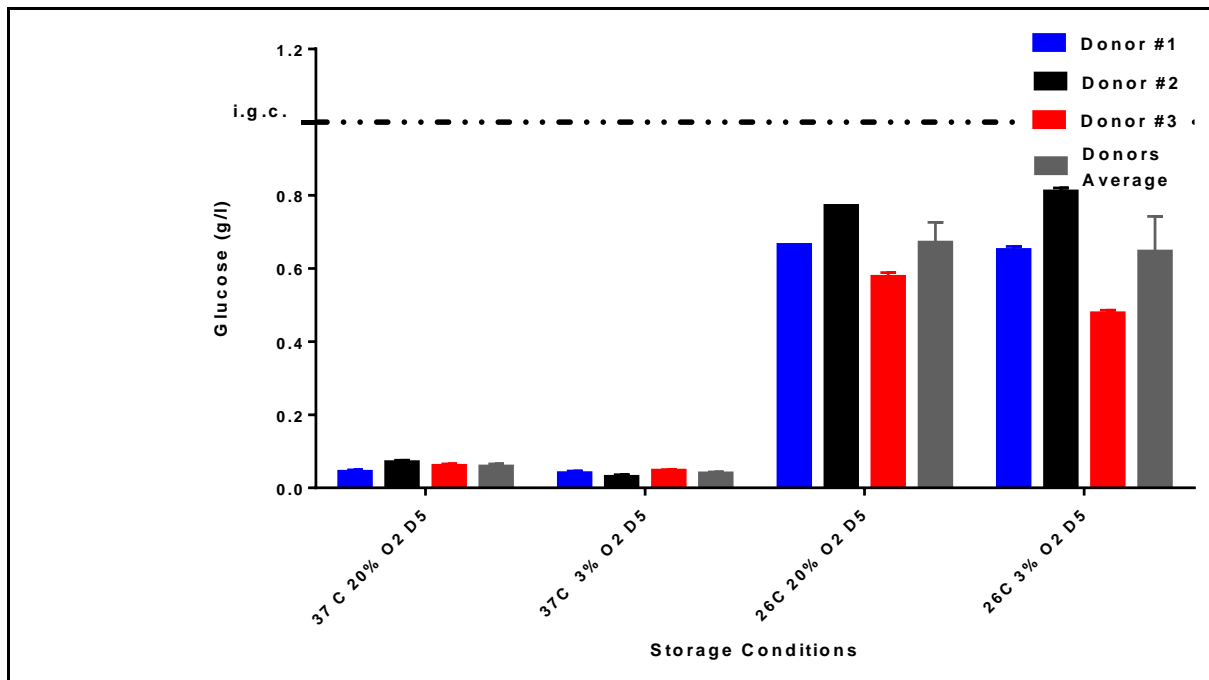


Fig. 4.3 Post-storage glucose concentrations (g/l) in spent medium for hMSCs seeded and stored in T25 flasks. hMSCs were isolated from three healthy donors and exposed to storage conditions listed in Table 4.1. Dashed line represents initial glucose concentration (i.g.c.)(1 g/l). Each measurement requires 1 ml of spent medium. Values are plotted as mean and standard error of the mean (n=3) for three technical replicates. For each storage condition, donors average represents the mean value of glucose concentration post storage for the three donors. (37 C= 37°C, O₂= pO₂, oxygen tension, D5= day 5).

This decreased to 33 % when the temperature was lowered to 26 °C while maintaining the same oxygen tension. For storage at 3 % oxygen, glucose consumption slightly increased to 96 % at 37 °C and 35 % at 26 °C. This might be explained by the increased proliferation which has been demonstrated by Dos Santos et al. (dos Santos et al., 2009) when hMSCs are cultured under hypoxia. Temperature has a statistically significant effect on glucose concentration after 5 day storage for all three donors (p=0.03). hMSCs from the three donors behaved in a consistent manner.

Consistently with glucose metabolism, storage at higher temperature (37 °C) increased the release of lactate at both oxygen tension levels (20 % and 3 %) (Fig. 4.4).

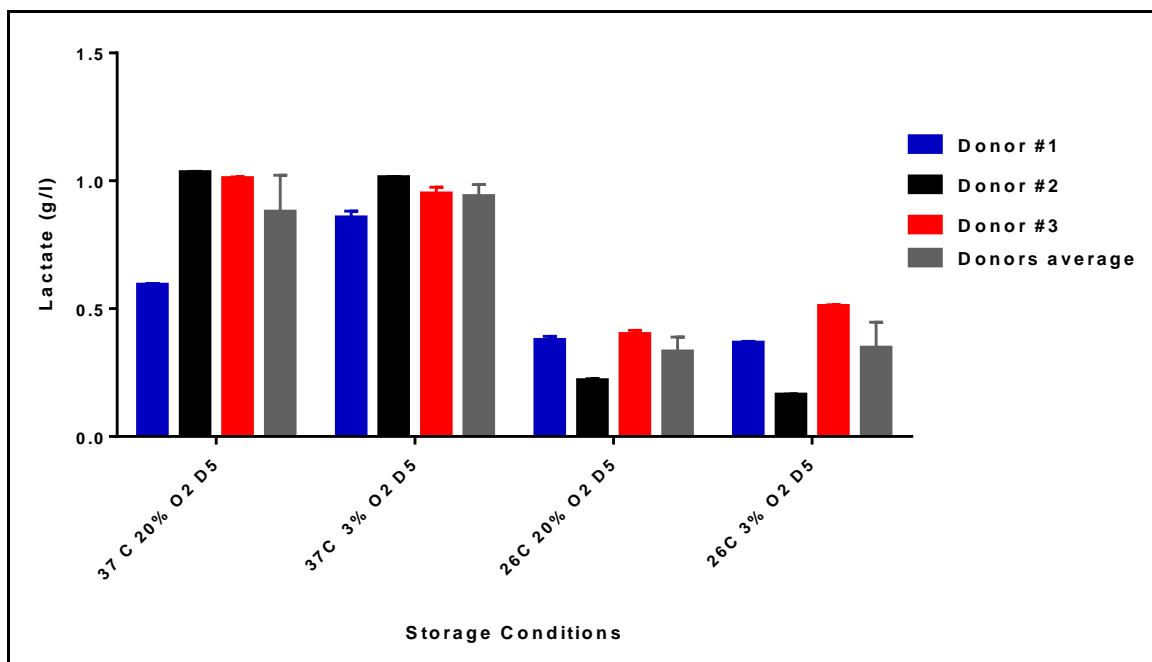


Fig. 4.4 Post-storage lactate concentrations (g/l) in spent medium for hMSCs seeded and stored in T25 flasks. hMSCs were isolated from three healthy donors and exposed to storage conditions listed in Table 4.1. Each measurement requires 1 ml of spent medium. Values are plotted as mean and standard error of the mean (n=3) for three technical replicates. For each storage condition, donors average represents the mean value of lactate concentration post storage for the three donors. (37 C= 37°C, O2= pO₂, oxygen tension, D5= day 5).

When stored at 3 % oxygen tension level, lactate released reached 1 g/l at 37 °C and 0.3 g/l at 26 °C. Decreasing storage temperature from 37 to 26 °C led to a 63 % decrease in lactate. This effect was reduced for storage at 20 % oxygen tension level, where lactate release decreased from 0.87 g/l at 37 °C to 0.34 g/l at 26 °C (61 % reduction). Temperature has a statistically significant effect on lactate concentration after 5 day storage for the three donors (p=0.02).

It is important to note that the lactate inhibitory concentration of 3.15 g/l identified by Schop et al (Schop et al., 2009) was not reached in any of the storage conditions following 5 day storage.

Glutamine metabolism was limited to 8.9 % of the initial glutamine concentration (3.1 mM) for both oxygen tension levels when the cells were stored at 26 °C (Fig.4.5).

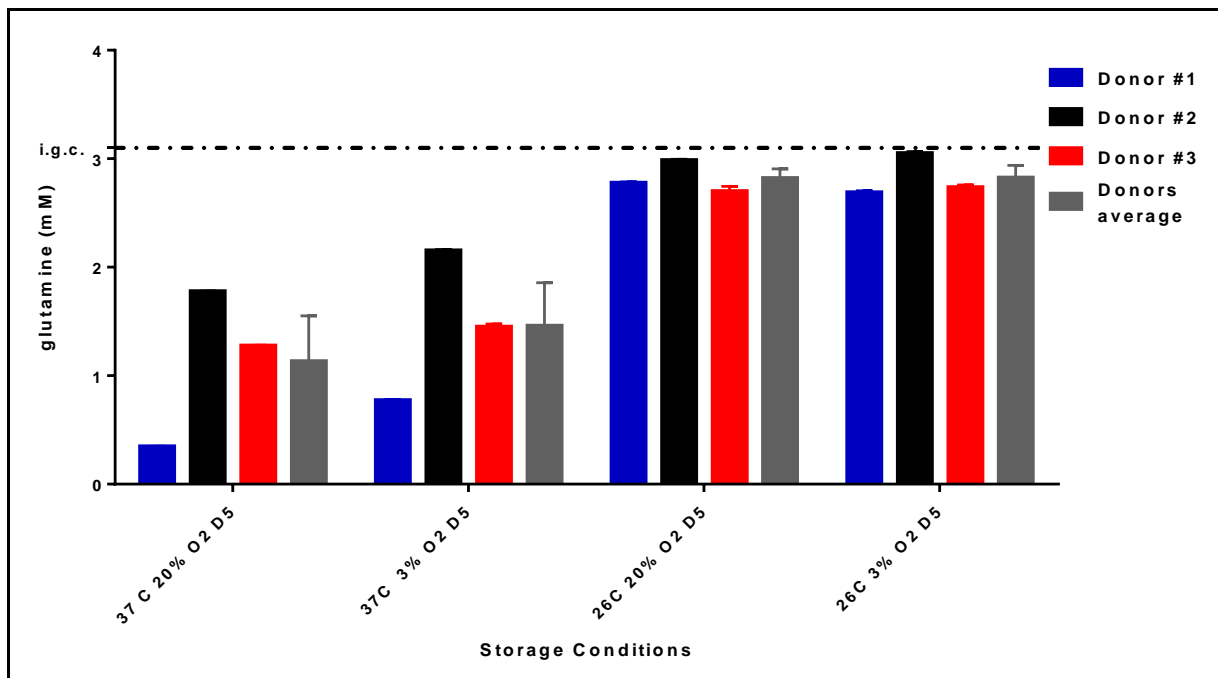


Fig. 4.5 Post-storage glutamine concentrations (mM) in spent medium for hMSCs seeded and stored in T25 flasks. hMSCs were isolated from three healthy donors and exposed to storage conditions listed in Table 4.1. Dashed line represents initial glutamine concentration (i.g.c.) (3.1 mM). Each measurement requires 1 ml of spent medium. Values are plotted as mean and standard error of the mean (n=3) for three technical replicates. For each storage condition, donors average represents the mean value of glucose concentration post storage for the three donors. (37 C= 37°C, O₂= pO₂, oxygen tension, D5= day 5).

At 37 °C, glutamine metabolism was considerably higher (63.44 % and 52.93 % for 20 and 3 % oxygen tension levels respectively). Temperature and oxygen (and their interaction) did not have a statistically significant effect on glutamine concentration after 5 day storage.

Consistently with glutamine metabolism, concentration of NH₃ when the cells were stored at 26 °C was 0.8 mM for both oxygen tension levels (Fig. 4.6).

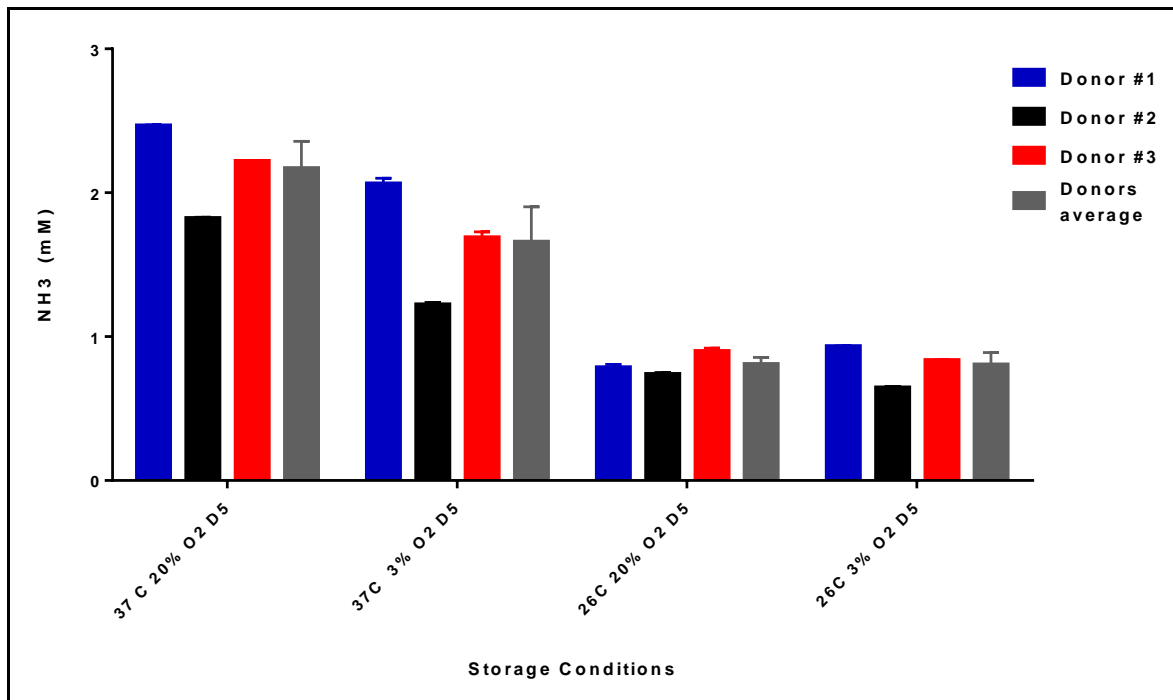


Fig. 4.6 Post-storage NH₃ concentrations (mM) in spent medium for hMSCs seeded and stored in T25 flasks. hMSCs were isolated from three healthy donors and exposed to storage conditions listed in Table 4.1. Each measurement requires 1 ml of spent medium. Values are plotted as mean and standard error of the mean (n=3) for three technical replicates. For each storage condition, donors average represents the mean value of glucose concentration post storage for the three donors. (37 C= 37°C, O₂= pO₂, oxygen tension, D5= day 5).

Storage at 37 °C led to an increase in NH₃ of 62.72 % and 51.23 % for 20% oxygen and 3 % oxygen respectively. Temperature and oxygen (and their interaction) did not have a statistically significant effect on NH₃ concentration after 5 day storage.

It was important to note that ammonia reached the inhibitory concentration value of 2.4 mM defined by Shop et al.(Schop et al., 2009) only for donor #1 when the cells were stored at 37°C and 20 % oxygen. This result was consistent with what Dos Santos et al. demonstrated for hMSCs cultured under normoxia (20 % O₂) (dos Santos et al., 2009).

4.2.2 Post storage chondrogenic differentiation of hMSC in micropellets

The chondrogenic differentiation potential of the hMSCs following storage was evaluated by gene expression and GAG quantification in micropellets as described in 4.1.2. Only when stored at 37 °C and 20 % oxygen, did hMSCs retain the ability to differentiate into chondrocytes (Fig. 4.7). In all other storage conditions, *COL2A1* was down regulated. All three donors showed consistent trends.

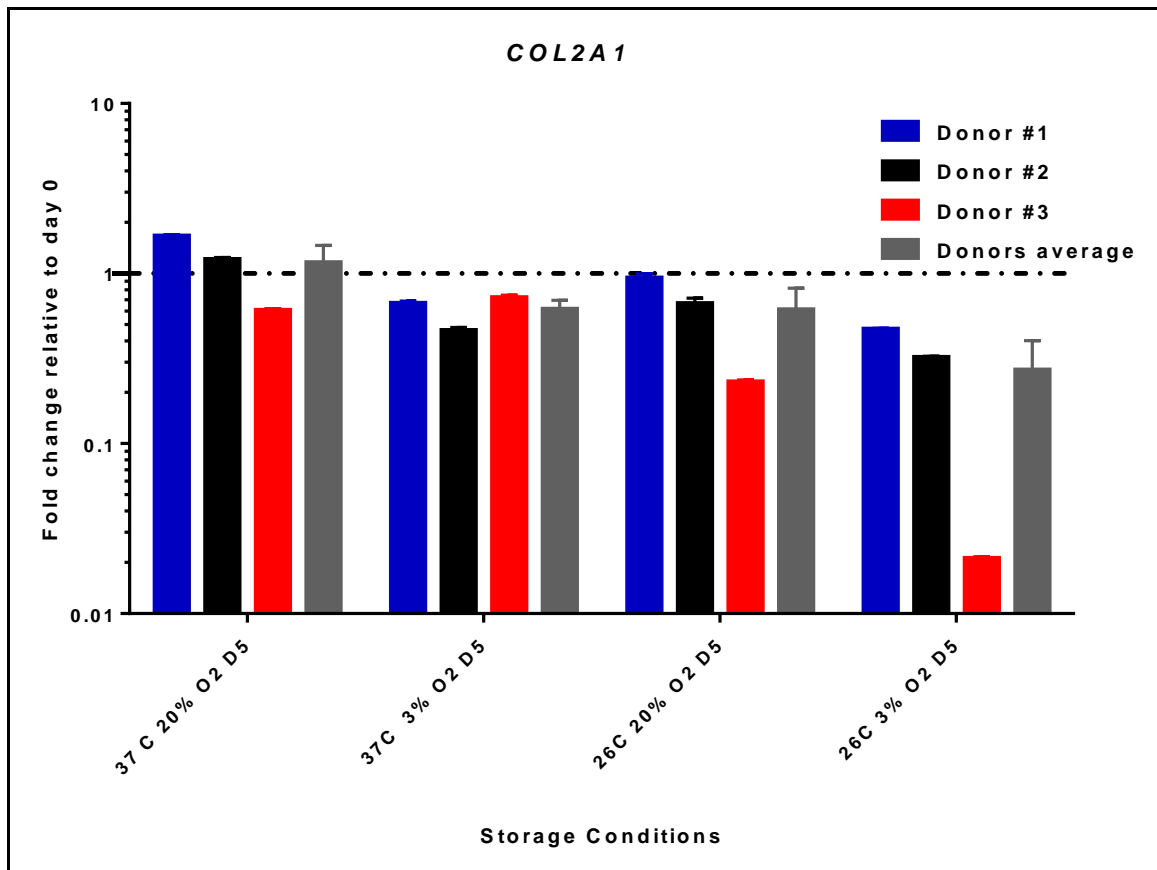


Fig. 4.7 Fold change in *COL2A1* gene expression in response to storage. hMSCs isolated from three healthy donors and exposed to storage conditions listed in Table 4.1. Fold changes values are relative to non-stored hMSCs (day 0) and are plotted as mean and standard error of the mean for three technical replicates for each donor. The average fold change values for the three healthy donors is also plotted for each storage condition. Data on y-axis are on logarithmic scale (log₁₀). (37 C= 37°C, O₂= pO₂, oxygen tension, D5= day 5).

Reduced oxygen tension and reduced temperature led to lower *COL2A1* expression compared to micropellets from non-stored hMSCs. While storage at 37 °C and 20 % oxygen corresponded to the highest *COL2A1* expression, storage at 26 °C and 3 % oxygen corresponded to the lowest. Temperature and oxygen and their interaction did not have a statistical significant effect on *COL2A1* expression.

Unlike *COL2A1*, *ACAN* was upregulated in all storage conditions for donor #1 and #3 (Fig.4.8).

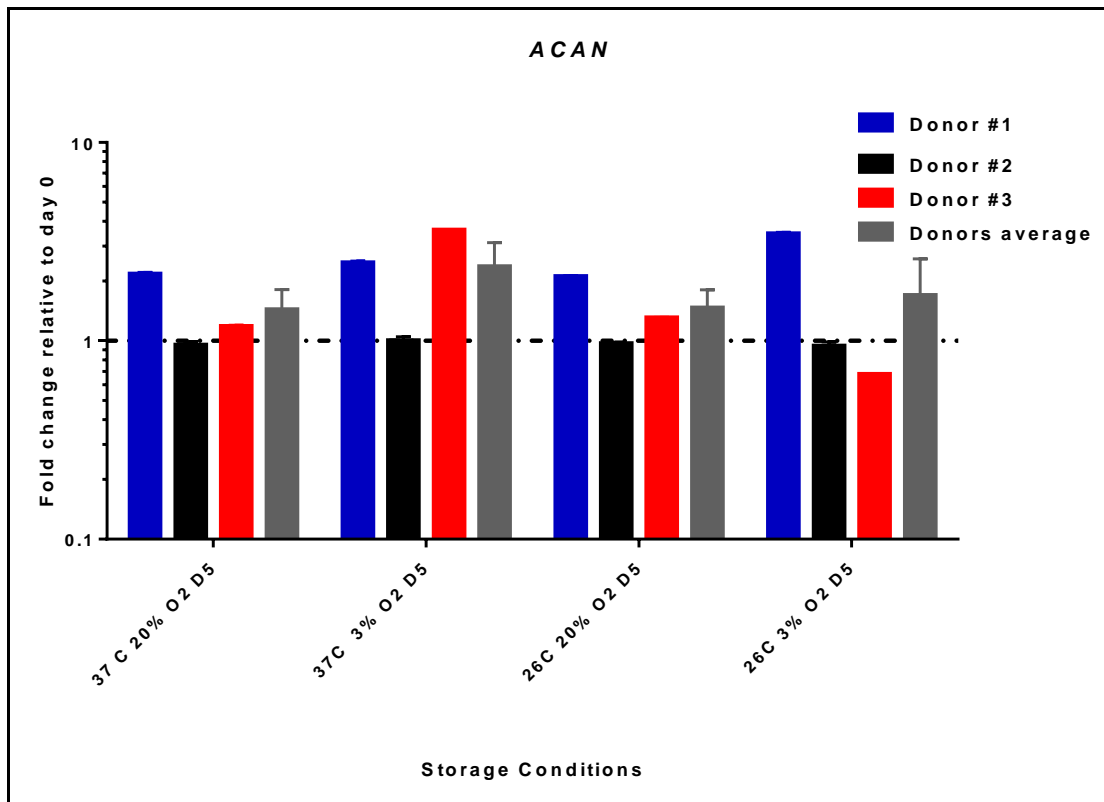


Fig. 4.8 Fold change in *ACAN* gene expression in response to storage. hMSCs isolated from three healthy donors and exposed to storage conditions listed in Table 4.1. Fold changes values are relative to non-stored hMSCs (day 0) and are plotted as mean and standard error of the mean for three technical replicates for each donor. The average fold change values for the three healthy donors is also plotted for each storage condition. Data on y-axis are on logarithmic scale (log₁₀). (37 C= 37°C, O₂= pO₂, oxygen tension, D5= day 5).

Donor #2 showed rather limited variations in *ACAN* expression compared to micropellets from untreated (non-stored) hMSCs in all storage conditions. hMSCs exposed to 5 day storage at 37 °C and 3 % oxygen showed the highest *ACAN* expression. Increase in storage temperature or decrease in oxygen tension led to higher *ACAN* expression. Temperature and oxygen and their interaction did not have a statistical significant effect on *ACAN* expression.

COL1A1, which encodes for the α 1 polypeptide chain of type 1 collagen, was not overexpressed for micropellets from hMSCs exposed to 5 day storage at 37 °C and 20 % oxygen (Fig.4.9).

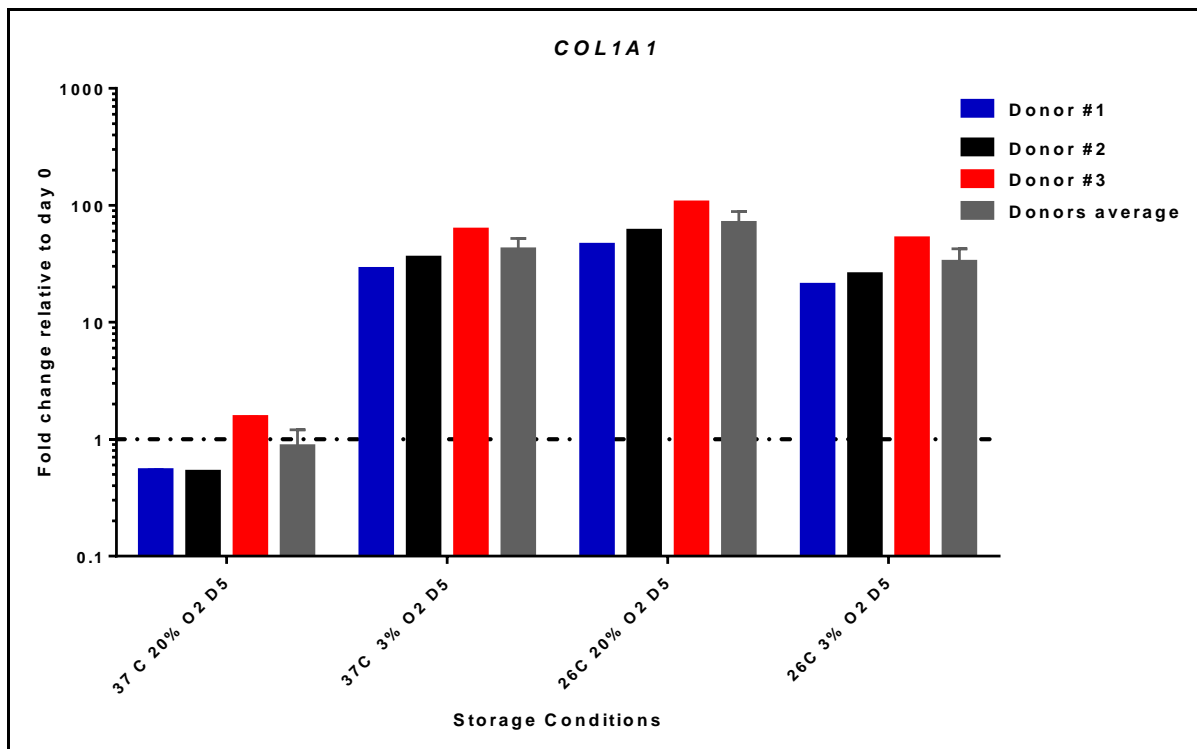


Fig. 4.9 Fold change in *COL1A1* gene expression in response to storage. hMSCs isolated from three healthy donors and exposed to storage conditions listed in Table 4.1. Fold changes values are relative to non-stored hMSCs (day 0) and are plotted as mean and standard error of the mean for three technical replicates for each donor. The average fold change values for the three healthy donors is also plotted for each storage condition. Data on y-axis are on logarithmic scale (log₁₀). (37 C= 37°C, O₂= pO₂, oxygen tension, D5= day 5).

For those cells, the storage did not inhibit but rather enhanced chondrogenesis leading to *COL2A1* upregulation (Fig 4.7). Consistently, *COL1A1* was downregulated. In all other storage conditions, *COL1A1* was considerably overexpressed and this correlates with *COL2A1* downregulation.

Temperature has a significant effect on *COL1A1* expression (p=0.0055). Oxygen did not have a statistically significant effect while the interaction with temperature was statistically significant (p=0.0016). This means that changes in *COL1A1* expression due to oxygen will be

dependent on the temperature level. The effect of oxygen on *COL1A1* was remarkably greater when the hMSCs were stored at 37 °C than at 26 °C.

Sulfated glycosaminoglycan (sGAG) synthesis and accumulation in pellets has been considered as a marker of chondrogenesis for hMSCs (Mackay et al., 1998). The assay used to measure GAGs was based on 1,9-dimethylmethylene blue which binds to the sulphated polysaccharide component of proteoglycans. hMSCs stored for 5 days at 37 °C and 20 % oxygen showed the greatest accumulation of sGAG relative to micropellets from non-stored hMSCs (Fig.4.10).

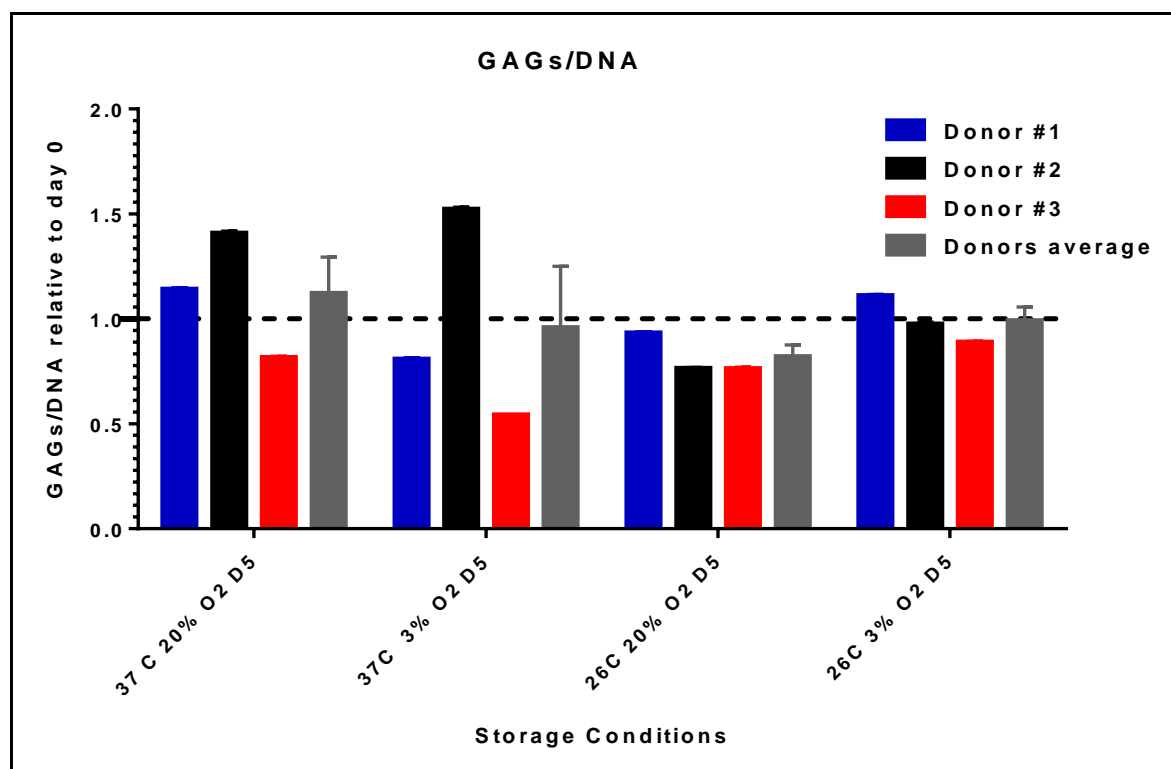


Fig. 4.10 Post storage GAGs accumulations in micropellets. hMSCs isolated from three healthy donors and exposed to storage conditions listed in Table 4.1. Fold changes values are relative to non-stored hMSCs (day 0) and are plotted as mean and standard error of the mean for three technical replicates for each donor. The average fold change values for the three healthy donors is also plotted for each storage condition. Data on y-axis are on logarithmic scale (\log_{10}). (37 C= 37 °C, O2= pO₂, oxygen tension, D5= day 5).

Lower temperature and oxygen tension level reduced the amount of sGAGs accumulated during the 14 day differentiation phase. Adesina et al. showed that hMSCs undergo a more robust chondrogenesis when differentiated under hypoxic conditions (Adesida, Mulet-Sierra, & Jomha, 2012). However, little to no evidence is available from others regarding the effect of hypoxia, alone or in combination with temperature, on hMSCs prior to a standard differentiation protocol under normoxia.

4.2.3 Post storage osteogenic differentiation of hMSC

The osteogenic differentiation potential of the hMSCs following storage was evaluated by gene expression using hMSCs stored in T25 flasks and ALP activity assay using cells stored in 24 well plates.

RUNX2, which encodes for runt related transcription factor 2 and which is required for bone formation, was upregulated in all storage conditions for donor #1 and donor 3 (Fig.4.11). For all three donors, *RUNX2* expression increased as temperature decreased from 37 °C to 26 °C, while no changes can be noticed due to oxygen level changes.

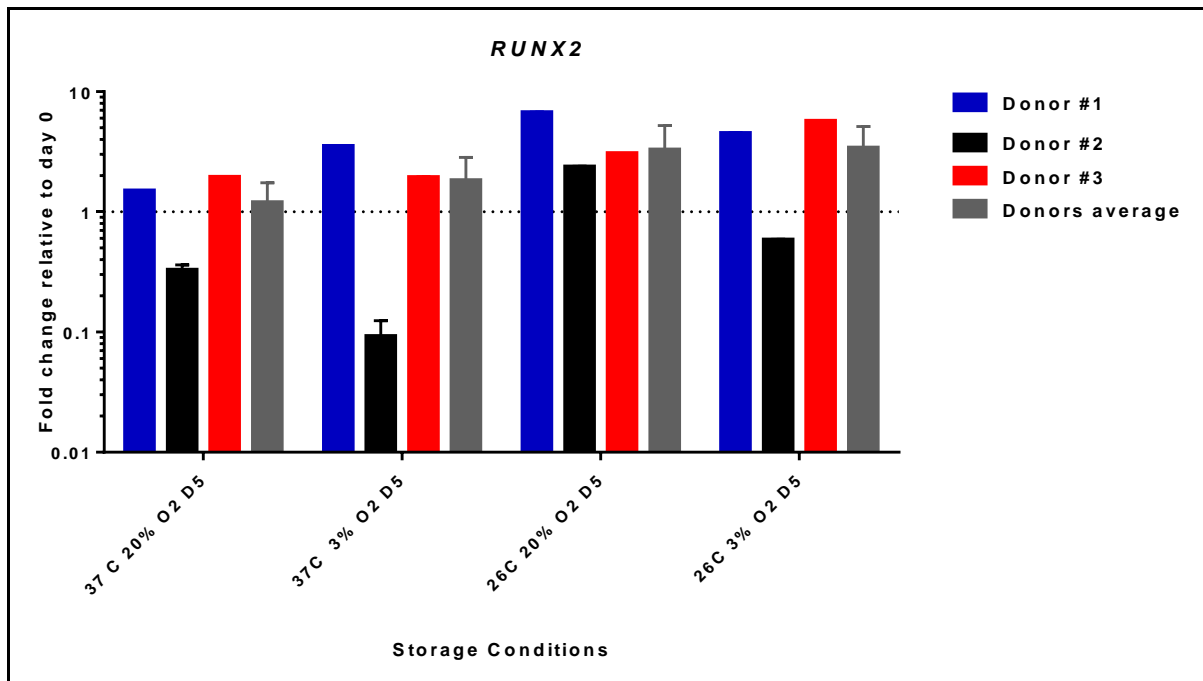


Fig. 4.11 Fold change in *RUNX2* gene expression in response to storage. hMSCs isolated from three healthy donors and exposed to storage conditions listed in Table 4.1. Fold changes values are relative to non-stored hMSCs (day 0) and are plotted as mean and standard error of the mean for three technical replicates for each donor. The average fold change values for the three healthy donors is also plotted for each storage condition. Data on y-axis are on logarithmic scale (\log_{10}). (37 C= 37 °C, O₂= pO₂, oxygen tension, D5= day 5).

ALPL, which encodes for the tissue non-specific form of the enzyme alkaline phosphatase (ALP), showed a similar trend to *RUNX2* (Fig. 4.12). *ALPL* expression slightly increased when temperature decreased for donor #1 and #3. When stored at 26 °C, hMSCs from donor #2 and #3 showed a slight increase in *ALPL* expression as oxygen tension decreased from 20 to 3 %.

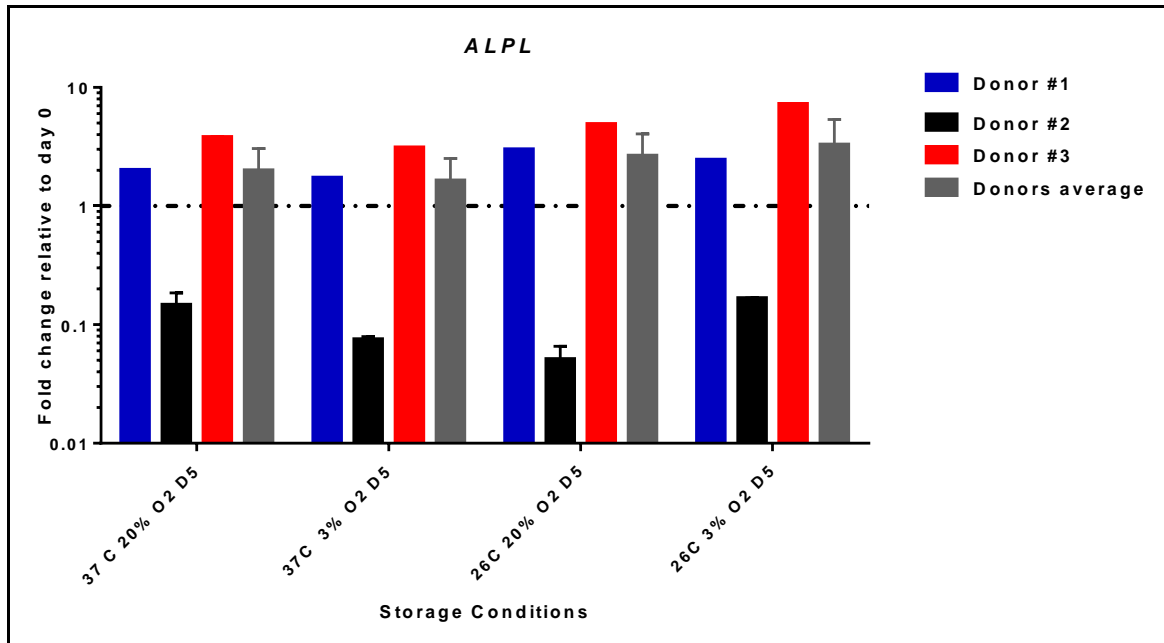


Fig. 4.12 Fold change in *ALPL* gene expression in response to storage. hMSCs isolated from three healthy donors and exposed to storage conditions listed in Table 4.1. Fold changes values are relative to non-stored hMSCs (day 0) and are plotted as mean and standard error of the mean for three technical replicates for each donor. The average fold change values for the three healthy donors are also plotted for each storage condition. Data on y-axis are on logarithmic scale (log₁₀). (37 C= 37 °C, O₂= pO₂, oxygen tension, D5= day 5).

In order to further investigate the effect of temperature and oxygen on the osteogenic differentiation potential, hMSCs from one donor (donor #1) were also seeded, stored and differentiated in 24 well plates. ALP enzymatic activity was assessed by pNPP assay as described in 4.1.7 at day 14 of osteogenic differentiation. ALP is a known marker of osteoblastic differentiation (Sheehy, Buckley, & Kelly, 2012). Cells stored at lower temperature and lower oxygen levels showed higher ALP activity (Fig. 4.13). The effect of temperature was statistically significant for all the three donors ($p=0.023$).

Following the pNPP assay, the cells were stained using Fast blue staining as described in 4.17. ALP stained cells showed a purple colour (Fig.4.14).

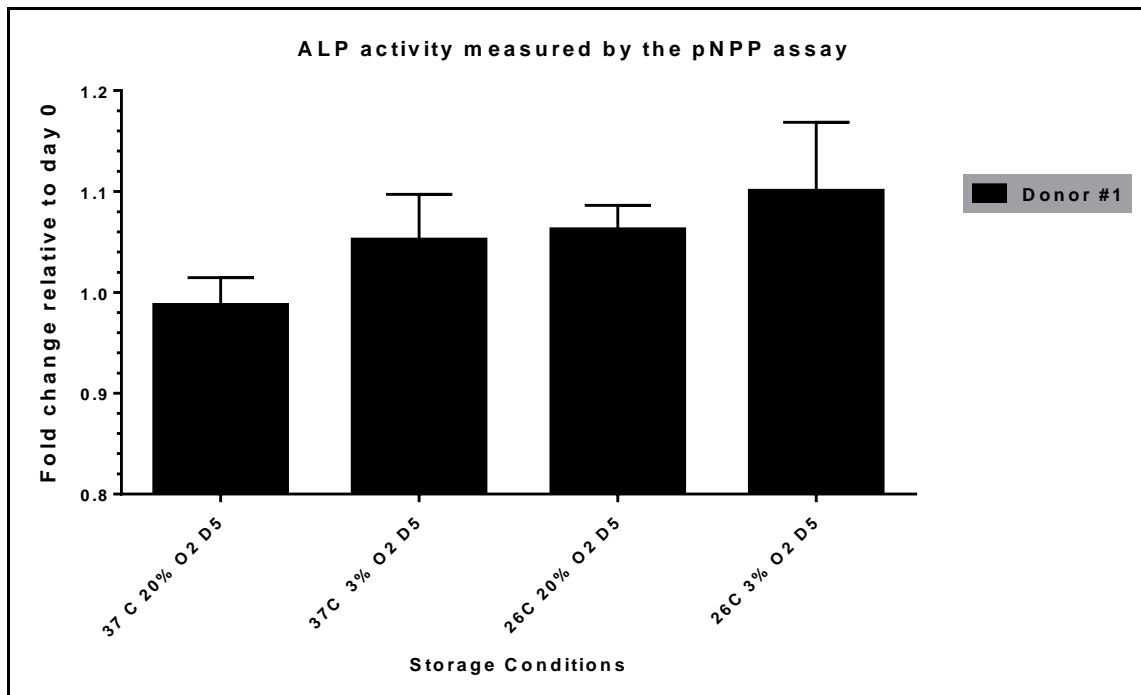


Fig. 4.13 Post storage ALP activity of hMSCs differentiated into osteogenic lineage. The ALP activity was measured with the pNPP assay and expressed relative to the ALP activity of differentiated non-stored hMSCs (day 0). hMSCs for one representative donor were used for this experiments. Data are expressed as mean and standard error of the mean for three biological replicates. (37 C= 37°C, O₂= pO₂, oxygen tension, D5= day 5).

ALP staining was highest at the lower temperature and oxygen levels. Compared to non stored differentiated hMSCs, ALP staining was lower for 5 day storage at 37 °C and 20 % oxygen. This result suggests a detrimental effect of temperature and oxygen on the osteogenic potential of hMSCs. Differences in ALP staining were also found for storage at different oxygen levels; lower oxygen level corresponds to higher ALP staining both at 37 °C and 26 °C storage.

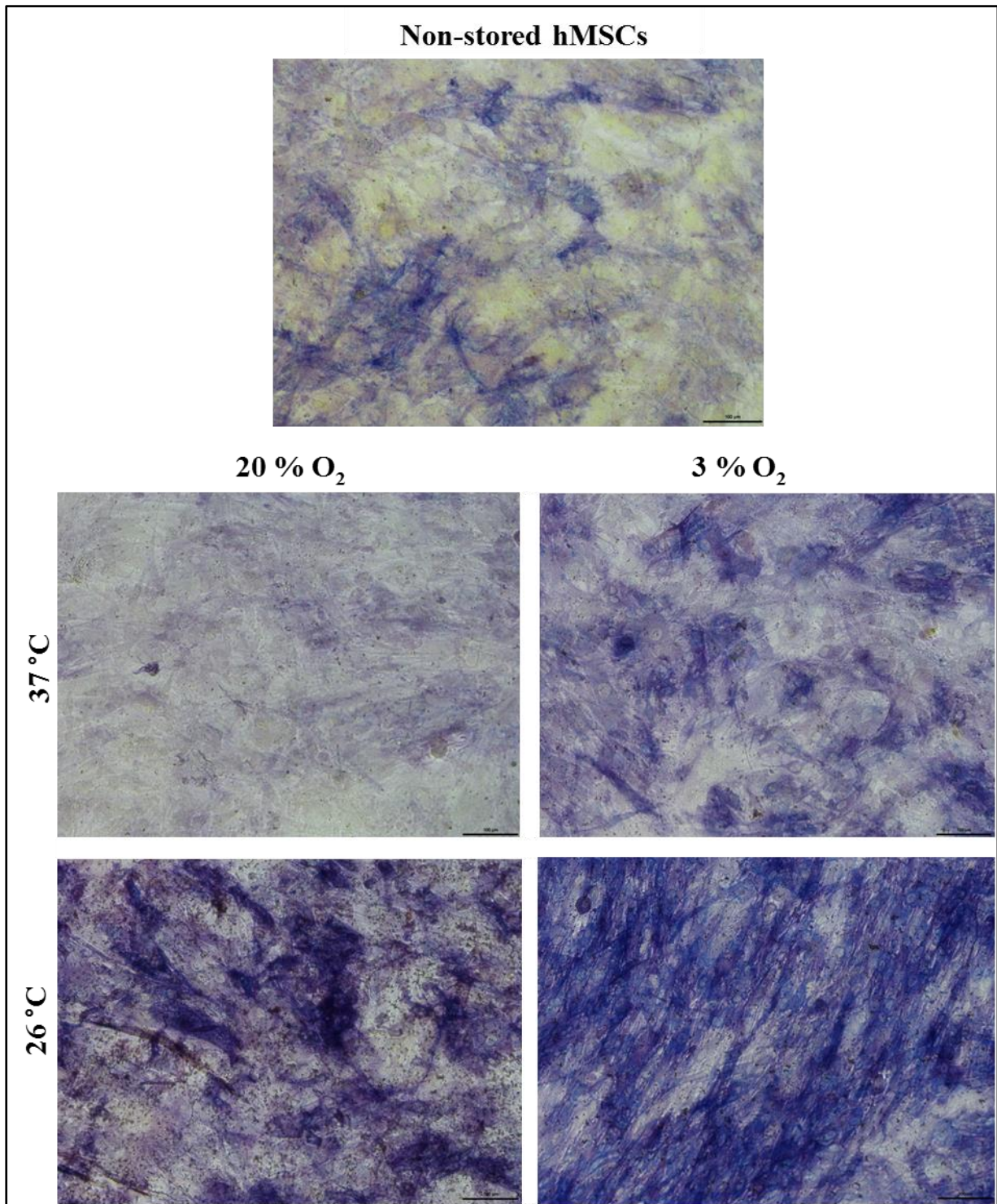


Fig. 4.14 ALP staining of differentiated hMSCs following 5 day storage. hMSCs from the donor were differentiated towards osteogenic lineage for 14 days before performing the ALP assay and staining using a Fast blue salt. Representative field of views are shown for all four storage conditions (Table 4.1) in a matrix format (oxygen versus temperature). Representative field of view of differentiated non-stored hMSCs is also shown (top). ALP positively stained cells are shown in purple. (Scale bar = 100 μ m).

4.2.4 Post storage adipogenic differentiation of hMSC

The adipogenic differentiation potential of the hMSCs following storage was evaluated by gene expression using hMSCs stored in T25 flasks and lipid vacuole quantification using hMSCs stored in plates as described in 4.1.8.

PPARG, which encodes for the peroxisome proliferator-activated receptor gamma linked to increased lipid uptake, and *FABP4*, which encodes for fatty acid binding protein 4, have been widely used as markers for adipogenic differentiation (Basciano et al., 2011). *PPARG* was upregulated in all four storage conditions for all three donors compared to non-stored cells (Fig. 4.15). Higher *PPARG* expression was linked to lower storage temperature and higher oxygen level.

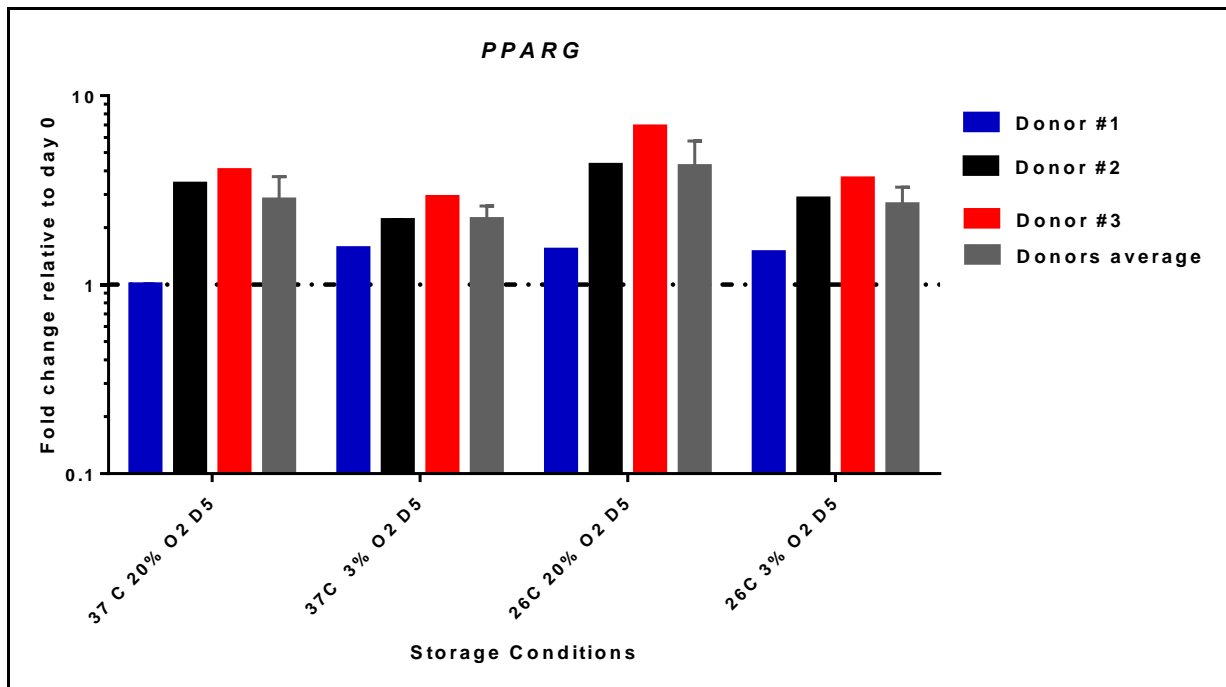


Fig. 4.15 Fold change in PPARG γ gene expression in response to storage. hMSCs isolated from three healthy donors and exposed to storage conditions listed in Table 4.1. Fold changes values are relative to non-stored hMSCs (day 0) and are plotted as mean and standard error of the mean for three technical replicates for each donor. The average fold change values for the three healthy donors are also plotted for each storage condition. Data on y-axis are on logarithmic scale (log₁₀). (37 C= 37°C, O2= pO₂, oxygen tension, D5= day 5).

FABP4 was also upregulated for all storage conditions for all three donors (Fig. 4.16). Higher storage temperature and higher oxygen level were linked to higher expression of *FABP4*. The effect of temperature was statistically significant for all three donors ($p=0.0032$).

In order to further investigate the effect of temperature and oxygen on the adipogenic differentiation potential, hMSCs from one representative donor (donor #3) were also seeded, stored and differentiated in 24 well plates. The presence of lipid vacuoles was assessed using AdipoRED staining (Lonza). Results are shown in Fig. 4.17. The number of adipocytes per field was quantified via imaging analysis using IMARIS software (www.bitplane.com). The highest number of adipocytes was observed for cells stored at 26 °C and 20 % oxygen, while storage at 37 °C led to a reduction in number compared to differentiated non-stored cells

(Fig.4.18). The effect of temperature on the number of adipocytes was statistically significant ($p=0.0038$).

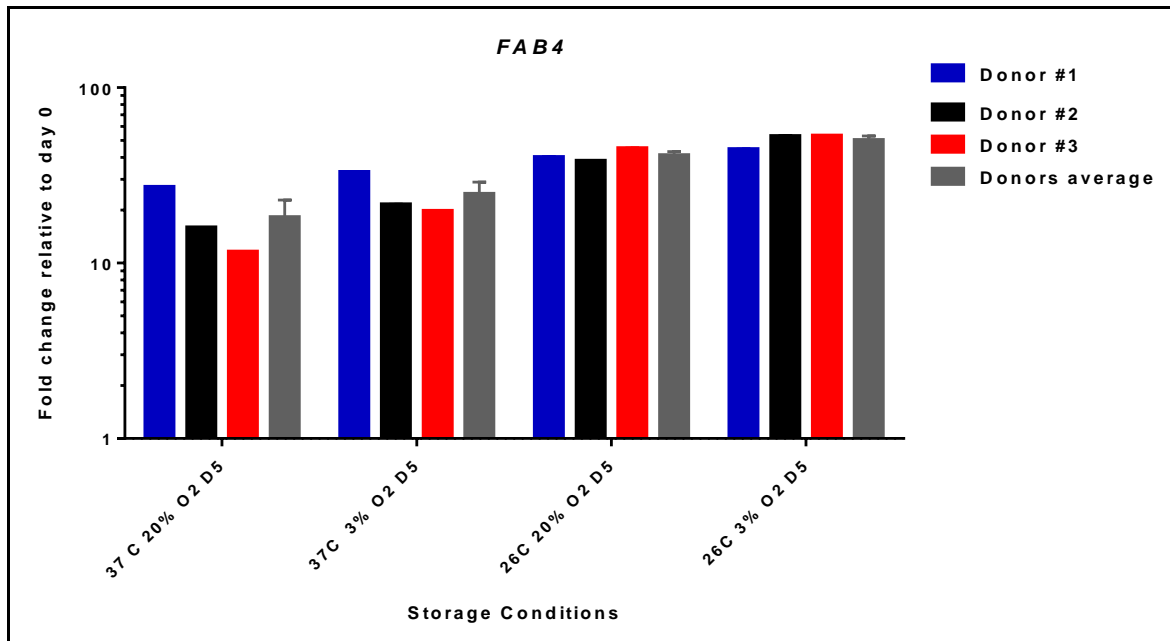


Fig. 4.16 Fold change in *FABP4* gene expression in response to storage. hMSCs isolated from three healthy donors and exposed to storage conditions listed in Table 4.1. Fold changes values are relative to non-stored hMSCs (day 0) and are plotted as mean and standard error of the mean for three technical replicates for each donor. The average fold change values for the three healthy donors are also plotted for each storage condition. Data on y-axis are on logarithmic scale (\log_{10}). (37 C= 37°C, O₂= pO₂, oxygen tension, D5= day 5).

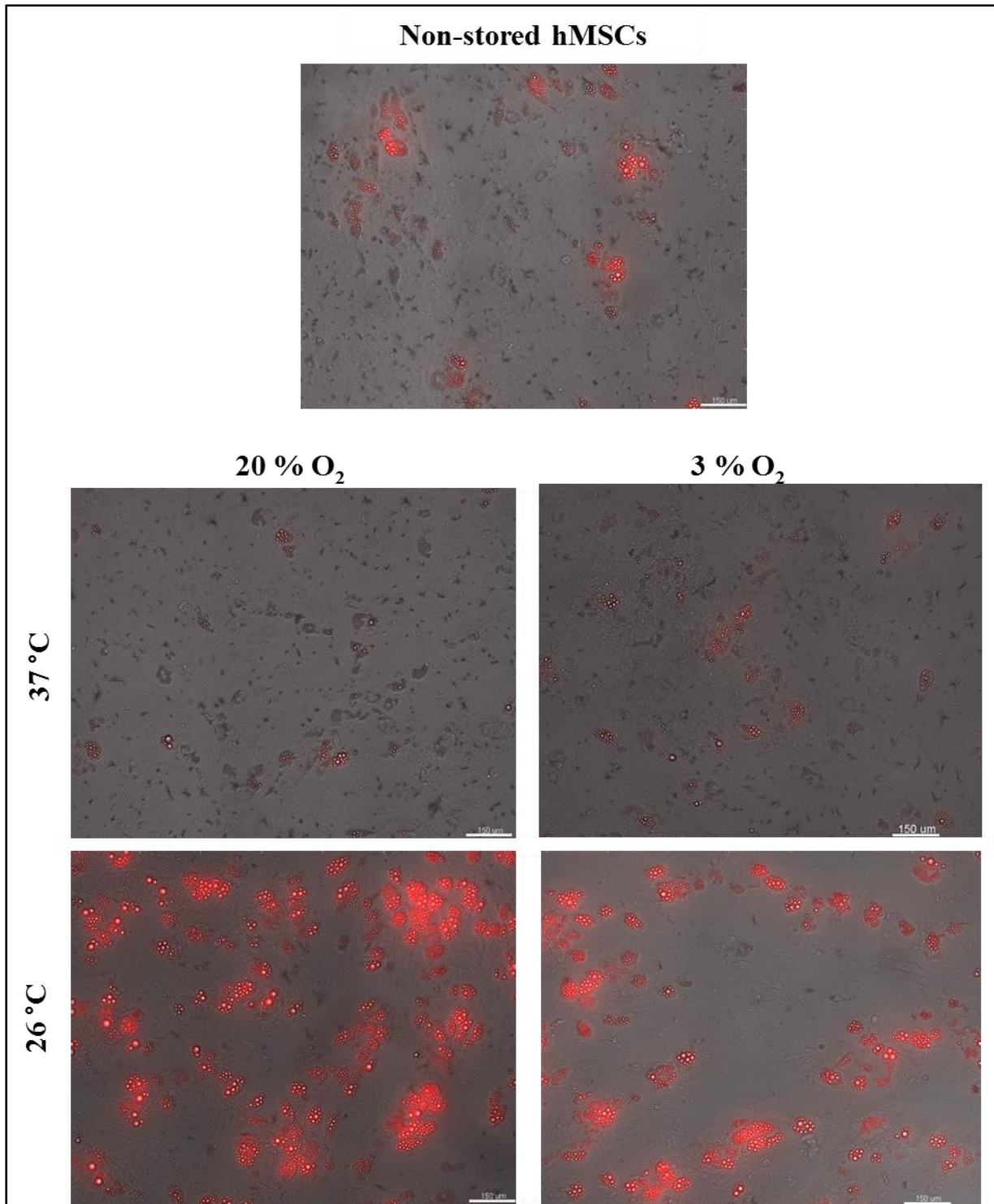


Fig. 4.17 AdipoRed staining of adipocytes following 5 day storage. hMSCs from one healthy donor were differentiated towards adipogenic lineage for 14 days before being stained using AdipoRed staining (Lonza). AdipoRed positive cells represent adipocytes (in red) and were visualized by fluorescence microscopy (Zeiss Axio Imager II microscope) (excitation $\lambda=485$ nm; emission $\lambda=535$ nm). Representative fields of stained adipocytes are shown for all four storage conditions (Table 4.1) in a matrix format (oxygen versus temperature). Representative field of differentiated non-stored hMSCs is also shown (top). (Scale bar = 150 μ m).

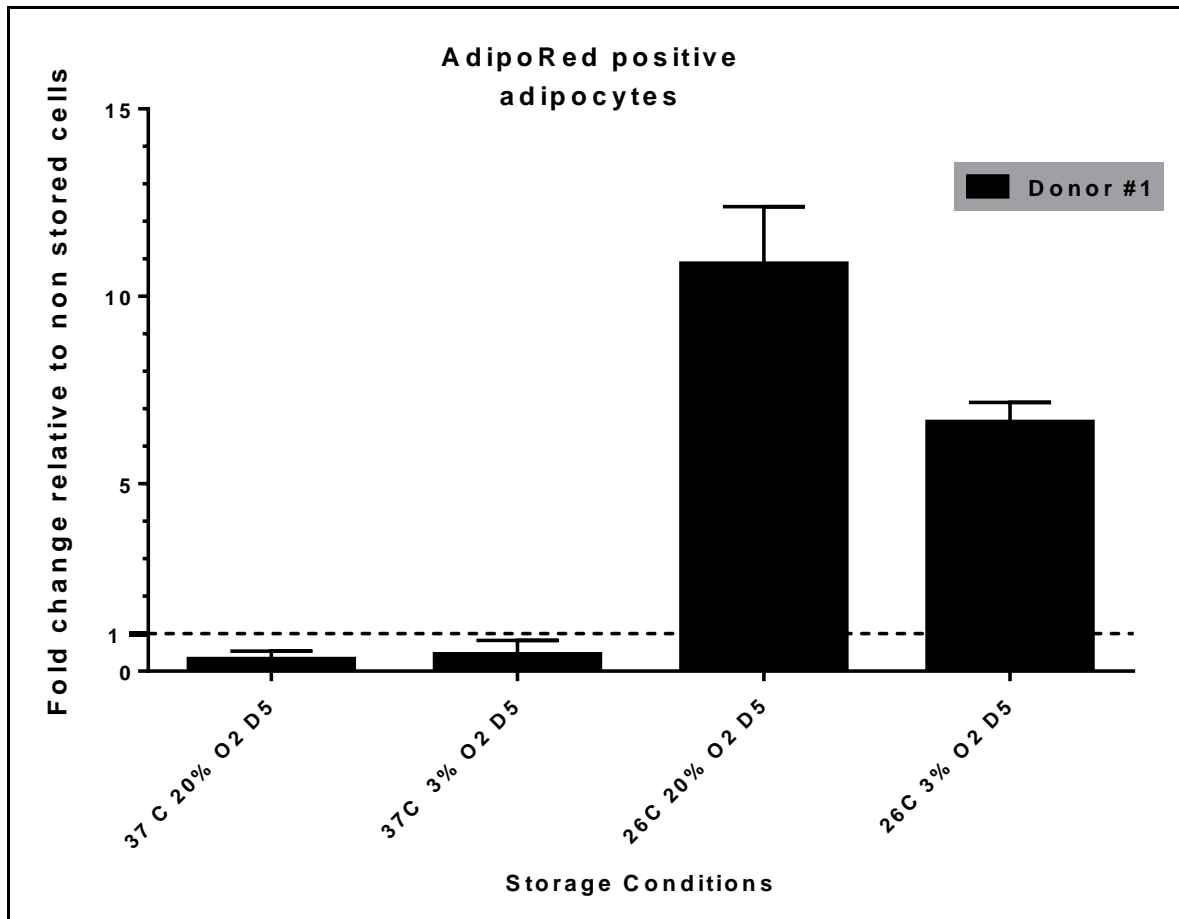


Fig. 4.18 Number of adipocytes for differentiated hMSCs following 5 day storage. Adipocytes were stained using the AdipoRed staining (Lonza), visualized by fluorescence microscopy (Zeiss Axio Imager II microscope) (excitation $\lambda=485$ nm; emission $\lambda=535$ nm) and counted by IMARIS software (BITPLANE, <http://www.bitplane.com/>). For each storage condition, three fields were taken for each of the three culture wells. The number of adipocytes has been calculated as the average of the three culture wells for each storage condition relative to differentiated hMSCs which were not exposed to any storage condition. (37 C= 37°C, O₂= pO₂, oxygen tension, D5= day 5). Dashed line represents fold change equal to 1 (no change in number of adipocytes compared to not stored cells.)

4.3 Brief summary of data described

In this chapter, the storage of hMSCs from three healthy donors has been studied. Table 4.9 summarizes the key findings.

Table 4.9 Brief summary of key findings for the storage of hMSCs in a controlled environment for 5 days.

	Key finding
Metabolites	
Glucose	Glucose concentration in spent medium increased as storage temperature decreased from 37 to 26 °C. The effect of temperature on glucose concentration was statistically significant.
Lactate	Lactate concentration increased as storage temperature increased from 26 to 37 °C. Lactate did not reach the inhibitory concentration of 3.15 g/l in any of the storage conditions.
Glutamine	Glutamine concentration was higher at lower temperature. Oxygen level only slightly affected glutamine concentration.
Ammonia	Ammonia concentration was higher for higher storage temperature. Ammonia concentration reached its inhibitory concentration 2.4 mM for donor 1 at 37 °C and 20 % oxygen.
Chondrogenic potential	
<i>COL2A1</i>	<i>COL2A1</i> was down regulated for all storage conditions except for 37 °C and 20 % O ₂ .
<i>ACAN</i>	<i>ACAN</i> was upregulated in all storage conditions for donor 1, while for donor 3 it was down regulated only for storage at 26 C and 3 % oxygen.
<i>COL1A1</i>	Lower storage temperature and lower oxygen tension lead to upregulation of <i>COL1A1</i> . For storage at 37 °C and 20 % oxygen, <i>COL1A1</i> was not upregulated. The effect of temperature and its interaction with oxygen levels were statistically significant.
GAGs/DNA	Lower temperature and oxygen tension level reduced the amount of sGAGs accumulated during the 14 day differentiation phase.
Osteogenic potential	
<i>RUNX2</i>	<i>RUNX2</i> expression increased as temperature decreased from 37 to 26 °C while no changes occurred due to oxygen level.
<i>ALPL</i>	Temperature and oxygen did not significantly affect <i>ALPL</i> expression.
ALP activity	ALP staining was higher at lower temperature and oxygen levels. The effect of temperature on ALP activity was statistically significant.
Adipogenic potential	
<i>PPARG</i>	<i>PPARG</i> was upregulated in all storage conditions. Higher expression was linked to lower storage temperature and higher oxygen levels.
<i>FABP4</i>	<i>FABP4</i> was upregulated for all storage conditions for all three donors. The effect of temperature was statistically significant.
adipocytes	The number of adipocytes was significantly higher following storage at 26 °C and 20 % oxygen.

4.4 Discussion

The aim of this chapter was to investigate the storage properties of hMSCs. The combined effect of temperature and oxygen over 5 day storage was studied.

The need for better cell product characterization to improve the manufacturing of cell therapy medicinal products has been highlighted (Bravery et al., 2013). This should include a deeper understanding of how process parameters, such as temperature and oxygen, affect the biological properties of the cells. This is even more important for the effective design of storage and transportation steps as these normally rely on passive containers where such parameters cannot be tightly controlled (PDA technical report 72).

In the undifferentiated hMSCs, temperature was the main factor affecting glucose, lactate, glutamine and ammonia metabolism. Unlike for the storage of cartilage discs, the effect of oxygen on ammonia metabolism was not statistically significant. However, hMSCs from donor#1 reached the reference inhibitory value for ammonia defined by Shop et al. (Schop et al., 2009) when stored at 37 °C and 20 % O₂ for 5 days.

A number of research groups have investigated the effect of low oxygen tension (hypoxia) on hMSCs differentiation potential, with emphasis on the effect that this has during the chondrogenic, osteogenic or adipogenic differentiation process (Markway et al., n.d.) (Malladi, Xu, Chiou, Giaccia, & Longaker, 2006)(Buravkova, Andreeva, Gogvadze, & Zhivotovsky, 2014). In this study, hMSCs have been exposed to four different combinations

of oxygen and temperature prior to the differentiation process, which more closely resembles the stimulation cells undergo during storage and transportation.

Storage of hMSCs at 37 °C and 20 % O₂ for 5 days increased the expression of *COL2A1* while reducing the expression of *COL1A1*. This suggests a greater chondrogenic potential which was not present for the other storage conditions. The amount of GAGs accumulated over the 14 days storage period was also higher for this storage condition. This demonstrates that when hMSCs are exposed to temperature and oxygen levels that move away from 37 °C and 20 % O₂ for 5 days, their chondrogenic potential is impaired. This might appear in contrast with the fact that during embryonic development, pluripotent stem cells differentiate into chondrocytes and form cartilage in a hypoxic environment (Adesida et al., 2012).

However, the difference might lay on the different role that hypoxia play during and prior to the differentiation process.

The osteogenic potential of the hMSCs from the three donors was not significantly affected by 5 day storage under the different combinations of temperature and oxygen. However, for donor#1, the effect of temperature was statistically significant and ALP activity reached its highest for hMSCs exposed to 5 day storage at 26 °C and 3 % oxygen. In a recent study, Sheehy et al. demonstrated that hypoxia pre-conditioning at 37 °C inhibits osteogenic differentiation (Sheehy et al., 2012). However, results described in this chapter demonstrate the effect of temperature on the osteogenic potential is even greater.

The 5 day storage led to upregulation of the adipogenic markers, such as *PPARG* and *FABP4* for all three donors. The effect of temperature was significant on *FABP4* regulation. Lower storage temperature increased the adipogenic potential of hMSCs and this was confirmed by the AdipoRed staining. The detrimental effect of hypoxia on the adipogenic and osteogenic potential of hMSCs has been documented (Hung et al., 2007). Results described in this

chapter showed that storage at a lower temperature (26 °C) remarkably increases their adipogenic potential. The significance of this key finding is not just limited to storage and transportation of hMSCs but could be used for the expansion of adipose derived human stem cells (hASCs) which are currently been investigated for a number of clinical applications, including but not limited to wound healing. (Keung et al., 2013)(clinicaltrials.gov).

Similarly to what was described in chapters 2 and 3 for the storage of cartilage discs, storage conditions should be defined depending on the biological property that needs to be preserved. Temperature and oxygen can be adequately selected to modulate chondrogenic, osteogenic and adipogenic potential of hMSCs. The selection of higher or lower values of these two parameters will depend upon the therapeutic applications the hMSCs are intended for as discussed in chapter 5.

Chapter 5

General discussion

The use of human cells as medicinal products has generated a great deal of interest worldwide for the potential to treat a broad range of high impact unmet clinical needs (Heathman et al., 2015). However, the ‘living’ nature of such products creates a number of challenges that are new to the biopharmaceutical community. The ability to ‘manufacture, store, transport and distribute regenerative medicine products’ has been identified by the UK’s Office for Life Science as a necessary step in order for these therapies to join ‘mainstream clinical practice’.

(https://www.gov.uk/government/uploads/system/uploads/attachment_data/file/32459/11-1056-taking-stock-of-regenerative-medicine.pdf)

As there is convincing evidence that cells are responsive to oxygen concentration within the growth medium, it is important to investigate its effect in combination with temperature.

The work described in this thesis aimed to investigate a novel temperature range (26-37 °C) for storage and transportation and, for the first time, to combine temperature with a variable oxygen tension over a simulated shelf life of 5 or 7 days.

5.1 Key findings

5.1.1 Post storage viability

For cell based medicinal product, viability can be considered as one important indicator to assess the stability over the shelf life. Although many assays are currently available (Ng et al., 2005), the assessment of viability can pose technical challenges when cells are organized into tissue. In such situations, metabolic dyes such as Alamar blue can provide an indicator of overall metabolic activity of the population of cells within the construct. The main limitation of metabolic assays, including Alamar blue, is that cellular metabolic activity varies greatly throughout the lifecycle of cells (Rampersad, 2012). On the other hand, alternative viability measurements which assess viability by monitoring cell membrane integrity could not be applied for cartilage discs as the cells could not be consistently isolated without altering their viability.

Viability of cartilage discs following storage in a controlled environment was tested using the Alamar blue assay as described in chapter 2. For all three donors, storage at 26 °C led to a better viability than storage at 37 °C after both 5 and 7 days. Oxygen tension did not have a large effect on modulating viability post-storage. Viability decreased over time but was on average no lower than 75.5 % even after 7 day storage at 37 °C and 20 % oxygen. As already noted, there are limited data on the storage of hMSCs at body temperature for 7 days.

However, other groups have investigated the viability of stem cells in a slightly different but related context. For example, Alves and colleagues also demonstrated that human pluripotent stem cell-derived cardiomyocytes (hPSC-CMs) showed high cell recovery (>70%) when stored for 7 days, although the cells were stored at 4 °C and with a clinical-compatible

preservation formulation (Serra, Brito, Correia, & Alves, 2012). Interestingly, hPSC-CM recovery was higher in three-dimensional aggregates than in 2D monolayers (Correia et al., 2016). While aggregation of therapeutic proteins is one of the most dangerous aspects of protein-based drugs (Chirino, Ary, & Marshall, 2004), for cell-based medicinal products this might provide a more physiological environment, enhancing their preservation over time. Interestingly, Bayouseff et al. recently demonstrated that aggregation of C2C12 myoblast cells maintained higher viability compared to single cells in suspension. (Bayoussef et al., 2012)

On the other hand, Patricia Gálvez-Martín and co-workers showed that the viability of adipose derived-hMSCs was maintained above 80 % for 48 hours storage at 4 °C but drastically decreased when the cells were stored at 25 °C and 37 °C (Galvez-Martin, Hmadcha, Soria, Calpena-Campmany, & Clares-Naveros, 2014) .

The ECM the cells are embedded in might also exert a protective effect while contributing to the proliferation of cells when lost which is not normally the case for cells stored in suspension. This ‘protective’ effect can also be created by encapsulating the cells into alginate, as recently demonstrated by Swioklo et al. (2015) for adipose derived mesenchymal stem cells and by Mahler and co-workers for hepatocytes (Mahler et al., 2003).

However, as discussed in chapter 2, the length of the shelf-life might also be dependent on the cell type as for commercially available engineered tissue products this varies from 36 hours for Holoclar to 15 days for Apligraf.

Therefore, for some cell types, aggregation and the presence of ECM enable longer shelf life even when the product is stored at temperatures closer to 37 °C.

5.1.2 Metabolites

When cells are stored at a temperature above $-150\text{ }^{\circ}\text{C}$, they will continue to metabolize glucose and glutamine while producing lactate and ammonia as waste products (Schop et al., 2009).

As part of more complex formulation studies, it is important to evaluate that the amount of glucose and glutamine available is sufficient to allow the cells to survive while lactate and ammonia do not reach or exceed values which might have a detrimental effect.

Chapters 2 and 3 demonstrated that the multifactorial approach can be used to identify temperature and oxygen as variables that can be engineered to modulate specific metabolic pathway during storage.

For cartilage discs, a decrease in storage temperature from $37\text{ }^{\circ}\text{C}$ to $26\text{ }^{\circ}\text{C}$ led to 34 % less glucose metabolized following 5 day storage while lactate release was 87% lower.

Lower oxygen tension had less of an effect on the amount of glucose and lactate. Even after 7 days storage, lower oxygen resulted in only a 4 % decrease of lactate release. Lactate release inversely matched glucose consumption with higher values for longer storage at higher temperature. Moreover, oxygen and temperature interaction showed a statistically significant effect on lactate metabolism. This implies that the temperature mediated decrease in lactate released in the medium will be dependent on the oxygen tension present in the medium.

For hMSC storage, lower temperature led to 61 % less glucose metabolized and 63 % less lactate released.

Storage at lower temperature and low oxygen condition also reduced glutamine metabolism. For cartilage discs, glutamine concentration in the spent medium post-storage ranged from 1% of the initial glutamine concentration (2 mM) after 5 day storage at 37 °C and 20 % oxygen to 76 % after 5 day storage at 26 °C and 3 % oxygen. Consequently, a lower amount of ammonia is produced after both 5 and 7 day storage. Interestingly, oxygen had a statistically significant effect on glutamine and ammonia concentration in the spent medium (along with storage temperature and length) for cartilage discs. This suggests that temperature and oxygen could be used to modulate the amount of waste products released, products that might have a detrimental effect on the cells.

However, for undifferentiated hMSC storage, glutamine and ammonia metabolism was less strongly influenced by oxygen tension, suggesting that the metabolic preferential pathway of undifferentiated hMSCs is different compared to the hMSC-derived chondrocytes. This was also demonstrated by Pattappa and co-workers (Pattappa, Heywood, de Bruijn, & Lee, 2011).

A limited number of studies have investigated the energy metabolism of MSCs with the aim to better understand it and improve growth conditions and cell yield for therapeutic applications. In an attempt to mimic more closely the bone microenvironment, with oxygen tension which varies from 1- 6 %, the effect of hypoxia on proliferation has been reported (Grayson, Zhao, Bunnell, & Ma, 2007b). Dos Santos et al. demonstrated that when cultured under low oxygen condition (2%), cells metabolized more glucose and glutamine but released lower quantities of lactate and ammonia (Dos Santos et al., 2010). The higher consumption of glucose was correlated to higher proliferation under hypoxia. This result was in contrast with

that reported by Schop et al (2009), who reported a lower glucose consumption rate for hMSCs cultured under low oxygen conditions (3%) on microcarriers (Schop et al., 2009).

Moreover, higher rate of glutamine consumption for the first 5 days of culture under hypoxia was not correlated to higher ammonia accumulation (Dos Santos et al., 2010), unlike what was found for cartilage discs (chapter 2) and undifferentiated hMSCs (chapter 4) in this thesis.

There is increasing evidence that metabolic pathways are strongly dependent on the proliferating state and cell type. Varum et al. (2011) demonstrated that iPSCs and hESCs, which are characterized by a high proliferating rate, mainly rely on glycolysis to meet their energy demand (Varum et al., 2011). Osteoblasts, with lower proliferative capacity compared to pluripotent stem cells, demonstrated the ability to alternate both glycolysis and oxidative phosphorylation for their ATP production (Komarova et al., 2000).

This suggests that glucose consumption and ammonia built-up in the final formulation should be evaluated for each cell-based product.

5.1.3 Chondrogenic potential

hMSCs have also been investigated for their potential to regenerate hyaline cartilage (Steinert et al., 2012). Because of the low engraftment rate of the cells *in situ*, these are often embedded in hydrogel matrix and can be applied or even directly injected into the knee (Spiller et al., 2011). The immunogenicity of allogeneic hMSCs have been investigated (Consentius et al., 2015). In a recent study, Nathalie Rouas-Freiss and co-workers demonstrated that hMSCs from bone marrow and adipose tissue maintained their

immunosuppressive properties even after chondrogenesis (Du et al., 2016). As chondrogenic differentiation potential is key, it is important to assess how temperature and oxygen can modulate this potential during storage.

Lower temperature and higher oxygen tension correspond to higher *COL2A1* fold change relative to non-stored cartilage discs following 5 and 7 day storage. As mentioned in chapter 2, this could be linked to *in-vivo* cartilage homeostasis. However, in these storage conditions (26 °C/20 % oxygen for 5 and 7 days storage), *COL1A1* was upregulated.

The effect of temperature and oxygen was also studied on undifferentiated hMSCs. Different trends were observed when investigating the effect of temperature and oxygen on hMSCs prior to chondrogenic differentiation. Unlike cartilage discs, *COL2A1* expression was highest following 5 day storage at higher temperature and higher oxygen (37 °C and 20 % oxygen). Only in this storage condition was *COL2A1* upregulated compared to non-stored hMSCs. Consistently with cartilage discs, *COL1A1* was downregulated for 37 °C/20 % oxygen (preferred condition for *COL2A1* expression) and significantly overexpressed for other storage conditions. Temperature and its interaction with oxygen were statistically significant. This implies that the effect of oxygen in modulating *COL1A1* expression will be dependent on temperature. Many groups have reported that hypoxia stimulation at 37 °C can increase the chondrogenic potential for hMSCs derived from a number of sources, such as bone marrow (Khan, Adesida, Tew, Lowe, & Hardingham, 2010), infrapatellar fat pad (Khan et al., 2007) , but not for adipose tissue derived hMSCs (Malladi et al., 2006).

For cartilage discs, storage at high temperature (37 °C) and oxygen (20 %) also led to higher *ACAN* expression both after 5 and 7 day storage. On the other hand, when storing undifferentiated hMSCs, *ACAN* expression was highest at 37 °C and 3 % oxygen for 5 days.

This was not confirmed by GAG accumulation, which was highest for storage at 37 °C and 20 % oxygen.

This suggests that temperature and oxygen can provide ‘contrasting’ stimuli to the cell product during storage, as discussed in chapter 3. As chondrogenesis can occur at both normoxic (20 %) and hypoxic (3 %) conditions, it can be hypothesised that some of the effect of hypoxia pre-stimulation is ‘lost’ when the cells are exposed again to 20 % oxygen.

5.1.4 Osteogenic potential

Although bone has a very high capacity to self-heal, the use of hMSCs for bone regeneration have been extensively studied mainly for the treatment of large bone defects or traumatic injuries (Steinert et al., 2012).

hMSCs stored for 5 days retained the potential to differentiate towards the osteogenic lineage as demonstrated by *RUNX2* and *ALPL* which were upregulated in all storage conditions.

Moreover, alkaline phosphatase (ALP) staining was highest at the lower temperature and oxygen levels. For both storage temperatures (26 and 37 °C), lower oxygen levels correlated to higher ALP staining.

The effect of hypoxia on hMSC osteogenic potential is controversial (Buravkova et al., 2014). Differences in culture conditions as well as donor make the comparison of results from different research groups difficult. If the effect of hypoxia is studied using a range of low oxygen levels (1-5 % oxygen) and variables levels of exposure (2 h to 60 h or more), hMSCs show a lower proliferation potential for 1% oxygen for 48 h (Epimenko et al 2011,

Hung et al 2007) but a slight increase in duration of incubation to 4 days at 1 % led to an enhanced proliferation potential for both umbilical cord and bone marrow derived hMSCs (Lavrienteva et al 2010). This suggests that hMSCs might possess a protective mechanism, such as an adaptation to low oxygen level, that can be reversed. While there is evidence that exposure to hypoxia during differentiation will inhibit osteogenic potential (Malladi et al. 2006, Fehrer et al. 2007, D'Ippolito et al. 2006), the data described in this thesis demonstrate that this potential can be restored once hMSCs are back to 37 °C and 20 % oxygen. Consistent results were also shown by Buravkova and colleagues (Buravkova, Grinakovskaya, Andreeva, Zhambalova, & Kozionova, 2009).

Other studies have demonstrated that the osteogenic potential of hMSCs can be preserved following low temperature storage (4 °C) for placenta derived (Pogozhykh, Prokopyuk, Pogozhykh, Mueller, et al., 2015) and bone marrow (Ginis, Grinblat, & Shirvan, 2012) derived hMSCs.

5.1.5 Adipogenic potential

PPARG and *FABP4*, two commonly used adipogenic gene markers, were also upregulated in all hMSCs following storage. In particular, *PPARG* expression was greatest for low temperature and high oxygen (26 °C 20 % oxygen) for all three donors and this correlates with the highest number of adipocytes stained. The effect of temperature on *FABP4* expression was also statistically significant for all three donors.

Valorani et al. showed that culturing adipose derived hMSCs for 7 days under 2 % oxygen and 37 °C increases their osteogenic potential (Valorani et al., 2012). However, data

described in chapter 4 showed that, for bone marrow derived hMSCs, exposure to lower temperature (26°C) has an even greater effect on enhancing the adipogenic potential.

5.1.6 DoE as an investigational and decision support tool

A DoE approach was applied to investigate the combined effect of temperature, oxygen and storage duration on cartilage discs and the combined effect of temperature and oxygen on undifferentiated hMSCs. This approach was preferred to the OFAT approach as it allows one to investigate the effect of interactions between factors and therefore a better understanding of how parameters effect the response, such as viability, metabolite concentration in spent medium and gene expressions changes. For cartilage disc storage, temperature had a statistically significant effect on viability, glucose, lactate, glutamine, ammonia and *COL1A1* expression. Oxygen had a statistically significant effect on glutamine, ammonia concentration and *COL1A1*. Interestingly, oxygen and temperature interaction showed a statistically significant effect on lactate metabolism, implying that the temperature mediated decrease in lactate released by the cartilage discs will be dependent on the oxygen tension. The effect of oxygen on glutamine and ammonia was confirmed but not statistically significant for undifferentiated hMSCs storage supporting the important finding that even when subjected to the same storage conditions, different cells might react in a different manner. Differences were also found in the expression of genes related to the chondrogenic potential of the two cell therapy products. The effect of oxygen on *COL1A1* was not statistically significant. However, its interaction with temperature was statistically significant, showing that oxygen will modulate the expression of *COL1A1* to a varying extent depending on the storage

temperature. Within the multidimensional space under investigation, the effect of different oxygen tension (3 and 20 %) was greater for storage at 37 °C than for storage at 26 °C.

Jakobsen et al. also applied a multifactorial approach to investigate the factors that induce chondrogenesis of hMSCs *in-vitro* (Jakobsen, Ostrup, Zhang, Mikkelsen, & Brinchmann, 2014). This enabled them to identify the optimal combination of growth factors (TGF- β and dexamethasone) leading to the highest expression of desirable hyaline cartilage markers.

However, they found that this optimal combination also introduced an induction of unwanted markers, such as an upregulation of *COL1A1*.

Similarly, data described in chapter 2 and 3 of this thesis have shown that preferential storage conditions for cartilage discs in terms of viability, lactate, ammonia, *COL2A1* and *ACAN* are the ones that led to upregulation of *COL1A1*, which should be minimal for cartilage-like tissue as collagen type I is abundant in bone ECM but nearly absent in hyaline cartilage (B Johnstone, Hering, Caplan, Goldberg, & Yoo, 1998).

This suggests that multiple factors should not be analysed nor controlled independently as the preferred outcome might be only achieved by adequately combining input factors. This was the basis for the case studies described in chapter 3. The eight response models created using the data from cartilage disc storage were combined together. Case study 1 showed how in a hypothetical scenario where two storage containers were available, values of viability, glucose, lactate, glutamine, ammonia and gene expression changes can be predicted. This simulation could be repeated for many more storage containers where temperature, oxygen tension and storage duration are the input parameters. This would support the screening phase of procurement for a storage container. Although the ‘shortlisted’ containers will then need to be tested and validated, the approach described in the case study will considerably reduce time and costs.

Case study 2 showed how the response models can be combined to predict the values that temperature and oxygen should have given set product specifications and assuming storage duration of 7 days. This hypothetical scenario represents the case where a storage container is not available for the cell therapy product and it aims to support its design. An ‘optimal’ operational space was identified and it includes all combinations of temperature and oxygen that are likely to meet the product specifications following 7 day storage.

As a decision support tool, DoE has the potential to limit the number of experiments required while maximising the understanding of multifactorial effect on the cell therapy product. This can be particularly useful where the amount of ‘raw’ material available for testing is limited, such as for autologous products (C. K. Schneider et al., 2010).

A similar approach has been suggested by Chen et al. for the characterization and optimization of cell seeding in scaffold for skeletal tissue engineering (Y. Chen et al., 2011).

5.2 Challenges and limitations

Data described in chapter 2 and 4 showed considerable donor to donor variability. The selection of ‘young healthy donors’ of Caucasian ethnicity to isolate bone marrow and hMSCs is very common among the scientific community. However, bone marrow and hMSCs isolated from this class of donors might be, in reality, very heterogeneous (Phinney & Prockop, 2007).

Given the inter donor variability observed in the data, the analysis of results was based on a technique known as ‘blocking’, which allows for more precise evaluation of main effects and interactions (Montgomery, 2012). It was not within the scope of this thesis to investigate the biological difference between donors. However, in order to increase the statistical power, at least two more donors could be tested.

In terms of biological differences between donors, it is important to consider its impact on process development of cell based medicinal products. For allogeneic therapies, hMSCs are expanded from one ‘universal’ donor to produce multiple doses for more patients. A master cell bank is normally developed (Salmikangas et al., 2015) as described in chapter 1. Bone marrow, or potentially any other source of biological material, is tested for safety (i.e. absence of pathogens). hMSCs derived from this donor can be extensively characterized during product development and a baseline can be generated. If a new donor needs to be introduced to comply with the demand of the product, the hMSCs will be characterized and compared with the baseline generated from the first donor. Only if no statistical significance can be observed, will the second donor will be used for production. The characterization should go beyond ISCT guidelines. If the product is the cartilage disc studied in this thesis, one additional parameter to monitor should be cell proliferation during chondrogenesis as high cell density correlates with better chondrogenesis (Murdoch et al., 2007).

All the storage experiments described in this thesis were carried out using tissue culture incubators where temperature and oxygen could be reproducibly set to specific levels. As only 4 dedicated incubators were available, it was not possible to confirm the presence of a non-linear relationship between the input parameters (temperature, oxygen and storage duration) and the output variables (viability, metabolites and gene expression). This would have required at least one additional storage condition and, therefore, at least one additional dedicated tissue culture incubator.

5.3 Future work

The work described in this thesis could be further developed as described below:

- As shown in Chapters 3 and 4, the concentration of ammonia in the spent medium following storage at 26 and 37 °C could be effectively reduced by lowering the oxygen level from 20 % to 3%. Building on this important finding, a new primary container for the storage of a cell-based product could be developed. The storage experiments described in this thesis were performed using culture plates or flasks as primary containers where the headspace was in equilibrium with the chamber of the incubator. If the oxygen tension was set at 3 %, this was kept constant within the incubator. In order to develop the primary container as mentioned above, the oxygen and carbon dioxide within the medium should be measured over 7 day storage at 26 and 37 °C and compared with the values of the same culture plate after being adequately sealed. If a significant drop in oxygen level is detected compared to the open container, then a ‘passive’ system could be devised to enable the oxygen tension to be constant for the duration of the storage. This would include a membrane with specific diffusion coefficient which would separate the sample from an “enriched” oxygen headspace (Fig 5.1). An optical patch could also be placed within the primary container to enable non-invasive oxygen monitoring during storage and transportation. Temperature monitoring is currently a requirement for transportation of temperature sensitive medicinal products. As standards for cell-based medicinal product transportation are developed, oxygen monitoring might prove necessary to ensure the quality of the product is not altered for non-cryopreserved products.

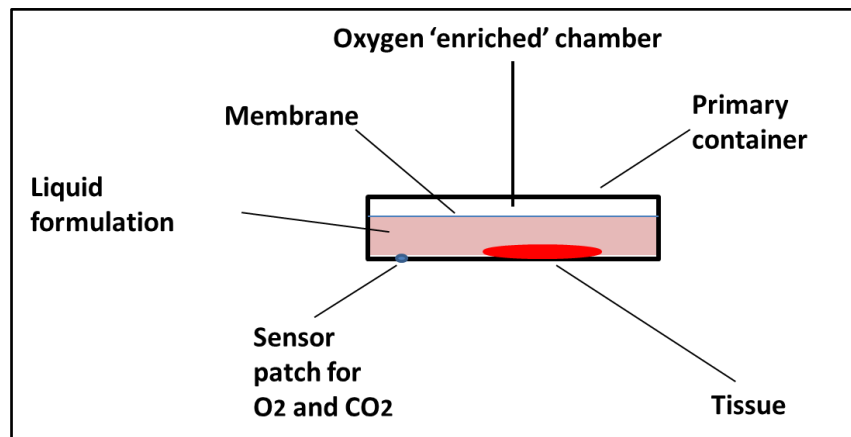


Fig. 5.1 Schematic of an innovative primary container for the storage and transportation of cell and tissue products. The oxygen 'enriched' chamber would provide through the membrane the adequate oxygen supply for the effective preservation of viability and biological function of the product.

- Data described in chapter 4 for the storage of undifferentiated hMSCs were generated using T25 flasks and culture plates. This provides the cells a surface to adhere to which does not normally occur when the cells are stored and transported in vials, bags or syringes. On the other hand, it is reasonable to assume that maintaining adherent cells in a more natural state would contribute to the preservation of their biological properties. This hypothesis is also supported from the 'protective' effect exerted by the ECM or biomaterials on cells, discussed earlier in this chapter. The potential beneficial effect of hMSC attachment during storage could be tested. If this hypothesis is confirmed, a new primary container could be devised which incorporates a temperature-sensitive polymer. This would allow for the cells to attach during storage and transportation and detach by adequately changing the temperature for delivery and administration of the product, negating the need for an enzymatic-mediated detachment reaction, which may not be optimal in a clinical setting. This approach is based on a technology developed by Professor Teruo Okano and currently

used to grow cells to confluency and detach them as a single sheet by lowering the temperature (J. Yang et al., 2005).

- The advantages of storing a cell therapy product between 26 and 37 °C could be compared with temperature that are commonly used for the transport of pharmaceuticals, such as controlled room temperature, hypothermic and -20 °C (Fig. 5.2). Chapter 3 demonstrated that the viability of the cartilage discs decreased as storage temperature increased for both a 5 and 7 day shelf life. However, storage and transport at a temperature that is closer to physiological, might significantly improve the preservation of the product's biological properties by limiting cold-induced stress. This hypothesis is also supported by data described in chapters 2 and 4; both cartilage discs and hMSCs showed enhanced expression of *COL2A1* and reduced *COL1A1* when stored at 37 °C and 20 % oxygen. However, this chondrogenic potential should be further investigated by introducing a protein level assays (such as western blotting or ELISA), in order to confirm that higher expression of *COL2A1* corresponds to higher production of collagen type II. Moreover, a live-dead staining of the cartilage discs following storage could also be introduced to provide additional information on the 'health' status of the cells within the disc. This could be used in combination with results generated from the Alamar blue assay and enable a better viability assessment.

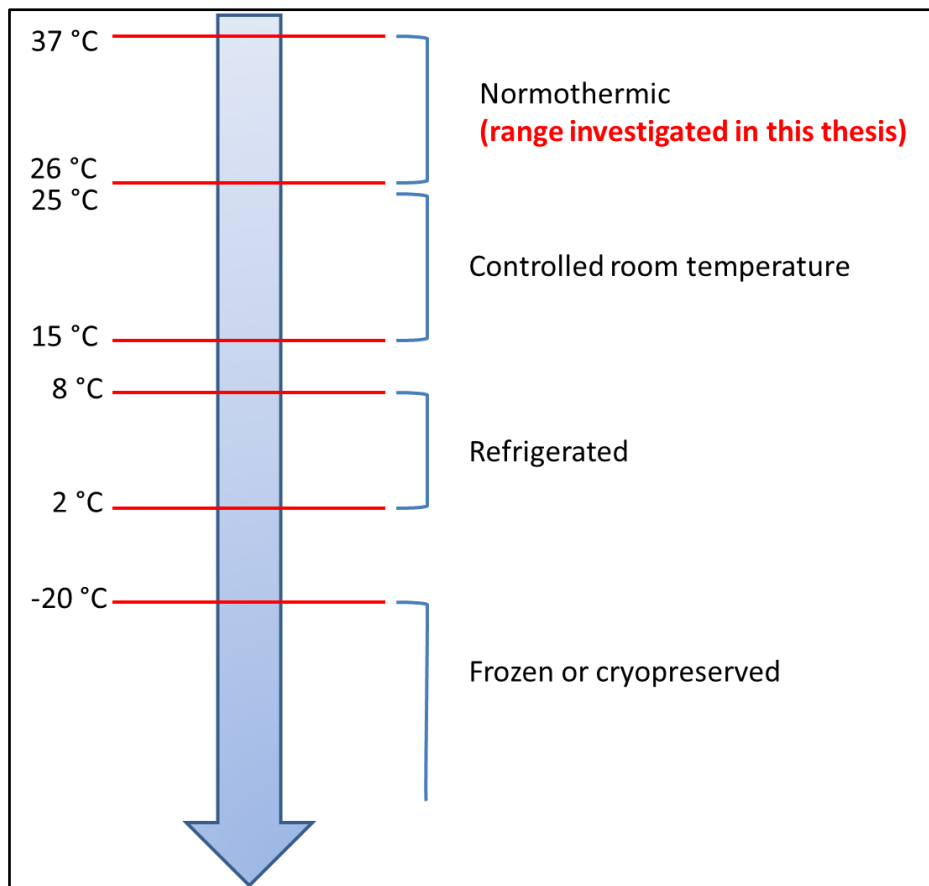


Fig. 5.2 Schematic illustration of the main temperature ranges that can be adopted for the transportation of pharmaceutical products.

- Although this research project was focused on storage, the results highlighted the potential for improvement of the current manufacturing process for a cell-based product. Mendicino et al., as part of a FDA review, reported that one of the main factors that can influence the manufacturing of hMSCs is the oxygen tension (Mendicino et al., 2014). The adoption of oxygen tension different than atmospheric (21%) has been successfully adopted for enhanced expansion of multipotent adult progenitor cells (MAPCs), where the cells are expanded at 3% oxygen (Subramanian, Park, Verfaillie, & Hu, 2011). Moreover, such hypoxic culture conditions can be used

to enhance the secretion of trophic factors, as already shown by Chang et al (2013) (Chang et al., 2013). The combined effect of temperature between 26 °C and 37 °C and oxygen could pave the way to innovative manufacturing processes which modulate the biological properties of the cells, including the production of trophic factors. Such approach is currently being investigated for robust production of hESCs and iPSCs (Silva et al., 2015).

5.4 Conclusion

The cell therapy market is growing at a fast pace and an increasing number of products are approaching late clinical development and the commercial phase. The preservation of the biological properties of a cell-based medicinal product throughout the supply chain will be paramount and effective solutions for storage and transportation will require deeper understanding and characterization of how these products are affected by process parameters.

This thesis demonstrates that within the normothermic range investigated in this thesis (26 °C and 37 °C), temperature and oxygen can modulate the properties of cartilage discs and undifferentiated hMSCs over a simulated shelf-life of 5 and 7 days.

The use of a DoE based approach as an investigation tool permitted the identification of interactions between temperature and oxygen that are very common for bioprocess systems.

The cell therapy industry is going through a similar product development path that traditional biopharmaceuticals faced 20 years ago. Similarly to what occurred for protein-based drug manufacturing, enhanced knowledge of the parameters that affect the cell during storage and

transportation will be necessary in order to realize the full potential of human cells as living therapeutic agents.

References

- Acker, J. (2013). 23. The challenges and limitations of current clinical methods for the hypothermic storage and cryopreservation of human red blood cells. *Cryobiology*, 66(3). <http://doi.org/10.1016/j.cryobiol.2013.02.029>
- Adesida, A. B., Mulet-Sierra, A., & Jomha, N. M. (2012). Hypoxia mediated isolation and expansion enhances the chondrogenic capacity of bone marrow mesenchymal stromal cells. *Stem Cell Research & Therapy*, 3(2), 9. <http://doi.org/10.1186/scrt100>
- Appelbaum, F. R. (2007). Hematopoietic-Cell Transplantation at 50. *New England Journal of Medicine*, 357(15), 1472–1475. <http://doi.org/10.1056/NEJMp078166>
- Arufe, M. C., De la Fuente, A., Fuentes, I., de Toro, F. J., & Blanco, F. J. (2010). Chondrogenic potential of subpopulations of cells expressing mesenchymal stem cell markers derived from human synovial membranes. *Journal of Cellular Biochemistry*, 111(4), 834–845. <http://doi.org/10.1002/jcb.22768>
- Back, S. A., Khan, R., Gan, X., Rosenberg, P. A., & Volpe, J. J. (1999). A new Alamar Blue viability assay to rapidly quantify oligodendrocyte death. *Journal of Neuroscience Methods*, 91(1-2), 47–54. [http://doi.org/10.1016/S0165-0270\(99\)00062-X](http://doi.org/10.1016/S0165-0270(99)00062-X)
- Baos, S., Sheehan, K., Culliford, L., Pike, K., Ellis, L., Parry, A. J., ... Rogers, C. A. (2015). Normothermic versus hypothermic cardiopulmonary bypass in children undergoing open heart surgery (thermic-2): study protocol for a randomized controlled trial. *JMIR Research Protocols*, 4(2), e59. <http://doi.org/10.2196/resprot.4338>
- Barbash, I. M., Chouraqui, P., Baron, J., Feinberg, M. S., Etzion, S., Tessone, A., ... Leor, J. (2003). Systemic delivery of bone marrow-derived mesenchymal stem cells to the infarcted myocardium: feasibility, cell migration, and body distribution. *Circulation*, 108(7), 863–8. <http://doi.org/10.1161/01.CIR.0000084828.50310.6A>
- Bartunek, J., Davison, B., Sherman, W., Povsic, T., Henry, T. D., Gersh, B., ... Terzic, A. (2016). Congestive Heart Failure Cardiopoietic Regenerative Therapy (CHART-1) trial design. *European Journal of Heart Failure*, 18(2), 160–168. <http://doi.org/10.1002/ejhf.434>
- Basciano, L., Nemos, C., Foliguet, B., de Isla, N., de Carvalho, M., Tran, N., & Dalloul, A. (2011). Long term culture of mesenchymal stem cells in hypoxia promotes a genetic program maintaining their undifferentiated and multipotent status. *BMC Cell Biology*, 12(1), 12. <http://doi.org/10.1186/1471-2121-12-12>
- Baust, J. G., & Baust, J. M. (2007). *Advances in biopreservation*. CRC/Taylor & Francis.
- Bayoussef, Z., Dixon, J. E., Stolnik, S., & Shakesheff, K. M. (2012). Aggregation promotes cell viability, proliferation, and differentiation in an in vitro model of injection cell therapy. *Journal of Tissue Engineering and Regenerative Medicine*, 6(10), e61–73. <http://doi.org/10.1002/term.482>
- Berg, Tymoczko, & Stryer. (2012). *Biochemistry*.
- Boeuf, S., & Richter, W. (2010). Chondrogenesis of mesenchymal stem cells: role of tissue source and inducing factors. *Stem Cell Research & Therapy*, 1(4), 31.

<http://doi.org/10.1186/scrt31>

- Boregowda, S. V., Krishnappa, V., Chambers, J. W., Lograsso, P. V., Lai, W. T., Ortiz, L. A., & Phinney, D. G. (2012). Atmospheric oxygen inhibits growth and differentiation of marrow-derived mouse mesenchymal stem cells via a p53-dependent mechanism: Implications for long-term culture expansion. *Stem Cells*, *30*(5), 975–987. <http://doi.org/10.1002/stem.1069>
- Brandenberger, R., Burger, S., Campbell, A., Fong, T., Lapinska, E., & Rowley, J. a. (2011). Cell therapy bioprocessing. *Bioprocess Int*, *9*, 30–37.
- Bravery, C. A., Carmen, J., Fong, T., Oprea, W., Hoogendoorn, K. H., Woda, J., ... Van't Hof, W. (2013). Potency assay development for cellular therapy products: an ISCT review of the requirements and experiences in the industry. *Cytotherapy*, *15*(1), 9–19. <http://doi.org/10.1016/j.jcyt.2012.10.008>
- Brederlau, A., Correia, A. S., Anisimov, S. V., Elmi, M., Paul, G., Roybon, L., ... Li, J.-Y. (2006). Transplantation of Human Embryonic Stem Cell-Derived Cells to a Rat Model of Parkinson's Disease: Effect of In Vitro Differentiation on Graft Survival and Teratoma Formation. *STEM CELLS*, *24*(6), 1433–1440. <http://doi.org/10.1634/stemcells.2005-0393>
- Bruder, S. P., Fink, D. J., & Caplan, A. I. (1994). Mesenchymal stem cells in bone development, bone repair, and skeletal regeneration therapy. *Journal of Cellular Biochemistry*, *56*(3), 283–294. <http://doi.org/10.1002/jcb.240560303>
- Buchanan, S. S., Pyatt, D. W., & Carpenter, J. F. (2010). Preservation of differentiation and clonogenic potential of human hematopoietic stem and progenitor cells during lyophilization and ambient storage. *PLoS ONE*, *5*(9), e12518. <http://doi.org/10.1371/journal.pone.0012518>
- Buravkova, L. B., Andreeva, E. R., Gogvadze, V., & Zhivotovsky, B. (2014). Mesenchymal stem cells and hypoxia: Where are we? *Mitochondrion*, *19*, 105–112. <http://doi.org/10.1016/j.mito.2014.07.005>
- Buravkova, L. B., Grinakovskaya, O. S., Andreeva, E. R., Zhambalova, A. P., & Kozionova, M. P. (2009). Characteristics of human lipoaspirate-isolated mesenchymal stromal cells cultivated under lower oxygen tension. *Cell and Tissue Biology*, *3*(1), 23–28. <http://doi.org/10.1134/S1990519X09010039>
- Cai, R., Nakamoto, T., Hoshihara, T., Kawazoe, N., & Chen, G. (2014). Control of Simultaneous Osteogenic and Adipogenic Differentiation of Mesenchymal Stem Cells. *Journal of Stem Cell Research & Therapy*, *04*(223). <http://doi.org/10.4172/2157-7633.1000223>
- Capelli, C., Pedrini, O., Valgardsdottir, R., Da Roit, F., Golay, J., & Introna, M. (2015). Clinical grade expansion of MSCs. *Immunology Letters*, *168*(2), 222–227. <http://doi.org/10.1016/j.imlet.2015.06.006>
- Carlsson, P.-O., Schwarcz, E., Korsgren, O., & Le Blanc, K. (2015). Preserved β -cell function in type 1 diabetes by mesenchymal stromal cells. *Diabetes*, *64*(2), 587–92. <http://doi.org/10.2337/db14-0656>

- Chamberlain, G., Fox, J., Ashton, B., & Middleton, J. (2007). Concise Review: Mesenchymal Stem Cells: Their Phenotype, Differentiation Capacity, Immunological Features, and Potential for Homing. *Stem Cells*, 25(11), 2739–2749. <http://doi.org/10.1634/stemcells.2007-0197>
- Chang, C.-P., Chio, C.-C., Cheong, C.-U., Chao, C.-M., Cheng, B.-C., & Lin, M.-T. (2013). Hypoxic preconditioning enhances the therapeutic potential of the secretome from cultured human mesenchymal stem cells in experimental traumatic brain injury. *Clinical Science*, 124(3), 165–176. <http://doi.org/10.1042/CS20120226>
- Chen, J.-L., Duan, L., Zhu, W., Xiong, J., & Wang, D. (2014). Extracellular matrix production in vitro in cartilage tissue engineering. *Journal of Translational Medicine*, 12(1), 88. <http://doi.org/10.1186/1479-5876-12-88>
- Chen, Y., Bloemen, V., Impens, S., Moesen, M., Luyten, F. P., & Schrooten, J. (2011). Characterization and optimization of cell seeding in scaffolds by factorial design: quality by design approach for skeletal tissue engineering. *Tissue Engineering. Part C, Methods*, 17(12), 1211–1221. <http://doi.org/10.1089/ten.tec.2011.0092>
- Chirino, A. J., Ary, M. L., & Marshall, S. A. (2004). Minimizing the immunogenicity of protein therapeutics. *Drug Discovery Today*, 9(2), 82–90. [http://doi.org/10.1016/S1359-6446\(03\)02953-2](http://doi.org/10.1016/S1359-6446(03)02953-2)
- Choudhery, M. S., Badowski, M., Muise, a, & Harris, D. T. (2013). Comparison of human mesenchymal stem cells derived from adipose and cord tissue. *Cytotherapy*, 15(August), 330–343. [http://doi.org/S1465-3249\(12\)00039-4](http://doi.org/S1465-3249(12)00039-4) [pii]r10.1016/j.jcyt.2012.11.010
- Choudhery, M. S., Badowski, M., Muise, A., & Harris, D. T. (2015). Effect of mild heat stress on the proliferative and differentiative ability of human mesenchymal stromal cells. *Cytotherapy*, 17(4), 359–68. <http://doi.org/10.1016/j.jcyt.2014.11.003>
- Conget, P. A., & Minguell, J. J. (1999). Phenotypical and functional properties of human bone marrow mesenchymal progenitor cells. *Journal of Cellular Physiology*, 181(1), 67–73. [http://doi.org/10.1002/\(SICI\)1097-4652\(199910\)181:1<67::AID-JCP7>3.0.CO;2-C](http://doi.org/10.1002/(SICI)1097-4652(199910)181:1<67::AID-JCP7>3.0.CO;2-C)
- Consentius, C., Reinke, P., & Volk, H.-D. (2015). Immunogenicity of allogeneic mesenchymal stromal cells: what has been seen *in vitro* and *in vivo* ? *Regenerative Medicine*, 10, 305–315. <http://doi.org/10.2217/rme.15.14>
- Coopman, K., & Medcalf, N. (2014). From production to patient : challenges and approaches for delivering cell therapies. *The Stem Cell Research Community, StemBook*, 44(0), doi/10.3824/stembook.1.97.1. <http://doi.org/10.3824/stembook.1.97.1.1>
- Correia, C., Koshkin, A., Carido, M., Espinha, N., ari , T., Lima, P. A., ... Alves, P. M. (2016). Effective Hypothermic Storage of Human Pluripotent Stem Cell-Derived Cardiomyocytes Compatible With Global Distribution of Cells for Clinical Applications and Toxicology Testing. *Stem Cells Translational Medicine*, 5(5), 658–669. <http://doi.org/10.5966/sctm.2015-0238>
- Corwin, W. L., Baust, J. M., Baust, J. G., & Van Buskirk, R. G. (2014). Characterization and modulation of human mesenchymal stem cell stress pathway response following hypothermic storage. *Cryobiology*, 68(2), 215–26.

<http://doi.org/10.1016/j.cryobiol.2014.01.014>

- D'Amour, K. A., Bang, A. G., Eliazar, S., Kelly, O. G., Agulnick, A. D., Smart, N. G., ... Baetge, E. E. (2006). Production of pancreatic hormone-expressing endocrine cells from human embryonic stem cells. *Nature Biotechnology*, 24(11), 1392–1401. <http://doi.org/10.1038/nbt1259>
- Dabiri, G., Heiner, D., & Falanga, V. (2013). The emerging use of bone marrow-derived mesenchymal stem cells in the treatment of human chronic wounds. *Expert Opinion on Emerging Drugs*, 18(4), 405–419. <http://doi.org/10.1517/14728214.2013.833184>
- Decaris, M. L., & Leach, J. K. (2011). Design of experiments approach to engineer cell-secreted matrices for directing osteogenic differentiation. *Annals of Biomedical Engineering*, 39(4), 1174–1185. <http://doi.org/10.1007/s10439-010-0217-x>
- DeLise, A. M., Fischer, L., & Tuan, R. S. (2000). Cellular interactions and signaling in cartilage development. *Osteoarthritis and Cartilage / OARS, Osteoarthritis Research Society*, 8(5), 309–34. <http://doi.org/10.1053/joca.1999.0306>
- Deshmukh, R. S., Kovacs, K. A., Dinnyes, A., An, Dinnyes, A., & s. (2012). Drug Discovery Models and Toxicity Testing Using Embryonic and Induced Pluripotent Stem-Cell-Derived Cardiac and Neuronal Cells. *Stem Cells International*, 2012, 1–9. <http://doi.org/10.1155/2012/379569>
- Djouad, F., Delorme, B., Maurice, M., Bony, C., Apparailly, F., Louis-Pence, P., ... Jorgensen, C. (2007). Microenvironmental changes during differentiation of mesenchymal stem cells towards chondrocytes. *Arthritis Research & Therapy*, 9(2), R33. <http://doi.org/10.1186/ar2153>
- Dominici, M., Le Blanc, K., Mueller, I., Slaper-Cortenbach, I., Marini, F., Krause, D. S., ... Horwitz, E. M. (2006). Minimal criteria for defining multipotent mesenchymal stromal cells. The International Society for Cellular Therapy position statement. *Cytotherapy*, 8(4), 315–317. <http://doi.org/10.1080/14653240600855905>
- dos Santos, F., Andrade, P. Z., Boura, J. S., Abecasis, M. M., da Silva, C. L., & Cabral, J. M. S. (2009). Ex vivo expansion of human mesenchymal stem cells: A more effective cell proliferation kinetics and metabolism under hypoxia. *Journal of Cellular Physiology*, (December), n/a–n/a. <http://doi.org/10.1002/jcp.21987>
- Dos Santos, F., Andrade, P. Z., Boura, J. S., Abecasis, M. M., Da Silva, C. L., & Cabral, J. M. S. (2010). Ex vivo expansion of human mesenchymal stem cells: A more effective cell proliferation kinetics and metabolism under hypoxia. *Journal of Cellular Physiology*, 223(1), 27–35. <http://doi.org/10.1002/jcp.21987>
- Dragan, A. I., Casas-Finet, J. R., Bishop, E. S., Strouse, R. J., Schenerman, M. A., & Geddes, C. D. (2010). Characterization of PicoGreen interaction with dsDNA and the origin of its fluorescence enhancement upon binding. *Biophysical Journal*, 99(9), 3010–9. <http://doi.org/10.1016/j.bpj.2010.09.012>
- Du, W., REPPEL, L., Avercenc, L., Schenowitz, C., HUSELSTEIN, C., bensoussan, daniele, ... Rouas-Freiss, N. (2016). Mesenchymal Stem Cells derived from Human Bone Marrow and Adipose Tissue maintain their immunosuppressive properties after chondrogenic differentiation: role of HLA-G. *Stem Cells and Development*,

scd.2016.0022. <http://doi.org/10.1089/scd.2016.0022>

- Eatock, J., Dixon, D., & Young, T. (2009). An exploratory survey of current practice in the medical device industry An exploratory survey of current practice in the medical device industry. *Journal of Manufacturing Technology Management*.
- Eberli, D. M., Pörtner, R., Kaiser, S. C., Kraume, M., Eibl, D., Eibl, R., & Biosystemtechnik, I. für B. (2014). *Cells and biomaterials in regenerative medicine*. InTech.
- Ebert, A. D., & Svendsen, C. N. (2010). Human stem cells and drug screening: opportunities and challenges. *Nature Reviews Drug Discovery*, 9(5), 367–372. <http://doi.org/10.1038/nrd3000>
- Eslaminejad, M. B., Fani, N., & Shahhoseini, M. (2013). Epigenetic regulation of osteogenic and chondrogenic differentiation of mesenchymal stem cells in culture. *Cell Journal*, 15(1), 1–10. Retrieved from <http://www.pubmedcentral.nih.gov/articlerender.fcgi?artid=3660019&tool=pmcentrez&rendertype=abstract>
- Fedorov, V. D., Sadelain, M., & Kloss, C. C. (2014). Novel Approaches to Enhance the Specificity and Safety of Engineered T Cells. *The Cancer Journal*, 20(2), 160–165. <http://doi.org/10.1097/PPO.0000000000000040>
- Frokjaer, S., & Otzen, D. E. (2005). Protein drug stability: a formulation challenge. *Nature Reviews. Drug Discovery*, 4(4), 298–306. <http://doi.org/10.1038/nrd1695>
- Galipeau, J. (2013). The mesenchymal stromal cells dilemma—does a negative phase III trial of random donor mesenchymal stromal cells in steroid-resistant graft-versus-host disease represent a death knell or a bump in the road? *Cytotherapy*, 15(1), 2–8. <http://doi.org/10.1016/j.jcyt.2012.10.002>
- Galvez-Martin, P., Hmadcha, A., Soria, B., Calpena-Campmany, A. C., & Clares-Naveros, B. (2014). Study of the stability of packaging and storage conditions of human mesenchymal stem cell for intra-arterial clinical application in patient with critical limb ischemia. *European Journal of Pharmaceutics and Biopharmaceutics : Official Journal of Arbeitsgemeinschaft Fur Pharmazeutische Verfahrenstechnik e.V.*, 86(3), 459–468. <http://doi.org/10.1016/j.ejpb.2013.11.002>
- Garrity, J. T., Stoker, a. M., Sims, H. J., & Cook, J. L. (2012). Improved Osteochondral Allograft Preservation Using Serum-Free Media at Body Temperature. *The American Journal of Sports Medicine*, 40, 2542–2548. <http://doi.org/10.1177/0363546512458575>
- Gibson, J. S., Milner, P. I., White, R., Fairfax, T. P. A., & Wilkins, R. J. (2008). Oxygen and reactive oxygen species in articular cartilage: modulators of ionic homeostasis. *Pflügers Archiv : European Journal of Physiology*, 455(4), 563–73. <http://doi.org/10.1007/s00424-007-0310-7>
- Ginis, I., Grinblat, B., & Shirvan, M. H. (2012). Evaluation of Bone Marrow-Derived Mesenchymal Stem Cells After Cryopreservation and Hypothermic Storage in Clinically Safe Medium. *Tissue Engineering Part C: Methods*, 18(6), 453–463. <http://doi.org/10.1089/ten.tec.2011.0395>
- Grayson, W. L., Zhao, F., Bunnell, B., & Ma, T. (2007a). Hypoxia enhances proliferation and

- tissue formation of human mesenchymal stem cells. *Biochemical and Biophysical Research Communications*, 358(3), 948–953. <http://doi.org/10.1016/j.bbrc.2007.05.054>
- Han, Y., Quan, G. B., Liu, X. Z., Ma, E. P., Liu, A., Jin, P., & Cao, W. (2005). Improved preservation of human red blood cells by lyophilization. *Cryobiology*, 51(2), 152–64. <http://doi.org/10.1016/j.cryobiol.2005.06.002>
- Hassell, T., Gleave, S., & Butler, M. (1991). Growth inhibition in animal cell culture. The effect of lactate and ammonia. *Applied Biochemistry and Biotechnology*, 30(1), 29–41. Retrieved from <http://www.ncbi.nlm.nih.gov/pubmed/1952924>
- Heathman, T. R., Nienow, A. W., McCall, M. J., Coopman, K., Kara, B., & Hewitt, C. J. (2015). The translation of cell-based therapies: clinical landscape and manufacturing challenges. *Regenerative Medicine*, 10(1), 49–64. <http://doi.org/10.2217/rme.14.73>
- Holzwarth, C., Vaegler, M., Gieseke, F., Pfister, S. M., Handgretinger, R., Kerst, G., & Müller, I. (2010). Low physiologic oxygen tensions reduce proliferation and differentiation of human multipotent mesenchymal stromal cells. *BMC Cell Biology*, 11, 11. <http://doi.org/10.1186/1471-2121-11-11>
- Hourd, P., Ginty, P., Chandra, A., & Williams, D. J. (2014). Manufacturing models permitting roll out/scale out of clinically led autologous cell therapies: regulatory and scientific challenges for comparability. *Cytotherapy*, 16(8), 1033–47. <http://doi.org/10.1016/j.jcyt.2014.03.005>
- Hung, S. C., Pochampally, R. R., Hsu, S. C., Sanchez, C. C., Chen, S. C., Spees, J., & Prockop, D. J. (2007). Short-term exposure of multipotent stromal cells to low oxygen increases their expression of CX3CR1 and CXCR4 and their engraftment in vivo. *PLoS ONE*, 2(5). <http://doi.org/10.1371/journal.pone.0000416>
- Hunt, C. J. (2011). Cryopreservation of Human Stem Cells for Clinical Application: A Review. *Transfusion Medicine and Hemotherapy*, 38(2), 107–123. <http://doi.org/10.1159/000326623>
- Im, G.-I., Jung, N.-H., & Tae, S.-K. (2006). Chondrogenic differentiation of mesenchymal stem cells isolated from patients in late adulthood: the optimal conditions of growth factors. *Tissue Engineering*, 12(3), 527–36. <http://doi.org/10.1089/ten.2006.12.527>
- Jakobsen, R. B., Ostrup, E., Zhang, X., Mikkelsen, T. S., & Brinchmann, J. E. (2014). Analysis of the effects of five factors relevant to in vitro chondrogenesis of human mesenchymal stem cells using factorial design and high throughput mRNA-profiling. *PLoS One*, 9(5), e96615. <http://doi.org/10.1371/journal.pone.0096615>
- Janmey, P. A., Winer, J. P., & Weisel, J. W. (2009). Fibrin gels and their clinical and bioengineering applications. *Journal of the Royal Society, Interface / the Royal Society*, 6(30), 1–10. <http://doi.org/10.1098/rsif.2008.0327>
- Johnstone, B., Alini, M., Cucchiari, M., Dodge, G. R., Eglin, D., Guilak, F., ... Stoddart, M. J. (2013). Tissue engineering for articular cartilage repair--the state of the art. *European Cells & Materials*, 25, 248–67. <http://doi.org/vol025a18> [pii]
- Johnstone, B., Hering, T. M., Caplan, A. I., Goldberg, V. M., & Yoo, J. U. (1998). In vitro chondrogenesis of bone marrow-derived mesenchymal progenitor cells. *Experimental*

Cell Research, 238(1), 265–72. <http://doi.org/10.1006/excr.1997.3858>

- Joshi, M. (1991). Design of Experiments in the semiconductor industry. *Statistical Methodology*.
- Kafienah, W., & Sims, T. J. (2004). Biochemical methods for the analysis of tissue-engineered cartilage. *Methods in Molecular Biology (Clifton, N.J.)*, 238, 217–30. Retrieved from <http://www.ncbi.nlm.nih.gov/pubmed/14970450>
- Kassis, I., Zangi, L., Rivkin, R., Levdansky, L., Samuel, S., Marx, G., & Gorodetsky, R. (2006). Isolation of mesenchymal stem cells from G-CSF-mobilized human peripheral blood using fibrin microbeads. *Bone Marrow Transplantation*, 37(10), 967–976. <http://doi.org/10.1038/sj.bmt.1705358>
- Kefalas, P. (2015). Reimbursement of licensed cell and gene therapies across the major European healthcare markets, 1, 1–14.
- Kern, S., Eichler, H., Stoeve, J., Klüter, H., & Bieback, K. (2006). Comparative analysis of mesenchymal stem cells from bone marrow, umbilical cord blood, or adipose tissue. *Stem Cells*, 24(5), 1294–1301. <http://doi.org/10.1634/stemcells.2005-0342>
- Keung, E., Nelson, P., & Conrad, C. (2013). Concise Review: Adipose-Derived Stem Cells as a Novel Tool for Future Regenerative Medicine. *Stem Cells*, 30, 804–810. <http://doi.org/10.1002/2012>
- Khan, W. S., Adesida, A. B., Hardingham, T. E., Brittberg, M., Lindahl, A., Nilsson, C., ... Clerici, C. (2007). Hypoxic conditions increase hypoxia-inducible transcription factor 2 α and enhance chondrogenesis in stem cells from the infrapatellar fat pad of osteoarthritis patients. *Arthritis Research & Therapy*, 9(3), R55. <http://doi.org/10.1186/ar2211>
- Khan, W. S., Adesida, A. B., Tew, S. R., Lowe, E. T., & Hardingham, T. E. (2010). Bone marrow-derived mesenchymal stem cells express the pericyte marker 3G5 in culture and show enhanced chondrogenesis in hypoxic conditions. *Journal of Orthopaedic Research*, 28(6), n/a–n/a. <http://doi.org/10.1002/jor.21043>
- Kinnaird, T., Stabile, E., Burnett, M. S., Lee, C. W., Barr, S., Fuchs, S., & Epstein, S. E. (2004). Marrow-Derived Stromal Cells Express Genes Encoding a Broad Spectrum of Arteriogenic Cytokines and Promote In Vitro and In Vivo Arteriogenesis Through Paracrine Mechanisms. *Circulation Research*, 94(5), 678–685. <http://doi.org/10.1161/01.RES.0000118601.37875.AC>
- Kirouac, D. C., & Zandstra, P. W. (2008). The systematic production of cells for cell therapies. *Cell Stem Cell*, 3(4), 369–81. <http://doi.org/10.1016/j.stem.2008.09.001>
- Kisiday, J. D., Kurz, B., DiMicco, M. A., & Grodzinsky, A. J. (2005). Evaluation of medium supplemented with insulin-transferrin-selenium for culture of primary bovine calf chondrocytes in three-dimensional hydrogel scaffolds. *Tissue Engineering*, 11(1-2), 141–51. <http://doi.org/10.1089/ten.2005.11.141>
- Kiviranta, I., Jurvelin, J., Säämänen, A. M., & Helminen, H. J. (1985). Microspectrophotometric quantitation of glycosaminoglycans in articular cartilage sections stained with Safranin O. *Histochemistry*, 82(3), 249–255.

<http://doi.org/10.1007/BF00501401>

- Komarova, S. V., Ataulakhanov, F. I., Globus, R. K., Aprille, J., Ataulakhanov, F., Martynov, M., ... Gay, C. (2000). Bioenergetics and mitochondrial transmembrane potential during differentiation of cultured osteoblasts. *American Journal of Physiology. Cell Physiology*, 279(4), C1220–9. <http://doi.org/10.1006/jtbi.1996.0222>
- Konomi, K., Tobita, M., Kimura, K., & Sato, D. (2015). New Japanese Initiatives on Stem Cell Therapies. *Cell Stem Cell*. <http://doi.org/10.1016/j.stem.2015.03.012>
- Lee, R. H., Pulin, A. A., Seo, M. J., Kota, D. J., Ylostalo, J., Larson, B. L., ... Prockop, D. J. (2009). Intravenous hMSCs Improve Myocardial Infarction in Mice because Cells Embolized in Lung Are Activated to Secrete the Anti-inflammatory Protein TSG-6. *Cell Stem Cell*, 5(1), 54–63. <http://doi.org/10.1016/j.stem.2009.05.003>
- Li, Y., Sattler, G. L., & Pitot, H. C. (1995). The effect of amino acid composition of serum-free medium on DNA synthesis in primary hepatocyte cultures in the presence of epidermal growth factor. *In Vitro Cellular {&} Developmental Biology - Animal*, 31(11), 867–870. <http://doi.org/10.1007/BF02634571>
- Lim, M., Shunjie, C., Panoskaltsis, N., & Mantalaris, A. (2012). Systematic experimental design for bioprocess characterization: Elucidating transient effects of multi-cytokine contributions on erythroid differentiation. *Biotechnology and Bioprocess Engineering*, 17(1), 218–226. <http://doi.org/10.1007/s12257-011-0422-y>
- Lim, M., Ye, H., Panoskaltsis, N., Drakakis, E. M., Yue, X., Cass, A. E. G., ... Mantalaris, A. (2007). Intelligent bioprocessing for haematopoietic cell cultures using monitoring and design of experiments. *Biotechnology Advances*, 25(4), 353–68. <http://doi.org/10.1016/j.biotechadv.2007.02.002>
- Lipsitz, Y. Y., Timmins, N. E., & Zandstra, P. W. (2016). Quality cell therapy manufacturing by design. *Nature Biotechnology*, 34(4), 393–400. <http://doi.org/10.1038/nbt.3525>
- M., H., MengGuoliang, E., R., D., G., & S., K. (2013). Factorial Experimental Design for the Culture of Human Embryonic Stem Cells as Aggregates in Stirred Suspension Bioreactors Reveals the Potential for Interaction Effects Between Bioprocess Parameters. <http://dx.doi.org/10.1089/ten.tec.2013.0040>.
- Ma, T., Tsai, A.-C., & Liu, Y. (2016). Biomanufacturing of human mesenchymal stem cells in cell therapy: Influence of microenvironment on scalable expansion in bioreactors. *Biochemical Engineering Journal*. <http://doi.org/10.1016/j.bej.2015.07.014>
- Mackay, A. M., Beck, S. C., Murphy, J. M., Barry, F. P., Chichester, C. O., & Pittenger, M. F. (1998). Chondrogenic Differentiation of Cultured Human Mesenchymal Stem Cells from Marrow. *Tissue Engineering*, 4(4), 415–428. <http://doi.org/10.1089/ten.1998.4.415>
- Mahler, S., Desille, M., Frémond, B., Chesné, C., Guillouzo, A., Campion, J.-P., & Clément, B. (n.d.). Hypothermic Storage and Cryopreservation of Hepatocytes: The Protective Effect of Alginate Gel Against Cell Damages.
- Makhoul, G., Chiu, R. C. J., & Cecere, R. (2013). Placental mesenchymal stem cells: A unique source for cellular cardiomyoplasty. *Annals of Thoracic Surgery*, 95(5), 1827–1833. <http://doi.org/10.1016/j.athoracsur.2012.11.053>

- Malladi, P., Xu, Y., Chiou, M., Giaccia, A. J., & Longaker, M. T. (2006). Effect of reduced oxygen tension on chondrogenesis and osteogenesis in adipose-derived mesenchymal cells. *American Journal of Physiology. Cell Physiology*, 290(4), C1139–46. <http://doi.org/10.1152/ajpcell.00415.2005>
- Markway, B. D., Tan, G.-K., Brooke, G., Hudson, J. E., Cooper-White, J. J., & Doran, M. R. (n.d.). Enhanced Chondrogenic Differentiation of Human Bone Marrow-Derived Mesenchymal Stem Cells in Low Oxygen Environment Micropellet Cultures. Cognizant Communication Corporation. Retrieved from <http://www.ingentaconnect.com/contentone/cog/ct/2010/00000019/00000001/art00005>
- Martin, I., Simmons, P. J., & Williams, D. F. (2014). Manufacturing challenges in regenerative medicine. *Science Translational Medicine*, 6(232), 232fs16. <http://doi.org/10.1126/scitranslmed.3008558>
- Martin, M. J., Muotri, A., Gage, F., & Varki, A. (2005). Human embryonic stem cells express an immunogenic nonhuman sialic acid. *Nature Medicine*, 11(2), 228–232. <http://doi.org/10.1038/nm1181>
- Mason, C., Brindley, D. A., Culme-Seymour, E. J., & Davie, N. L. (2011). Cell therapy industry: billion dollar global business with unlimited potential. *Regenerative Medicine*, 6(3), 265–272. <http://doi.org/10.2217/rme.11.28>
- Massie, I., Selden, C., Hodgson, H., Fuller, B., Gibbons, S., & Morris, G. J. (2014). GMP Cryopreservation of Large Volumes of Cells for Regenerative Medicine: Active Control of the Freezing Process. *Tissue Engineering Part C: Methods*, 20(9), 693–702. <http://doi.org/10.1089/ten.tec.2013.0571>
- Mathew, A. J., Baust, J. M., Van Buskirk, R. G., & Baust, J. G. (2004). Cell Preservation in Reparative and Regenerative Medicine: Evolution of Individualized Solution Composition. *Tissue Engineering*, 10(11-12), 1662–1671. <http://doi.org/10.1089/ten.2004.10.1662>
- Mathiasen, A. B., Qayyum, A. A., Jørgensen, E., Helqvist, S., Fischer-Nielsen, A., Kofoed, K. F., ... Atsma, D. (2015). Bone marrow-derived mesenchymal stromal cell treatment in patients with severe ischaemic heart failure: a randomized placebo-controlled trial (MSC-HF trial). *European Heart Journal*, 36(27), 1744–53. <http://doi.org/10.1093/eurheartj/ehv136>
- Matsubara, T., Tsutsumi, S., Pan, H., Hiraoka, H., Oda, R., Nishimura, M., ... Kato, Y. (2004). A new technique to expand human mesenchymal stem cells using basement membrane extracellular matrix. *Biochemical and Biophysical Research Communications*, 313(3), 503–508. <http://doi.org/10.1016/j.bbrc.2003.11.143>
- Mendicino, M., Bailey, A. M., Wonnacott, K., Puri, R. K., & Bauer, S. R. (2014). MSC-Based Product Characterization for Clinical Trials: An FDA Perspective. *Cell Stem Cell*. <http://doi.org/10.1016/j.stem.2014.01.013>
- Montgomery, D. C. (2012). *Design and Analysis of Experiments. Design* (Vol. 2). <http://doi.org/10.1198/tech.2006.s372>
- Müller, P., Bulnheim, U., Diener, A., Lüthen, F., Teller, M., Klinkenberg, E.-D., ... Rychly, J. (2007). Calcium phosphate surfaces promote osteogenic differentiation of

- mesenchymal stem cells. *Journal of Cellular and Molecular Medicine*, 12(1), 281–291. <http://doi.org/10.1111/j.1582-4934.2007.00103.x>
- Munneke, J. M., Spruit, M. J. A., Cornelissen, A. S., van Hoeven, V., Voermans, C., & Hazenberg, M. D. (2015). The Potential of Mesenchymal Stromal Cells as Treatment for Severe Steroid-Refractory Acute Graft-Versus-Host Disease: A Critical Review of the Literature. *Transplantation*. <http://doi.org/10.1097/TP.0000000000001029>
- Murdoch, A. D., Grady, L. M., Ablett, M. P., Katopodi, T., Meadows, R. S., & Hardingham, T. E. (2007). Chondrogenic Differentiation of Human Bone Marrow Stem Cells in Transwell Cultures: Generation of Scaffold-Free Cartilage. *Stem Cells*, 25(11), 2786–2796. <http://doi.org/10.1634/stemcells.2007-0374>
- Ng, K. W., Leong, D. T. W., & Hutmacher, D. W. (2005). The Challenge to Measure Cell Proliferation in Two and Three Dimensions. *Tissue Engineering*, 11(1-2), 182–191. <http://doi.org/10.1089/ten.2005.11.182>
- Nombela-Arrieta, C., Ritz, J., & Silberstein, L. E. (2011). The elusive nature and function of mesenchymal stem cells. *Nature Publishing Group*, 12(2), 126–131. <http://doi.org/10.1038/nrm3049>
- Panchalingam, K. M., Jung, S., Rosenberg, L., & Behie, L. A. (2015). Bioprocessing strategies for the large-scale production of human mesenchymal stem cells: a review. *Stem Cell Research & Therapy*, 6(1), 225. <http://doi.org/10.1186/s13287-015-0228-5>
- Panés, J., García-Olmo, D., Van Assche, G., Colombel, J. F., Reinisch, W., Baumgart, D. C., ... Danese, S. (2016). Expanded allogeneic adipose-derived mesenchymal stem cells (Cx601) for complex perianal fistulas in Crohn's disease: a phase 3 randomised, double-blind controlled trial. *The Lancet*. [http://doi.org/10.1016/S0140-6736\(16\)31203-X](http://doi.org/10.1016/S0140-6736(16)31203-X)
- Pattappa, G., Heywood, H. K., de Bruijn, J. D., & Lee, D. A. (2011). The metabolism of human mesenchymal stem cells during proliferation and differentiation. *Journal of Cellular Physiology*, 226(10), 2562–2570. <http://doi.org/10.1002/jcp.22605>
- Pei, D., Xu, J., Zhuang, Q., Tse, H.-F., & Esteban, M. a. (2010). Induced pluripotent stem cell technology in regenerative medicine and biology. *Advances in Biochemical Engineering/biotechnology*, 123(July 2015), 127–141. <http://doi.org/10.1007/10>
- Phinney, D. G., & Prockop, D. J. (2007). Concise Review: Mesenchymal Stem/Multipotent Stromal Cells: The State of Transdifferentiation and Modes of Tissue Repair-Current Views. *Stem Cells*, 25(11), 2896–2902. <http://doi.org/10.1634/stemcells.2007-0637>
- Pogozhykh, D., Prokopyuk, V., Pogozhykh, O., Mueller, T., Prokopyuk, O., Bárcena, A., ... Kierulf, P. (2015). Influence of Factors of Cryopreservation and Hypothermic Storage on Survival and Functional Parameters of Multipotent Stromal Cells of Placental Origin. *PLOS ONE*, 10(10), e0139834. <http://doi.org/10.1371/journal.pone.0139834>
- Rafalski, V. a, Mancini, E., & Brunet, A. (2012). Energy metabolism and energy-sensing pathways in mammalian embryonic and adult stem cell fate. *Journal of Cell Science*, 125, 5597–608. <http://doi.org/10.1242/jcs.114827>
- Ramalho-Santos, M., Yoon, S., Matsuzaki, Y., Mulligan, R. C., Melton, D. A., Bongso, A., ... Cheshier, S. H. (2002). "Stemness": transcriptional profiling of

- embryonic and adult stem cells. *Science (New York, N.Y.)*, 298(5593), 597–600.
<http://doi.org/10.1126/science.1072530>
- Rampersad, S. N. (2012). Multiple applications of Alamar Blue as an indicator of metabolic function and cellular health in cell viability bioassays. *Sensors (Basel, Switzerland)*, 12(9), 12347–60. <http://doi.org/10.3390/s120912347>
- Rasini, V., Dominici, M., Kluba, T., Siegel, G., Lusenti, G., Northoff, H., ... Schäfer, R. (2013). Mesenchymal stromal/stem cells markers in the human bone marrow. *Cytotherapy*, 15(3), 292–306. <http://doi.org/10.1016/j.jcyt.2012.11.009>
- Rathore, A. S., & Winkle, H. (2009). c o m m e n t a r y Quality by design for biopharmaceuticals, 27(1).
- Rayment, E. A., & Williams, D. J. (2010). Mind the Gap: Challenges in Characterising and Quantifying Cell- and Tissue-Based Therapies for Clinical Translation. *STEM CELLS*, 28(5), N/A–N/A. <http://doi.org/10.1002/stem.416>
- Reissis, Y., Garcia-Gareta, E., Korda, M., Blunn, G., & Hua, J. (2013). The effect of temperature on the viability of human mesenchymal stem cells. *Stem Cell Research & Therapy*, 4(6), 139. <http://doi.org/10.1007/s00580-014-1915-9>
- Reissis, Y., García-Gareta, E., Korda, M., Blunn, G. W., & Hua, J. (2013). The effect of temperature on the viability of human mesenchymal stem cells. *Stem Cell Research & Therapy*, 4(6), 139. <http://doi.org/10.1186/scrt350>
- Rippon, H. J., & Bishop, A. E. (2004). Embryonic stem cells. *Cell Proliferation*, 37(1), 23–34. <http://doi.org/10.1111/j.1365-2184.2004.00298.x>
- Robinson, N. J., Picken, A., & Coopman, K. (2014). Low temperature cell pausing: An alternative short-term preservation method for use in cell therapies including stem cell applications. *Biotechnology Letters*, 36(2), 201–209. <http://doi.org/10.1007/s10529-013-1349-5>
- Rosen, E. D., & MacDougald, O. A. (2006). Adipocyte differentiation from the inside out. *Nature Reviews Molecular Cell Biology*, 7(12), 885–896.
<http://doi.org/10.1038/nrm2066>
- Salmikangas, P., Menezes-Ferreira, M., Reischl, I., Tsiftoglou, A., Borg, J. J., Ruiz, S., ... Schneider, C. K. (2015). Manufacturing , characterization and control of cell-based medicinal products: challenging paradigms toward commercial use. *Regenerative Medicine*, 10(1), 65–78. <http://doi.org/10.2217/rme.14.65>
- Sasaki, M., Abe, R., Fujita, Y., Ando, S., Inokuma, D., & Shimizu, H. (2008). Mesenchymal Stem Cells Are Recruited into Wounded Skin and Contribute to Wound Repair by Transdifferentiation into Multiple Skin Cell Type. *The Journal of Immunology*, 180(4), 2581–2587. <http://doi.org/10.4049/jimmunol.180.4.2581>
- Schäck, L. M., Noack, S., Winkler, R., Wißmann, G., Behrens, P., Wellmann, M., ... Hoffmann, A. (2013). The Phosphate Source Influences Gene Expression and Quality of Mineralization during In Vitro Osteogenic Differentiation of Human Mesenchymal Stem Cells. *PLoS ONE*, 8(6). <http://doi.org/10.1371/journal.pone.0065943>
- Schneider, C. K., Salmikangas, P., Jilka, B., Flamion, B., Todorova, L. R., Paphitou, A., ...

- Celis, P. (2010). Challenges with advanced therapy medicinal products and how to meet them. *Nature Reviews. Drug Discovery*, 9(3), 195–201. <http://doi.org/10.1038/nrd3052>
- Schneider, W., Bortfeld, T., & Schlegel, W. (2000). Correlation between CT numbers and tissue parameters needed for Monte Carlo simulations of clinical dose distributions. *Physics in Medicine and Biology*, 45(2), 459–478. <http://doi.org/10.1088/0031-9155/45/2/314>
- Schnitzler, A. C., Verma, A., Kehoe, D. E., Jing, D., Murrell, J. R., Der, K. A., ... Rook, M. S. (2015). Bioprocessing of human mesenchymal stem/stromal cells for therapeutic use: Current technologies and challenges. *Biochemical Engineering Journal*, 108, 3–13. <http://doi.org/10.1016/j.bej.2015.08.014>
- Schop, D., Janssen, F. W., van Rijn, L. D. S., Fernandes, H., Bloem, R. M., de Bruijn, J. D., & van Dijkhuizen-Radersma, R. (2009). Growth, metabolism, and growth inhibitors of mesenchymal stem cells. *Tissue Engineering. Part A*, 15(8), 1877–86. <http://doi.org/10.1089/ten.tea.2008.0345>
- Schwartz, S. D., Hubschman, J.-P., Heilwell, G., Franco-Cardenas, V., Pan, C. K., Ostrick, R. M., ... Lanza, R. (2012). Embryonic stem cell trials for macular degeneration: a preliminary report. *The Lancet*, 379(9817), 713–720. [http://doi.org/10.1016/S0140-6736\(12\)60028-2](http://doi.org/10.1016/S0140-6736(12)60028-2)
- Scott, M. A., Nguyen, V. T., Levi, B., & James, A. W. (2011). Current Methods of Adipogenic Differentiation of Mesenchymal Stem Cells. <http://dx.doi.org/10.1089/scd.2011.0040>.
- Serra, M., Brito, C., Correia, C., & Alves, P. M. (2012). Process engineering of human pluripotent stem cells for clinical application. *Trends in Biotechnology*, 30(6), 350–359. <http://doi.org/10.1016/j.tibtech.2012.03.003>
- Sessarego, N., Parodi, A., Podestà, M., Benvenuto, F., Mogni, M., Raviolo, V., ... Frassoni, F. (2008). Multipotent mesenchymal stromal cells from amniotic fluid: solid perspectives for clinical application. *Haematologica*, 93(3), 339–46. <http://doi.org/10.3324/haematol.11869>
- Sheehy, E. J., Buckley, C. T., & Kelly, D. J. (2012). Oxygen tension regulates the osteogenic, chondrogenic and endochondral phenotype of bone marrow derived mesenchymal stem cells. *Biochem Biophys Res Commun*, 417(1), 305–310. <http://doi.org/10.1016/j.bbrc.2011.11.105>
- Shintani, N., & Hunziker, E. B. (2011). Differential effects of dexamethasone on the chondrogenesis of mesenchymal stromal cells: influence of microenvironment, tissue origin and growth factor. *European Cells & Materials*, 22, 302–19; discussion 319–20. Retrieved from <http://www.ncbi.nlm.nih.gov/pubmed/22116649>
- Silva, M. M., Rodrigues, A. F., Correia, C., Sousa, M. F. Q., Brito, C., Coroadinha, A. S., ... Alves, P. M. (2015). Robust Expansion of Human Pluripotent Stem Cells: Integration of Bioprocess Design With Transcriptomic and Metabolomic Characterization. *Stem Cells Translational Medicine*, 4(7), 731–42. <http://doi.org/10.5966/sctm.2014-0270>
- Simaria, A. S., Hassan, S., Varadaraju, H., Rowley, J., Warren, K., Vanek, P., & Farid, S. S. (2014). Allogeneic cell therapy bioprocess economics and optimization: Single-use cell

- expansion technologies. *Biotechnology and Bioengineering*, 111(1), 69–83.
<http://doi.org/10.1002/bit.25008>
- Sotiropoulou, P. A., Perez, S. A., Salagianni, M., Baxevanis, C. N., & Papamichail, M. (2006). Characterization of the optimal culture conditions for clinical scale production of human mesenchymal stem cells. *Stem Cells (Dayton, Ohio)*, 24(2), 462–71.
<http://doi.org/10.1634/stemcells.2004-0331>
- Spiller, K. L., Maher, S. A., & Lowman, A. M. (2011). Hydrogels for the Repair of Articular Cartilage Defects. *Tissue Engineering Part B: Reviews*, 17(4), 281–299.
<http://doi.org/10.1089/ten.teb.2011.0077>
- Steinert, A. F., Rackwitz, L., Gilbert, F., Noth, U., & Tuan, R. S. (2012). Concise Review: The Clinical Application of Mesenchymal Stem Cells for Musculoskeletal Regeneration: Current Status and Perspectives. *Stem Cells Translational Medicine*, 1(3), 237–247.
<http://doi.org/10.5966/sctm.2011-0036>
- Stolzing, A., & Scutt, A. (2006). Effect of reduced culture temperature on antioxidant defences of mesenchymal stem cells. *Free Radical Biology and Medicine*, 41(2), 326–338. <http://doi.org/10.1016/j.freeradbiomed.2006.04.018>
- Stolzing, A., Sethe, S., & Scutt, A. M. (2006). Stressed stem cells: Temperature response in aged mesenchymal stem cells. *Stem Cells and Development*, 15(4), 478–87.
<http://doi.org/10.1089/scd.2006.15.478>
- Subramanian, K., Park, Y., Verfaillie, C. M., & Hu, W. S. (2011). Scalable expansion of multipotent adult progenitor cells as three-dimensional cell aggregates. *Biotechnology and Bioengineering*, 108(2), 364–375. <http://doi.org/10.1002/bit.22939>
- Sun, H., Wu, C., Dai, K., Chang, J., & Tang, T. (2006). Proliferation and osteoblastic differentiation of human bone marrow-derived stromal cells on akermanite-bioactive ceramics. *Biomaterials*, 27(33), 5651–5657.
<http://doi.org/10.1016/j.biomaterials.2006.07.027>
- Swioklo, S., Constantinescu, A., & Connon, C. J. (2016). Alginate-Encapsulation for the Improved Hypothermic Preservation of Human Adipose-Derived Stem Cells. *Stem Cells Translational Medicine*, 5(3), 339–49. <http://doi.org/10.5966/sctm.2015-0131>
- Takahashi, K., & Yamanaka, S. (2006). Induction of Pluripotent Stem Cells from Mouse Embryonic and Adult Fibroblast Cultures by Defined Factors. *Cell*, 126(4), 663–676.
<http://doi.org/10.1016/j.cell.2006.07.024>
- Tew, S. R., Murdoch, A. D., Rauchenberg, R. P., & Hardingham, T. E. (2008). Cellular methods in cartilage research: Primary human chondrocytes in culture and chondrogenesis in human bone marrow stem cells. *Methods*, 45(1), 2–9.
<http://doi.org/10.1016/j.ymeth.2008.01.006>
- Trainor, N., Pietak, A., & Smith, T. (2014). Rethinking clinical delivery of adult stem cell therapies. *Nature Biotechnology*, 32(8), 729–735. <http://doi.org/10.1038/nbt.2970>
- Trounson, A., & DeWitt, N. D. (2016). Pluripotent stem cells progressing to the clinic. *Nature Reviews Molecular Cell Biology*, 17(3), 194–200.
<http://doi.org/10.1038/nrm.2016.10>

- Tye, H. (2004). Application of statistical “design of experiments” methods in drug discovery. *Drug Discovery Today*, 9(11), 485–491. [http://doi.org/10.1016/S1359-6446\(04\)03086-7](http://doi.org/10.1016/S1359-6446(04)03086-7)
- Valles, A., & Sanchez, J. (2009). Implementation of Six Sigma in a Manufacturing Process: A Case Study. *International Journal of Industrial Engineering*, 16(3), 171–181.
- Valorani, M. G., Montelatici, E., Germani, A., Biddle, A., D’Alessandro, D., Strollo, R., ... Alison, M. R. (2012). Pre-culturing human adipose tissue mesenchymal stem cells under hypoxia increases their adipogenic and osteogenic differentiation potentials. *Cell Proliferation*, 45(3), 225–238. <http://doi.org/10.1111/j.1365-2184.2012.00817.x>
- Van Campenhout, A., Swinnen, L., Klykens, J., Devos, T., & Verhoef, G. (2014). Post-cryopreservation viability of mesenchymal stem cells. *Cytotherapy*, 16(4), S83. <http://doi.org/10.1016/j.jcyt.2014.01.301>
- Varum, S., Rodrigues, A. S., Moura, M. B., Momcilovic, O., Easley, C. A., Ramalho-Santos, J., ... Schatten, G. (2011). Energy Metabolism in Human Pluripotent Stem Cells and Their Differentiated Counterparts. *PLoS ONE*, 6(6), e20914. <http://doi.org/10.1371/journal.pone.0020914>
- Wang, D. W., Fermor, B., Gimble, J. M., Awad, H. A., & Guilak, F. (2005). Influence of oxygen on the proliferation and metabolism of adipose derived adult stem cells. *Journal of Cellular Physiology*, 204(1), 184–91. <http://doi.org/10.1002/jcp.20324>
- Wang, H.-S., Hung, S.-C., Peng, S.-T., Huang, C.-C., Wei, H.-M., Guo, Y.-J., ... Chen, C.-C. (2004). Mesenchymal Stem Cells in the Wharton’s Jelly of the Human Umbilical Cord. *Stem Cells*, 22(7), 1330–1337. <http://doi.org/10.1634/stemcells.2004-0013>
- Wang, X., Wang, Y., Gou, W., Lu, Q., Peng, J., & Lu, S. (2013). Role of mesenchymal stem cells in bone regeneration and fracture repair: a review. *International Orthopaedics*, 37(12), 2491–2498. <http://doi.org/10.1007/s00264-013-2059-2>
- Wurth, C., Demeule, B., Mahler, H.-C., Adler, M., Rathore, A. S., Rathore, A. S., ... Roberts, C. J. (2016). Quality by Design Approaches to Formulation Robustness—An Antibody Case Study. *Journal of Pharmaceutical Sciences*, 105(5), 1667–1675. <http://doi.org/10.1016/j.xphs.2016.02.013>
- Yang, J., Yamato, M., Kohno, C., Nishimoto, A., Sekine, H., Fukai, F., & Okano, T. (2005). Cell sheet engineering: Recreating tissues without biodegradable scaffolds. *Biomaterials*, 26(33), 6415–6422. <http://doi.org/10.1016/j.biomaterials.2005.04.061>
- Yang, Z., & Xiong, H. (2012). Culture Conditions and Types of Growth Media for Mammalian Cells. *Biomedical Tissue Culture, Chapter 1*, 3–18. <http://doi.org/10.5772/52301>
- Ying, Q.-L., Wray, J., Nichols, J., Battle-Morera, L., Doble, B., Woodgett, J., ... Smith, A. (2008). The ground state of embryonic stem cell self-renewal. *Nature*, 453(7194), 519–523. <http://doi.org/10.1038/nature06968>
- Zhang, X., Hirai, M., Cantero, S., Ciubotariu, R., Dobrila, L., Hirsh, A., ... Takahashi, T. A. (2011). Isolation and characterization of mesenchymal stem cells from human umbilical cord blood: Reevaluation of critical factors for successful isolation and high ability to proliferate and differentiate to chondrocytes as compared to mesenchymal stem cells fro.

Journal of Cellular Biochemistry, 112(4), 1206–1218. <http://doi.org/10.1002/jcb.23042>

Zhou, S., Cui, Z., & Urban, J. P. G. (2004). Factors influencing the oxygen concentration gradient from the synovial surface of articular cartilage to the cartilage-bone interface: a modeling study. *Arthritis and Rheumatism*, 50(12), 3915–24. <http://doi.org/10.1002/art.20675>

Appendix I

Donor details for the bone marrow derived hMSCs used in this thesis

Donor	Sex	Ethnicity	Age
1	Female	Caucasian	24
2	Male	Caucasian	29
3	Male	Caucasian	25